UNDERSTANDING POSTRANSLATIONAL MODIFICATIONS INVOLVED IN ADI3 PROGRAMMED CELL DEATH SIGNALING

A Dissertation

by

JULIAN RICARDO AVILA PACHECO

Submitted to the Office of Graduate Studies of
Texas A&M University
in partial fulfillment of the requirements for the degree of

DOCTOR OF PHILOSOPHY

Approved by:

Chair of Committee,	Timothy Devarenne
Committee Members,	Mikhailo Kolomiets
	Jean-Philippe Pellois
	Paul Straight
Head of Department,	Gregory Reinhart

December 2012

Major Subject: Biochemistry

ABSTRACT

Programmed cell death (PCD) is an active process by which organisms coordinate the controlled destruction of cells. In tomato, the protein kinase Adi3 (AvrPto-dependent Pto-interacting kinase 3), acts as a negative regulator of PCD and shares important functional homologies with the mammalian anti-apoptotic AGC kinase PBK/Akt. Adi3 was originally identified as an interactor of the complex formed by the tomato resistance protein Pto and the *Pseudomonas syringae pv. tomato* (*Pst*) effector protein AvrPto. The complex formed by AvrPto and Pto causes a resistance response characterized by a rapid form of PCD that limits the spread of *Pst* and prevents the onset of the tomato bacterial speck disease.

In an effort to characterize the mechanisms by which Adi3 regulates PCD, we identified Adi3 interacting partners in a Y2H screen. Here, I describe the interaction of Adi3 with two interacting partners identified: the Sucrose Non-fermenting (SNF1) kinase complex (SnRK) which is a eukaryotic master regulator of energy homeostasis and the E3 RING Ubiquitin ligase AdBiL.

Using a combination of *in vitro* and *in vivo* approaches I found that AdBiL is an active ubiquitin ligase that ubiquitinates Adi3. Interestingly, Adi3 was found to be degraded in a proteasome-dependent manner suggesting ubiquitination could play a role in its degradation. On the other hand, Adi3 was found to inhibit the SnRK complex by directly interacting with its catalytic subunit as well as by phosphorylating the regulatory subunit *Sl*Gal83 at Ser26. *Sl*Gal83 is phosphorylated at multiple sites *in vivo*, and this

phosphorylation state, as well as its intracellular localization was found to depend on a myristoylation signal present at its N-terminus. Phosphorylation at Ser26 by Adi3 was found to alter the localization of this subunit in a myristoylation-dependent manner.

The interactions studied in this dissertation provide additional evidence on the functional homologies shared by Adi3 and PKB. In addition, the regulatory control of SnRK activity and cellular localization offers a novel connection between pathways involved in energy homeostasis and pathogen-mediated PCD.

DEDICATION

To my mother and father who have never given up on me and have invested their lives making sure I grew up to be a good man, thanks to you both from the bottom of my heart.

Ma, pa, gracias por siempre estar a mi lado y por invertir sus vidas intentando hacerme de mí un hombre mejor, gracias desde lo más profundo de mi corazón.

ACKNOWLEDGEMENTS

I would like to thank my advisor Dr. Timothy Devarenne for giving me the opportunity to work with him. But, especially for giving me the time and freedom to find direction in my research and letting me make and learn from my own mistakes. I could have not learned this much if I had been under his mentorship.

I would also like to thank my committee, Dr. Straight, Dr. Pellois, and Dr. Kolomiets for their time and support throughout my six years in graduate school, but more importantly for the diverse vision about science and academia they have given me.

This work is the outcome of the fantastic support the faculty and staff have provided in the Department of Biochemistry and Biophysics. I am tremendously grateful for all the help and encouragement I have received throughout the years from this great place and its people. I would like to particularly thank Dr. Dorothy Shippen for sharing her insightful knowledge in science, academia, and life, but especially for always being an advocate for my scientific career. Also, I would like to thank Dr. Ping He and Dr. Libo Shan for their fantastic work, which has served as an inspiration for me in the past few years, and for their feedback during our joint lab meetings.

I would like to thank my friends for being my friends and being there in good or bad times, Andrew, Anna, Joel, Carlos, Katie, and Catalina. Life in this town would have not been the same without them.

Finally, to Garrett Nichols, for saving my life and giving me more love I could I have ever had asked for.

NOMENCLATURE

Adi3	AvrPto-dependent Pto-interacting protein 3
PDK1	3-Phosphoinositide dependent protein kinase 1
AdBiL	Adi3 Binding Ligase
SnRK	Sucrose non-fermenting related kinase
SnRK1	Tomato α-subunit of the SnRK complex
HR	Hypersensitive Response
PCD	Programmed cell death
Ub	Ubiquitin
UBC	Ubiquitin conjugating enzyme (E2)
UBA	Ubiquitin activating enzyme (E1)
HECT	Homologous to the E6-AP carboxyl terminus
RING	Really interesting new gene domain
Pst	*Pseudomonas syringae pathovar Tomato*
Sl	*Solanum lycopersicum* (Tomato)
At	*Arabidopsis thaliana* (Thale cress)

TABLE OF CONTENTS

Page

LIST OF FIGURES

Page

LIST OF TABLES

CHAPTER I

INTRODUCTION AND LITERATURE REVIEW

1.1 Programmed cell death (PCD)

1.1a Initial studies on cell death

Cell death has been subject of study since the 19th century when dying cell types and tissues were subject to extensive histological characterization (Khosravi-Far et al., 2007). Early observations like the absorption of tadpole tail cells in the developing frog and the webbing between digits in humans and mice are among some of the examples of the multiple developmental processes that were described in great detail (Glücksmann, 1951). While rich in detail, these studies were limited to morphological comparisons among dying tissues and lacked any biological explanation on the underlying processes that were taking place (Khosravi-Far et al., 2007).

At the time, the puzzling occurrence of cell death, especially in developing embryos, seemed counterintuitive since selective killing of cell types and even entire organs appeared wasteful during such energy demanding stages (Saunders, 1966). It was not until the mid 20th century that the concept of programmed cell death (PCD) was proposed. Developmental biologists working on the changes that take place during metamorphosis and embryonic development recognized that certain types of cell death were not accidental but biologically controlled (Khosravi-Far et al., 2007). The destruction and further reutilization of tissues in the development of insects and chick embryos were some of the very first PCD processes studied. Using grafting of chicken

embryos Saunders (1966) observed that certain cells in the developing wings and digits carried an irrevocable "death sentence" upon them. Similarly, physiological studies of the degradation of the larval muscle tissues used for the unfurling of the wings of the silk moth *Antheraea pernyi* revealed that the quick yet organized death of cells was a "programmed" process that involved hormone-signaling, protein synthesis, and the formation of lysosomes (Lettre & Hengartner, 2006, Lockshin, 1969).

The work conducted on the nematode *Caenorhabditis elegans,* which was awarded with a Medicine Nobel Prize in 2002, revealed the identity of the first genes involved in controlling the death of 131 out of the worm's 1090 somatic cells. This work paved the way for the elucidation of PCD controllers in animals (Ellis & Horvitz, 1986, Vaux & Korsmeyer, 1999). These seminal studies, among others, helped coin the concept of PCD under which the reconstruction of tissues and entire organs rely on a detailed genetic blue-print with instructions on the timing and identity of the cells and tissues that are to commit suicide.

1.1b Definition of PCD

Programmed cell death (PCD) is now recognized as the active process by which organisms coordinate the controlled destruction of cells (Lam, 2004, Pennell & Lamb, 1997). PCD can be initiated by metabolic and developmental requirements or as a response to biotic or abiotic environmental factors (Lam, 2004). In both animals and plants, PCD is crucial for the removal of cells that are no longer required, have been damaged, or are infected (Lam, 2004). Studies on plants have shown the involvement of PCD in a plethora of processes such as the differentiation of the tracheary elements

(TEs), root cap shedding, aleurone development, trichome development, anther dehiscence, leaf morphogenesis, systemic resistance, and the hypersensitive response (HR; Figure 1; Fukuda, 2000, Wang et al., 1996).

1.2 Types of PCD

1.2a Apoptosis

One of the best studied examples of PCD is apoptosis which is a term used to group animal cells undergoing cell death that exhibit cellular shrinkage, chromatic condensation, DNA nucleosomal fragmentation, and plasma membrane blebbing (Vaux & Korsmeyer, 1999). These physiological steps end with the formation of apoptotic bodies; particles containing condensed cytosol and tightly packed organelles that are to be cleaned out by phagocytic macrophages (Elmore, 2007). Unlike apoptosis, the remnants of plant PCD do not appear to be engulfed by adjacent cells as they generally remain trapped within the confinement of the cell wall (Lam, 2004). In fact, several physiological types of PCD have been characterized in plants that, despite sharing physiological components with animal PCD, have unique features (Vaux & Korsmeyer, 1999).

1.2b Senescence

Senescence is age-dependent and usually takes longer than other types of PCD. During plant senescence, large sections of tissue are compromised, such as in the leaf senescence of perennial plants that allows for the coordinated foliage color changes in the fall (Lim et al., 2007). During leaf senescence, a dramatic metabolic switch takes place in which photosynthesis is replaced by the dismantling of the chloroplasts,

accompanied by the synthesis and mobilization of lipids, carbohydrates, and proteins (Lim et al., 2007). Nutrients salvaged during the chloroplast breakdown lead to the formation of droplets rich in lipids called plastoglobuilli (Figure 1). During most of senescence, however, organelles like mitochondria and nuclei are retained, indicating that senescent cells remain functional for the proper coordination of nutrient recycling. In the later stages of plant senescence vacuolar collapse, chromatin condensation, and DNA laddering are commonly observed (Cao et al., 2003, Lim et al., 2003, Simeonova et al., 2000).

1.2c Vacuole-mediated PCD

A typical example of plant PCD involving the destruction of the vacuole is the differentiation of tracheary elements (TEs; Fukuda, 2000, Lam, 2004). A type of conductive tissues in plants, TEs comprise tracheids and vessel members, both of which are hollow tubes used in the transport of water in the xylem (Fukuda, 2000). A good model for plant PCD study has been the TE formation model Zinnia which has allowed for the study of PCD *in vivo* using undifferentiated cells (Fukuda, 2000). During TE formation in Zennia cells, the vacuole swells and accumulates a hydrolytic cocktail of cysteine proteases, aspartate proteases, and nucleases (Fukuda, 2000). Meanwhile, secondary cell walls are deposited forming the reticulated structure that will serve as the scaffolding structure for the xylem once the cell dies (Lam, 2004). Finally, DNA fragmentation occurs followed by the collapse of the vacuole (Groover et al., 1997). The collapse of the vacuole causes the degradation of single-membrane organelles (i.e. Endoplasmic reticulum, Golgi) followed by the degradation of double-membrane

organelles (i.e. mitochondria, chloroplasts; Groover et al., 1997). The hydrolytic components of the vacuole can either be released to the cytosol by the collapse of the vacuole membrane or they can be released to the apoplast as a result of the fusion of the vacuole with cell membranes (Hara-Nishimura & Hatsugai, 2011). Unlike other types of plant PCD, no chromatin condensation is observed during the formation of tracheary elements (Fukuda, 2000, Lam, 2004). Other examples of this type of cell death include the death of the endosperm and the aleurone layer (Kuo et al., 1996).

1.2d Hypersensitive Response (HR)

HR is a rapid and localized type of plant PCD that takes place during the resistance response to pathogen infections (Figure 1). The purpose of HR is to contain the spread of the pathogen and block its access to plant nutrients (Coll et al., 2011, Dangl & Jones, 2001, Greenberg & Yao, 2004). This type of cell death was first described by H. Marshal Ward in 1902 using wheat cultivars and the fungal leaf rust caused by members of the *Puccinia* genus (Coll et al., 2011) and in 1915 the term hypersensitivity was used by Elvin Stackman who observed the quick cell death that takes place in resistant cereals exposed to rust fungi (Mur et al., 2008, Stakman, 1915). In all HR responses observed cell death is confined to a defined area that has come in contact with the pathogen and a sharp limit is established between cells that are dying and cells that are to remain alive (Mur et al., 2008).

Despite the plasticity in physiological plant HR responses some histological features appear to be shared with forms of animal PCD such as chromatin condensation, cytochrome c release, endonucleolytic cleavage, cytoplasmic shrinkage, and

mitochondrial swelling while having unique characteristics such as the collapse of the vacuole, the disruption of the chloroplasts, and the lack of apoptotic body formation (Mur et al., 2008). Cells undergoing HR usually shrink with a concomitant drop in cytoplasmic mobility due to the depolymerization of the cytoskeleton (Shimmen & Yokota, 2004). However, the occurrence of chromatin condensation and nucleolytic cleavage appears to depend on both the host and the type of pathogenic interaction as both phenomena are not observed in all HR responses (Mur et al., 2008).

Being 1.5 billion years apart from animals (Wang et al., 1999), it is clear that plants have evolved unique cell death programs with features that share no perfect homology to metazoan PCD programs. This can be seen in the great variety of mechanisms described in this section and the subtle differences observed even within similar types of plant PCDs. The classification of plant PCD based on histological features is useful in the characterization of cell deaths and the study of conserved mechanisms. However, it is hindered by the lack of information in the regulatory components and the molecular elements involved. The mechanisms involved in the regulation of HR are linked to the way plants interact with the pathogens that attack them. The molecular components of HR as well as the plant pathogen interactions will be reviewed in more detail as they constitute the framework for this dissertation.

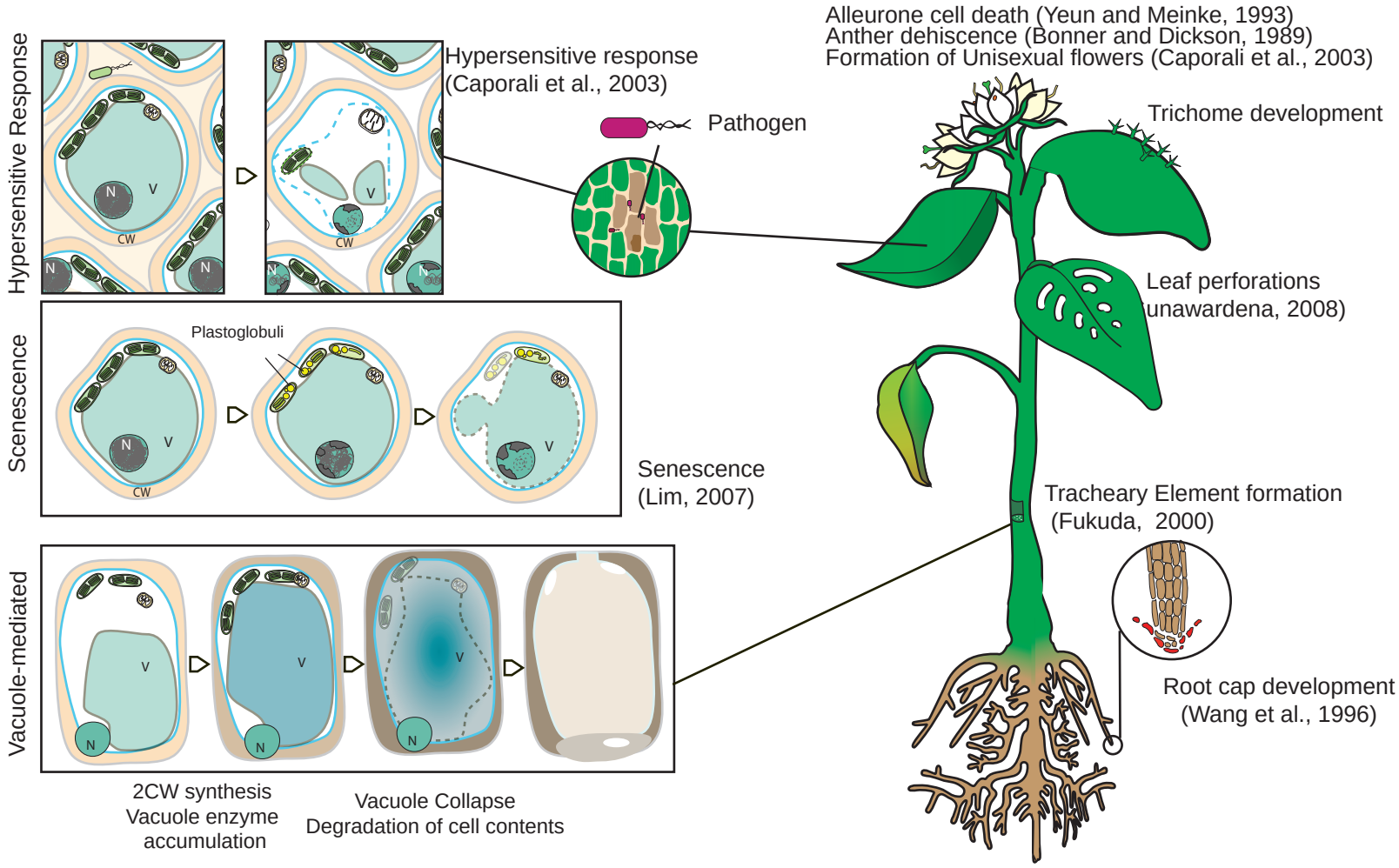

Figure 1. Physiology and function of PCD in vascular plants. PCD in plants takes place during several developmental stages and in response to biotic and abiotic stimuli. V. Vacuole, N. Nucleus, CW, Cell Wall. See text for details. This figure was adapted from (Coll et al., 2011; Greenberg and Yao, 2004b; Lam, 2004; Pennell and Lamb, 1997)

1.3 Plant pathogen interactions

Like their animal counterparts, plants are constantly challenged to identify and respond to organisms that are detrimental to their fitness such as pathogens and herbivores and beneficial organisms such as symbionts, altogether while discerning them from their own cells. However, unlike animals, plants lack immune specific components such as phagocytes, leukocytes, and antibodies, perhaps because of their unique circulatory system and the sessile nature of their cell-wall encased cells (Nürnberger et al., 2004, Ronald & Beutler, 2010, Sanabria et al., 2008, Zipfel & Felix, 2005). Despite these evident physiological differences plants and animals have independently evolved strikingly similar defense strategies (Ronald & Beutler, 2010). Like animals, plants have two primary mechanisms of defense: a pathogen triggered immunity (PTI) and an effector-triggered immunity (ETI; Dangl & McDowell, 2006, Jones & Dangl, 2006, Sanabria et al., 2008).

1.4 Pathogen-triggered immunity (PTI)

Similar to innate mammalian immunity, plants have a basal line of defense that involves the recognition of highly conserved pathogen- or microbial-associated molecular patterns (PAMPs, MAMPs; Jones & Dangl, 2006). Uniquely microbial, PAMPs are highly conserved structural motifs used by plants to identify the presence of foreign biological elements that may be potentially pathogenic. Some examples include the fungal cell wall protein chitin or the bacterial lipopolysaccharide, elongation factor Tu (EF-Tu), and the flagellum component flagellin (Sanabria et al., 2008). A plethora of PAMPs from bacterial, fungal, and viral pathogens have been identified and include

peptides, proteins, lipids, glycoproteins, and oligosaccharides (Erbs et al., 2008, Felix & Boller, 2003, Lochman & V, 2006, Schuhegger et al., 2006, Silipo et al., 2008, Tang et al., 2012). This diversity of molecules indicates that plants must have a versatile and extensive detection mechanism to cope with the number of eliciting molecules and activate the appropriate responses (Nürnberger et al., 2004).

1.4a Receptors involved in PTI

PAMPs receptor proteins (PRRs) are usually transmembrane receptors with an extracellular ligand binding domain and may contain an intracellular kinase domain (Figure 2). The presence of the cytosolic kinase can help divide PRRs into receptor-like kinases (RLKs) which contain a cytosolic kinase domain, and the receptor-like proteins (RLPs) which lack it (Fritz-Laylin et al., 2005). An additional type of receptor can be found directly bound to the cell wall. These receptors are referred to as polygalacturonase-inhibiting proteins (PGIP) and are capable of binding and inhibiting the action of polygalacturonases produced by pathogens (Chisholm et al., 2006). Leucine-rich repeats (LRR) are often found in the extracellular PAMP binding domains of PRRs and PGIPs because of their versatility in binding diverse molecules such as proteins, lipids, glycans, and nucleic acids (Beutler, 2009). However, other PAMP binding mechanism might exist such as the S-domain containing RLKs that are induced during defense responses but for which no PAMPs have yet been identified (Fritz-Laylin et al., 2005). A genomic analysis of *Arabidopsis thaliana* indicates it has over 200 RLKs containing LRR domains (Shiu & Bleecker, 2003). This vast number of receptors suggests evolutionary pressure may have caused this group to expand in order

to allow plants to recognize different pathogens and modulate specific responses accordingly.

1.4b FLS2: a case study

The fine tuning and regulation of PRR triggered signaling can also involve the oligomerization of receptors providing "adaptor" components that integrate pathogen responses (Sanabria et al., 2008). The complexity of this multi-protein recognition system is illustrated by the flagellin receptor flagellin-sensing 2 (FLS2; Gomez-Gomez & Boller, 2000, Zipfel et al., 2006). FLS2 is an LRR-RLK that, upon binding flagellin, forms a complex with Brassinosteroid Associated Kinase 1 (BAK1; Chinchilla et al., 2007). BAK1, a member of the SERK (Somatic Embryogenesis Receptor Kinase) family of LRR-RLKs, was originally described for its role in the signaling of the plant hormone brassinosteroid and most likely works as an adaptor of, in this particular case, convergent PAMP and hormone signaling (Lu et al., 2010). Recently, the BAK1/FLS2 complex has been shown to oligomerize with additional SERKs, suggesting PAMP receptors operate in multimeric complexes (Segonzac & Zipfel, 2011). The complex formed by BAK1 and FLS2 interacts with BIK1 (Botrytis-induced kinase 1), a protein involved in the response to necrotrophic fungal pathogens. BIK1 is an RLK that lacks any extracellular domain and is likely to remain in the cytosol where it mediates PTI signal transduction (Figure 3, Lu et al., 2010). The interconnection of hormone signaling and the defense responses against fungal and bacterial pathogens, is becoming a common feature in plant immunity studies and demonstrates the complexity of the responses plant utilize to

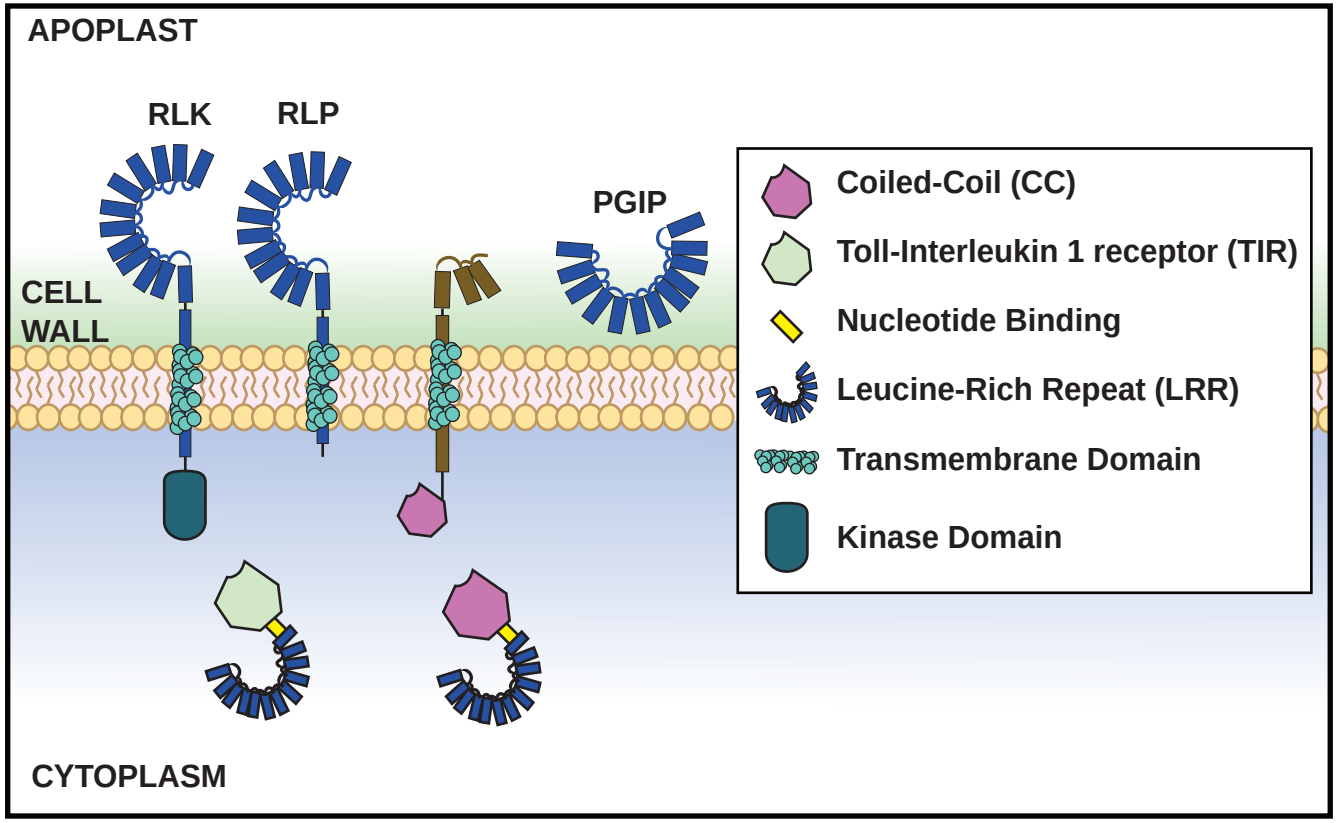

Figure 2. Receptors involved in plant immunity. Plants have receptor proteins to identify potentially pathogenic microorganisms. These receptors can be cytosolic, membrane-bound, or extracellular. The cytosolic nucleotide-binding leucine-rich repeat (NB-LRR) containing receptors are some of the most abundant. Members of this group contain either amino-terminal coiled-coil (CC) or Toll-Interleukin 1 receptor (TIR) domains. Membrane bound receptors can be RLKs (Receptor-like kinases) and RLPs (Receptor-like proteins); LRR containing proteins that may have or lack an intracellular kinase domain respectively. Finally, a group of LRR-containing proteins can be found in the cell wall. These proteins known as Polygalacturonase-inhibiting proteins (PGIPs) are involved in blocking polygalacturonases produced by pathogens. Image adapted from Chisholm et al., (2006).

successfully counteract a pathogenic infection (Figure 3). Interestingly, animal PRRs Toll and Toll-like receptor 5 (TLR5) are also capable of binding flagellin, despite sharing little sequence similarity with the flagellin binding LRR of FLS2 (Hayashi, 2001) However, FLS2 is capable of triggering responses by binding a 22 amino acid stretch in flagellin (flg22) that does not elicit a response in TLR5.The differences between FLS2 and TLR5 amino acid sequence and the differential binding of flagellin peptides suggest that animal and plant basal recognition systems are the outcome of convergent evolution (Nürnberger et al., 2004).

1.4c PTI responses

Activation of PRRs leads to a rapid depolarization of the plasma membrane caused by an influx of Ca^{++} ions into the cytosol which is required for the activation of calcium-dependent protein kinases and the production of reactive oxygen species (ROS) (Jeworutzki et al., 2010). Upon detection of a PAMP, PTI is activated and with it, by poorly understood mechanisms, responses such as: stomatal closure, MAP kinase activation, cell wall thickening by callose deposition, programmed cell death (PCD), and systemic acquired resistance (SAR); a mechanism by which hormone signaling activates defense responses in uninfected areas of the plant (Asai et al., 2002, Melotto et al., 2006, Navarro et al., 2004). PTI responses may be coordinated in part by the activation of the zinc-finger containing WRKY transcription factors. In *A. thaliana* for instance the WRKY gene family contains 74 members, and the expression of more than 70% of them appears to be affected by pathogen-induced responses (Eulgem et al., 2000).

1.5 Effector proteins: pathogens strike back

Phytopathogenic organisms have developed mechanisms to interfere with the host's defense signaling altering its metabolism by targeting host cell proteins or DNA (Grant et al., 2006). This highly specialized set of biochemical tools include effector proteins; molecules that are secreted by the pathogen and often delivered directly into the host's cells (Chisholm et al., 2006, Jones & Dangl, 2006). For instance, phytopathogenic gram negative bacteria deliver effector proteins directly into plant cells using the type III system (TTSS) which forms an injectosome-like structure spanning into the host cell membrane and allowing for the controlled transfer of proteins without exposing the cell to the extracellular milieu (Abramovitch & Martin, 2005). Biotrophic fungi on the other hand, don't appear to have a TTSS and most likely rely on the haustorium, a pathogenesis structure that is in intimate contact with the cell membrane to the deliver effectors that primarily remain apoplastic or may enter the cell by a yet uncharacterized mechanism (Chisholm et al., 2006).

1.5a Effector mechanisms of action

Effector repertoires can be quite diverse in function and number varying among pathogens of the same host and even within strains of the same pathogen. For instance the tomato (*Solanum lycopersicum*) pathogens *X. campestris pv vesicatoria* and *Pseudomonas syringae pv tomato* (*Pst*) DC3000 have 17 and 28 confirmed effector proteins each of which only three are homologous in both species (Chang et al., 2005).

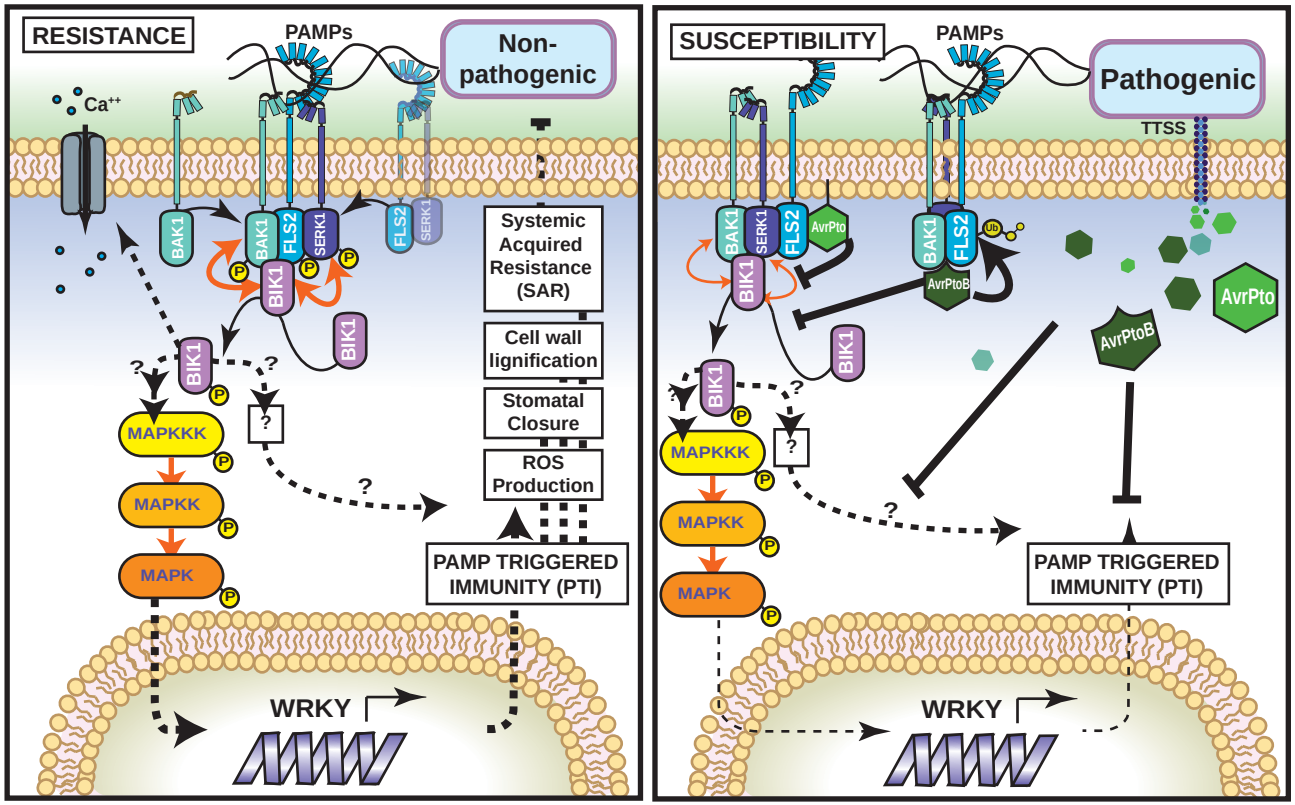

Figure 3. Resistance and susceptibility in plant pathogen interactions. Left. Perception of Pathogen-associated molecular patterns (PAMPs) such as the flagellum component flagellin by the receptor-like kinase (RLK) FLS2 triggers the activation of Pathogen-triggered immunity (PTI). Upon perception of flagellin FLS2 rapidly forms a complex with BAK1 and BIK1, and potentially SERKs. The FLS2/BAK1/BIK1 complex triggers a series of trans- and auto-phosphorylation events (orange arrows) to transmit the signal, by yet uncharacterized mechanisms, into the nucleus. Upon phosphorylation BIK1 is released from the complex. PTI activation involves a MAPK phosphorylation cascades, Ca^{++} influx into the cytosol, and the induction of WRKY gene transcription. PTI responses activated by this mechanism include: cell wall lignification, stomatal closure, and systemic acquired resistance (SAR). Right. Pathogenic bacteria inject effector proteins (depicted in green) into the cytosol using a type III secretion system (TTSS) injectosome. Effectors interfere with the establishment of PTI. For instance, AvrPto and AvrPtoB interfere with FLS2 signalling by interfering with the recruitment of BIK1 and phosphorylation, as well as by ubiquitinating FLS2 and potentially targeting it to 26S-proteasomal degradation. Adapted from Chisholm et al., (2006) and Zegonzac and Ziepfel (2011).

Strikingly, the *Pst* strains DC3000 and T1, both causative agents of the tomato bacterial speck disease, share only half of their effector proteins (Collmer et al., 2009). Studying effector proteins and their targets is fundamental to understand how a particular plant-pathogen interaction takes place, in terms of the type of defense responses that are activated as well as the metabolic pathways affected by the pathogen. One of the first bacterial effector proteins for which a target was identified was the *Pst* effector HopM1. HopM1 functions by binding the *A. thaliana At*MIN7; a protein with important roles in defense responses and localized in the trans-Golgi network/early endosome (TGN/EE) (Nomura et al., 2006, Nomura et al., 2011). HopM1 mimics an ubiquitin ligase and ubiquitinates *At*MIN7 targeting it to 26S mediated degradation (Nomura et al., 2006). In the absence of *At*MIN7, plants are hyper susceptible to infection by *Pst* as plants are impaired in their ability to establish a successful defense response (Nomura et al., 2011). This targeted degradation of a host protein involved in immunity signaling is part of the strategy in which bacterial proteins mimic eukaryotic functions; ubiquitination in this particular case. Despite recent advances in our understanding of a few of the mechanisms by which effector proteins hijack the host's defenses and metabolism, studies of the effector protein role in pathogenesis are still challenged by effector abundance, the difficulty in identifying their targets, and their lack of homology with known proteins or conserved catalytic domains (Grant et al., 2006).

1.5b Effector triggered immunity (ETI)

Effector proteins can efficiently blind the plant's basal immunity; with no means to counteract the effect of effector proteins a plant is doomed to fall victim of infection. To counteract this apocalyptic scenario, plants possess a mechanism to recognize effector proteins and activate a quick set of defense mechanisms known as effector-triggered immunity (ETI; Jones & Dangl, 2006)

1.5c ETI responses

ETI can rapidly activate defenses, some of which overlap with those triggered by PAMP perception (Delaney, 1997, Sanabria et al., 2008). For instance, both responses involve the development of systemic acquired resistance, which induces defenses in uninfected regions in the plant (Mishina & Zeier, 2007). Additional R-triggered responses include rapid alkalinization of the extracellular space, influx of calcium ions, production of reactive oxygen intermediates and nitric oxide, changes in transcription, and HR (Dangl & McDowell, 2006, Greenberg & Yao, 2004)

1.5d ETI receptors

The recognition of effector proteins relies on a set of intracellular receptors characterized by containing a C-terminal LRR domain with central nucleotide binding domains (NB-LRR), and sometimes an N-terminal domain that can be either a coiled-coil domain (CC) or similar to the effector domains of *Drosophila melanogaster* and human Toll-and interleukin-1 receptor (TIR) domains (Hammond-Kosack & Jones, 1997; Figure 2). Plant NB-LRRs directly bind and recognize pathogen-derived effector molecules (DeYoung & Innes, 2006, Dodds, 2006) or indirectly by forming complexes

with intermediate plant proteins. These plant proteins can either be the direct target of the effector proteins or decoys (Coll et al., 2011, DeYoung & Innes, 2006). These different effector recognition mechanisms have lead to the proposal of the gene-for-gene, guard, and decoy models (van der Hoorn & Kamoun, 2008).

1.5e The gene-for-gene model

The genetics of ETI were first genetically described by Flor in 1955. Using resistant and susceptible varieties of flax to the rust disease pathogen *Melampsora lini*, Flor observed that resistance depended on a system in which the presence of a matching pair of genes in both the pathogen and the host were required. This observation lead to the widely accepted proposal of a "gene-for-gene" resistance model in which plants depend on a particular resistance (R) gene to counteract infection only, if the pathogen carries a matching avirulence (Avr) factor, named this way because hosts carrying it are unable to cause disease and are therefore avirulent. (Abramovitch & Martin, 2004, Bent & Mackey, 2007, Takken et al., 2006). Molecular characterization of this system has revealed that some Avr gene products are indeed effector proteins that can be recognized directly by R-proteins. For instance, the rice blast fungus (*Magnaporthe grisea*) effector AVR-Pita directly interacts with the LRR-like domain of the R gene Pi-ta (Jia et al., 2000) and the *A. thaliana* RRS1(Resistance to *Ralstonia solanacearum* 1) directly interacts with the effector protein PopP2 of the bacterial wilt pathogen *Ralstoni solanacearum* (Deslandes, 2003).

In evolutionary terms, plants and pathogens are engaged in a red queen theory evolutionary model, in which pathogens are under constant selective pressure to evolve

modifications in Avr genes to avoid detection by R-proteins, while preserving their pathogenic nature. Similarly, plants are constantly evolving R-proteins to keep up with the new forms of Avr proteins developed by the pathogen (Toft & Andersson, 2010).

1.5f The guard hypothesis

The limited number of R-genes, however, fails to explain the ability plants have to detect the immense number of pathogenic effector molecules (DeYoung & Innes, 2006). To reconcile this limitation, a recognition system was characterized in which plant NB-LRR can detect the modifications caused by effector proteins on their plant targets (Dangl & Jones, 2001, Van der Hoorn et al., 2002). This model, known as the guard hypothesis, allows for the monitoring of individual plant proteins targeted by multiple effector molecules. Consequently, one R gene to recognize multiple Avr proteins simultaneously (Coll et al., 2011, DeYoung & Innes, 2006, Van der Hoorn et al., 2002). A classical example that has been used in support of the guard hypothesis, is the ETI initiated by the *A. thaliana* NB-LRR RPM1. RPM1 confers resistance to the *P. syringae* effector proteins AvrPm1 and AvrB (Debener et al., 1991, Mackey et al., 2002). However, direct interaction of RPM1 with any of these Avr proteins has not been demonstrated (DeYoung & Innes, 2006). Instead, RPM1 was found to interact with the plant protein RIN4 (RPM1-interacting protein 4), which is a phosphorylation target of both AvrPm1 and AvrB (van der Hoorn & Kamoun, 2008). The modifications caused on RIN4 by the Avr proteins are detected by RPM1, which triggers ETI (Mackey et al., 2002). This indirect mechanism of activation has also been refer to as a 'bait and switch', in which RPM1 acts as an inactive switch that becomes activated by the bait

RIN4 when it is modified by Avr proteins (Block & Alfano, 2011, Collier & Moffett, 2009). The guard hypothesis implies, however, that the guarded molecules (guardees) are involved in regulating plant defenses (Van der Biezen & Jones, 1998). So far, it is not completely known if RIN4 is the primary target of the virulence caused by AvrRpm1 or AvrB, as these effectors can still enhance virulence in its absence (Lim & Kunkel, 2004). Similar observations with guarded molecules have lead to the proposal of a modified guard hypothesis known as the decoy hypothesis (van der Hoorn & Kamoun, 2008).

1.5g The decoy hypothesis

The decoy hypothesis states that guardee molecules act as decoys that resemble the original virulence targets of effector molecules, but do not functionally resemble the guarded molecule (van der Hoorn & Kamoun, 2008). This way, plants are able to bypass the bidirectional evolutionary pressure imposed by the targeting by bacterial virulence effectors and the defense function they perform in the plant (Collier & Moffett, 2009, van der Hoorn & Kamoun, 2008). A case for the decoy hypothesis has been made with the *Pst* effectors AvrPto and AvrPtoB, which will be explored in greater detail in the following section as it serves as an introduction to the proteins studied in this dissertation.

1.6 The AvrPto/AvrPtoB and Pto/Prf model

The tomato bacterial speck disease is caused by *Pst* and it affects leaves and fruits causing economic losses by decreasing yields and rendering the tomatoes unmarketable (Jones, 1991). The identification of a resistant variety of tomato in the late

1970s (Abramovitch & Martin, 2004, Ptiblado & Kerr, 1980), along with the genetic and molecular amenability of both pathogen and host, has led to the identification of key genes and their role in the development of resistance or disease in this model system (Pedley & Martin, 2003).

The study of the tomato R-genes Pto and Prf and their ability to trigger defense responses against Pst strains carrying the effector genes AvrPto or AvrPtoB has been one of the most discussed and studied examples of plant resistance (van Ooijen et al., 2007).

1.6a AvrPto and AvrPtoB virulence targets

AvrPtoB has two N-terminal kinase interacting domains capable of binding FLS2 and Bti9/chitin elicitor receptor kinase 1 (CERK1) which is a component of fungal chitin detection system (Gimenez-Ibanez et al., 2009, Zeng et al., 2012). In both situations AvrPtoB interferes with the defense signaling activated by these two PPRs. AvrPtoB also has a C-terminal ubiquitin ligase domain that, like HopM1 imitates ubiquitin ligases and targets FLS2 for degradation (Gohre & Robatzek, 2008). Remarkably, AvrPtoB exhibits striking structural similarity to eukaryotic ubiquitin ligases despite sharing no sequence homology (Janjusevic et al., 2006).

AvrPto is targeted to the plasma membrane by the N-terminal addition of myristate and palmitate, where it acts as a kinase inhibitor of both PPRs FLS2 and the elongation factor Tu receptor (EFR) preventing signaling by interfering with their autophosphoporylation activity (Xiang et al., 2008). Interestingly, despite being recognized by Pto, both AvrPto and AvrPtoB are structurally unrelated highlighting an

interesting evolutionary constrain to the recognition of two unrelated effectors by an individual R-protein (Mucyn, 2006).

1.6b AvrPto and AvrPtoB recognition models, gene-for-gene, guard, or decoy?

Originally described as an example for the gene for gene model, the absence of both AvrPto and AvrPtoB in strains of *Pst* blocks the plant's ability to recognize the pathogen (Lin & Martin, 2007). Likewise, mutations affecting either one of the plant R-encoding genes, Pto or Prf, render the effector proteins from *Pst* undetectable, enabling AvrPto and AvrPtoB to fulfill their role as virulence facilitators by manipulating PAMP-triggered responses.

Pto is a myristoylated Ser/Thr kinase that physically interacts with either AvrPto and AvrPtoB (de Vries et al., 2006, Pedley & Martin, 2003) whereas Prf has the typical R-protein structure; it has the CC and NB-LRR domains, in addition to a non-conserved N-terminal domain (Oldroyd & Staskawicz, 1998).

The role of Prf and Pto in defense signaling has puzzled researchers given their lack of identifiable function. Recent evidence suggests Pto forms a complex by interacting with the non-conserved N-terminus of Prf (Mucyn, 2006). The interaction of Pto with an NB-LRR molecule resembles the regulatory components that follow the guard hypotheses. In this particular case, Prf acts as the guard of Pto, which upon the disturbance caused by AvrPto/AvrPtoB, triggers ETI (Mucyn, 2006). However, some observations do not support the guard model. For instance, Pto does not appear to act as PTI-related protein, since its removal does not confer an advantage to the pathogenesis caused by *Pst* strains carrying AvrPto (Chang et al., 2000). Also, Pto is not present in

susceptible cultivars, making it an unlikely conserved guarded target involved in basal defense (Mucyn, 2006, van der Hoorn & Kamoun, 2008) Furthermore, the AvrPtoB domain that interacts with the basal defense target CERK1 also binds Pto (Cheng et al., 2011, Gimenez-Ibanez et al., 2009, Zeng et al., 2012), similarly, the AvrPtoB domain that interacts with BAK1and suppresses PTI, interacts with Fen; a Pto-related allele (Abramovitch et al., 2003, Jia et al., 1997, Rosebrock, 2007). These observations suggest that Pto and Fen act as decoys of the PTI elements BAK1 and CERK, and the defense responses activated are dependent on Prf (van der Hoorn & Kamoun, 2008).

Until recently, the mechanisms by which Prf-mediated signaling was activated by the formation of AvrPto/AvrPtoB – Pto complexes, remained largely speculative. Recent evidence has lead to the proposal of a model in which Pto functions as an inhibitor of Prf activity, by binding its N-terminus (Oh & Martin, 2011). Such inhibition is released when Pto binds AvrPto. This binding inhibits Pto kinase activity, but this appears to be a remnant of AvrPto function inhibiting the kinase activity of PAMP receptors, rather than the direct mechanism of activation of Prf-mediated ETI (Xing et al., 2007). Instead, structural studies indicate that, by binding AvrPto, Pto undergoes a conformational change that leads to the release of Prf (Xing et al., 2007).

The precise function of Prf as a defense activator is not yet known. However, it has been proposed that the release of Prf by Pto, relieves the inhibition of the Prf NB-domain that, in NB-LRR proteins, appears to be inhibited by the LRR domain (Collier & Moffett, 2009). Once activated, Prf is able to interact with yet to be identified downstream signaling components involved in ETI activation (Du et al., 2012).

In conclusion, the kinase Pto, acting as either a guarded molecule or a decoy, keeps Prf in an inhibited state. This inhibition is disrupted by a conformation change on Pto, caused by the binding of AvrPto or AvrPtoB, followed by the release of Prf which causes the activation of ETI (Oh & Martin, 2011).

1.6c Activation of downstream signaling

In an effort to understand the signaling components involved in ETI activation, several Pto interacting partners (Pti) have been identified using yeast two hybrid screens (Zhou et al., 1995). One of these proteins, Pti1, can induce HR when over expressed even in the absence of the effector AvrPto, suggesting that it acts downstream of Pto (Sessa et al., 2000, Zhou et al., 1995). However, it is not clear whether this kinase plays a role in pathogen induced HR, and the role of this and other Pti proteins in plant defenses is not known (Gu, 1998). Given that Pto could act as a decoy for AvrPto/AvrPtoB target receptors, it is possible Pti molecules are not biological substrates of Pto, but instead natural substrates of its guarded molecules.

1.6d AvrPto-dependent Pto-interacting proteins

An alternative signaling mechanism is presented by the identification of proteins that interact with Pto in an Avr-dependent way (Adi proteins). Using a yeast three-hybrid screen five proteins were identified: the catalase Adi1, the Ser/Thr kinases Adi2 and Adi3, a truncated proteasome α-subunit Adi5, and a protein with no conserved homology Adi4 (Bogdanove & Martin, 2000). The study of Adi3 has revealed it negatively regulates AvrPto-Pto mediated cell death. Understanding Adi3 function might

provide tools for devising the molecular mechanisms underlying cell death triggered during a susceptible and resistance pathogenic interaction.

1.7 AGC kinases

Phosphorylation is one of the most ubiquitous eukaryotic postranslational modifications; its reversible nature integrates stimuli to generate regulatory networks in which protein localization, activity, and interaction with other proteins is altered (Manning et al., 2002). The complexity of the regulatory networks involving phosphorylation is illustrated by the number of kinases that, in *A. thaliana* for instance, can be as many as 1,000 (Bögre et al., 2003). These kinases are classified into several groups, for instance: receptor-like kinases, cyclin-dependent kinases (CDKs), Calcium dependent protein kinases (CDPKs), the Snf1-related protein kinases (SnRK), and mitogen-activated protein kinases (MAPK), and the AGC group of kinases which comprises cAMP-dependent protein kinases (PKA), cGMP-dependent protein kinase (PKG), phospholipid dependent protein kinases (PKC), and protein kinase B (Bögre et al., 2003).

Members of the metazoan AGC family of kinases play fundamental roles in processes as diverse as growth, metabolism, protein synthesis, gene transcription, and apoptosis (Bögre et al., 2003, Pearce et al., 2010) Plant AGC kinases on the other hand, have been poorly studied and their function is not as well understood as their mammalian counterparts (Hirt et al., 2011). Mutagenesis and expression analysis indicate plant AGC kinases are involved in processes such as the transport of the plant

hormone auxin (PINOID), phototropism (PHOT1/2), pollen tube growth (AGC1.5), root hair growth (AGC1.6), and stress responses (OXI1, Adi3; Zhang & McCormick, 2009).

1.7a AGC kinase regulation

A common feature of AGC kinases is their ability to translate signals derived from messengers such as cAMP, cGMP, lipids, and Ca^{++} (Zhang & McCormick, 2009). Furthermore, a subset of plant AGC kinases appears to be regulated by the upstream phosphorylation by the 3-phosphoinositide dependent kinase-1 (Pdk1; Vivanco & Sawyers, 2002). PDK1 is a highly conserved eukaryotic Ser/Thr kinase that, in animals, responds to the production of the signaling phospholipid phosphatidylinositol 3,4,5-triphosphate (PIP3) and localizes to the membrane aided by a pleckstrin homolgy (PH) domain where PDK1 phosphorylates its targets. In plants, activation of PDK1 might rely on other phospholipids, such as PtdIns3, PtdIns $(4,5)P_2$, and PtdIns $(3,4,5)P_3$, but not PIP3, as plants lack the ability to produce PIP3 Kinases and thus cannot produce it (Deak et al., 1999, Munnik & Testerink, 2009). Animal and some plant AGC kinases rely on a hydrophobic motif named PIF (PDK1-interacting fragment) to interact with PDK. Upon interaction PDK1 phosphorylates a residue in the activation region known as the T-Loop extension. This residue can be either a Thr in animals or a Ser in plant AGC kinases (Anthony et al., 2004).

1.7b Adi3

Adi3 shares structural and functional features with the mammalian AGC protein kinase B (PKB; also known as AKT), which is an important negative regulator of mammalian apoptosis (Vivanco & Sawyers, 2002). Adi3 belongs to the group VIIa of

plant AGC kinases and is characterized by containing a large (74 amino acids) T-Loop extension, a conserved DFG motif for Mg++ binding and a C-terminal PDK-interacting fragment known as the PIF motif (Devarenne et al., 2006; Figure 4). Adi3 appears to work upstream of MAPKKKs cell death-inducing cascade signaling (Devarenne et al., 2006). Downregulation of Adi3 expression in tomato plants using virus-induced gene silencing promotes the appearance of spontaneous cell death lesions in leaves and stems suggesting that it is, like PKB, a negative regulator of PCD (Devarenne et al., 2006).

Furthermore, overexpression of Adi3 promotes cell survival and decreases the PCD triggered by Pto signaling (Devarenne et al., 2006, Ek-Ramos et al., 2010). In animals, PKB negatively regulates apoptosis by posphorylation and inactivation of proapoptotic factors such as BAD and activation of antiapoptotic factors such the IκB kinase (IKK; Devarenne et al., 2006, Vivanco & Sawyers, 2002). As opposed to PKB, neither the mechanisms by which Adi3 regulates cell death nor its substrates are known. Since Adi3 is unable to phosphorylate an artificial PKB substrate and mammalian apoptosis shares no perfect homology to plant PCD, its substrates might differ from those of PKB (Devarenne et al., 2006).

1.7c Models for Adi3 role in pathogenesis and resistance

It has been proposed that in uninfected plants is Adi3 is activated by phosphorylation of the T-loop Ser539 by PDK and subsequently transits into the nucleus (Ek-Ramos et al., 2010; Figure 5). Nuclear shuttling of Adi3 depends on both a nuclear localization signal present in its activation loop and a nuclear export signal close to its N-terminus (Ek-Ramos et al., 2010; Figure 4). The Adi3 phosphorylation at Ser539

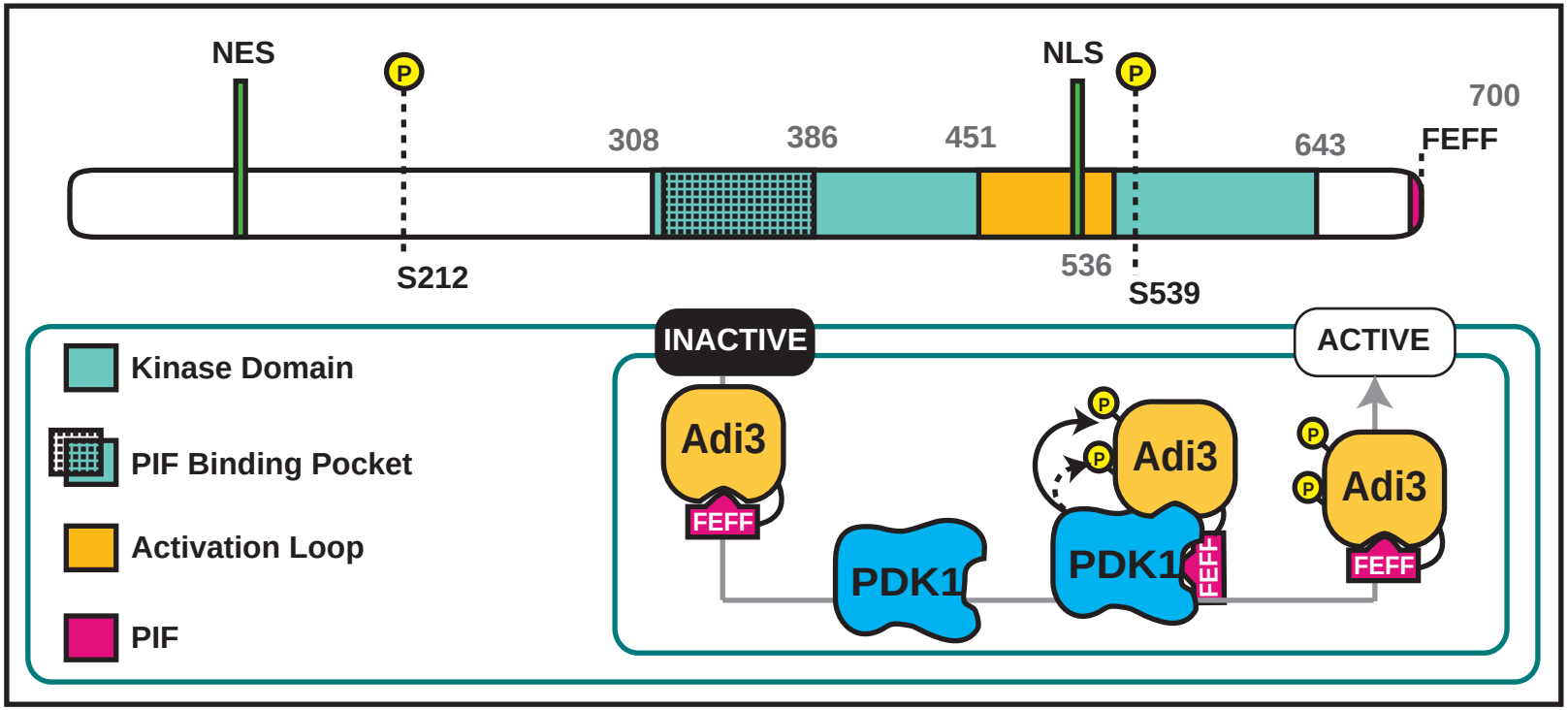

Figure 4. Adi3 features and activation model by PDK1. The PDK1-interacting fragment (PIF) located at the C-terminal end of Adi3 comprises the hydrophobic residues FFEF. Both Adi3 and PDK1 contain a PIF binding pocket. During interaction with PDK, the PIF domain leaves the binding pocket in Adi3 and is docked within the PIF-binding pocket in PDK1(Biondi, 2004). Next Adi3 is activated by PDK via phosphorylation at Ser539. Recently, Ser212 has been characterized as a potential second phosphorylation site of Adi3 that matches the motif surrounding Ser539. The location of the phosphorylation sites, domains, and nuclear exportation and localization signals are shown. Numbers in grey represent approximate amino acid locations in the protein. Image adapted from (Devarenne, 2011; Ek-Ramos et al., 2010)

directs the protein to the nucleus where its cell PCD function manifests (Ek-Ramos et al., 2010). Likewise, mutations affecting the nuclear localization of Adi3 prevent its PCD suppressing activity and the protein localizes to punctate structures that appear to be part of the endosomal trafficking system (Figure 5). Similarly, activation of PKB by PDK1 at the plasma membrane causes its migration to the nucleus, where it prevents the execution of apoptosis by either phosphorylating or interacting with nuclear proteins (Ahn et al., 2006, Brunet et al., 1999, Lee et al., 2008, Masuyama et al., 2001).

In infected plants, Adi3 activation could be disrupted during ETI upon recognition of the AvrPto/Pto complex leading to Pto dependent signaling and HR. Alternatively, the interaction of the Adi3/Pto complex with the effector AvrPto suggests that Adi3 could be manipulated to control cell death by *Pst* similarly to the PKB inhibition by mammalian pathogens such as *Yersinia enterocolitica.* The *Y. enterocolitica* effector protein YopH interferes with the synthesis of PIP3 and thus, interferes with activation of PDK1 and subsequent phosphorylation of PKB (Devarenne et al., 2006, Sauvonnet et al., 2002). In an effort to understand the regulatory properties of Adi3 over cell death a Y2H screen using Adi3 as a bait and a cDNA library of *Pst* infected tomato revealed a set of interaction partners including a member of the SnRK family of kinases and an E3 ubiquitin ligase.

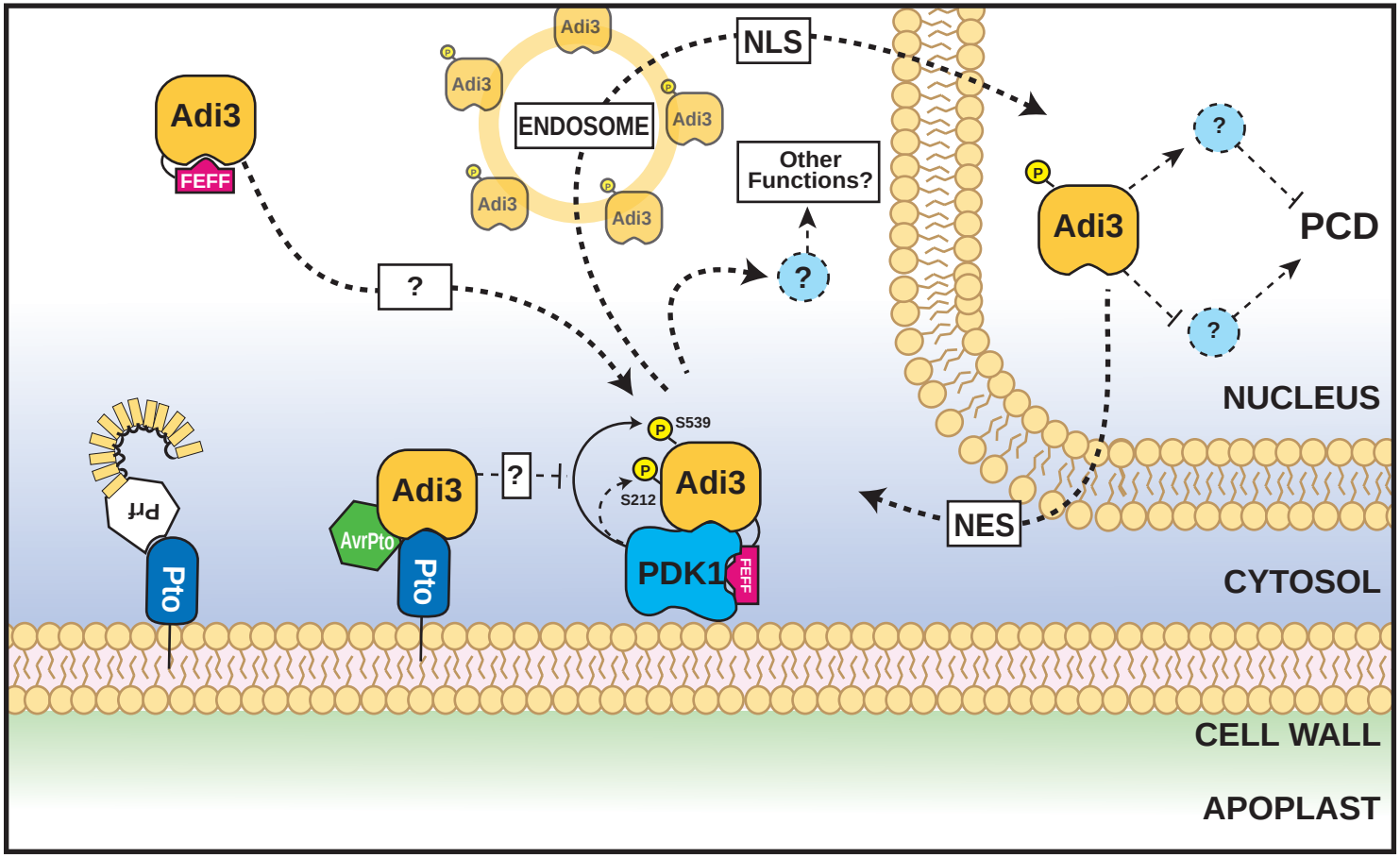

Figure 5. Model for Adi3 function. Tomato PDK1 phosphorylates and activates Adi3 which results in its relocalization to the nucleus. Removal of Adi3 nuclear localization signal (NLS) results in the accumulation of Adi3 in vesicles that appear to be part of the endomembrane system, and results in cell death induction. Therefore Adi3 PCD suppressing seems to require nuclear localization. During the response to *Pseudomonas syringae* infection, the complex formed by Pto/AvrPto and Adi3 is proposed to prevent Adi3 PCD-supressing activity by disrupting its ability to localize to the nucleus, potentially by preventing its phosphorylation by PDK. Dotted lines and question marks indicate hypotheses currently being investigated. Image adapted from Devarenne et al., (2006), Ek-Ramos et al., (2010).

1.8 The SnRK complex

Organisms must survey the metabolic status of a cell and respond the metabolic challenges that may arise, whether they are presented by developmental, environmental, or stress responses. One of the central players involved in this process is the eukaryotic Sucrose Non-fermenting (Snf1) kinase complex. Snf1 is a widely conserved Ser/Thr protein kinase that coordinates metabolic homeostasis and stress responses in eukaryotes. First identified in yeast (Carlson et al., 1981, Celenza & Carlson, 1986), homologues of the Snf1 complex have been identified in roundworms (AMP-Activated Kinase, AKK), mammals (AMP-activated protein kinase, AMPK) and plants (Snf1-related kinase, SnRK; Polge & Thomas, 2007). In all organisms where it has been characterized, Snf1 functions as a heterotrimer comprised of a catalytic α subunit and the non-catalytic γ and β subunits (Halford et al., 2000, Hardie et al., 1998). Organisms, have varying numbers of Snf1 subunit isoforms, which are used to regulate the multiple functions of the complex by both transcriptional as well as post-translational mechanisms (Hardie et al., 1998).

1.8a SnRK complex structure and regulation

SnRKs function as heterotrimeric complex that may contain different combinations of α, β, and γ isoforms. In mammals two α- (AMPKα1,α2), two β- (AMPKβ1/β2) and three γ- subunits (AMPKγ1, γ2, γ3) can be found (Steinberg & Kemp, 2009). Yeast, on the other hand, has one α- (Snf1), one γ- (SNF4), and three β- subunits (GAL83/SIP1/SIP2; Hardie et al., 1998). In addition to these genes, multiple alternate splice variants can be found for some of these subunits increasing the possible

combination of complexes variants (Steinberg & Kemp, 2009). In plants two α- subunits can be found in *A. thaliana* (AKIN10, AKIN11) and Tomato (*Sl*SnRK1.1, *Sl*SnRK1.2), one γ subunit (AKINγ: *A. thaliana*, Snf4: Tomato), and three β-subunits in *A. thaliana* (AKINβ1, β2, β3) and two in tomato (*Sl*Gal83, *Sl*Sip1).

Most plant, yeast, and animal subunits are functionally conserved and can complement mutations in the respective genes in yeast knockout strains (Ghillebert et al., 2011). However, plants have a large family of α-related catalytic subunits (SnRK2 and SnRK3) which have diverged and are no longer functionally homologous to any of the yeast or animal subunits. Additionally, plants have a modified subunit that appears to have arisen from a fusion of a γ and a β-subunit, this subunit is nevertheless, capable of complementing an SNF4 deletion in yeast (Lumbreras et al., 2001; Gissot et al., 2006). These observations suggest plants can use a larger number of complexes in order to respond to metabolic situations that other organisms do not encounter (Ghillebert et al., 2011).

1.8b Catalytic α-subunits

The α-subunits typically have an auto-inhibitory domain at their C-terminus and require the phosphorylation of a conserved Threonine residue located on the activation loop within kinase domain in order to produce a fully activated catalytic enzyme. This activation residue corresponds to Thr172 in the mammalian AMPKα, Thr210 in Snf1, and Thr175 in plant SnRKs (Hedbacker & Carlson, 2006, Polge & Thomas, 2007, Steinberg & Kemp, 2009). Three kinases have been identified that phosphorylate AMP: LKB1, Calmodulin-dependent kinase (CaMKKβ), and Tak1 kinase (Steinberg & Kemp,

2009). Likewise yeast kinases that phosphorylate SNF1 have been identified and are: Tos3, Pak1, and Elm1 (Hong et al., 2003). Recently, SnRK1-activating kinases (SnAK) 1 and 2 were shown to be the upstream activating kinases in *A. thaliana.* These kinases were previously named GRIKs (gemnivirus Rep-interacting kinases) because of their ability to interact with the gemnivirus replication protein AL1 (Halford & Hey, 2009, Hey et al., 2007, Shen & Hanley-Bowdoin, 2006, Shen et al., 2009).

1.8c Regulatory β-subunits

The β- subunits of the SnRK complex have a glycogen-binding domain (GBD) towards the middle of the protein, a C-terminal association with Snf1 complex (ASN) domain, and a variable N-terminal region. The GBD domain is required for the interaction of α- and β- subunits in both plant and yeast, but appears to be dispensable in animals for the formation of the complex. Besides this, the function of the GBD domain and its glycogen binding activity remains largely speculative (Ghillebert et al., 2011). The ASN domain is required in plants and yeast for the interaction with the γ-subunits, while in animals it mediates the interaction with both γ and α subunits (Jiang & Carlson, 1997). The N-terminus of the β-subunits regulates the cellular localization of the complex. For instance glucose deprivation in yeast causes cytosolic GAL83 and Sip1 containing complexes to re-locate to the nucleus and the vacuole respectively (Vincent et al., 2001).

1.8d Post-translational modifications of β-subunits

Post-translational modifications are common among β-subunits and seem to play an important role in their regulatory functions. For instance, β-subunits are subject to N-

myristoylation; the covalent attachment of the 14 carbon fatty acid myristate to a Gly residue. Thanks to its hydrophobic nature, myristoylation facilitates protein tethering to membranes and is potentially important in mediating the interaction of the β subunits with the complex (Hedbacker & Carlson, 2006, Steinberg & Kemp, 2009).

Additionally, β-subunits are extensively phosphorylated. For instance, the mammalian AMPKβ1 subunit is phosphorylated by the α-subunit of the complex (AMPKα) at Ser24, Ser25, Ser108, and phosphorylated by an unknown upstream kinase at Ser182 (Mitchelhill et al., 1997). AMPKβ1 phosphorylation at Ser24, Ser25 and Ser182 is involved in localizing the protein to the nucleus, while a mutation removing Ser108 inhibits the catalytic activity of the complex (Warden et al., 2001). In yeast, the β subunits are also phosphorylated (by Snf1) or trans-phosphorylated by casein kinase II (Mangat et al., 2010). However, the exact location of the phosphorylation sites in yeast β-subunits has not been experimentally addressed. In plants, no information on the phosphorylation state of β-subunits has been directly studied. However, searches for *A.thaliana* β-Subunits in the Arabidopsis Protein Phosphorylation Site Datatabase (PhosPhat, http://phosphat.mpimp-golm.mpg.de/; Durek et al., 2010, Heazlewood et al., 2008) reveal the presence of a peptide with Ser197 phosphorylated on AKINβ1 obtained in an *in vivo* phosphoproteomic analysis (Reiland et al., 2009).

The role of β-subunits phosphorylation in the regulation of cellular localization, SnRK complex assembly, and kinase activity has not been studied in depth and is, in general, still poorly understood (Ghillebert et al., 2011).

1.8e Regulatory γ-subunits

Like β-subunits, γ-subunits generally possess a variable N-terminal domain. However, unlike any other subunit, γ-subunits are characterized for containing four tandem Bateman repeats which are involved in binding adenosine derivatives (Steinberg & Kemp, 2009). These domains bind AMP and allosterically make the γ subunit relief the catalytic auto-inhibition of the α-catalytic subunit (Xiao et al., 2007). In support of this model, a domain within γ containing a pseudo-substrate for the catalytic α-subunit was found, indicating that γ-subunits can act as inhibitors of the complex in the absence of AMP (Scott et al., 2007). However, this regulatory mechanism has only been demonstrated in animal complexes and the activator of plant and yeast complexes remains a matter of controversy (Ghillebert et al., 2011).

1.8f SnRK function in yeast

The SnRK complex functions in response to metabolic stresses but is also involved in regulating normal growth and development (Ghillebert et al., 2011). In yeast, the Snf1 complex is required during glucose starvation, when the yeast must switch from fermentative to oxidative metabolism because only alternative carbon sources are available (Celenza & Carlson, 1986, Halford et al., 2000). In the absence of glucose for instance, the activity of the complex increases dramatically, a phenomenon correlated with an increase in the AMP/ATP ratio. However, the direct mechanism by which the complex becomes activated is not fully understood (Steinberg & Kemp, 2009). In addition to its role in sugar metabolism, Snf1 is involved in diverse processes such as: the recycling of nutrients through autophagy, the synthesis of reserve carbohydrates, the

regulation of meiosis and sporulation, the coordination of filamentous and biofilm formation, and senescence (Ashrafi et al., 2000, Kuchin et al., 2002, Lorenz et al., 2009, Wang et al., 2001).

1.8g SnRK function in animals

Like its yeast counterpart, the animal AMPK complex monitors the energy status of cells by activating ATP generating pathways or repressing ATP consuming pathways (Ghillebert et al., 2011). In order to do so, AMPK senses the AMP/ATP ratio, which can be affected by: glucose deprivation, hypoxia, ischemia, prolonged exercise, and oxidative stress (Hardie, 2007). When activated by a drop in ATP, AMPK turns on energy producing pathways such as glycolysis, fatty acid oxidation, and autophagy while downregulating energy-consuming pathways such as protein and fatty acid synthesis (Stapleton et al., 1996). While directly affecting biochemical processes involved in the production of ATP, AMPK also controls the endocrine processes involved in whole body energy homeostasis through the action of several cytokines known as adipokines (Steinberg & Kemp, 2009). Not surprisingly, AMPK is fundamental for survival and its improper regulation is linked to a plethora of metabolic disorders such as obesity, diabetes, insulin resistance, and cardiovascular disease among others (Steinberg & Kemp, 2009).

1.8h SnRK function in plants

Accumulating evidence indicates plant SnRKs function in similar metabolic challenges as its animal and yeast counterparts by sensing the energy state of the cells and responding to biotic and abiotic stress (Polge & Thomas, 2007; Figure 6). For

instance, SnRKs can phosphorylate and inactivate important metabolic enzymes such as 3-hydroxymethyl-3-methylglutaryl-CoA reductase (HMGR), sucrose phosphate synthase, nitrate reductase, and trehalose phosphate synthase 5 (Dale et al., 1995, Harthill et al., 2006, Sugden et al., 1999; Figure 6). These enzymes are all involved in key regulatory steps of sucrose, lipid and amino acid biosynthesis as well as the production of trehalose-6-phosphate; a sugar signaling molecule that regulates plant metabolism and development (Delatte et al., 2011). SnRKs also regulate the expression of several genes controlling metabolic pathways such as amylase and sucrose synthase, enzymes involved in sucrose and starch degradation respectively (Polge & Thomas, 2007; Figure 6). Furthermore, SnRKs appear to be involved in pollen, root, and tuber formation (Lovas et al., 2003, Zhang et al., 2001). Furthermore, SnRK is required to mobilize photosynthates to the roots in response to herbivory (Schwachtje et al., 2006; Figure 6). Despite these recent advances in our understanding of SnRK involvement in energy regulation and stress responses the molecular mechanisms controlling and regulating such processes are not yet understood (Polge & Thomas, 2007).

1.9 The SnRK complex in cell death

1.9a Yeast

The yeast SNF complex plays an important role in regulating cell death. Loss of the activation γ-subunit Snf4 causes a 20% increase in life span. On the other hand, removal of the β-subunit Sip2, a negative regulator of Snf1 kinase activity, exhibits accelerated aging, presumably linked with an increase in Snf1 kinase activity (Ashrafi et al., 2000). With age, the β-Subunit Sip2 transits from the membrane to the cytosol. This

change in localization causes Sip2 to release Snf4 allowing it to localize to the nucleus where it is required for the activation of nuclear Snf1 and senescence. This change in localization depends on the myristoylation state of Sip2; when myristoylation of Sip2 is blocked by an N-terminal Gly to Ala substitution, Sip2 switches to a nucleo-cytoplasmic localization and accelerated senescence ensues (Lin et al., 2003).

1.9b Mammals

The AMPK complex phosphorylates molecules involved in growth, survival, and autophagy (Luo et al., 2010). AMPK and the tumor suppressor protein p53 are mutually regulated. For instance, the β-subunit AMKβ1 is up-regulated in a p53 dependent manner by diverse stress stimuli; this mechanism seems to work in synchrony with the cell death pathway regulated by PKB and mammalian target of rapamycin (mTOR) to facilitate stress-growth inhibition and cell death (Feng et al., 2007). In fact, genetic and biochemical evidence suggests that PKB activates the mTOR pathway by inhibiting the AMPK complex (Hahn-Windgassen et al., 2005, Horman et al., 2006). While the involvement of AMPK in several metabolic and PCD related-pathways has been established it is still unclear how stress affects AMPK activity in aging, as some reports indicate increase activity while others report inactivation (Steinberg & Kemp, 2009).

1.9c Plants

In plants, the SnRK complex seems to be involved in innate antiviral defenses and a plant specific SnRK in *A. thaliana* interacts with proteins involved in nematode resistance (Hao et al., 2003). The characterization of the SnRK β-subunits in the *A. thaliana* SnRK complex showed increased levels of SnRK β1 and β2 mRNA in

senescent tissue, suggesting a possible role of this subunit and the SnRK complex in programmed cell death in plants (Polge et al., 2008; Figure 6). Recently, the α-catalytic subunit was found to be required for protecting plants against oxygen deprivation and subsequent cellular energy depletion (Cho et al., 2012). Furthermore, plants overexpressing the catalytic subunit display delayed senescence while expression of their inactive forms causes accelerated senescence potentially by manipulating autophagy (Cho et al., 2012; Figure 6).

1.10 Ubiquitination

1.10a Ubiquitin

Ubiquitination is a process by which ubiquitin, a 76 residue polypeptide, is covalently attached to a Lys residue in a target protein. Living up to its name, ubiquitin (Ub) can be found in all eukaryotic species where it has been looked for and being identical in higher plants and differing at only two and three residues in comparison to yeast and mammals respectively (Callis et al., 1995). Structurally, Ub is a globular molecule that is remarkably stable thanks to the hydrogen bonds formed between an α-helix that sits on a fold of five strand β-sheets. This tridimensional make-up is known as the Ub-fold (Smalle & Vierstra, 2004). Ub contains a Glycine residue at its C-terminal end (Gly76), essential for the linkage formed with the Lys residue on the target proteins (Busch & Goldknopf, 1981). An additional conserved and unique feature of Ub is its expression. Ub is encoded as a polypeptide chain compromise of variable numbers of monomeric units. These fusion proteins are rapidly processed into individual Ub units by proteases (Smalle & Vierstra, 2004).

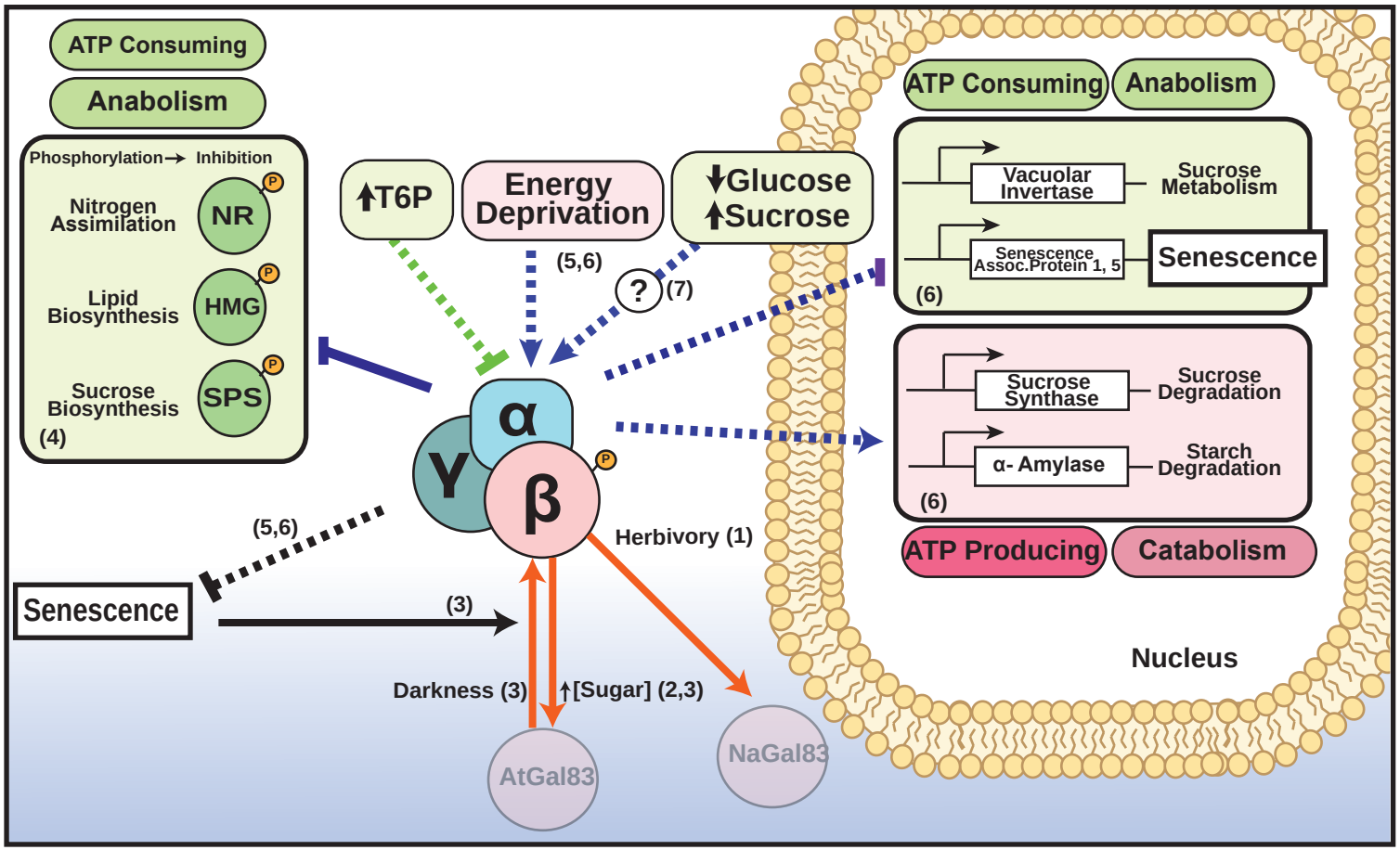

Figure 6. SnRK function in plants. Cartoon representation of a few of the SnRK complex functions characterized in plants. Plant SnRK functions as a heterotrimers with α, β, and γ subunits. The complex is activated under energy deprivation and under high sucrose or low glucose concentrations, although the effect of sugars on SnRK activation remains a controversial topic (Halford and Hey, 2009). For details see main text. 1.(Schwachtje et al., 2006), 2, (Li et al., 2009), 3, (Polge et al., 2008), 4, (Dale et al., 1995a; Dale et al., 1995b; Sugden et al., 1999b), 5: (Cho et al., 2012; Thelander et al., 2004), 6, (Baena-Gonzalez et al., 2007), 7, (Baena-Gonzalez et al., 2007; Halford and Hey, 2009).

1.10b The ubiquitination reaction

The specific attachment of Ub moieties is accomplished through the coordinated action of a Ub activating enzyme E1 (UBA), a Ub conjugating enzyme E2 (UBC), and a Ub ligase (E3). The conjugation of Ub takes place in a multi-step reaction in which the E1 enzyme catalyzes the formation of an acyl phosphoanhydride bond between adenosine monophosphate (AMP) and the Ub C-terminal glycine carboxyl group, using adenosine tri-phosphate (ATP) as a substrate. Activated Ub is then attached to a cysteine in the E1 enzyme through a thiol-ester linkage with the subsequent release of AMP. Next, Ub is transferred to another cysteine on an E2 enzyme via transesterification (Hershko & Ciechanover, 1998). Finally, Ub is linked to a substrate's lysyl ε-amino group through and isopeptidic bond. This final step is catalyzed with the aid of an E3 conjugating enzyme (or complex of proteins), which is also used as a substrate-recognition element, but may be used as a temporary receptor for the Ub to be transferred. Ub can be transferred individually (mono-ubiquitination) or multiply attached to lysines present on the Ub moiety of already ubiquitinated substrates (poly-ubiquitination).

1.10c Ubiquitination enzymes

A. thaliana contains two E1 enzymes (Hatfield et al., 1997). On the other hand, E2s are more diverse as *A. thaliana* contains approximately 37 proteins containing the characteristic E2 ligase UBC domain; a 150- amino acid patch that surrounds the cysteine to which Ub is attached prior to substrate transfer (Bachmair et al., 2001, Hamilton et al., 2001). The most diverse ubiquitination enzymes are the E3 Ub ligases

since they dictate the identity of the ubiquitinated substrate as well as the type of ubiquitination (mono or poly). For instance, approximately 1,300 E3s can be found in *A. thaliana* (Smalle and Vierstra, 2004). The different types of E3s have been grouped into four categories according to their mechanism of action and their subunit composition: HECT, RING, U-box, and Cullin-RING ligases (Vierstra, 2009).

1.10d Homologous to the E6-AP carboxyl terminus (HECT) domain E3s

HECT E3 ligases are individual proteins that, unlike any other ligase, directly carry activated ubiquitin in a cysteine thio-ester bond before transferring it to the substrate (Downes et al., 2003). In order to accomplish this, members of this group have a HECT domain which consists of a 350-amino acid region containing a cysteine to which Ub is attached. HECT ligases owe their name to the domain found on the E6-associated protein, an E3 ligase involved in the degradation of p53 in mammals (Huibregtse et al., 1995).

1.10e Really interesting new gene (RING) and U-box domain E3s

RING ligases are individual proteins that share a zinc-binding cysteine-rich motif (Freemont, 1993). The RING motif contains an octet of Cys or His residues that chelate two zinc ions. Unlike other RING finger motifs which mediate protein-DNA interactions, this domain is used to establish physical interactions with the Ub-loaded E2 (Borden, 2000). Meanwhile, the rest of the protein functions to mediate the interaction with the substrates to be ubiquitinated (Vierstra, 2009). U-box ligases on the other hand, lack a the RING domain amino acid organization but share the structural fold used to establish interactions with the E2 ligases using electrostatic interactions instead (Wiborg

et al., 2008). The *A. thaliana* genome contains approximately 480 RING-finger containing proteins and 64 proteins with a U-box domain (Smalle & Vierstra, 2004, Stone, 2005).

1.10f SCF-RING E3 ligases

Ligases belonging to this group are RING-Box 1 (RBX1) proteins that contain a RING domain that mediates the interaction with the E2 ligases, but posses a multi-subunit recognition system that mediates the interaction of the ligase with its substrates (Smalle and Vierstra, 2004). This recognition system is known as SCF for its subunits: SKP1, CDC53 (or Cullin), and F-box proteins (Deshaies, 1999). The F-box protein is the direct substrate recognition module that is tethered to the RING domain with the aid of the SKP and CUL proteins. This is possibly one of the most widespread ligase groups in plants. *A. thaliana* has approximately 700 F-box proteins, at least two RBX1 subunits, five Cullin, and about 21 SKPs. The different subunit combinations could in theory recognize a limitless number of substrates (Smalle and Vierstra, 2004). This system is used in the signaling pathways of various plant hormones such as auxin, in which the TIR1 ubiquitin ligase ubiquitinates AUX/IAA proteins which are involved in auxin signaling. The ubiquitination of these proteins only takes place when the recognition complex is stabilized by the binding of auxin which acts as a molecular glue. This remarkably specific system is now recognized as the long sought after auxin receptor (Tan, 2007).

1.10g Fates of ubiquitination

Ubiquitination has been linked to processes as diverse as protein degradation, endocytosis, histone modification, protein activation, stress response, DNA damage repair, and changes in intracellular protein localization (Pickart, 2001). Translating ubiquitination into a particular outcome often depends not only on the presence or absence of Ub, but the type of ubiquitination (mono- or poly-) and the topology of the poly-Ub chains. For instance, proteins that carry polyubiqutin chains that are linked by a Lys48 to Gly76 bond are targeted to degradation by the 26S proteasome; an ATP-dependent protease complex that breaks down proteins into individual amino acids, but is capable of recycling Ub moieties (Chau et al., 1989, Yang et al., 2004).

An example of a non-proteasomal ubiquitination is the iron-regulated transporter 1 (IRT1) in *A. thaliana*. Monoubiquitination of IRT1 mediates its endocytosis from the plasma membrane into lytic vacuoles, where it is subsequently degraded (Barberon et al., 2011). This system is used to adjust the number of channel molecules present in the plasma membrane and prevent metal cytotoxicity and an example of 26S proteasome-independent degradation mediated by ubiquitination (Barberon et al., 2011).

1.10h Ubiquitination in PCD

Evidence suggests ubiquitination plays a role in the regulation of PCD. For instance, Ub is found in high amounts in vascular elements and xylem precursors and inhibition of the proteasome-mediated degradation machinery prevents the development of tracheary elements (Bachmair et al., 2001, Fukuda, 2000, Woffenden et al., 1998). Recently, several E3 ligases have been reported to play a role in defense signaling and

PCD (Stulemeijer & Joosten, 2008). For instance, the U-box containing E3 ligase PUB17 in *A. thaliana* was found to be required for resistance against *Pst* expressing the effector proteins RPM1 and RPS4 (Yang et al., 2006). Furthermore, the *A. thaliana* PUB13 E3 ligase was characterized as an important negative regulator of cell death that interferes with the resistance to biotrophic pathogens, but facilitates resistance against necrotrophic pathogens (Li et al., 2012). The tobacco E3 ligase (*Nt*CMPG1) was also reported to be required for defense signaling induced by the AvrPto/Pto complex and the *Phytophtora infestans* elicitor Inf1 (Gonzalez-Lamothe, 2006). Furthermore, a membrane integrated RING1 E3-ligase (At5g10380) in *A. thaliana* was shown to be a positive regulator of programmed cell death in response to the fungal toxin Fumonisin B1 (FB1) or *Pst* carrying the effector protein RPM1 (Lin et al., 2008). Surprisingly, the role of FB1- or RPM1-mediated stress was to stabilize RING1 *in vivo*, probably by interfering with its autoubiquitination activity (Lin et al., 2008). Finally, the *A. thaliana* RING domain E3 ligase benzoic acid hypersensitive1-Dominant (BAH1) seems to function as a regulator of immune responses involving pathogen associated salicylic acid accumulation and cell death (Yaeno & Iba, 2008). Despite the genetic body of evidence presented, the roles of only a few of these proteins have been characterized *in vivo* (Lin et al., 2008).

CHAPTER II

METHODS*

2.1 Cloning and site directed mutagenesis

2.1a Cloning of tomato AdBiL, UBC8, UBC10 and A. thaliana AtUBA1, AtUBC8, AtUBC11 (CHAPTER III)

All primers and restriction sites used in this study for ORF amplification, cloning, and mutagenesis are listed in Table 1 and the primers used to amplify all genes were designed using sequence data obtained from the Sol Genomics Network (SGN) databases (http://solgenomics.net/) and The Arabidopsis Information Resource (TAIR). The ORF of *AdBiL* was obtained by RT-PCR using leaf total RNA. *AdBiL* corresponds to the SGN Unigene U580180. Full length ORF cDNA clones were obtained from TAIR and use to clone the sequences of: the E1 ligase *AtUBA1*(AT2g30110) from clone U218214, *AtUBC8* (AT5g41700) from the clone U15399, *AtUBC11* (AT3g08690) from the clone U18004. Tomato homologous UBCs were identified using BLAST searches against the SGN databases. *SlUBC8* corresponds to the unigenes SGN-U578242/U312900 and was isolated from the EST clone cTOA-26-L24. *SlUBC10* (UBC2) corresponds to the unigenes SGN U312900/U581187 and was isolated from the EST clone cTOF-12-E20.

---

* Portions of the following chapter have been reprinted with permission from: **Avila J, Gregory O, Su D, Deeter T, Chen S, Silva-Sanchez C, Xu S, Martin G, Devarenne T** (2012) The β-Subunit of the SnRK1 Complex Is Phosphorylated by the Plant Cell Death Suppressor Adi3. Plant Physiology **159:** 1277-1290.

2.1b Cloning of tomato SnRK1, Gal83, Sip1, Tau1, Tau2, and Snf4 (CHAPTER IV)

The ORFs for *SlSnRK1*, *SlSip1*, *SlSnf4*, *Tau1*, and *Tau2* were obtained by RT-PCR using cDNA generated with Superscript III (Invitrogen) from tomato total RNA isolated from 4-week-old leaves. Primers used to amplify *SlSnRK1* (accession #AF143743) were based on the unigene SGN-U564382. The cDNA for *SlSip1* (accession #AF322108) in unigene SGN-U575258 and reported in Bradford et al. (2003) appeared to lack a portion of the 5' end of the cDNA when compared to homologous β-subunits from yeast and Arabidopsis. Consequently, the tomato genome sequence was searched on SGN for the *SlSip1* gene using unigene SGN-U575258. An *Sl*Sip1 gene was found in genomic sequence SL2.31ch05:63330625..63325020 and primers were designed based on this sequence to amplify the ORF by RT-PCR. The reported *SlGal83* cDNA (accession #AY245177) lacked the 5' end and the full length cDNA was identified in unigene SGN-U564868. Primers based on this unigene were used to amplify the ORF by PCR using SGN EST clone cTOF-18-D18 as a template. The *Tau1* (accession #JQ846034) and *Tau2* (accession #JQ846035) ORFs were isolated using primer sequences based on the unigenes U571217 and U565213, respectively. The *SlSnf4* ORF (accession #AF419320) was amplified by PCR using the published sequence (Bradford et al., 2003). Mutagenesis of *SlSnRK1* and *SlGal83* was performed using Pfu Turbo Polymerase (Stratagene) and the primer pairs listed in Table 1. Cloning of Adi3 and its kinase activity mutants were described previously (Devarenne et al., 2006).

Table 1. Primers used in this study

Gene	Primer Name	Purpose	Direction	Restriction site	Sequence
Adi3	Adi3 BamHI-F	Cloning into pGEX	Forward	BamHI	CACGGATCC**ATG**GAAAGGATACCTGAAGTT
Adi3	Adi3 EcoRI-R	Cloning into pGEX	Reverse	EcoRI	CACGAATTC**CTA**AAAGAACTCAAAGTCAAG
*Sl*SnRK1	SnRK EcoRI-F	ORF Amplification Cloning into pEG202/pJG4-5	Forward	EcoRI	CACGAATTC**ATG**GACGGAACAGCAGTG
*Sl*SnRK1	SnRK BamHI-R	ORF Amplification Cloning into pEG202	Reverse	BamHI	CACGGATCC**TTA**AAGTACTCGAAGCTG
*Sl*SnRK1	SnRK PstIR	Cloning into pMAL	Reverse	PstI	CACCTGCAG**TTA**AAGTACTCGAAGCTG
*Sl*SnRK1	SnRK T175D-F	Mutagenesis	Forward		GGTCATTTTCTGAAG**GAT**AGTTGCGGAAGCCCA
*Sl*SnRK1	SnRK T175D-R	Mutagenesis	Reverse		TGGGCTTCCGCAACT**ATC**CTTCAGAAAATGACC
*Sl*SnRK1	SnRK K48Q-F	Mutagenesis	Forward		CACAAAGTTGCTGTC**CAG**ATTCTTAATCGTCGA
*Sl*SnRK1	SnRK K48Q-R	Mutagenesis	Reverse		TCGACGATTAAGAAT**CTG**GACAGCAACTTTGTG
*Sl*Snf4	SNF4 EcoRI	ORF Amplification Cloning into	Forward	EcoRI	CACGAATTC**ATG**CAGGCAACAGCGGAG
*Sl*Snf4	SNF4 SalI	ORF Amplification Cloning into	Reverse	SalI	CACGTCGAC**TCA**CTGCAAAAACTCAG
*Sl*Sip1	SIP1 EcoRI	ORF Amplification Cloning into pMAL	Forward	EcoRI	CACGAATTC**ATG**TTTAGACCTGAGATG
*Sl*Sip1	SIP1 BamHI	ORF Amplification Cloning into pMAL	Reverse	BamHI	CACCTCGAG**TCA**CCTCTGTATTGACTTG
*Sl*Gal83	GAL83 EcoRI	ORF Amplification Cloning into pMAL,	Forward	EcoRI	CACGAATTC**ATG**GGGAATGCGAACGCC

Table 1. Continued

Gene	Primer Name	Purpose	Direction	Restriction site	Sequence
*Sl*Gal83	S147A	Mutagenesis	Reverse		GTAATGATATATACC**CGC**TGGAAGGACCAAAAG
*Sl*Gal83	S192A	Mutagenesis	Forward		CCAGAGAACCTCGAA**GCT**GTTGCAGAGTTTGAG
*Sl*Gal83	S192A	Mutagenesis	Reverse		CTCAAACTCTGCAAC**AGC**TTCGAGGTTCTCTGG
*Sl*Gal83	S204/205A	Mutagenesis	Forward		CCACCATCACCT**GACGCT**GCCTATGCGCAAGCTTTG
*Sl*Gal83	S204/205A	Mutagenesis	Reverse		CAAAGCTTGCGCATAGG**CAGCGTC**AGGTGATGGTGG
*Sl*Gal83	S234A	Mutagenesis	Forward		CTAACTGTTCTTGGT**GCT**GAAAACTCAGAAGAAGC
*Sl*Gal83	S234A	Mutagenesis	Reverse		GCTTCTTCTGAGTTTTG**AGC**ACCAAGAACAGTTAG
*Sl*Gal83	S237A	Mutagenesis	Forward		GGTTCTGAAAAC**GCA**GAAGAA GCACCTTC
*Sl*Gal83	S237A	Mutagenesis	Reverse		GAAGGTGCTTC TTC**TGC**GTTTTC AGAACC
*Sl*Gal83	S242/243A	Mutagenesis	Forward		CAGAAGAAGCACCT**GCTGCT** CCAAAACCCCAGCACG
*Sl*Gal83	S242/243A	Mutagenesis	Reverse		GTGCTGGGGTTTTGG**AGCAGC**AGGTGCTTCTTCTG
*Sl*Gal83	S262A/S264R	Mutagenesis	Forward		GAGAAAGGATGGGCT**GCT**CAA**GCC**ATTGTTGCTCTTGG
*Sl*Gal83	S262A/S264R	Mutagenesis	Reverse		CCAAGAGCAACAAT**CCG**TTG**AGC**AGCCCATCCTTTCTC
Tau1	Tau1-F	ORF Amplification	Forward		ATGGGGAATGTGAGTGGG
Tau1	Tau1-R	ORF Amplification	Reverse		TCACTTTTTCAAGGACTTAAAAAG
Tau1	Tau1-F	Cloning into pMAL	Forward	EcoRI	CACGAATTCATGGGGAATGTGAGTGGG
Tau1	Tau1-R	Cloning into pMAL	Reverse	SalI	CACGTCGACTCACTTTTTCAAGGACTTAAAAAG
Tau2	Tau2-F	ORF Amplification	Forward		ATGGGGAATGTTAATGGAAGAG

Table 1. Continued

Gene	Primer Name	Purpose	Direction	Restriction site	Sequence
Tau2	Tau2-R	ORF Amplification	Reverse		TCACCTCTGTATGGACTTGTAAAG
Tau2	Tau2-F	Cloning into pMAL	Forward	EcoRI	CACGAATTCATGGGGAATGTTAATGGA
Tau2	Tau2-R	Cloning into pMAL	Reverse	SalI	CACGTCGACTCACCTCTGTATGGACTTGTA
AdBiL	RING XhoI-F	Cloning into pEG202, pJG4-5, pFLAG	Forward	XhoI	CACCTCGAGTCATGACCGGTTCTGGGACGGC
AdBiL	RING XhoI-R	Cloning into pEG202, pJG4-5	Reverse	XhoI	CACCTCGAGATGGGATTGAATGGTGTGGATC
AdBiL	RING BamHI-F	Cloning into pMAL	Forward	BamHI	CACGGATCCATGGGATTGAATGGTGTG
AdBiL	RING BamHI-R	Cloning into pMAL	Reverse	BamHI	CACGGATCCTCATGACCGGTTCTGGG
AdBiL	RING SalI-R NS	Cloning into pFLAG	Reverse	SalI	CACGTCGACTGACCGGTTCTGGGACGG
*Sl*UBC8	*Sl*UBC8 EcoRI-F	Cloning into pMAL, pGEX	Forward	EcoRI	CACGAATTCATGGCATCCAAGCGG
*Sl*UBC8	*Sl*UBC8 SalI-R	Cloning into pMAL, pGEX	Reverse	SalI	CACGTCGACCTATCCCATGGCAAATT
*Sl*UBC10	*Sl*UBC10 EcoRI-F	Cloning into pMAL, pGEX	Forward	EcoRI	CACGAATTCATGGCTTCGAAACGAATA
*Sl*UBC10	*Sl*UBC10 SalI-R	Cloning into pMAL, pGEX	Reverse	SalI	CACGTCGACCTACATACACAAACATTC
*At*UBC8	*At*UBC8 EcoRI-F	Cloning into pMAL, pGEX	Forward	EcoRI	CACGAATTCATGGCGTCGAAGCGG
*At*UBC8	*At*UBC8 SalI-R	Cloning into pMAL, pGEX	Reverse	SalI	CACGTCGACTTAGCCCATGGCATAC
*At*UBC11	*At*UBC11 EcoRI-F	Cloning into pMAL, pGEX	Forward	EcoRI	CACGAATTCATGGCTTCTAAGAGGATC
*At*UBC11	*At*UBC11 SalI-R	Cloning into pMAL, pGEX	Reverse	SalI	CACGTCGACTCAACCCATTGCGTAC
*At*UBA1	*At*UBA1 EcoRI-F	Cloning into pMAL, pGEX	Forward	EcoRI	CACGAATTCATGCTTCACAAGCGAGCTAGTC
*At*UBA1	*At*UBA1 XbaI-R	Cloning into pMAL	Reverse	XbaI	CACTCTAGATCACCTGAAGTAGATAGAGAC

Table 1. Continued

Gene	Primer Name	Purpose	Direction	Restriction site	Sequence
*At*UBA1	*At*UBA1 NotI-R	Cloning into pGEX	Reverse	NotI	CACGCGGCCGCTCACCTGAAGTAGATAGAGAC
*Sl*Gal83 P	*Sl*Gal83 pM-F	Amplifying *Sl*Gal83 promoter	Forward	None	GAGCGTAACGTTTGCATACAGTC
*Sl*Gal83 P	*Sl*Gal83 pM-R	Amplifying *Sl*Gal83 promoter	Reverse	None	GTCTTCCCAATAATGCTAGTG
*Sl*Gal83 P	*Sl*Gal83 pM-EcoRIF	Cloning into pTEX	Forward	EcoRI	CACGAATTCGAGCGTAACGTTTGCATAC
*Sl*Gal83 P	Gal83 pM-BamHIR	Cloning into pTEX	Reverse	BamHI	CACGGATCCCATGTCTTCCCAATAATGCTAGTG

2.2 Recombinant protein expression and purification

2.2a SnRK complex enzymes and GST-Adi3 (CHAPTER IV)

The ORFs for *SlSnRK1*, *SlGal83*, and *SlSip1* were cloned as N-terminal MBP fusions into pMAL-c2 vector (New England Biolabs). Recombinant proteins were expressed in *E. coli* BL21 Star (DE3) as described previously (Devarenne et al., 2006) and purified using maltose binding resin (New England Biolabs) manufacturer protocols. For GST-Adi3, the *Adi3* ORF was cloned into the pGEX-4T N-terminal GST fusion vector (GE-Healthcare) and protein was expressed and purified as recommended by the manufacturer. After elution, all fusion proteins were concentrated using Amicon Ultra centrifugal filters (Millipore) and added to buffer for final concentrations of 50% glycerol, 50 mM Tris-HCl pH7.5, 0.5 mM EDTA, 100 mM NaCl. Protein concentrations were quantified using Bio-Rad Protein Assay Kit before storage at -20C.

2.2b Ubiquitination enzymes (CHAPTER III)

In order to obtain MBP- and GST- tagged proteins, the ORF of *AdBiL*, *AtUBA1*, *AtUBC8*, *AtUBC11*, *SlUBC8*, *SlUBC11* were cloned into the expression vectors -c2 vector (New England Biolabs) and pGEX-4T N-terminal GST fusion vector (GE-Healthcare). Proteins were expressed in *E. coli* BL21 Star (DE3). Cells were grown in 30 ml of TB media an induced with isopropyl β-D-1-thiogalactopyranoside 100 μM. Proteins were expressed for 4 hours at 30°C. Next, bacterial cells were resuspended in Adi3 extraction buffer (Devarenne et al., 2006) and lysed by the addition of lysozyme followed by sonication. Bacterial lysates containing MBP- or GST-fusions were cleared by centrifugation and bound for 2 hours at 4°C to 300 μl of immobilized amylose (New

England BioLabs) or glutathione (Thermo Scientific) beads respectively. Bound proteins were washed in 2 ml of extraction buffer and proteins were eluted in elution buffer (50 mM Tris pH 8.0, 50mM NaCl, 1 mM DTT) containing 10 mM reduced glutathione or 10 mM maltose. Eluted fractions were concentrated using Amicon Ultra centrifugal filters (Millipore) and glycerol was added to a final concentration of 50%. Protein concentrations were estimated using Bio-Rad Protein Assay Kit before storage at -20C. MBP-tagged Adi3 and kinase activity mutants were purified as previously described (Avila et al., 2012). For pull down assays, C-terminal FLAG-tagged AdBiL was obtained cloning AdBiLs ORF into the pFLAG-CTC expression vector (Sigma-Aldrich). Cells expressing AdBiL-FLAG and MBP-Adi3 were aliquoted and frozen at -20°C and cleared lysates were prepared as described above, except AdBiL-FLAG cells were lysed in the presence of 0.2% Sarkosyl, 1 mM PMSF, and 1% Triton.

2.3 Yeast two-hybrid assay (CHAPTERs III and IV)

Y2H assays where conducted using pEG202 for the bait vector and pJG4-5 for the prey vector as described previously (Devarenne et al, 2006). Constructs were transformed into yeast strain EGY48 containing the pSH18-34 reporter vector and analyzed for *LacZ* gene expression on X-Gal containing plates. Protein expression was confirmed by western blot. All other procedures for the Y2H assays and Y2H library screen for identifying Adi3 interactors followed standard procedures as previously described (Golemis et al., 2008).

2.4 Yeast complementation and invertase assays (CHAPTER IV)

The ORF for *SlGal83* and its Ser26 mutants were fused to a C-terminal eGFP tag under the control of the *glyceraldehyde-3-phosphate dehydrogenase* (GPD) promoter in the modified vector MBB263. The yeast β-subunit knockout strain MCY4040 (*MATα sip1Δ::KanMX6 sip2Δ3::LEU2 gal83::TRP1 his3-Δ200 leu2-3,112 trp1Δ1 ura3-52 lys2-801*) (Vincent et al., 2001) was transformed with the *Sl*Gal83 constructs using the standard lithium acetate/PEG method. Transformants were screened on plates of complete minimal (CM) media with 2% glucose and lacking leucine, tryptophan, and uracil. Recovered colonies were grown in liquid CM 2% glucose medium for 48 hrs and 5-fold serial dilutions were spotted on selective media supplemented with either 2% glucose or 2% sucrose and incubated at 30˚C for 2 days (2% glucose) or 6-7 days (2% sucrose). Invertase assays were performed as previously reported (Celenza and Carlson, 1989; Bradford et al., 2003). Invertase activity of derepressed (0.05% glucose) and glucose-repressed (2% glucose) cells was estimated as a measure of the amount of sucrose metabolized into glucose using the Glucose (GO) Assay kit (Sigma) as described by the manufacturer.

2.5 Pull down assays

2.5a Interaction of Adi3 with AdBiL (CHAPTER III)

Cleared bacterial lysates expressing AdBiL-FLAG were incubated for 1 hour at 4°C in the presence or absence of MBP- tagged Adi3, Adi3^{K337Q}, Adi3^{S539D} and proteins were pulled down using immobilized amylose beads (New England BioLabs). Resin with bound proteins were washed 6 times with buffer containing 10 mM Tris, 150mM

NaCl, 1mM EDTA, 1% Triton pH8.0. Bound proteins were boiled at 95°C in SDS-Sample buffer and resolved by 12% SDS-PAGE. Western blotting with α-FLAG at 1:1000 (Sigma-Aldrich) or α-MBP (New England BioLabs) at 1:5,000 was used for pull downs and α-FLAG at 1:10,000 or α-MBP at 1:50,000 for loading controls and immunoblotting detection was done using the ECL kit (Amersham Pharmacia Biotech).

2.5b Interaction of Adi3 with the SnRK1 complex (CHAPTER IV)

Immobilized glutathione beads (Thermo Scientific) were equilibrated by washing three times with 200 µl of binding buffer (50 mM NaCl, 50 mM Tris-HCl pH 7.5, 0.1% Triton X-100, 5 mM EDTA). For each pull down 1 µg of either GST or GST-Adi3 and equivalent protein amounts of MBP, MBP-*Sl*Gal83, MBP-*Sl*Sip1, and MBP-*Sl*SnRK1 were mixed in a final volume of 30 µl. Samples were incubated for 15 min at room temperature followed by addition of buffer pre-equilibrated glutathione resin to each sample and incubation for 1 hr at 4˚C on an orbital shaker. The resin with bound proteins was pelleted by centrifugation at 100 x g and washed 5 times with 200 µl of wash buffer (500 mM NaCl, 50 mM Tris-HCl pH 7.5, 0.1% Triton X-100, 5 mM EDTA). Bound proteins were eluted using 1x SDS-PAGE sample buffer, resolved by 12% SDS-PAGE, and analyzed by western blotting using α-GST (Santa Cruz Biotechnology) at 1:15,000 and α-MBP (New England BioLabs) at 1:5,000 for pull downs or 1:10,000 for loading controls.

2.6 Ubiquitination assays

In vitro ubiquitination assays were done as described before with modifications (Lu et al., 2011, Rosebrock, 2007). Reactions were conducted in 30 µl of ubiquitination

buffer containing 50 mM Tris-HCl pH 7.5, 5 mM MgCl2, 0.5 mM dithiothreitol (DTT), and 5 mM ATP, and 5 µg of FLAG tagged ubiquitin (Boston Biochem), 50 ng of purified AtUBA1, 250 ng of AtUBC, 400ng of AdBiL and 1 µg of MBP-Adi3 or 3 µg of GST-Adi3 for pull downs. The reactions were incubated at 30°C and stopped with the addition of 4X SDS sample buffer and boiling at 95°C for 5 minutes. Proteins were separated by 8% SDS-PAGE and western blotting was used to identify ubiquitinated proteins using α-FLAG at 1:1000, α-MBP at 1:5000, α-GST at 1:5000, and α-Adi3 at 1:500. Ubiquitination reactions used for the preliminary screening of human ubiquitin conjugating enzymes used 250 µg of each enzyme from the UbcH (E2) Enzyme Set (Boston Biochemical). For pull down experiments, ubiquitination reactions were done as described above and, after completion, bound for 1 hour at 4°C to glutathione beads pre-equilibrated in binding buffer (50 mM Tris, 0.5 mM DTT, 50 mM NaCl, 5 mM EDTA, 0.1% Triton X100). Beads were washed 6 times in binding buffer containing 500 mM NaCl and pulled down proteins analyzed by 8% SDS PAGE and western blotting as done before.

2.7 Kinase assays (CHAPTER IV)

In vitro kinase assays were done in 30 µl reactions in Adi3 kinase buffer (10 mM Tris-HCl pH 7.5, 10 mM $MgCl_2$, 1mM DTT, 20 µM ATP) or *Sl*SnRK1 kinase buffer (10 mM Tris-HCl pH 8, 10 mM $MnCl_2$ or $MgCl_2$, 1mM DTT, 20 µM ATP). *Sl*SnRK1 autophosphorylation appeared to be slightly stronger using $MnCl_2$ and therefore, was used for all *Sl*SnRK1 autophosphorylation assays. However, *Sl*SnRK1 substrate phosphorylation was comparable using $MnCl_2$ or $MgCl_2$ as a cofactor. Therefore, $MgCl_2$

was used for all *Sl*SnRK1 substrate phosphorylation experiments. Adi3 substrate phosphorylation assays contained 5 μg of purified MBP-Adi3 or MBP-Adi3^{S539D} and 2 μg of MBP-Gal83, MBP-Gal83 mutants, or MBP-Sip1. For *Sl*SnRK1 kinase assays, 3 μg of MBP-SnRK1, MBP-SnRK1^{K48Q}, or MBP-SnRK1^{T175D} were used. Reactions were initiated upon addition of 0.25 μCi of γ-[^{32}P]ATP (6000Ci/mmole, Perkin Elmer) per sample and were incubated for 15 min at room temperature for Adi3 or 30 min at 30˚C for *Sl*SnRK1. Reactions were terminated by addition of 4x SDS-PAGE sample buffer and samples resolved by 7.5% SDS-PAGE. Sample radioactive incorporation imaging and quantification was done with a phosphorimager (Bio-Rad Molecular Imager).

SAMS peptide (HMRSAMSGLHLVKRR) phosphorylation assays were performed as described previously (Davies et al., 1989). Assay conditions for *Sl*SnRK1 phosphorylation of the SAMS peptide were as for the *Sl*SnRK1 substrate phosphorylation assays above plus 100 μM SAMS peptide (AnaSpec). Reactions were spotted on phosphocellulose p81 paper (Whatman), washed three times in 1% H_3PO_4, once in acetone, the paper dried, and the incorporated radioactivity counted using a Beckman LS5000TA scintillation counter. For SAMS phosphorylation with protoplast lysates, 4 x 10^5 tomato protoplasts expressing empty pTEX vector, *Sl*GAL83-GFP, and *Sl*GAL83^{S26D}-GFP were lysed by vortexing in a buffer containing 50mM Tris pH8.0, 1mM EDTA, 50mM NaCl, 8% Glycerol, 5mM DTT, 2% plant protease inhibitor cocktail (Sigma) and 2% plant phosphatase inhibitor cocktail (Sigma). Extracts were cleared by centrifugation at 4°C, 13,000 g for 10 minutes. Protein concentration was estimated as described above and lysates were adjusted to equal protein concentrations

with lysis buffer. Reactions were done as described above, but using a buffer containing 40 mM HEPES-KOH pH 7.6, 10 mM $MgCl_2$, 1mM DTT, 200 μM ATP, 2 μCi of γ-[^{32}P]ATP, and 100μM SAMS peptide (buffer adapted from (Fragoso et al., 2009)). Reactions were initiated with the addition of 8 μl of the protein extract. Phosphate incorporation was analyzed as described above and the remaining lysates were used for α-GFP western blotting to evaluate expression efficiency of the proteins.

2.8 Cell-free degradation assays (CHAPTER III)

Cell free degradation assays were done as described before (Lee, 2008; Osterlund et al., 2000) with modifications. Three-week old tomato leaves were ground in liquid nitrogen and homogenized in reaction buffer containing 25mM Tris, 10 mM MgCl2, 5 mM DTT, and 10 mM NaCl. Cell debris was removed by centrifugation and soluble protein concentration was quantified using Bio-Rad Protein Assay Kit. Cell-free degradation reactions were conducted in reaction buffer supplemented with 10mM ATP, 10 μg of leaf extracts, and in the presence of 500 ng of purified MBP-Adi3 or MBP-Adi3^{K337Q}. Reactions were incubated at 30°C for 30, 90, or 180 minutes. Subsequently, reactions were stopped with the addition of 4X SDS sample buffer, boiled at 95°C, and proteins resolved in a 10% SDS-PAGE and analyzed with western blotting using α-Adi3 (at 1:500) and α-MBP (at 1:5000) antibodies.

2.9 Mass spectrometry (CHAPTER IV)

For sample preparation, coomassie stained gel bands were in-gel digested with trypsin overnight and phosphopeptides were enriched using a NuTip metal oxide

phosphoprotein enrichment kit according to manufacturer's instructions (Glygen, Columbia, MD).

For LC-MS/MS analysis, phosphopeptides were injected onto a capillary trap (LC Packings PepMap, Amsterdam, Netherlands) and desalted for 5 min with 0.1% v/v acetic acid at a flow rate of 3 μl/min. The samples were loaded onto an LC Packings C_{18} PepMap nanoflow HPLC column. The elution gradient of the HPLC column started at 97% solvent A, 3% solvent B and finished at 60% solvent A, 40% solvent B for 30 min. Solvent A consisted of 0.1% v/v acetic acid, 3% v/v ACN, and 96.9% v/v H_2O. Solvent B consisted of 0.1% v/v acetic acid, 96.9% v/v ACN, and 3% v/v H_2O. LC-MS/MS analysis was carried out on a LTQ Orbitrap XL mass spectrometer (Thermo Scientific, Bremen, Germany). The instrument under Xcalibur 2.07 with LTQ Orbitrap Tune Plus 2.55 software was operated in the data dependent mode to automatically switch between MS and MS/MS acquisition. Survey scan MS spectra (from m/z 300 – 2000) were acquired in the orbitrap with resolution R=60,000 at m/z 400. During collisionally induced dissociation (CID), if a phosphate neutral loss of 98, 49, 32.66 and 24.5 m/z below the precursor ion mass was detected, there was an additional activation of all four neutral loss m/z values. This multistage activation was repeated for the top five ions in a data-dependent manner. Dynamic exclusion was set to 60 seconds. Typical mass spectrometric conditions include a spray voltage of 2.2 kV, no sheath and auxiliary gas flow, a heated capillary temperature of 200˚C, a capillary voltage of 44V, a tube lens voltage of 165V, an ion isolation width of 1.0 m/z, a normalized CID collision energy of 35% for MS/MS in LTQ. The ion selection threshold was 500 counts for MS/MS. The

mass spectrometer calibration was performed according to the manufacturer's guidelines using a mixture of sodium dodecyl sulphate, sodium taurocholate, MRFA and Ultramark.

For the protein search algorithm, all MS/MS spectra were analyzed using Mascot (Matrix Science, London, UK; version 2.2.2). Mascot was set up to search a current Arabidopsis database assuming the digestion enzyme trypsin. Mascot was searched with a fragment ion mass tolerance of 0.50 Da and a parent ion tolerance of 10 ppm. Iodoacetamide derivative of Cys, deamidation of Asn and Gln, oxidation of Met and phosphorylation of Ser, Thr and Tyr are specified as variable modifications. The MS/MS spectra of the identified phosphorylated peptides were manually inspected to ensure confidence in phosphorylation site assignment.

2.10 Phosphatase treatment (CHAPTER IV)

Gal83-GFP proteins were expressed in tomato protoplasts from pTEX for 22 hrs and were lysed in ice-cold extraction buffer containing 50 mM Tris-HCl pH 7.5, 100 mM NaCl, 0.1% Triton X-100, 2 mM DTT, 2.5% plant protease inhibitor cocktail (Sigma), and 6 μM epoxymicin (Enzo Life Sciences). Lysates were split into two fractions; one for phosphatase treatment and one for a no treatment control. Both fractions were adjusted to 3 mM $MnCl_2$ in λ phosphatase buffer (50mM HEPES pH7.5, 100mM NaCl, 2mM DTT, 0.01% Brij-35) in a final volume of 100 μl. The no treatment fraction was additionally adjusted to 2% phosphatase inhibitors (Sigma, phosphatase inhibitor cocktail 1). Reactions were started with the addition of 800 units of λ phosphatase (New England BioLabs), incubated at 30˚C for 30 min, and reactions

terminated by addition of 1x SDS-PAGE sample buffer. Samples were then resolved by 7.5% SDS-PAGE with a 1:500 bis-acrylamide:acrylamide ratio and analyzed by α-GFP western blotting.

2.11 Protoplast protein expression and cell death assays (CHAPTER IV)

The ORFs for *Gal83* and *Gal83*^{S26A} were cloned into the BamHI and SalI restriction sites of pTEX-eGFP (Ek-Ramos et al., 2010) to yield an in frame C-terminal GAL83-GFP fusion under the control of the 35S promoter. Cloning of Adi3 into pTEX-eGFP for an N-terminal tagged GFP-Adi3 was previously described (Ek-Ramos et al., 2010). The resulting constructs were purified using CsCl gradient centrifugation. Protoplasts were isolated from expanded leaves of 4-week-old PtoR tomato plants and transformed as previously reported (Devarenne et al., 2006; Ek-Ramos et al., 2010) using 8 x 10^5 protoplasts and 25 μg of plasmid DNA. For NaCl-induced cell death experiments transformed protoplasts expressing proteins for 18 hrs were suspended in 200 μl of WI buffer (0.5M mannitol, 4 mM MES pH5.7, 20mM KCl) with or without 200 mM NaCl, incubated in the dark at 25˚C, and aliquots taken over a 5.5 hr time-course. Cell viability was estimated by treating 30 μl protoplast aliquots with 0.05% Evans blue for 5 min and counting a minimum of 200 cells as previously described (Devarenne et al., 2006; Ek-Ramos et al., 2010). Cell viability estimates are a measurement of at least three independent transformation experiments. Protein expression was confirmed by western blot with 4 x 10^5 transformed protoplast resuspended in 1x SDS-PAGE sample buffer and boiled at 95˚C for 5 min. GFP-fusion

proteins were detected with an HRP-conjugated α-GFP antibody (Santa Cruz Biotechnology) at 1:1000.

2.12 Microscopy (CHAPTER V)

Transformed protoplasts were incubated in the dark for 16 hours at 22°C prior to visualization using a Zeiss Axioplan 2 fluorescent microscope. Nuclear staining was done by treating the protoplasts with 10μM HOECHST 33342 (Sigma), for 30 minutes. All cell localization experiments were carried out at least three independent times.

2.13 Cellular fractionation (CHAPTER V)

Nuclear fractionation was done as previously described (Ek-Ramos et al., 2010). Briefly, 400,000 transformed protoplasts were harvested 18-20 hours after transformation, and gradually lysed with three consecutive washes in Buffer A with centrifugation at 5,000g for 5 minutes at 4°C to pellet the nuclei. Isolated nuclei (N) were lysed in SDS Sample buffer and pooled supernatants were centrifuged at 100,000rpm for 1 hour at 4°C to separate soluble from insoluble proteins. The 100K supernatant was then concentrated either by using Amicon Ultra centrifugal filters (Millipore) or by acetone precipitation and resuspension in SDS sample buffer, whereas pellets with insoluble protein and membranes were resuspended in SDS sample buffer and sonication. The fractionation of membranes and soluble protein in the absence of detergent were essentially done as described in (Jung et al., 2002). Protein concentrations were quantified with Bio-Rad Protein Assay Kit and western blotting analysis was conducted using HRP-conjugated α-GFP antibody (Santa Cruz Biotechnology) at 1:1000.

CHAPTER III

UBIQUITINATION OF ADI3 BY THE RING UBIQUITIN LIGASE ADBIL

3.1 Rationale

Studies on the anti-apoptotic properties of mammalian PKB, suggest that it can suppress cell death by controlling the activation and expression of proapoptotic proteins, as well as by protecting proliferation and survival factors from PCD-triggered degradation (Brunet et al., 1999, Datta et al., 1997, Dijkers et al., 2000, Lee et al., 2008, Plas & Thompson, 2002). Based on this information and the knowledge that, like PKB, Adi3 is a Ser/Thr kinase that suppresses cell death, we sought to identify potential Adi3 phosphorylation substrates with the goal of finding proteins involved in PCD regulation in plants.

3.2 Adi3 interacts with AdBiL

In an effort to identify Adi3-interacting proteins a previous student carried out a yeast two-hybrid (Y2H) screen using a cDNA prey library that has been previously used to identify proteins that interact with the tomato resistance protein kinase Pto (Zhou et al., 1995). Approximately 15 million yeast transformants were screened for Adi3-interacting proteins using selection on Leu- plates and 1,366 transformants were followed-up in a *LacZ* screen. The prey inserts from 85 random positive clones were sequenced and screened against GenBank by BLAST for identification. Of these clones, SnRK1, encoding the α-subunit of the SnRK1 protein complex (CHAPTER IV) and a

RING-domain containing protein were identified four and six times, respectively (Devarenne, 2011).

The RING-domain protein obtained was named AdBiL (Adi3 Binding ligase). The partial Y2H *AdBiL* cDNA sequence was used in BLAST searches against the SOL Genomics Network (SGN) database (http://solgenomics.net/) to identify the full length ORF. The SGN Unigene *U580180* was found to be identical to *AdBiL* and this sequence was used to design primers for cloning the full length ORF, which was obtained from RT-PCR using leaf total RNA. Surprisingly no additional related E3 ligases were found in the tomato genome suggesting there are no redundant AdBiL genes. Using the Arabidopsis information resource (TAIR) databases, the closest sequence homologue to AdBiL was found to be the gene At3g05545 (similarity: 58.5%, identity: 46.6%, Figure 7). The next closest sequence identified corresponds to the red and far-red insensitive 2 protein (RFI2 – AT2g47700; similarity 39.9%, identity 29.5%; Figure 7). The full-length AdBiL ORF was used to confirm the interaction with Adi3 in a Y2H assay (Figure 8 A, B). The *Drosophila melanogaster* transcription factors BICOID and DORSAL were used as a control for false positive interactions. In the Y2H assay, AdBiL does not auto-activate when expressed either in the prey or bait vectors or in the presence or absence of BICOID or DORSAL Figure 8 A, B). A Y2H interaction is observed only when AdBiL is expressed in the presence of Adi3 regardless of its expression as prey or bait (Figure 8A). This interaction was found to be independent of the kinase activity of Adi3. For instance, AdBiL still displays interaction with Adi3 when expressed in the presence of

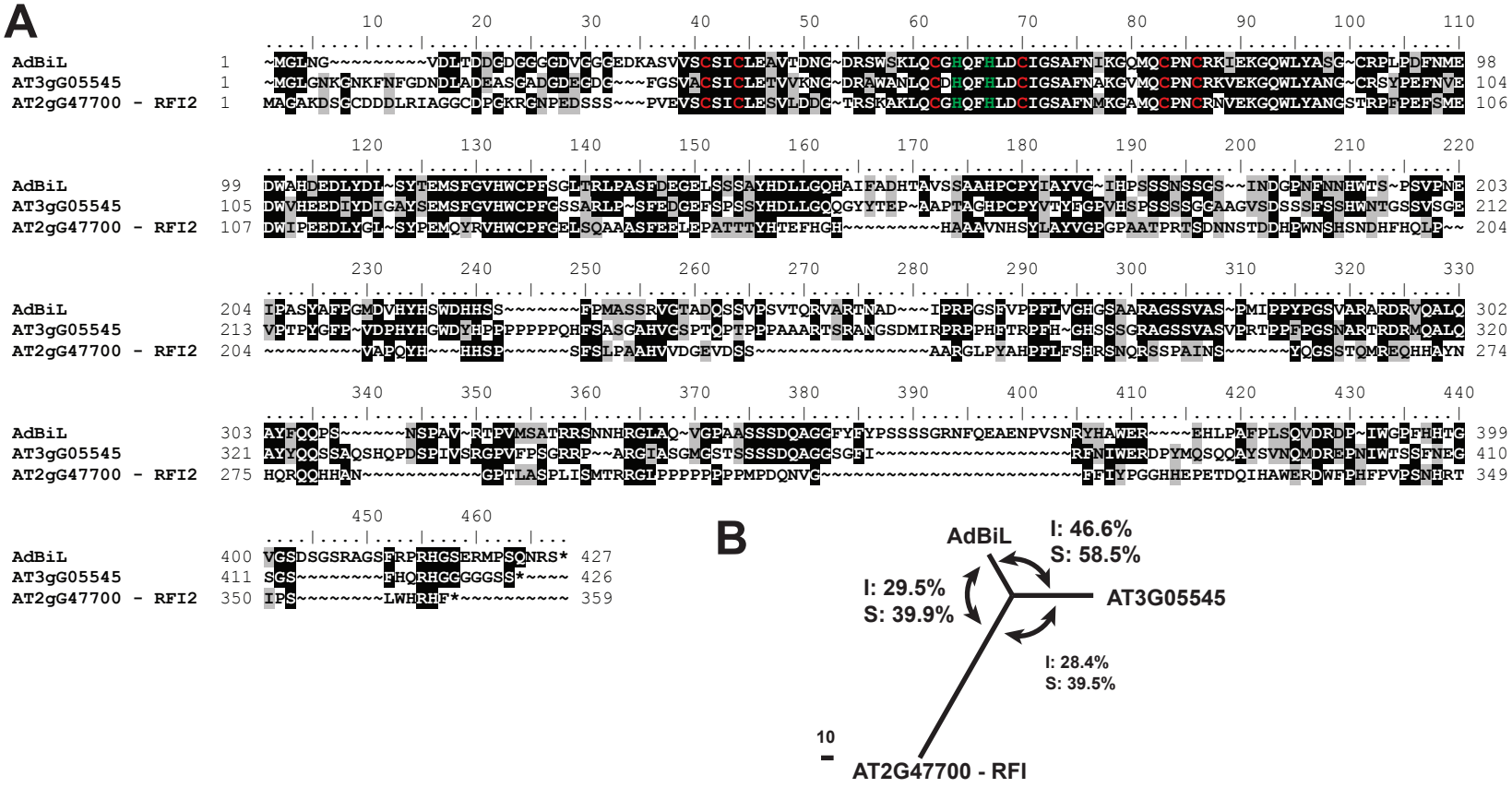

Figure 7. Arabidopsis thaliana AdBiL related sequences. A, alignment of AdBiL with *A. thaliana* related sequences At3g05545 and RFI2. Cys in red and His in green show the position of the C3H2C4 RING domain B, Phylogenetic comparison of AdBiL and *A. thaliana* related sequences. The tomato *AdBiL* DNA sequence was used for a BLASTX search against the Arabidopsis information resource (TAIR) DNA databases. The top three hits obtained correspond to: three RING-Ubox proteins; two of unknown function (At3g05545, E-value:1e-74 and At4g13490 E-value:1e-16) and one -the Red and Far-Red Insensitive 2 protein (At2g47700 , E-value:2e-54), which is involved in phytochrome and circadian signaling. Only At3g05545 and RFI are shown in the alignment, At4g13490 was excluded because of the reduced sequence similarity to AdBiL (Identity (I): 13.4%, Similarity (S): 23%). Protein and DNA sequences were aligned using ClustalW (Larkin et al., 2007) and the trees were produced using the maximum likelihood (DNAml, PROml) package in the BioEdit Sequence Alignment Editor (Hall, 1999). Trees were analyzed using Treeview (Page, 1996) and Adobe Illustrator.

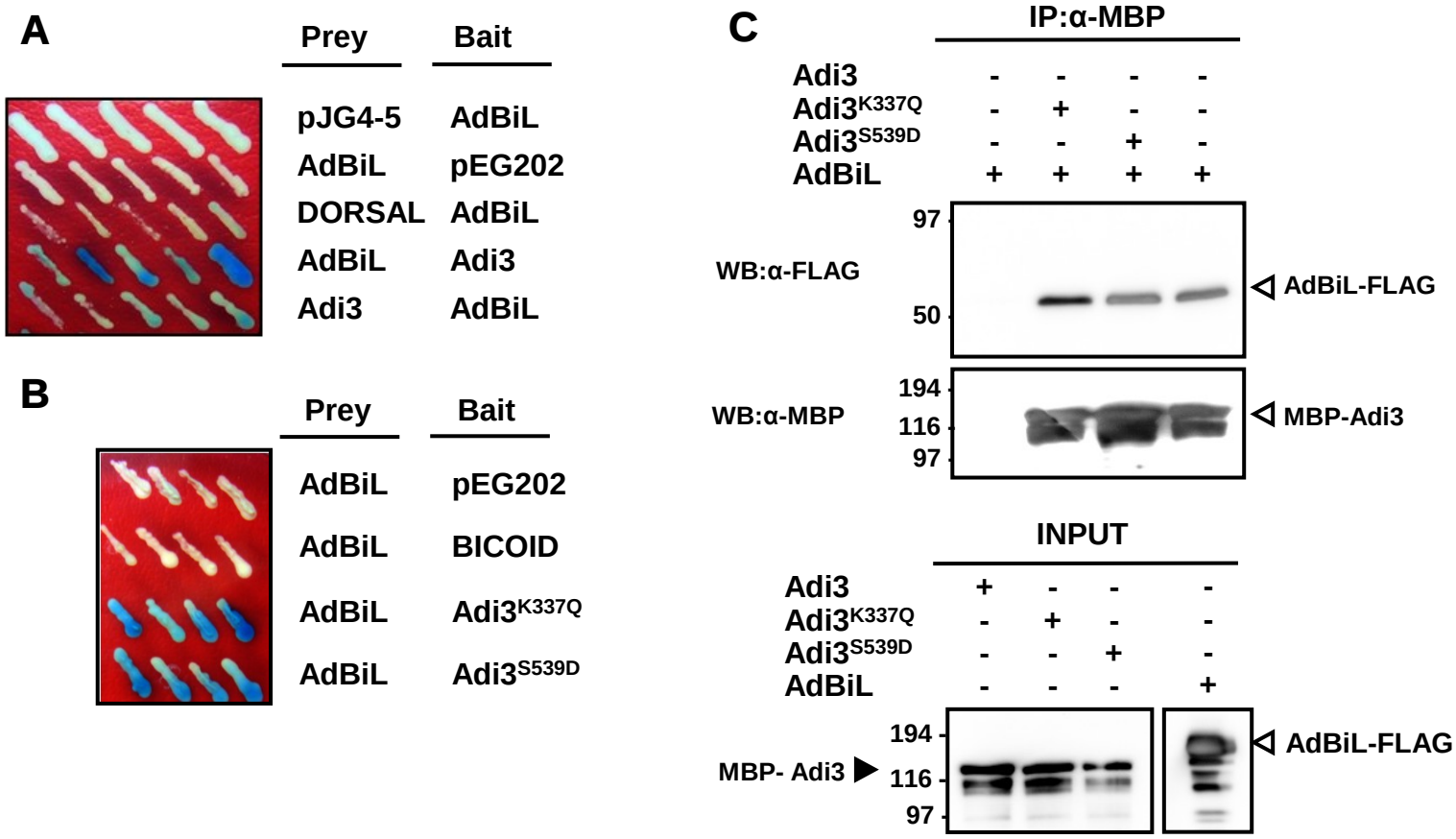

Figure 8. Adi3 interaction with AdBiL. AdBiL interacts with Adi3 (A) and Adi3 kinase activity mutants (B) in a Y2H assay. Interaction was estimated by the expression of *LacZ* on CM plates containing X-Gal (blue = interaction). For A and B, the *Drosophila melanogaster* proteins BICOID and DORSAL were used as negative interaction controls. C. Adi3 interacts with AdBiL in vitro. Bacterial lysates containing MBP and FLAG tagged proteins were bound to amylose resin for one hour at 4°C. Co-immunoprecipitated proteins were analyzed by western blotting with α-MBP and α-FLAG antibodies. Bottom panels, input for each fusion protein was analyzed by α-MBP and α-FLAG western blot.

kinase inactive (K337Q) and constitutively active (S539D) Adi3 mutants (Figure 8 B). These interactions were tested in an *in vitro* pull down experiment. AdBiL was expressed as a C-terminal FLAG tagged fusion and protein extracts were bound in the presence or absence of MBP-tagged Adi3. AdBiL was pulled down only in the presence of Adi3 and, in accordance to the Y2H results obtained, was found to be unaffected by the kinase activity of Adi3 (Figure 8 C). Collectively, this data suggest Adi3 can interact with AdBiL and this interaction does not rely on the kinase activity of Adi3. In support of these observations, an *in vitro* kinase assay revealed Adi3 does not *trans*-phosphorylate AdBiL (Figure 9).

3.3 AdBiL is an E3 ubiquitin ligase

AdBiL contains a characteristic RING finger domain. This motif contains an octet of Cys and His residues that bind zinc; RING domains can either have two His (RING-H2: C3H2C3) or one His (RING-HC: C3HC4) residues (Smalle and Vierstra, 2004). The motif found in AdBiL corresponds to a RING-H2 domain: Cys1-X(2)-Cys2-X(16)-X-His1-X(2)-His2-X(2)-Cys3-X(12)-Cys4- in which X can be any amino acid (Figure 7). RING domains are found in several protein families in which they function in mediating protein-protein or protein-DNA interactions (Freemont, 1993, Kraft, 2005, Smalle & Vierstra, 2004). Since the closely related AdBiL sequence At3g05545 has been shown to behave as an E3 ubiquitin ligase that specifically auto-ubiquitinates in the presence of the *A. thaliana* E2s *At*UBC8, *At*UBC11, and to a lesser extent *At*UBC10 (Kraft, 2005, Stone, 2005), we examined if AdBiL behaves as an E3 ligase.

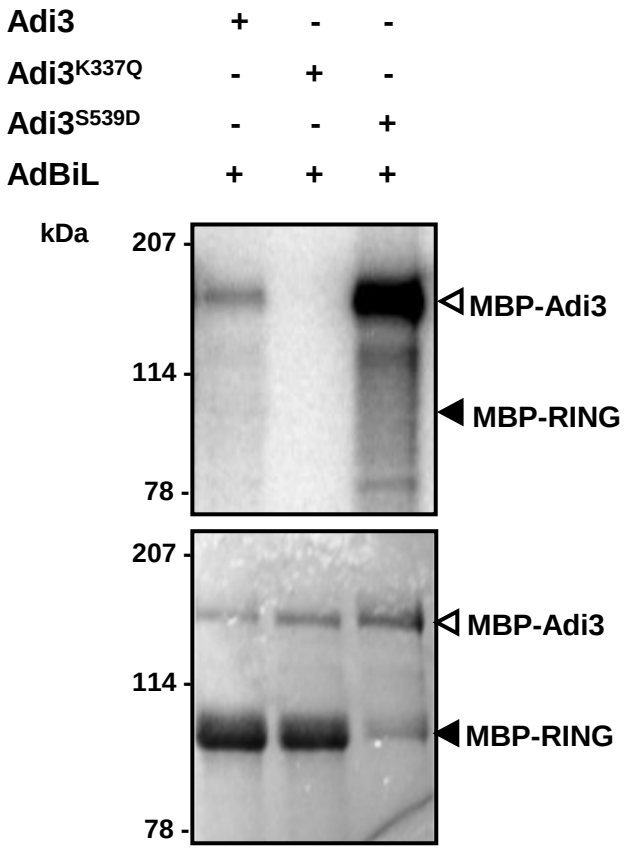

Figure 9. Adi3 does not phosphorylate AdBiL. Top panels: phosphorimage; bottom panel: coomassie stained gel. Recombinant MBP-AdBiL and MBP-Adi3 (S539D: kinase active; K337Q: kinase-inactive) were used to test the transphosphprylaton of AdBiL using γ-[^{32}P]ATP in *in vitro* kinase assays.

We conducted *in vitro* ubiquitination assays using MBP- tagged *At*UBA1 as the E1 enzyme and a set of human E2s. The transfer of FLAG tagged Ub to AdBiL was used as an indicator of the ubiquitination efficiency for the reaction.

Western blotting using α-FLAG antibodies revealed that no single human E2 was capable of transferring Ub to AdBiL (Figure 10, lanes 3 to 8). Two different possibilities for this result were considered. First, *in vitro* ubiquitination assays routinely use commercially available recombinant yeast (NP012712) or human (NP003325) E1s which are only 41% similar to the *A. thaliana* E1. Thus, it is possible the E1 sequence differences could interfere with the Ub loading onto human E2s. The reciprocal situation however does not hold true, as multiple studies have successfully used human and yeast E1s in order to activate plant E2s (Kraft, 2005). Second, the human E2s tested might be unable to interact with and transfer ubiquitin to AdBiL.

In order to overcome these possible situations, *A. thaliana* and tomato E2s were used instead. Recombinant GST- tagged *At*UBC8 and *At*UBC11 were produced and used in *in vitro* ubiquitination assays. *At*UBC8, but not *At*UBC11 was found to transfer Ub onto AdBiL as observed by the appearance of multiple bands in the α-FLAG western blotting (Figure 10, lanes 9, 10 top panel). These bands would correspond to the transfer of one or multiple Ub moieties to AdBiL. To the best of our knowledge, no previous characterization of tomato E2s has been done, so BLAST searches against the SGN databases were used to identify tomato E2s related to *At*UBC8 and *At*UBC11 using, not only these sequences, but closely related members of the *A. thaliana* group VI of E2s (Kraft, 2005). From this search, seven E2-related sequences were identified. The first

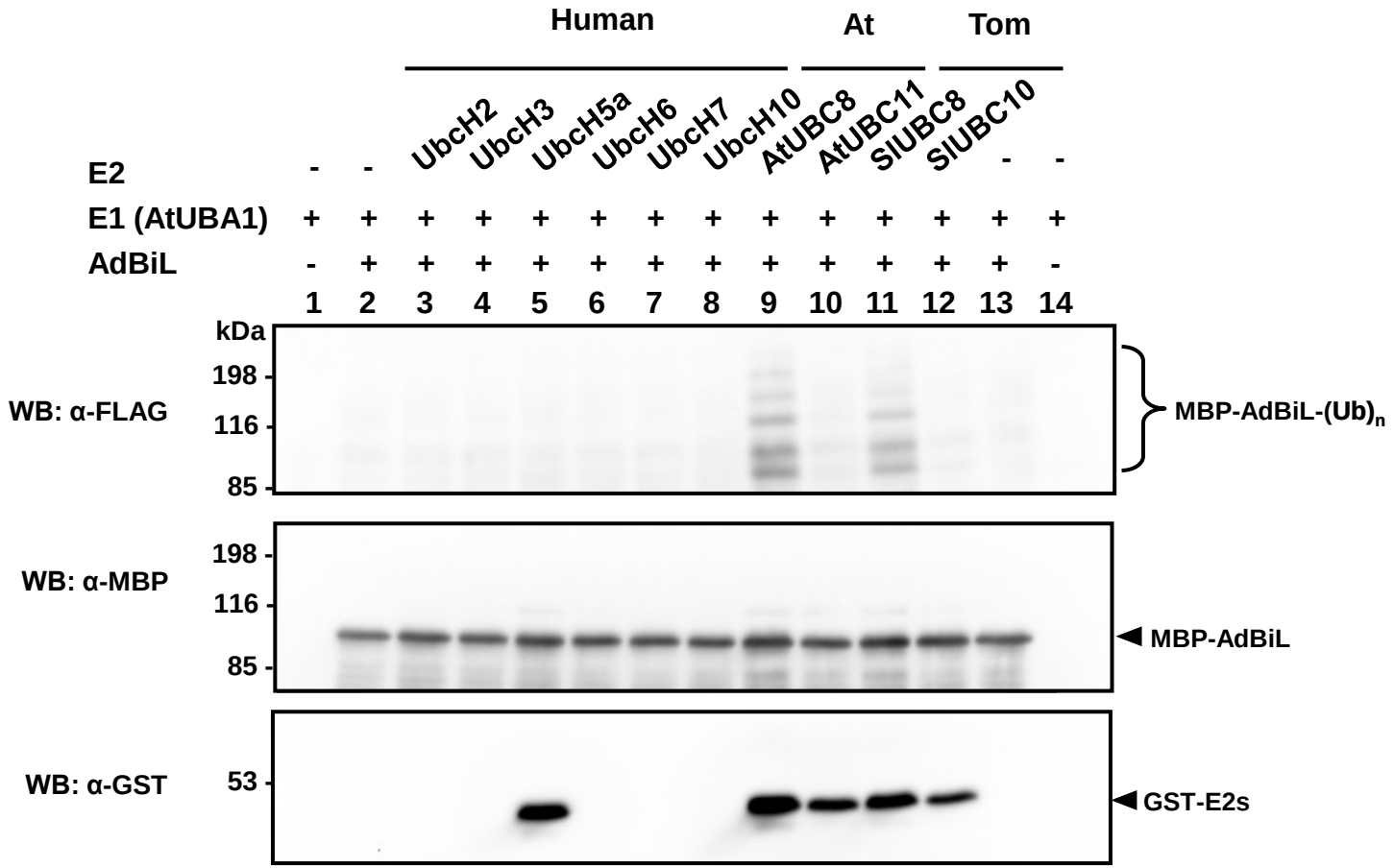

Figure 10. *At*UBC8 and *Sl*UBC8 are required for the ubiquitination of AdBiL. Recombinant human, *A. thaliana*, and tomato E2s were screened for their ability to transfer FLAG-tagged ubiquitin to MBP-tagged AdBiL in an *in vitro* ubiquitination assay containing the *A. thaliana* E1 *At*UBA1 as the ubiquitin activating enzyme. Ubiquitination reactions were separated in SDS-PAGE and western blot was conducted using α-FLAG to identify ubiquitinated proteins and α-MBP or α-GST antibodies to confirm assay inputs.

five were named *SlUBC*a-e and did not have any noticeable sequence identity to *A. thaliana* E2s (Figure 11C). The final two sequences were named *SlUBC8* and *SlUBC10* for sequence similarity (Figure 11C) and phylogenetic clustering with *AtUBC8* and *AtUBC10* (Figure 11A, B). The tomato *UBC8* and *UBC10* CDS were isolated from cDNA clones in the SGN EST library and tested for their ability to transfer Ub to AdBiL. Out of the two E2s, only *Sl*UBC8 was capable of transferring Ub to AdBiL (Figure 10, lane 11). Altogether these data indicate AdBiL is specifically ubiquitinated in the presence of *At*UBC8 or *Sl*UBC8.

3.4 AdBiL ubiquitinates Adi3

In order to determine if AdBiL mediates the transfer of Ub to Adi3 *in vitro* ubiquitination assays were carried out using *Sl*UBC8 as the E2 enzyme. As seen previously, *Sl*UBC8 is capable of ubiquitinating AdBiL (Figure 12, lane 4). The addition of Adi3 to the ubiquitination reaction caused a drastic increase in the Ub signal obtained when only E1, E2, and AdBiL are present (Figure 12, compare lanes 4 and 11). This would suggest that Adi3 is in fact ubiquitinated by AdBiL. However, since the background generated by ubiquitination of AdBiL made it difficult to determine if Adi3 is being ubiquitinated, we next used a GST pull down assay to selectively isolate GST-Adi3 from the assay after ubiquitination. This assay showed that Ub-FLAG was detected in several distinct Adi3 bands suggesting that Adi3 is ubiquitinated by AdBiL (Figure 13, lane 8). The presence of a few bands and a lack of a high molecular weight smear suggest Adi3 is not poly-ubiquitinated, but instead incorporates a few Ub moieties (Figure 13, Lane 8). Interestingly, the same ubiquitinated Adi3 bands were

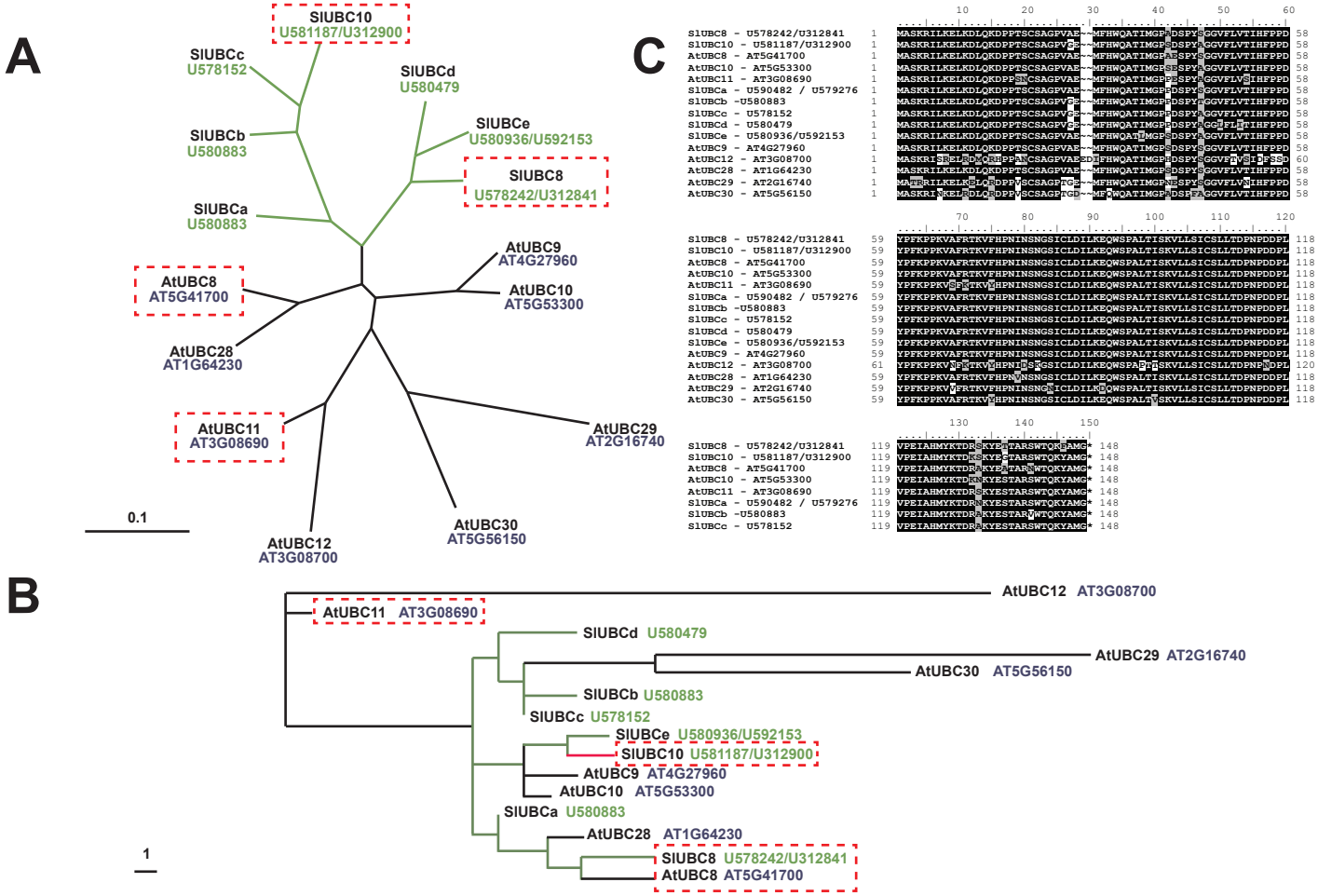

Figure 11. Tomato and *Arabidopsis thaliana group* VI E2 ubiquitin conjugating enzymes (UBCs). Phylogenetic comparison of related DNA (A) and (B) protein E2 ligases from tomato and *A. thaliana* belonging to the group VI of E2 ligases (Kraft, 2005). C, Alignment of the amino acid sequences for the generation of (B) is shown, amino acids identical and similar to the consensus sequence are highlighted in black and grey respectively with BLOSUM62 used as the similarity matrix. Lines on the bottom left of A and B indicate base or amino acid substitutions per site respectively. Tree clades in green lines correspond to tomato and black ones to the *A. thaliana* genes. Text in green and blue font shows the Sol Genomics Network and Arabidopsis Information Resource (TAIR) gene identifiers respectively. The genes used in this study are boxed in red-dashed lines.

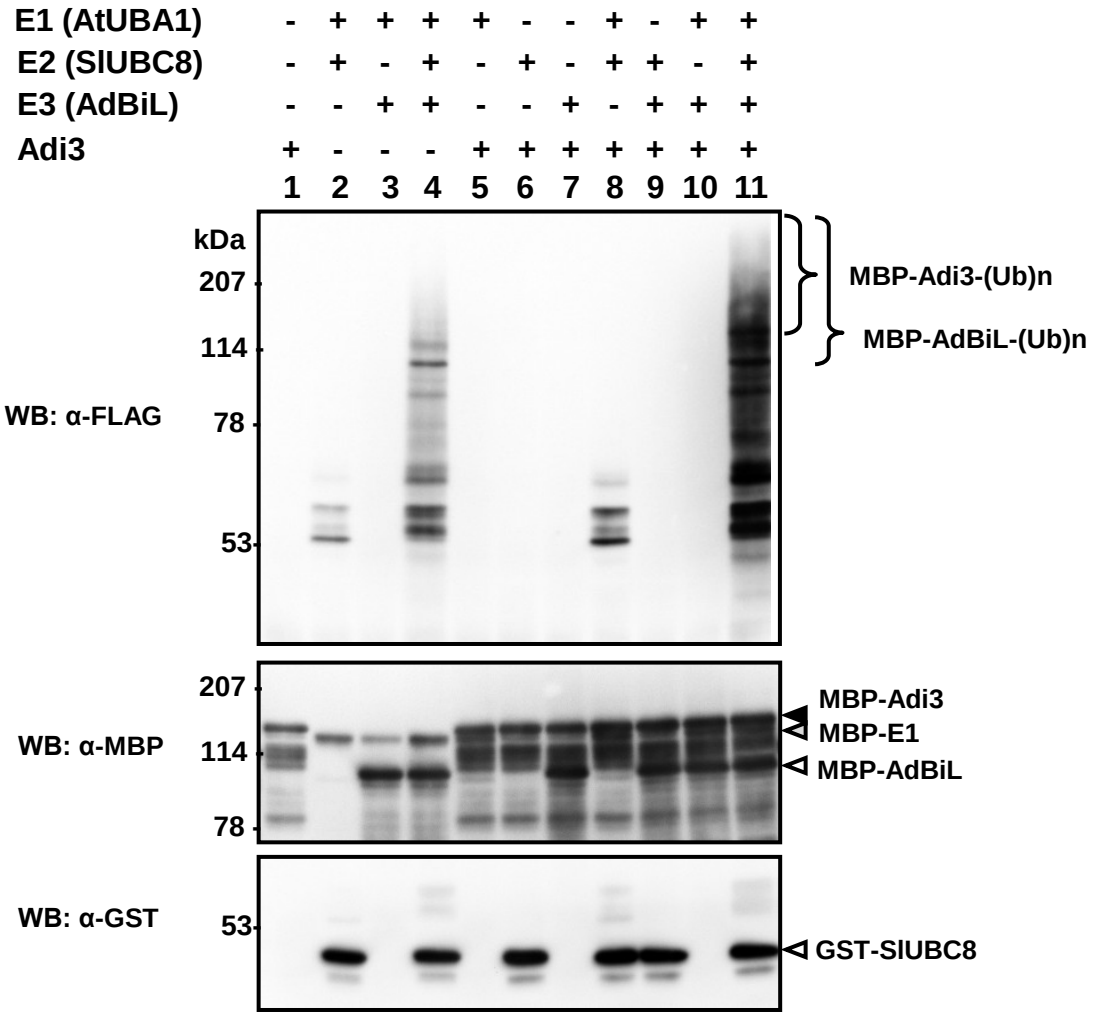

Figure 12. Adi3 is ubiquitinated by AdBiL. *In vitro* ubiquitination assay using MBP-*At*UBA1, GST-*Sl*UBC8, and MBP-AdBiL as the E1, E2, and E3 enzymes respectively. MBP-Adi3 was used as the final substrate for the ubiquitination reaction. Western blot was conducted using α-FLAG to identify the addition of ubiquitin-FLAG to substrates and α-MBP or α-GST antibodies to confirm assay inputs.
.

detected at a low level when only the E1, E2, or E3 were in the assay (Figure 13, lanes 1-6) suggesting there is a low level of Ub transfer to Adi3 without the full enzyme complex.

3.5 Adi3 is degraded in a cell-free system

An Adi3-specific antibody was developed in order to aid in the *in vitro* and *in vivo* study of Adi3 ubiquitination and degradation. A peptide encompassing residues 465 to 479 (IRISSDDPSKRGAAF) in Adi3 T-Loop extension, was synthesized and conjugated (KHL) to develop polyclonal antibodies (Figure 14C). Serum from rabbits before and after immunization was tested for its ability to recognize recombinant Adi3 in western blots (Figure 14A). Next, antibodies were affinity purified from serum using the immunization peptide in affinity chromatography, and the purified antibody was tested in western blotting with decreasing amounts of recombinant Adi3 (Figure 14B). The produced antibody immunoreacts with recombinant Adi3 in western blotting, however, the titer obtained was too low to detect any endogenous expression of Adi3 in plant samples (data not shown) and thus, was used only for *in vitro* experiments.

One of the most common and best characterized outcomes of ubiquitination is the degradation by the 26S proteasome (Smalle & Vierstra, 2004). In order to explore this possibility for Adi3 ubiquitination, we used a cell-free system to test the stability of Adi3 in tomato leaf extracts in the presence or absence of increasing concentrations (0 – 100μM) of the proteasomal inhibitor MG132 (Osterlund et al., 2000). Recombinant MBP-tagged Adi3 was incubated with tomato leaf extracts and protein degradation was estimated by western blotting α-Adi3 or α-MBP antibodies. Adi3 is rapidly degraded in

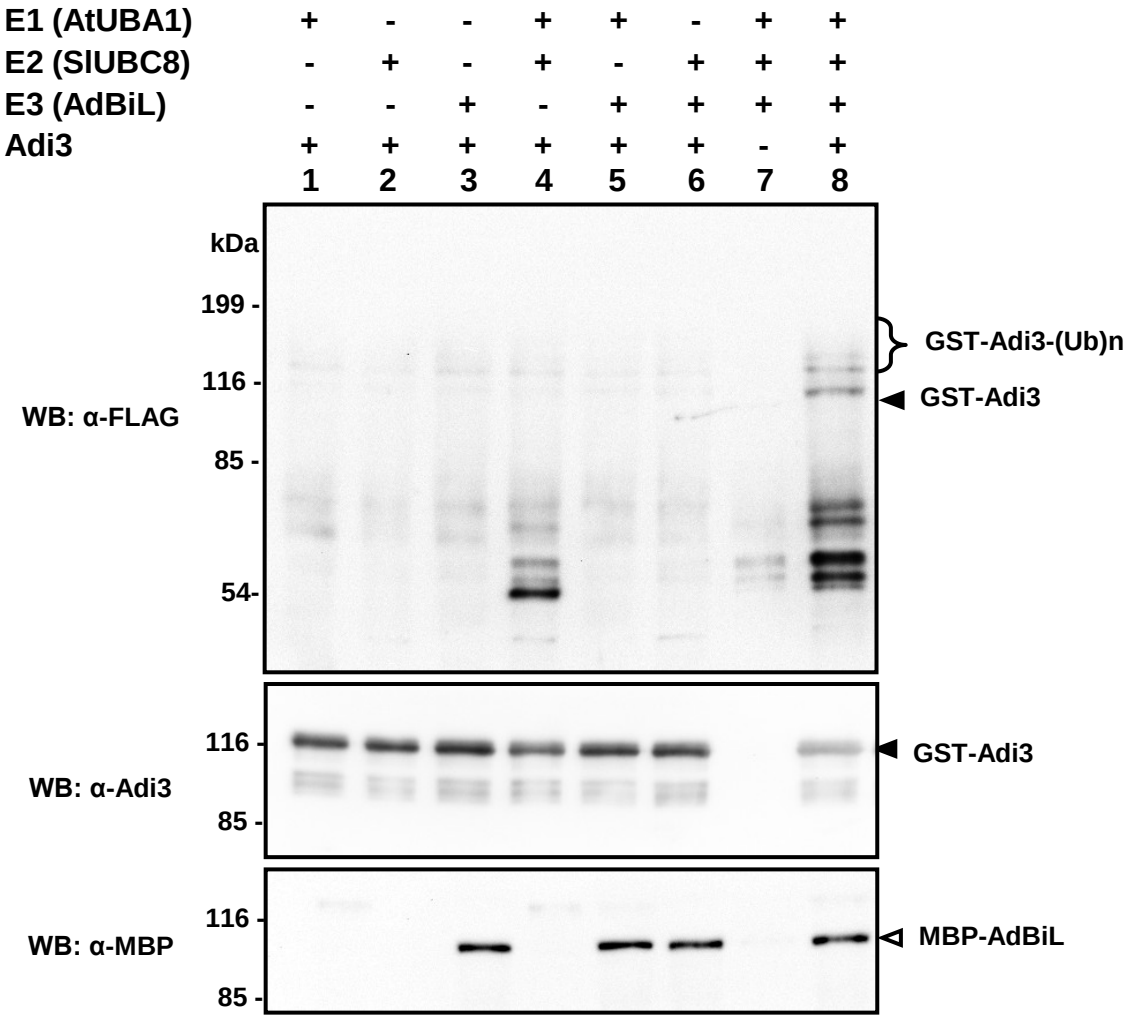

Figure 13. Pull down of Adi3 ubiquitinated by AdBiL. *In vitro* ubiquitinated GST-Adi3 was immunoprecipitated using glutathione resin and resolved by SDS-PAGE. Western blot was conducted using α-FLAG to identify ubiquitinated Adi3 (upper panel), α-Adi3 was used to detect the position of MBP-Adi3 in the blot (middle panel). The residual MBP-AdBiL bound to Adi3 was detected with α-MBP antibodies (lower panel).

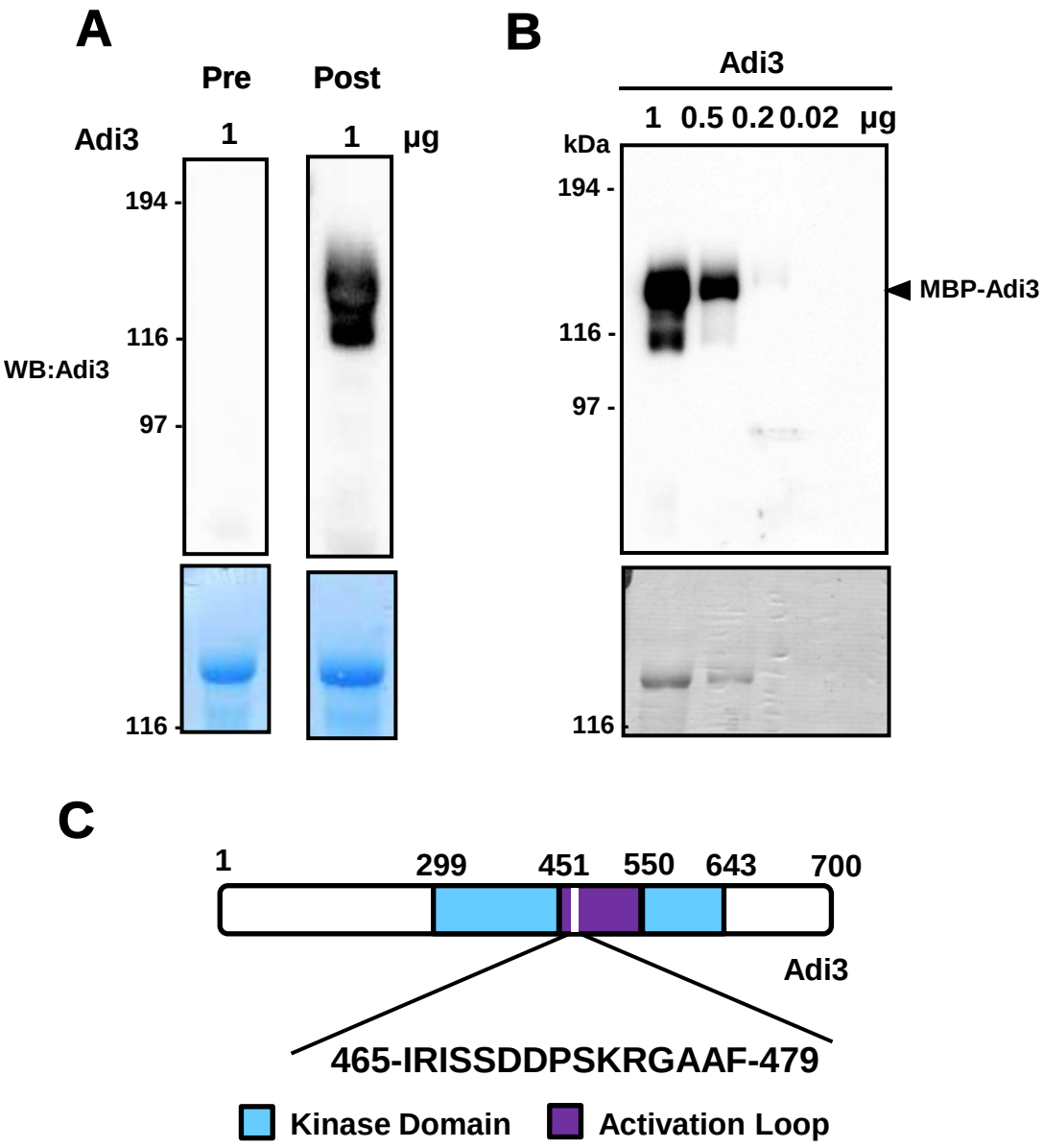

Figure 14. Production of α-Adi3 antibodies. A. Rabbit serum pre- and post-immunization with the Adi3 synthetic peptide IRISSDDPSKRGAAF was used in western blotting analysis of recombinant MBP-Adi3. B. Affinity purified α-Adi3 antibody was tested using decreasing concentration of MBP-Adi3. C. Location of the region in which the sequence used for the peptide design is located.

the presence of plant extract in the absence of MG132 and virtually no protein remained after 1.5 hours (Figure 15, lanes 1-4). Interestingly, the degradation of Adi3 is accompanied by the appearance of two cleavage products; one that immunoreacts with the α-Adi3 antibody at approximately 60kDa and one recognized by the α-MBP antibody at approximately 47kDa. The addition of MG132 partially protected Adi3 from being completely degraded after 3 hours of incubation, indicating that the 26S proteasome is involved in the degradation of Adi3. The level of Adi3 after MG132 treatment does not reach that at the start of the assay since MG132 is a reversible inhibitor of the proteasome and does not offer full protection against proteasomal degradation (Lee & Goldberg, 1996).

3.6 Discussion

We successfully reconstituted an *in vitro* ubiquitination system in which plant E1, E2s, and the AdBiL E3 were used. This system allowed us to demonstrate that AdBiL has ubiquitin ligase activity *in vitro*. The *in vitro* ubiquitination of AdBiL is an unexpected observation since RING ligases are thought to act as scaffolding molecules that bring substrates and E2s together rather than incorporating activated ubiquitin into themselves; an activity that had previously been exclusive to HECT domain containing E3 ligases (Smalle and Vierstra, 2004). Characterization of several RING containing ligases in cell-free systems shows however, that auto-ubiquitination is a common and perhaps auto-regulatory mechanism (Häkli et al., 2004). Both the significance of this auto-ubiquitination activity as well as the precise catalytic action of RING E3 ligases is not known (Dikic & Robertson, 2012).

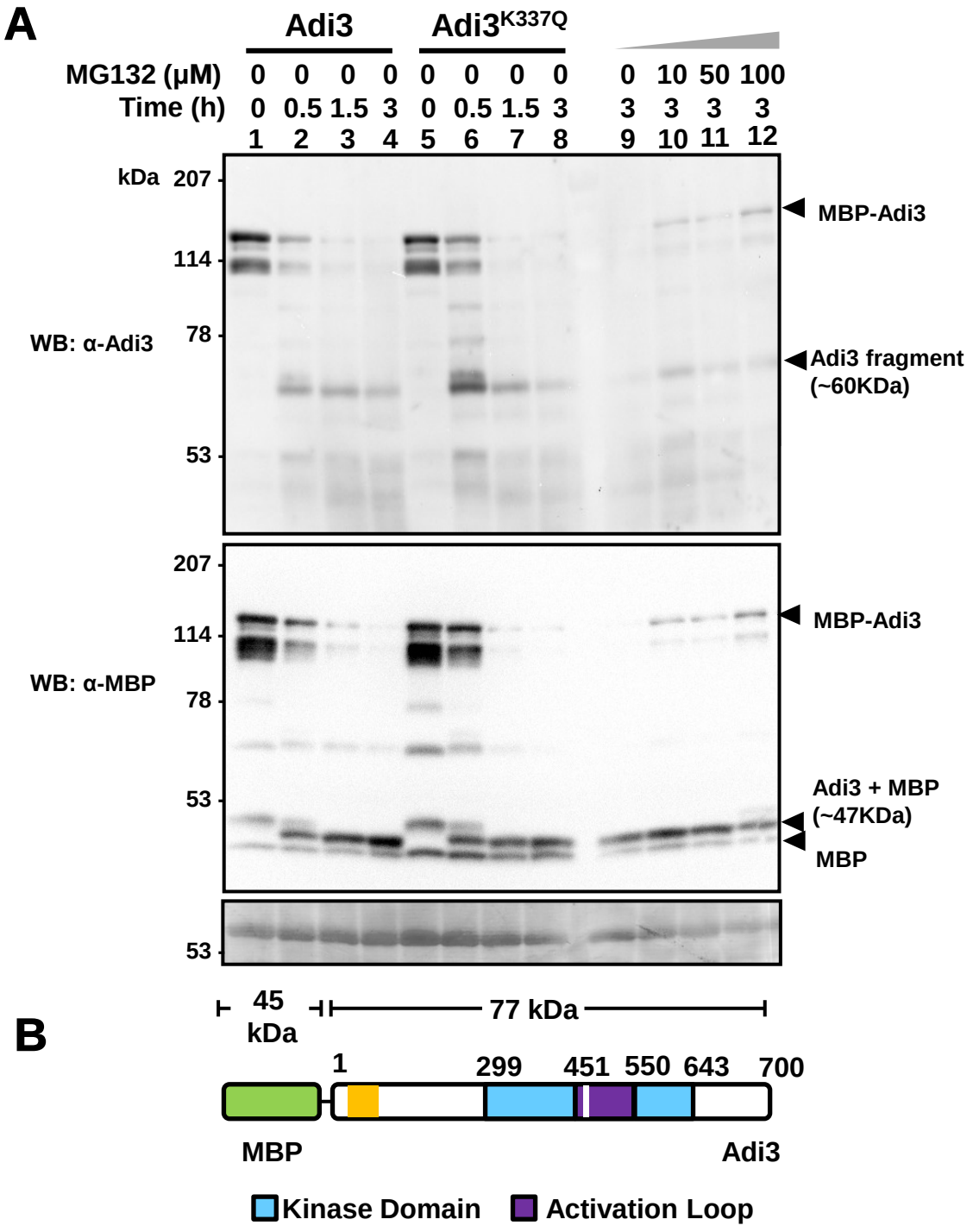

Figure 15. Cell-free degradation of Adi3. A. Recombinant Adi3 and kinase-inactive Adi3^{K337Q} are degraded in a proteasomal-dependent manner. MBP-Adi3 was incubated with tomato leaf protein extracts (10μg) for the indicated times at 30°C in the presence or absence of increasing MG132 concentrations. Adi3 levels were estimated by western blotting with α-Adi3 (upper panel) or α-MBP (middle panel) antibodies. Lower panel, coomasie stained blots indicating loading controls for plant extracts. B. Cartoon representation of MBP-Adi3 and the potential region in which Adi3 is cleaved (yellow).

The auto-ubiquitination of E3 ligases has been used previously in plant E3 ligases as an indicator of ubiquitination efficiency (Kraft, 2005, Stone, 2005) and in this study allowed for the identification of UBC8s from either tomato or *A. thaliana* as the cognate E2s for AdBiL. Surprisingly, even closely related E2s such as *At*UBC11 or *Sl*UBC10, failed to deliver Ub onto AdBiL. All of the E2s analyzed are nearly identical at the amino acid level, except for a few polymorphic sites at residues 42, 47, and 133 (Figure 11 C). Both UBC8s share an Ala at position 42 and a Ser at position 47, residues that are not conserved in either *Sl*UBC10 or *At*UBC11. This observation suggests that the differences in Ub transfer efficiency are caused by these two residues.

Ubiquitination assays with Adi3 by AdBiL suggest that only a few Ub moieties are transferred to Adi3 by AdBiL *in vitro*. The number of Ub molecules is often an indicator of the fate of the protein. For instance, mono-ubiquitination can affect intracellular localization, whereas polyubiquitination could trigger proteasomal degradation (Glickman & Ciechanover, 2002). Adi3 is rapidly degraded in the presence of plant extracts and this degradation is partially reversed with the addition of the 26S proteasome inhibitor MG132. This observation implies that Adi3 poly-ubiquitination is taking place, which was not seen in our *in vitro* assays. Thus, it is possible that *in vivo* AdBiL is capable of polyubiquitinating Adi3 or that another E3 ligase mediates Adi3 poly-ubiquitination. The direct involvement of AdBiL-mediated ubiquitination for the proteasomal degradation of Adi3 will require further testing.

The identification of cleavage products when Adi3 is incubated with plant extracts suggests that proteases are involved in the degradation process (Figure 15, lane

2 and 6). During apoptosis, the Adi3 functional homologue PKB is down-regulated at the protein level *via* ubiquitination and 26S proteasomal degradation. This degradation process depends on a type of pro-apoptotic Cys-dependent proteases known as caspases (Medina et al., 2005, Rokudai et al., 2000). Direct cleavage of PKB has been observed both *in vivo* and *in vitro* and inhibition of caspase activity *in vivo* completely abrogates the degradation of PKB (Medina et al., 2005). It is unclear whether caspases accomplish this by inactivating PKB de-ubiquitinating enzymes or activating enzymes involved in PKB ubiquitination. Furthermore, it is possible that caspase-mediated cleavage of PKB is a pre-requisite for its ubiquitination and proteasomal degradation (Medina et al., 2005). Using caspase inhibitors plants have been shown to possess caspase activity (Tsiatsiani et al., 2011). This activity is now asserted to a group of caspases known as metacaspases which are involved in several regulatory processes including PCD (Coll et al., 2010, Tsiatsiani et al., 2011). For instance, treatment with caspase inhibitors can block the HR caused by an incompatible interaction of tobacco and *P. syringae* pv. *phaseolicola* as well as the PCD induced by oxidative stress in soybean (del Pozo & Lam, 1998, Solomon et al., 1999). The catalytic cleavage of Adi3 by metacaspases could offer an explanation for the partial MG132 protection observed in Adi3 cell-free degradation experiments (Figure 15, compare lane 1 and 12). Further testing should address whether metacaspase inhibition protects Adi3 from degradation.

In addition to protein stability, ubiquitination is known to play an important role in protein trafficking (Pickart, 2001). For instance, PKB ubiquitination by the E3 ligase TRAF6 causes it to be recruited to the plasma membrane where it is activated by growth

factor stimuli (Yang et al., 2009). We have previously shown that Adi3 PCD suppressing activity depends on its ability to localize to the nucleus upon activation at the plasma membrane and this trafficking involves the association of Adi3 with punctuate membrane structures that resemble endosomal vesicles (Ek-Ramos et al., 2010). Since it is known that protein monoubiquitination is a target for endosomal localization (Pickart, 2001) it is possible that as an alternative to mediating its degradation, ubiquitination of Adi3 by AdBiL could be involved in regulating localization and the kinase activation state.

Ubiquitination of PKB is a versatile post-translational modification that regulates its multiple functions by means of affecting protein stability, localization, and activation state. The ubiquitination of Adi3 as well as its proteasomal dependent and independent degradation resemble mechanisms used in PKB regulation and provides additional evidence in support of Adi3 functioning similarly to PKB. Further characterization of Adi3 ubiquitination by AdBiL and its direct effect on protein stability and localization should help us understand the implication of this modification on Adi3 functions and in PCD.

CHAPTER IV

CHARACTERIZATION OF THE INTERACTION OF ADI3 WITH THE SNRK COMPLEX*

4.1 Identification of SnRK1 as an Adi3 interacting protein

In an effort to identify Adi3-interacting proteins we carried out a yeast two-hybrid (Y2H) screen using a cDNA prey library that has been previously used to identify proteins that interact with the tomato resistance protein kinase Pto (Zhou et al., 1995). Approximately 15 million yeast transformants were screened for Adi3-interacting proteins using selection on Leu- plates and 1,366 transformants were followed-up in a *LacZ* screen. The prey inserts from 85 random positive clones were sequenced and screened against GenBank by BLAST for identification. Of these clones, *SnRK*, encoding the α-subunit of the SnRK1 protein complex, was identified four times. The *SnRK* insert in the prey library was a partial ORF and a full-length ORF was identified by searching the tomato EST data base (http://solgenomics.net/) by BLAST with the *SnRK* Y2H fragment. Unigene SGN-U564382 was identified as containing a full-length *SnRK* ORF and this sequence was amplified from tomato leaf tissue RNA by RT-PCR. A BLAST search against GenBank with the full-length *SnRK* sequence showed that it was identical to a previously identified tomato *SnRK* cDNA (Bradford et al., 2003). In *A.*

---

* Portions of the following chapter have been reprinted with permission from: **Avila J, Gregory O, Su D, Deeter T, Chen S, Silva-Sanchez C, Xu S, Martin G, Devarenne T** (2012) The β-Subunit of the SnRK1 Complex Is Phosphorylated by the Plant Cell Death Suppressor Adi3. Plant Physiology **159:** 1277-1290.

thaliana, SnRK proteins are separated into three distinct families, SnRK1, SnRK2, and SnRK3 (Halford and Hey, 2009). BLAST and alignment comparison of the protein encoded by the *SnRK* sequence cloned here with members of the *A. thaliana* SnRK (*At*SnRK) family indicated that it belongs to the SnRK1 family (Figure 16). The tomato gene identified here will be referred to as *Sl*SnRK1 throughout this study.

The full-length *SlSnRK1* ORF was used to confirm the Y2H interaction with Adi3 and test the interaction with kinase activity mutants of Adi3. *Sl*SnRK1 does not autoactivate in the Y2H assay when expressed from either the prey or bait vectors (Figure 17A). Our previous studies have shown that mutation of the Pdk1 phosphorylation site on Adi3 (S539) to Asp ($Adi3^{S539D}$) confers constitutive kinase activity on Adi3, and mutation of Lys337 to Gln ($Adi3^{K337Q}$) in the ATP-binding pocket eliminates Adi3 kinase activity (Devarenne et al., 2006). The interaction of *Sl*SnRK1 with Adi3 was not abolished by either of these Adi3 kinase activity mutants (Figure 17A). This was the case whether the proteins were in the bait or prey vectors (Figure 17A) suggesting that kinase activity is not required for this interaction. The *Sl*SnRK1 and Adi3 interaction was also tested by immunoprecipitation. GST-Adi3 immunoprecipitated with an α-GST antibody was not capable of pulling down MBP, but was capable of pulling down MBP-*Sl*SnRK1 (Figure 17B, compare lanes 5 and 6).

4.2 Adi3 also interacts with two *Sl*SnRK1 β-subunits

We also tested if Adi3 could interact with two of the previously identified *Sl*SnRK1 β-subunits. First, cDNAs for these two tomato β-subunits, *Sl*Gal83 and *Sl*Sip1 (Bradford et al., 2003), were cloned. The reported *Sl*Gal83 sequence is not a full-length

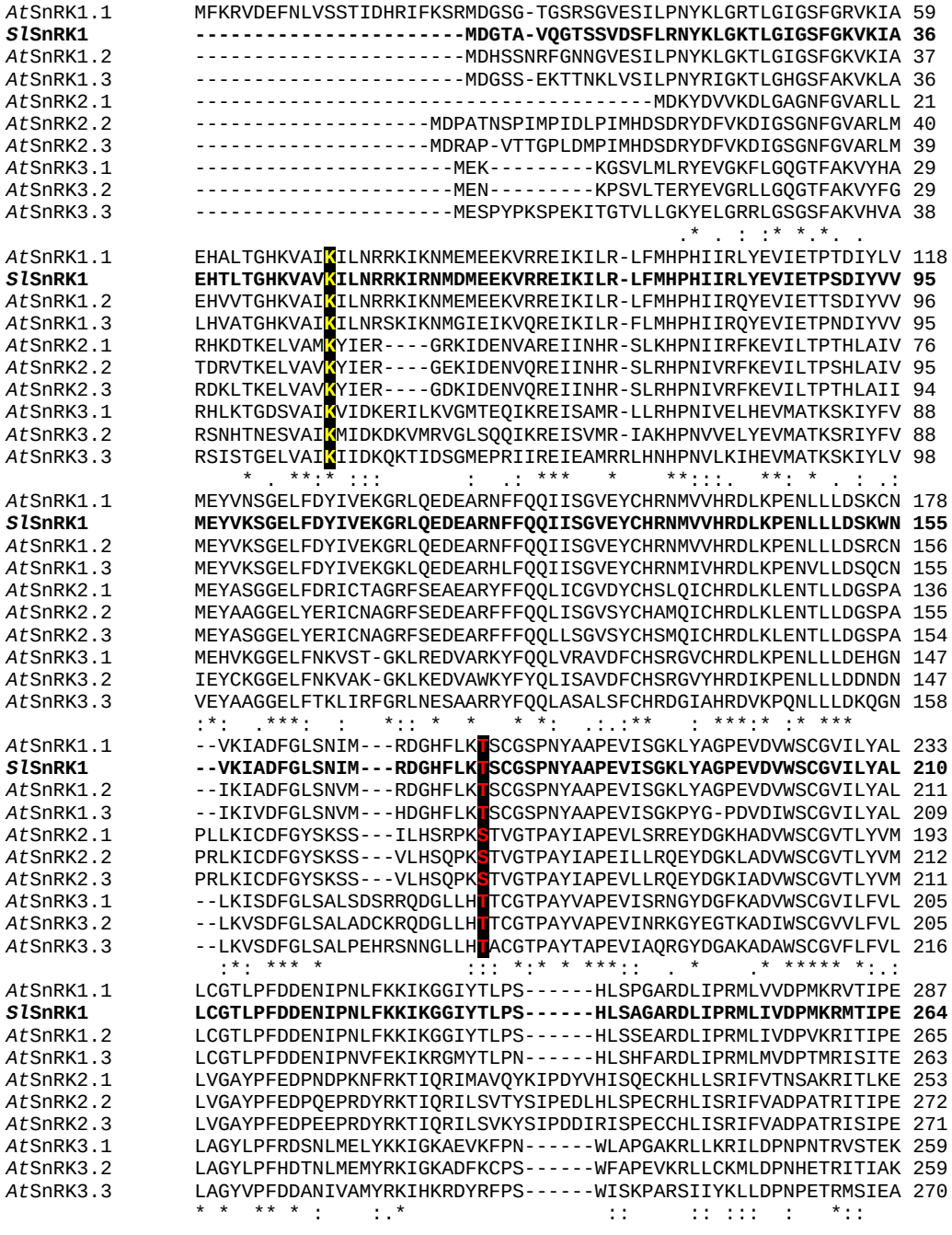

Figure 16. Alignment of SnRK proteins from tomato and *Arabidopsis thaliana*. The following SnRK sequences were aligned using clustalW: SlSnRK1 (shown in bold; AF143743), *At*SnRK1.1 (NP850488), *At*SnRK1.2 (NP974375), *At*SnRK1.3 (NP198760), *At*SnRK2.1 (P43292), *At*SnRK2.2 (Q39192), *At*SnRK2.3 (Q39193), *At*SnRK3.1 (P92937), *At*SnRK3.2 (Q9LYQ8), *At*SnRK3.3 (Q9SUL7). The invariant lysine responsible for ATP binding is shown in yellow outlined in black; K48 in SlSnRK1. The activation phosphorylation site, T175 in *Sl*SnRK1, is shown in red outlined in black.

```
AtSnRK1.1       IRQHPWFQAHLPRYLAVPPPDTVQQAKKI------------DEEILQEVINMGFDRNHL 334
SlSnRK1         IRLHPWFQAHLPRYLAVPPPDTTQQAKKI------------DEEILQEVVKMGFDRNNL 311
AtSnRK1.2       IRQHRWFQTHLPRYLAVSPPDTVEQAKKI------------NEEIVQEVVNMGFDRNQV 312
AtSnRK1.3       IRQHPWFNNHLPLYLSIPPLDTIDQAKKI------------EEEIIQNVVNIGFDRNHV 310
AtSnRK2.1       IKNHPWYLKNLPKELLESA-QAAYYKRDT------------SFSLQSVEDIMKIVGEAR 299
AtSnRK2.2       ITSDKWFLKNLPGDLMDEN-RMGSQFQEP------------EQPMQSLDTIMQIISEAT 318
AtSnRK2.3       IKTHSWFLKNLPADLMNES-NTGSQFQEP------------EQPMQSLDTIMQIISEAT 317
AtSnRK3.1       IMKSSWFRKGLQEEVK--ESVEEETEVDA----EAEGNASAEK----EKKRCINLNAFEI 309
AtSnRK3.2       IKESSWFRKGLHLKQKKMEKMEKQQVREATNPMEAGGSGQNENGENHEPPRLATLNAFDI 319
AtSnRK3.3       VMGTVWFQKSLEISEFQSSVFELDRFLEK-----------------EAKSSNAITAFDL 312
                :    *:   *               .                   .      :

AtSnRK1.1       IESLRNRTQNDGTVTYYLILDNRFR--ASSGYLGAEFQETMEG-TPRMHPAESVASPVSH 391
SlSnRK1         TESLRNRVQNEGTVAYYLLLDNRHR--VSTGYLGAEFQESMEYGYNRINSNETAASPVGQ 369
AtSnRK1.2       LESLRNRTQNDATVTYYLLLDNRFR--VPSGYLESEFQETTWF----------------- 353
AtSnRK1.3       VDSLANRIQNEATVAYHLILDNRNQNSVPNDPFQSKFKEISDGIFNSTLPVQNITSHVGH 370
AtSnRK2.1       NPAPSTSAVKSSGSGADEEEEEDVEAEVEEEEDDEDEYEKHVKEAQSCQESDKA------ 353
AtSnRK2.2       IPTVRNRCLDDFMADN-LDLDDDMDDFDSESEIDVDSSGEIVYAL--------------- 362
AtSnRK2.3       IPAVRNRCLDDFMTDN-LDLDDDMDDFDSESEIDIDSSGEIVYAL--------------- 361
AtSnRK3.1       ISLSTGFDLSGLFEKGEEKEEMRFTSNREASEITEKLVEIGKDLKMKVRKK-EHEWRVKM 368
AtSnRK3.2       IALSTGFGLAGLFGDVYDKRESRFASQKPASEIISKLVEVAKCLKLKIRKQGAGLFKLER 379
AtSnRK3.3       ISLSSGLDLSGLFER-RKRKEKRFTARVSAERVVEKAGMIGEKLGFRVEKK--EETKVVG 369
                                :              .

AtSnRK1.1       RLPGLMEYQGVGLRSQYPVERKWALGLQSRAHPREIMTEVLKALQDLNVCWKKIGHYNMK 451
SlSnRK1         RFPGIMDYQQAGAR-QFPIERKWALGLQSRAHPREIMTEVLKALQELNVCWKKIGQYNMK 428
AtSnRK1.2       --------------------------QSYAHT--------------------------- 359
AtSnRK1.3       SFSALYGLKSNVKD-----DKTWTLGLQSQGSPYDIMTEIFKALQNLKICWKKIGLYNIK 425
AtSnRK2.1       ------------------------------------------------------------
AtSnRK2.2       ------------------------------------------------------------
AtSnRK2.3       ------------------------------------------------------------
AtSnRK3.1       SAEAT----VVEAEVFEIAPSYHMVVLKKSGGDTAEYKRVMK--ESIRPALIDFVLAWH- 421
AtSnRK3.2       VKEGKNGILTMDAEIFQVTPTFHLVEVKKCNGDTMEYQKLVE--EDLRPALADIVWVWQG 437
AtSnRK3.3       LGKGR---TAVVVEVVEFAEGLVVADVKVVVEGEEEEEEVESHWSELIVELEEIVLSWHN 426


AtSnRK1.1       CRWVPNSS--ADGMLSNSMHDNNYFGDESSIIENEAAVKSPNVVKFEIQLYKTRDDKYLL 509
SlSnRK1         CRWVPSLPGHHEGMGVNSMHGNQFFGDDSSIIENDGATKLTNVVKFEVQLYKTREEKYLL 488
AtSnRK1.2       ------------------------------------------------------------
AtSnRK1.3       CRWVRSFAYYKN----------------HTIEDECAIILPTVIKFEIQLYKVREGKYLL 468
AtSnRK2.1       ------------------------------------------------------------
AtSnRK2.2       ------------------------------------------------------------
AtSnRK2.3       ------------------------------------------------------------
AtSnRK3.1       ------------------------------------------------------------
AtSnRK3.2       EKEKEEQLLQDEQGEQEPS--------------------------------------- 456
AtSnRK3.3       ------------------------------------------------------------


AtSnRK1.1       DLQRVQGPQFLFLDLCAAFLAQLRVL 535
SlSnRK1         DLQRLQGPQFLFLDLCAAFLAQLRVL 514
AtSnRK1.2       -------------------------
AtSnRK1.3       DILRIDGPQFIFFDLCVAFLRELGVL 494
AtSnRK2.1       -------------------------
AtSnRK2.2       -------------------------
AtSnRK2.3       -------------------------
AtSnRK3.1       -------------------------
AtSnRK3.2       -------------------------
AtSnRK3.3       -------------------------
```

Figure 16. Continued

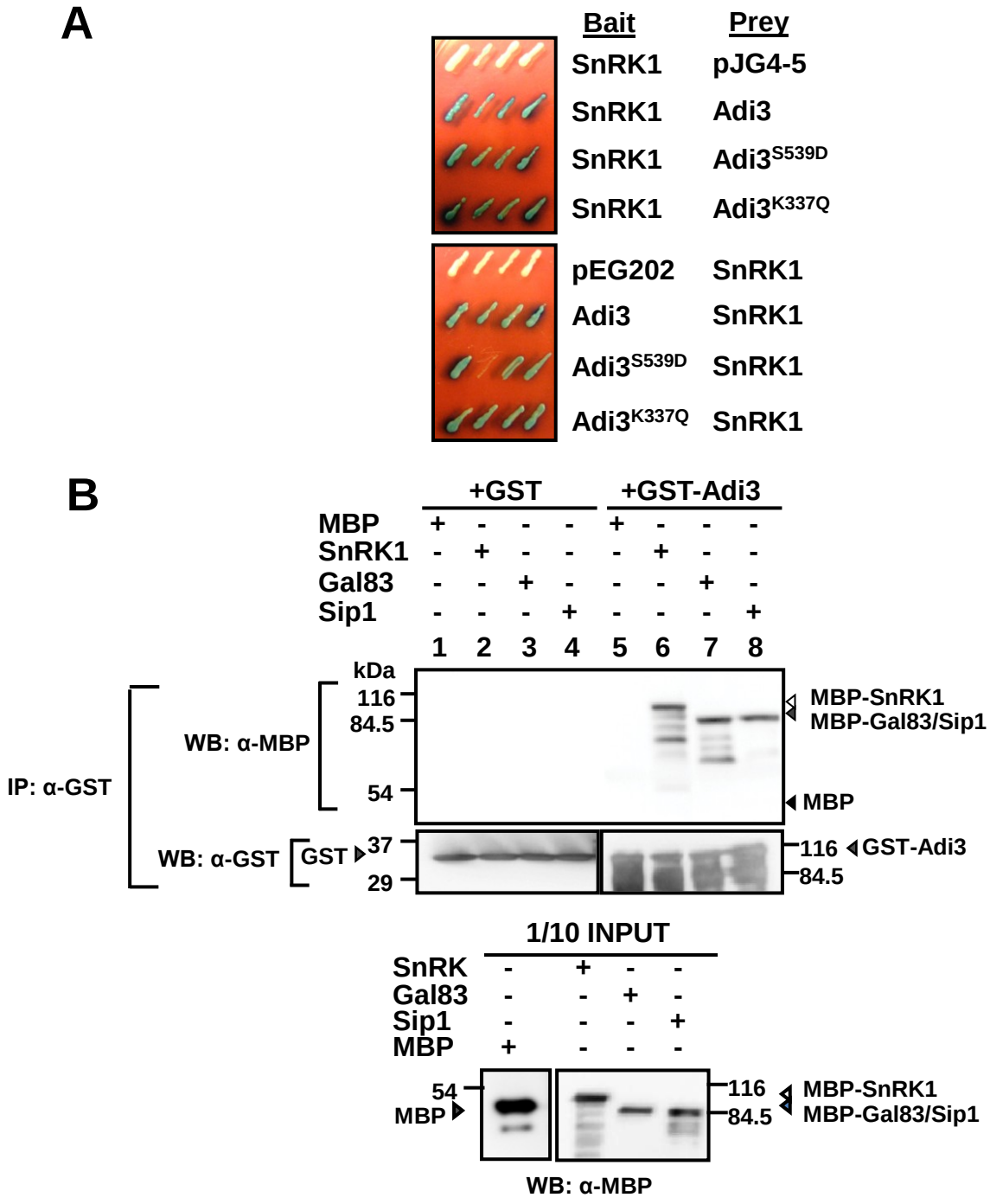

Figure 17. Adi3 interaction with SnRK1 complex members. A, Adi3 and *Sl*SnRK1 interact in the Y2H assay. The indicated bait and prey constructs were expressed in yeast and tested for expression of the *lacZ* gene on X-Gal plates (blue = interaction). B, Adi3 interacts with SnRK1 complex members by immunoprecipitation. Top panels, GST or a GST-Adi3 fusion protein was incubated at 4˚C for 1 hr with MBP fusion proteins of *Sl*SnRK1, *Sl*Gal83, or *Sl*Sip1, immunoprecipitated with an α-GST antibody, and the proteins associated with GST-Adi3 analyzed by α-MBP western blot. Bottom panels, a 1/10 aliquot of each MBP fusion protein was analyzed by α-MBP western blot for loading control.

ORF and is missing a portion of the 5' end (Bradford et al., 2003). Thus, we used the tomato EST and genomic databases to identify the remaining 5' end of the *Sl*Gal83 sequence and to make sure the published *Sl*Sip1 sequence contained the full-length ORF.

A BLAST search of the tomato ESTs with the published *Sl*Gal83 sequence identified a full-length ORF within unigene SGN-U564868, which indicated the published *Sl*Gal83 sequence was missing 51 bp from the 5' end, or 17 N-terminal amino acids (Figure 18). The original *Sl*Gal83 sequence also had a mis-identification of nucleotide 58 as guanine when EST and genomic sequence indicates nucleotide 58 is a cytosine (not shown). The full-length *Sl*Gal83 ORF was amplified by PCR from SGN clone cTOF-18-D18.

A BLAST search with the published *Sl*Sip1 sequence (Bradford et al., 2003) against the tomato genomic database identified the *Sl*Sip1 gene within genomic locus AC186291.2. The deduced ORF from this genomic sequence was longer than the published sequence and indicated the published *Sl*Sip1 ORF was missing 177 bp of 5' sequence, or 59 N-terminal amino acids (Figure 18; Figure 19A). The full-length ORF sequence of *Sl*Sip1 was cloned by RT-PCR based on the deduced ORF sequence confirming the presence of this transcript in tomato (Figure 19A). Both of these cloned full length tomato sequences were used for all subsequent studies reported here.

The interaction of *Sl*Gal83 and *Sl*Sip1 with Adi3 was tested by α-GST IP as with *Sl*SnRK1. The results indicated that both β-subunits were capable of interacting with Adi3 (Figure 17, lanes 7, 8). For reasons that will become apparent below, we made *Sl*Gal83 the main subject of our research and have shown that Adi3 also interacts with

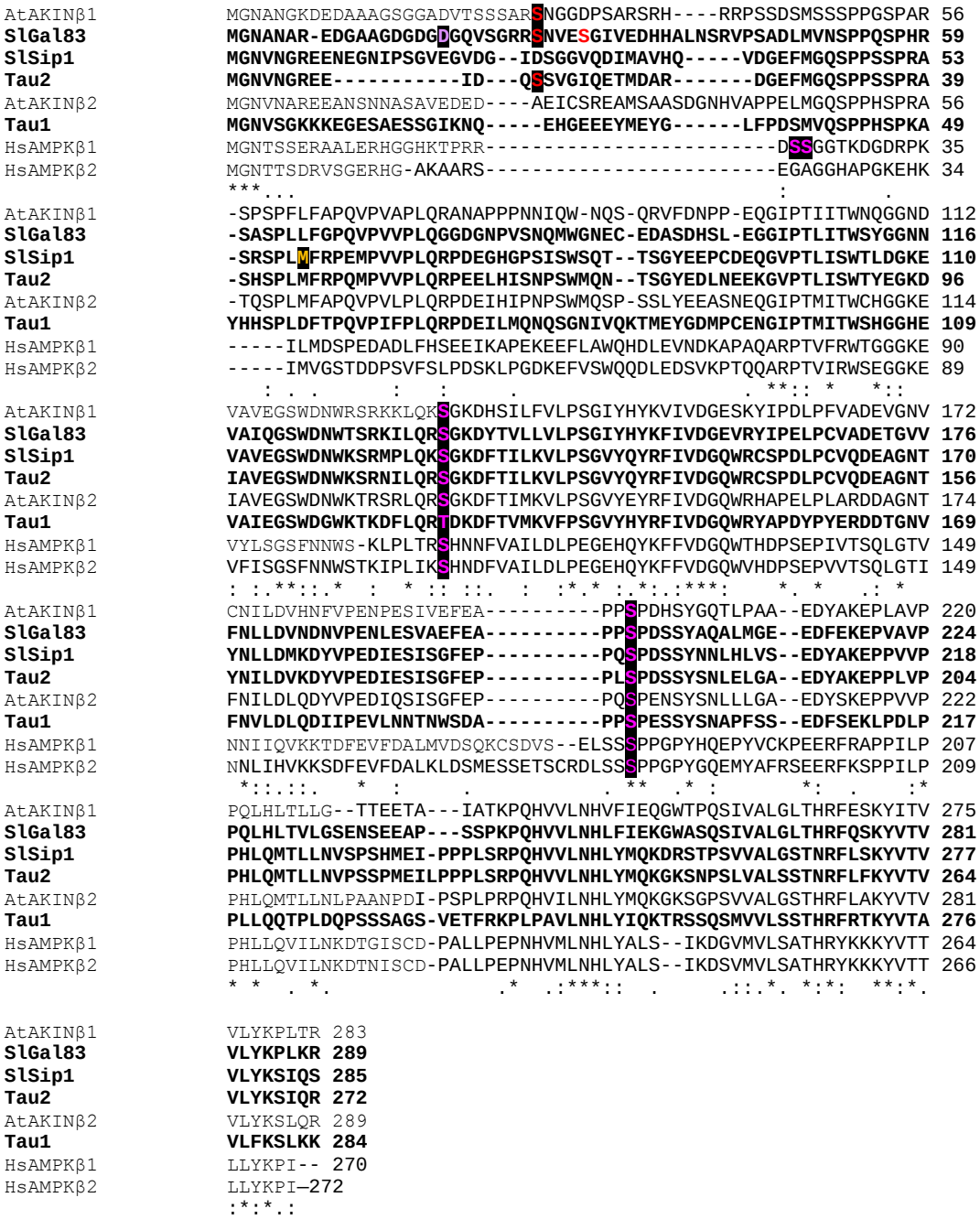

Figure 18. Alignment of SnRK complex β-subunits. The following β-subunit protein sequences were aligned using clustalW: *Sl*Gal83 (JF895513), *Sl*Sip1 (JF8955212), *Tau*1 (JQ846034), *Tau*2 (JQ846035), *At*AKINβ1 (AAM6584), *At*AKINβ2 (CAB64719), HsAMPKβ1 (NP_006244), and HsAMPKβ2 (NP_005390). The N-terminal end of the original *Sl*Gal83 (D18) is shown in purple and outlined in black. The Adi3 phosphorylation site on *Sl*Gal83 (S26) and the MS identified phosphorylation site S30 are shown in red outlined in black. The originally identified *Sl*Sip1 start site (M33) is shown in orange outlined in black. The HsAMPKβ1 phosphorylation sites are shown in pink outlined in black

.

*Sl*Gal83 in the Y2H assay (Figure 19B). These results indicated that Adi3 is capable of interacting with several members of the *Sl*SnRK1 complex.

4.3 Adi3 phosphorylates *Sl*Gal83

Since Adi3 interacts with the *Sl*SnRK1 α-subunit it is possible that Adi3 acts as an upstream activator of *Sl*SnRK1. Thus, we analyzed Adi3 kinase activity toward *Sl*SnRK1. First, a kinase-inactive *Sl*SnRK1 was generated by mutating Lys48 to Gln, *Sl*SnRK1^{K48Q} (Figure 20, lane 12). This Lys corresponds to the invariant Lys45 in AMPK required for ATP binding (Dyck et al., 1996; Figure 16). Phosphorylation of *Sl*SnRK1^{K48Q} by the constitutively-active Adi3^{S539D} was not seen (Figure 20A, lane 14), suggesting Adi3 is not an upstream activator of *Sl*SnRK1.

Because Adi3 can interact with *Sl*Gal83 and *Sl*Sip1 it is possible that Adi3 can phosphorylate these β-subunits. The β-subunits from yeast and mammals are known to be phosphorylated (Mangat et al., 2010, Mitchelhill et al., 1997, Warden et al., 2001), while phosphorylation of the plant β-subunits has not been reported to date. Thus, the ability of Adi3 to phosphorylate the *Sl*Gal83 and/or *Sl*Sip1 β-subunits was examined. Kinase assays showed that both wild-type Adi3 and constitutively-active Adi3^{S539D} were able to phosphorylate *Sl*Gal83 with Adi3^{S539D} phosphorylating *Sl*Gal83 ~ 6 times more than wild-type (Figure 20A, compare lanes 6 and 8). Interestingly, neither form of Adi3 was capable of phosphorylating *Sl*Sip1 (Figure 20A, lanes 9-11) even though Adi3 can interact with *Sl*Sip1 (Figure 17B, lane 8). This would suggest there is some catalytic specificity of Adi3 towards *Sl*Gal83 over that of *Sl*Sip1.

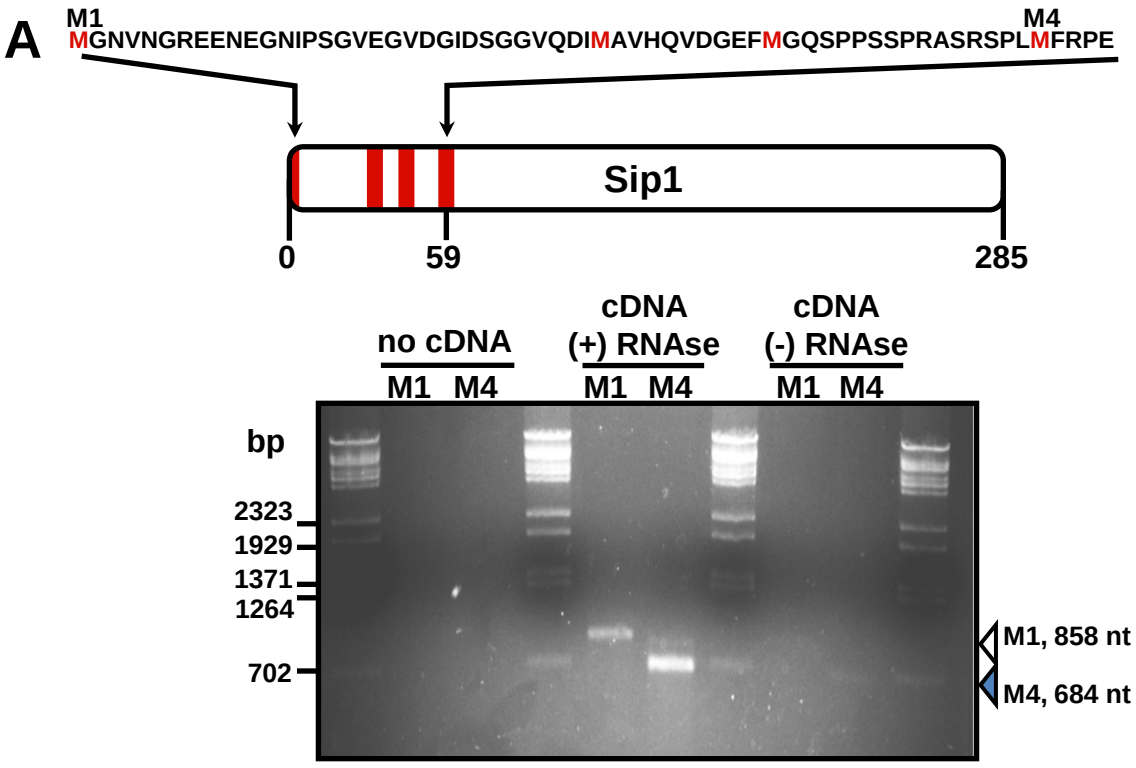

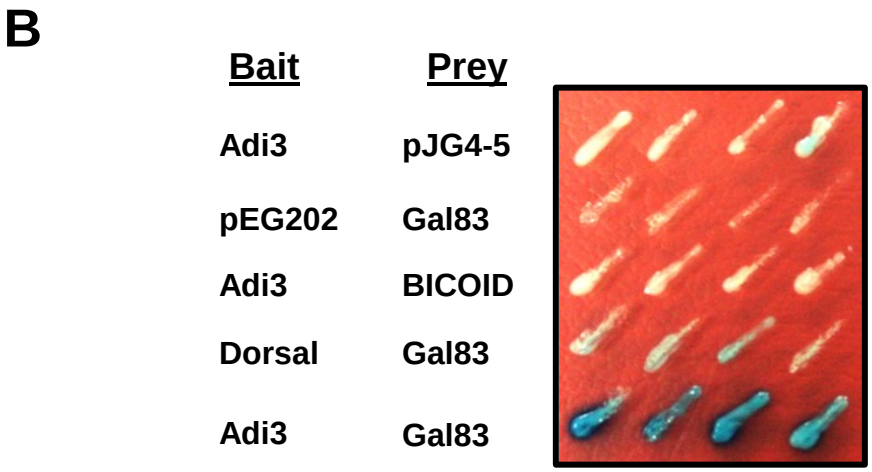

Figure 19. RT-PCR amplification of *Sl*Sip1 and Adi3/*Sl*Gal83 yeast two-hybrid interaction. A, Schematic of *Sl*Sip1 showing originally identified start site (M4) and newly identified start site (M1). Also shown below is the RT-PCR gel showing amplification of the larger *Sl*Sip1 from tomato leaf total RNA. B, Yeast two-hybrid interaction between Adi3 and Gal83. The indicated bait and prey constructs were tested in a standard yeast two-hybrid assay for expression of the *lacZ* gene on X-Gal plates.

The phosphorylation of *Sl*Gal83, but not *Sl*Sip1 by Adi3, lead us to search the tomato genome for additional *Sl*SnRK1 β-subunits that may be phosphorylated by Adi3. The *Sl*Gal83 sequence was used to search the tomato genome by BLAST against the SGN Tomato Combined Database (whole genome, BAC, and unigene sequences) and two additional sequences with high similarity to *Sl*SnRK1 β-subunits were discovered and termed Tau1 and Tau2 (Figure 18). Additionally, BLAST of the Tau1 and Tau2 proteins against GenBank returned the *A. thaliana* β-subunit AKINβ2 (E values 1E-90 and 3E-136, respectively) as a top hit suggesting these proteins are SnRK1 β-subunits. The Tau1 and Tau2 cDNAs were amplified from leaf RNA by RT-PCR (Figure 21) and the proteins derived from these ORFs appear to be more related to *Sl*Sip1 and the *A. thaliana* β-subunit AKINβ2 than to *Sl*Gal83 (Figure 20B). Next, the phosphorylation of Tau1 and Tau2 by Adi3^{S539D} was tested using *in vitro* kinase assays, which showed that Adi3 did not phosphorylate Tau1 or Tau2 to a significant level and only phosphorylated *Sl*Gal83 (Figure 20C).

Since Adi3 only phosphorylates *Sl*Gal83 and not the other β-subunits we focused on *Sl*Gal83, and confirmed that it is a functional SnRK1 β-subunit using yeast complementation that was not done in the initial *Sl*Gal83 study (Bradford et al., 2003). In yeast the Snf1 complex functions to allow growth on alternative carbon sources such as sucrose (Carlson et al., 1981, Polge & Thomas, 2007) and loss of the three yeast β-subunits (*Sc*Sip1, *Sc*Sip2, and *Sc*Gal83; *sip1Δsip2Δgal83Δ* yeast) does not allow for growth on sucrose (Schmidt & McCartney, 2000).

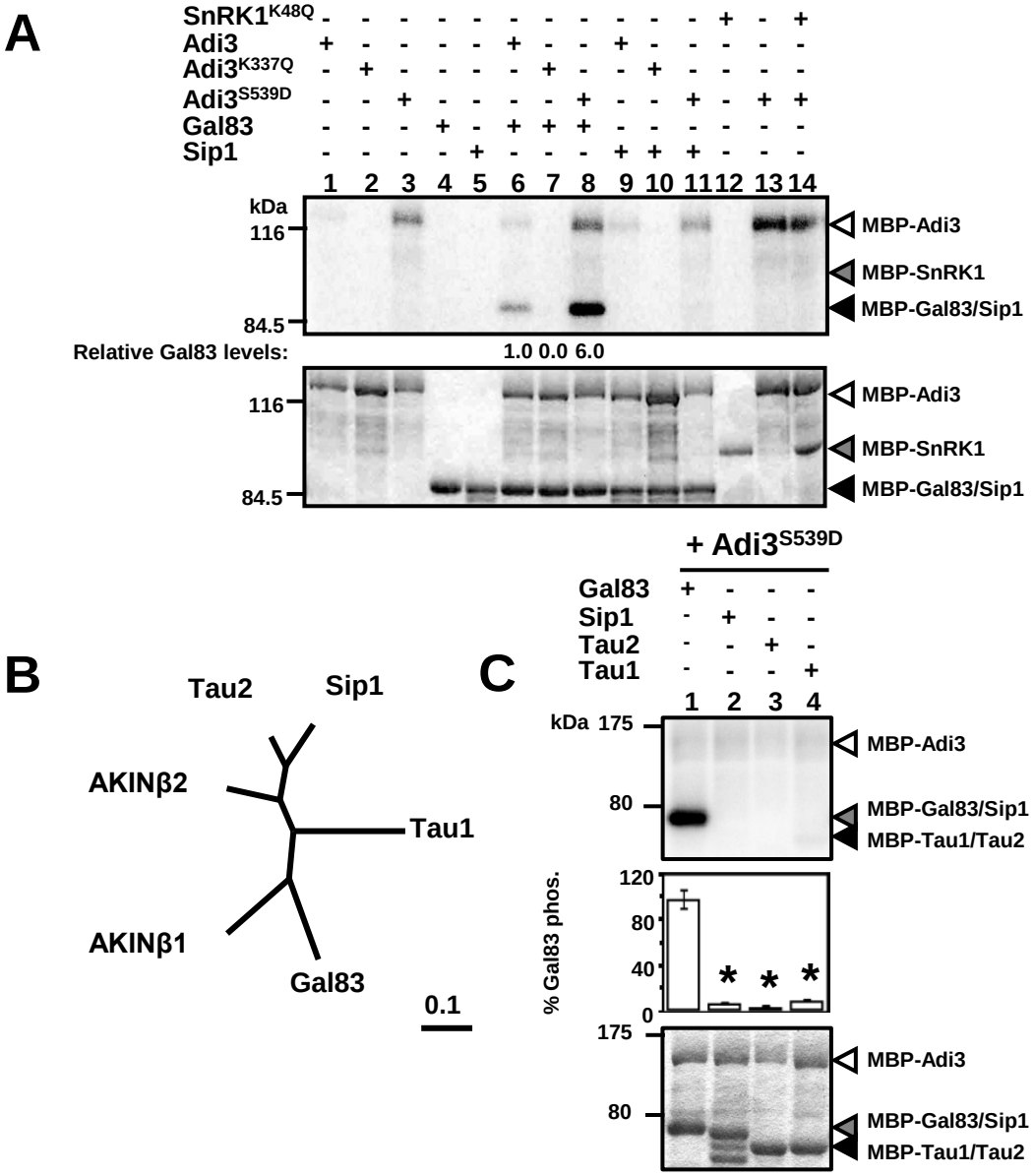

Figure 20. Adi3 phosphorylates *Sl*Gal83. In A and C, top panels show phosphor images and bottom panels show Coomassie blue-stained gels. Quantity One software was used to normalize the phosphorylation levels to the protein levels in each assay. A, Analysis of *Sl*SnRK1 α- and β-subunit phosphorylation by Adi3. Kinase-active and -inactive MBP-Adi3 proteins were tested for phosphorylation of MBP-*Sl*Gal83, MBP-*Sl*Sip1, and kinase inactive MBP-SnRK1^{K48Q} in *in vitro* kinase assays. *Sl*Gal83 phosphorylation values are reported as a percentage of wild-type Adi3 phosphorylation of *Sl*Gal83 and are representative of two independent experiments. B, Phylogenetic relationship between tomato and *A. thaliana* β-subunits. Proteins were aligned using ClustalW (Larkin et al., 2007), and the tree produced was analyzed using TreeView (Page, 1996). The scale bar indicates the number of amino acid substitutions per site. C, Adi3 only phosphorylates the Gal83 β-subunit. Kinase-active MBP-Adi3^{S539D} was tested for phosphorylation of MBP-*Sl*Gal83, MBP-*Sl*Sip1 MBP-Tau1, and MBP-Tau2 as in A. Values are averages of three independent experiments. Error bars represent SE. Asterisks indicate significant decreases in b-subunit phosphorylation as compared with *Sl*Gal83 phosphorylation (Student's t test, P , 0.01).

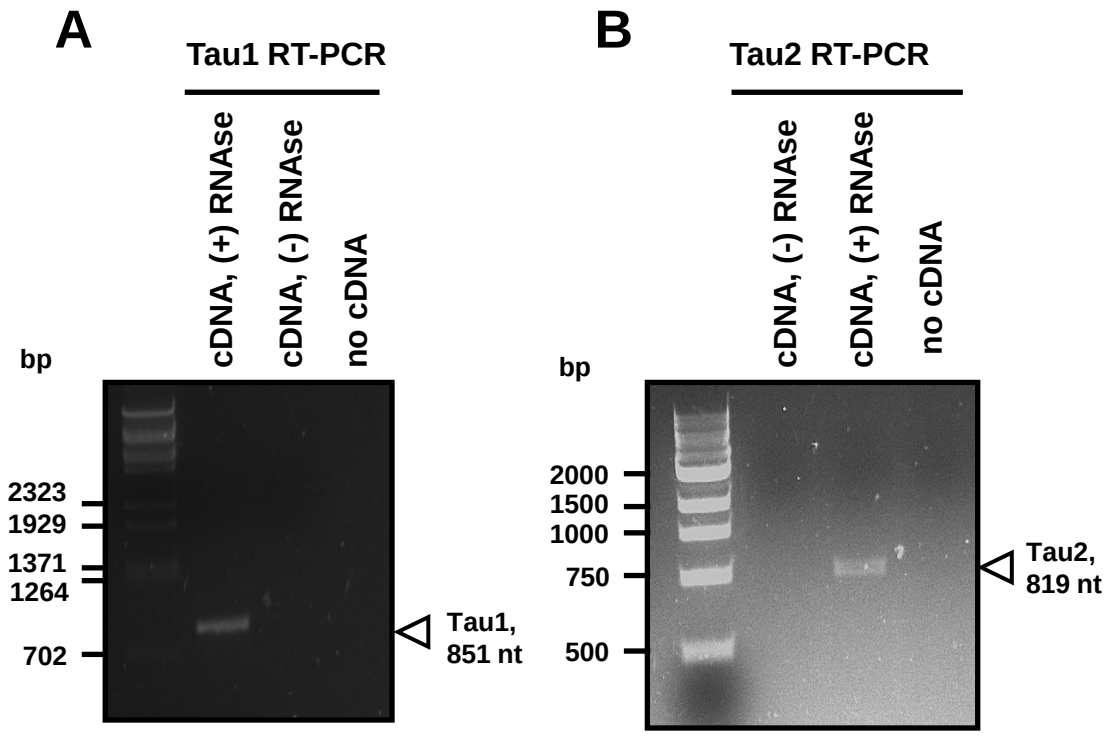

Figure 21 RT-PCR amplification of *Tau1* and *Tau2*. A, RT-PCR gel showing amplification of the *Tau1* cDNA from tomato leaf total RNA. B, RT-PCR gel showing amplification of the *Tau2* cDNA from tomato leaf total RNA**.**

Complementation of *sip1Δsip2Δgal83Δ* cells and restoration of growth on sucrose can be accomplished by introducing any one of the β-subunits (Schmidt & McCartney, 2000). Individually, each of the *A. thaliana* β-subunits (AKINβ1, AKINβ2, AKINβ3) are also capable of complementing the *sip1Δsip2Δgal83Δ* cells (Gissot et al., 2004, Polge & Thomas, 2007). We carried out this assay and showed that *Sl*Gal83-GFP was capable of restoring *sip1Δsip2Δgal83Δ* growth on sucrose, confirming complementation (Figure 22A). As an additional confirmation of *Sl*Gal83 complementation of *sip1Δsip2Δgal83Δ* yeast, we tested for restoration of invertase activity, which is regulated by the Snf1 complex under low glucose conditions (Carlson et al., 1984). Our results show that *Sl*Gal83-GFP was able to restore basal and low glucose-induced invertase activity to *sip1Δsip2Δgal83Δ* yeast (Figure 22B). These studies confirm *Sl*Gal83 as a true SnRK1 β-subunit and that *Sl*Gal83-GFP is functional *in vivo*.

4.4 Identification of Ser26 as the Adi3 phosphorylation site on *Sl*Gal83

In an effort to identify the *Sl*Gal83 residue phosphorylated by Adi3 we carried out a kinase assay screen of several *Sl*Gal83 Ser mutants. Within the *Sl*Gal83 protein there are 28 Ser amino acids (Figure 18), 17 of which were mutated to Ala and tested for loss of phosphorylation by Adi3 using *in vitro* kinase assays. Once the assays were completed, the *Sl*Gal83 phosphorylation levels were normalized to the *Sl*Gal83 and Adi3 protein levels in each assay, and the amount of *Sl*Gal83 phosphorylation was expressed

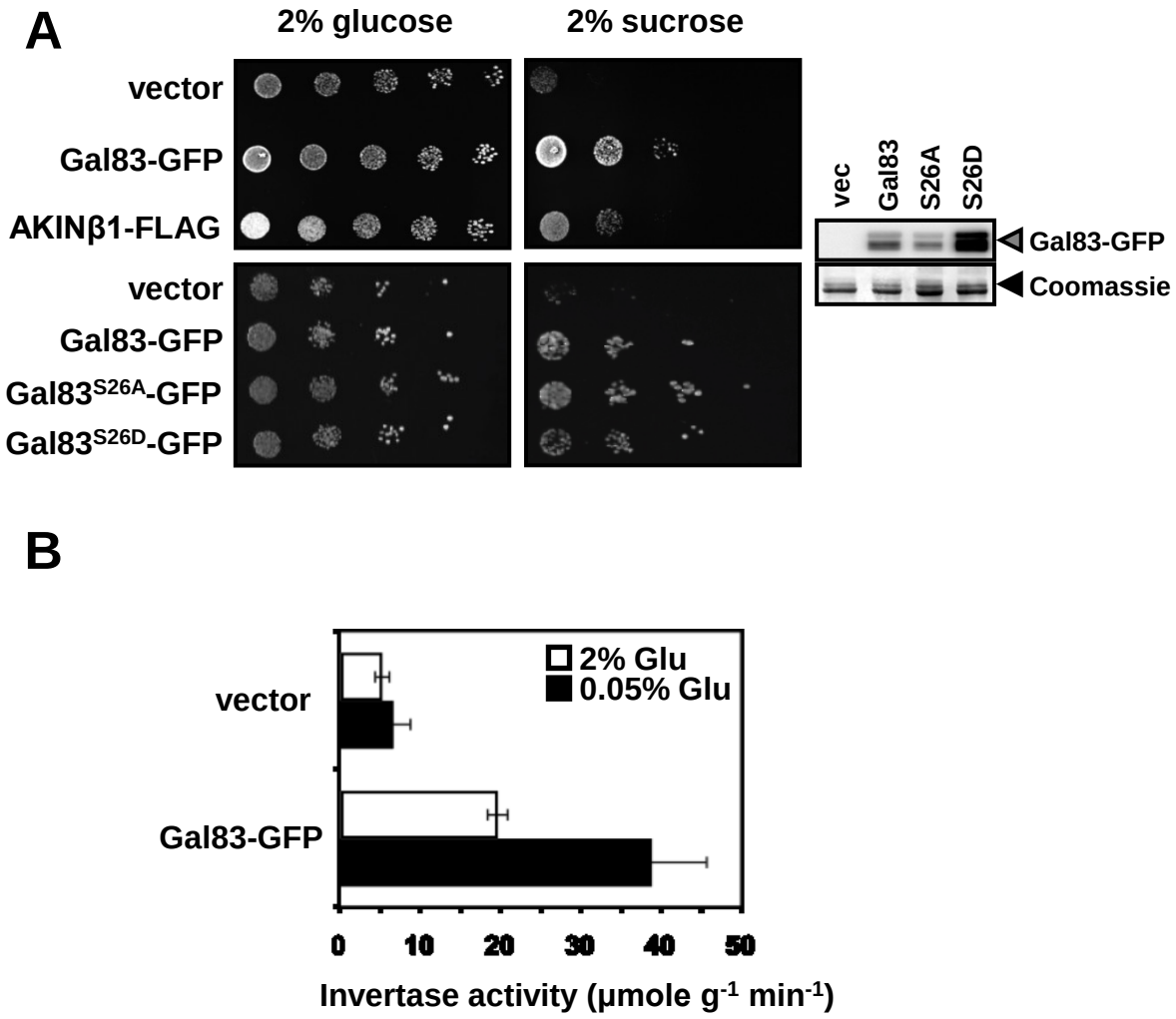

Figure 22. *Sl*Gal83 complementation of *sip1Δsip2Δgal83Δ* yeast. A, Tomato *Sl*Gal83 can complement the yeast β-subunit triple knockout. *sip1Δsip2Δgal83Δ* yeast cells were transformed with empty vector, the indicated *Sl*Gal83 constructs, or AKINβ1 and plated on 2% glucose or sucrose CM plates at 5-fold dilutions. *Sl*Gal83-GFP protein expression detected by α-GFP western blot is shown on the right. B, *Sl*Gal83 complementation of yeast invertase activity. The indicated constructs were transformed into *sip1Δsip2Δgal83Δ* yeast and extracts from the yeast tested for invertase activity in the presence of high (2%) and low (0.05%) glucose. Values are averages of three independent experiments and error bars are standard error.

as a percentage of wild-type *Sl*Gal83 phosphorylation. The results indicate that while many of the mutations slightly increased or decreased the ability of Adi3 to phosphorylate *Sl*Gal83, only the Ser26A mutation completely eliminated phosphorylation by Adi3 (Figure 23A, lane 3). There are 8 Thr residues in *Sl*Gal83 (Figure 18). Ala mutation of one Thr residue did not eliminate Adi3 phosphorylation (data not shown) and the remaining 7 Thr were not tested since Ser26A was a complete knockout of Adi3 phosphorylation of *Sl*Gal83 (Figure 23A). These results indicate that while Adi3 can interact with several members of the *Sl*SnRK1 complex, it can only phosphorylate *Sl*Gal83. The β-subunit protein alignment indicates that *Sl*Sip1, Tau1, and Tau2 do not contain a Ser corresponding to *Sl*Gal83 Ser26 (possibly marginally conserved in Tau2; Figure 16) supporting the inability of Adi3 to phosphorylate these proteins.

Phosphorylation of *Sl*Gal83 Ser26 was confirmed by mass spectrometry (MS) analysis. Trypsin digestion of *Sl*Gal83 will produce two possible peptides containing Ser26, **S**NVESGIVEDHHALNSR and R**S**NVESGIVEDHHALNSR (Ser26 bold and underlined), and MS/MS analysis of *in vitro* Adi3 phosphorylated, trypsin digested *Sl*Gal83 identified Ser26 phosphorylation in both peptides (Figure 23B; Figure 24A). The *in vivo* phosphorylation of Ser26 was also analyzed by first expressing *Sl*Gal83-GFP in tomato protoplasts and immunoprecipitating the protein with an α-GFP antibody (Figure 24B, C). The trypsin digested protein was analyzed by MS/MS and Ser26 phosphorylation was identified in the SNVESGIVEDHHALNSR peptide (Figure 23C), but not the RSNVESGIVEDHHALNSR peptide. These data indicates that Adi3

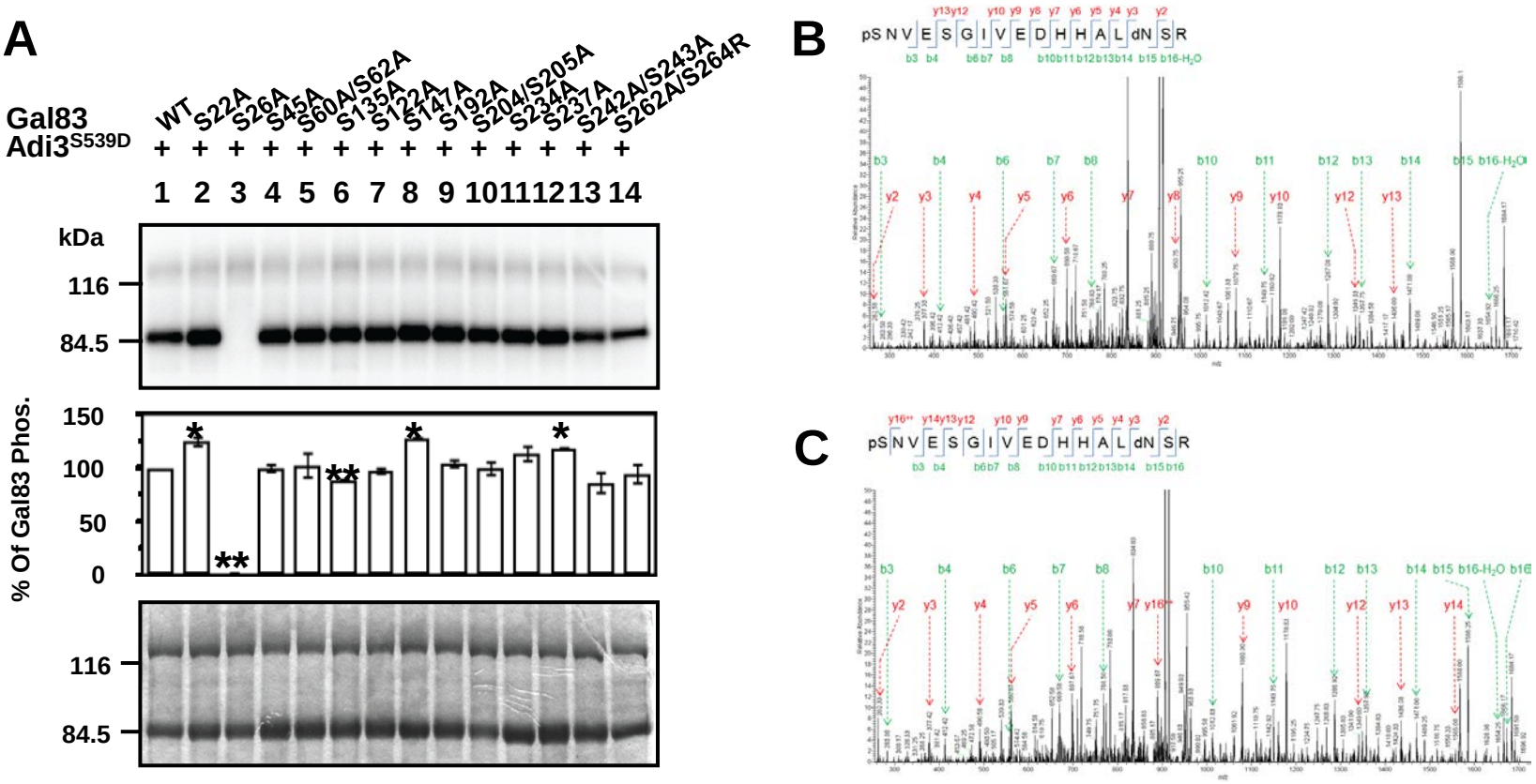

Figure 23. Adi3 phosphorylates *Sl*Gal83 at Ser26. A, Adi3 phosphorylates Ser26 of *Sl*Gal83. Kinase-active MBP-Adi3^{S539D} was used to phosphorylate the indicated MBP-Gal83 Ser to Ala mutants using γ-[^{32}P]ATP in *in vitro* kinase assays. Quantity One software was used to normalize the phosphorylation levels to the protein levels in each assay. *Sl*Gal83 phosphorylation values are reported as a percentage of wild-type Gal83 phosphorylation and are the average of three independent experiments. Error bars are standard error. One asterisk and two asterisks indicate significant increase or decrease, respectively, in phosphorylation of *Sl*Gal83 Ser to Ala mutants compared to wild-type *Sl*Gal83 phosphorylation (Student's t test, $p < 0.05$). Top panels, phosphorimage; bottom panels, Coomassie stained gel. B, MS identification of Gal83 Ser26 *in vitro* phosphorylation by Adi3. *in vitro* Adi3 phosphorylated *Sl*Gal83-MBP as in (A) was digested with trypsin, passed over an IMAC column, and eluted peptides analyzed by MS/MS. C, MS identification of *Sl*Gal83 Ser26 *in vivo* phosphorylation. *Sl*Gal83-GFP was expressed in tomato protoplasts, α-GFP immunopreciptated, the protein digested with trypsin, passed over an IMAC column, and eluted peptides analyzed by MS/MS.

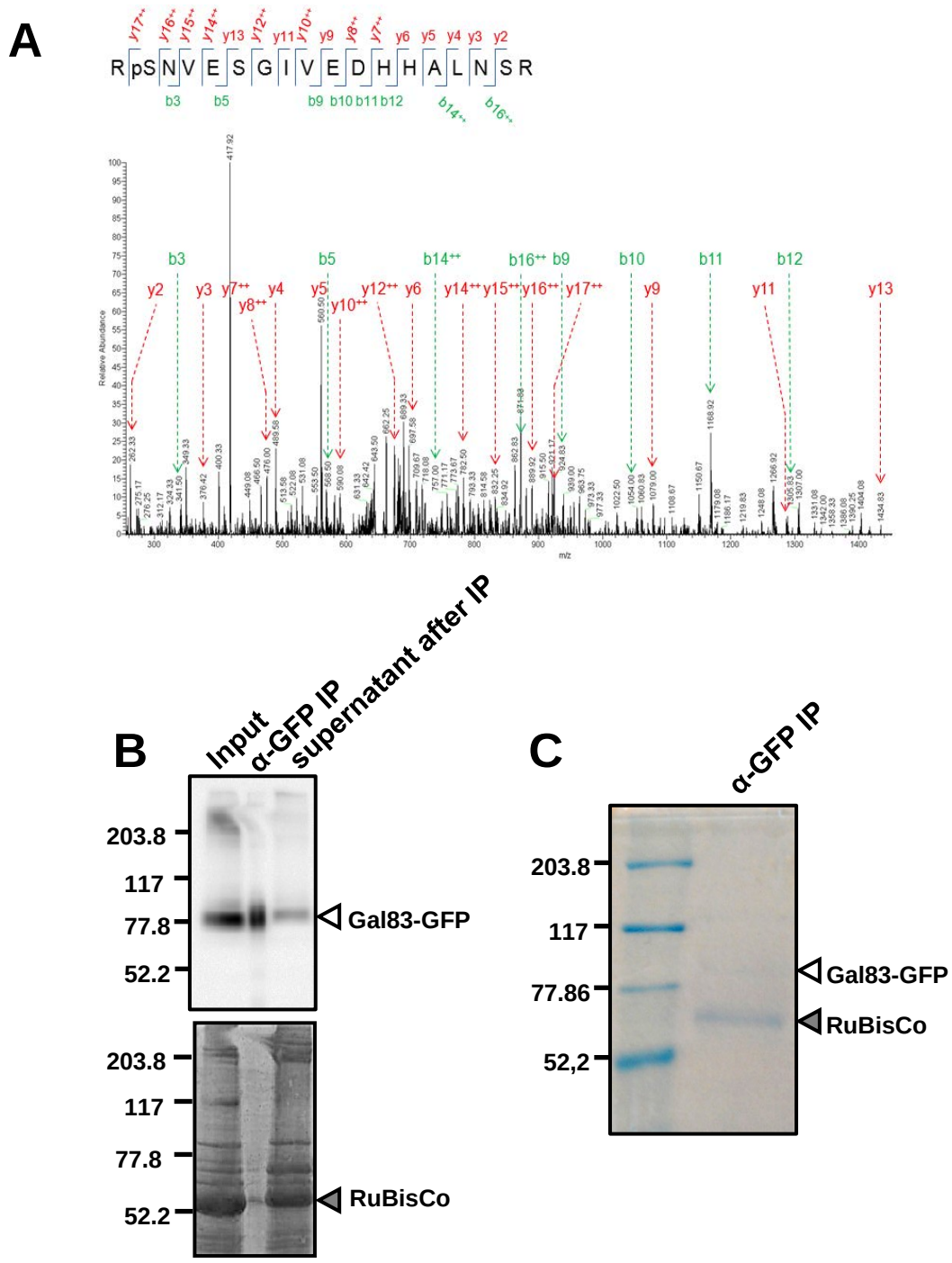

Figure 24. MS identification of *Sl*Gal83 S26 phosphorylation and α-GFP immunoprecipitation of *Sl*Gal83-GFP. A, Identification of *Sl*Gal83 S26 phosphorylation *in vitro* in peptide RpSNVESGIVEDHHALNSR. B, *Sl*Gal83-GFP can be pulled down with an α-GFP antibody. Protoplasts expressing *Sl*Gal83-GFP for 16 hrs were lysed, immunoprecipitated with α-GFP antibody, and analyzed by α-GFP western blot. C, Immunoprecipitated *Sl*Gal83-GFP used for MS analysis. *Sl*Gal83-GFP was expressed and immunoprecipitated as in (A) and the sample separated by SDS-PAGE. The band corresponding to *Sl*Gal83-GFP was cut from the gel, trypsin digested and analyzed by MS.

phosphorylates *Sl*Ga83 Ser26 *in vitro* and supports the possibility that Adi3 also performs this phosphorylation event *in vivo*.

An additional *Sl*Gal83 phosphorylation site was identified *in vitro* and *in vivo* in peptide RSNVEpSGIVEDHHALNSR corresponding to Ser30 (Figure 25 A, B) suggesting that Adi3 may also phosphorylate Ser30. The Ser30 to Ala mutation was not initially tested as shown in Figure 23. So, the *Sl*Gal83^{S30A} protein was produced and tested for loss of Adi3 phosphorylation as in Figure 23. The results indicate that the S30A mutation does not significantly reduce the *Sl*Gal83 phosphorylation by Adi3 *in vitro* (Figure 25C). While Adi3 could be responsible for this phosphorylation event *in vivo*, it remains to be positively determined. It should be noted that for both the *in vitro* and *in vivo* MS/MS analysis, peptides with the Ser26 phosphorylation were approximately twice as prevalent as those with Ser30 phosphorylation and no peptides were found with both Ser26 and Ser30 phosphorylation.

4.5 Tomato Gal83 is phosphorylated *in vivo*

In order to analyze the *in vivo* phosphorylation status of *Sl*Gal83 we used an alteration to the standard SDS-PAGE by adjusting the ratio of bis-acrylamide to acrylamide. This method has been used to distinguish different phosphorylation states of yeast phosphatidylinositol 4-kinase (Demmel et al., 2008). *Sl*Gal83-GFP transgenic *A. thaliana* plants were created and the *Sl*Gal83-GFP protein analyzed by α-GFP western blot using increasing ratios of bis-acrylamide to acrylamide. The 1:200 bis-acrylamide:acrylamide ratio was capable of separating five different forms of *Sl*Gal83-GFP and two of these forms are lost when expressing the *Sl*Gal83^{S26A}-GFP protein

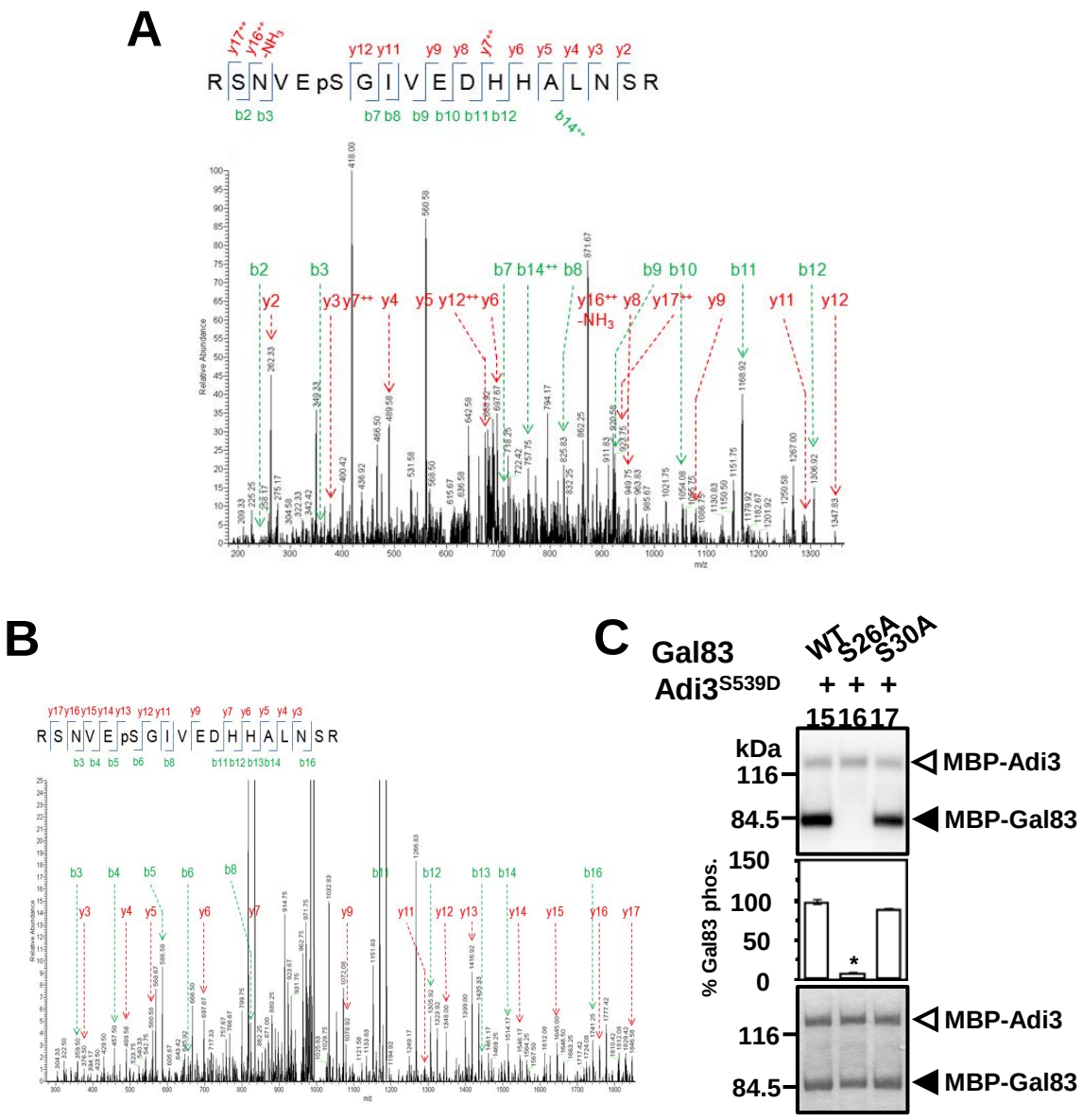

Figure 25. MS identification of *Sl*Gal83 S30 phosphorylation. A, Identification of *Sl*Gal83 S30 phosphorylation *in vitro* in peptide RSNVEpSGIVEDHHALNSR. B, Identification of *Sl*Gal83 S30 phosphorylation *in vivo* in peptide RSNVEpSGIVEDHHALNSR. C, Adi3 does not phosphorylate *Sl*Gal83 S30 *in vitro*. One asterisk indicates significant decrease in phosphorylation of *Sl*Gal83 Ser to Ala mutants compared to wild-type *Sl*Gal83 phosphorylation (Student's t test, $p < 0.05$).

(Figure 26). This would suggest that the 1:200 SDS-PAGE/α-GFP western blot can be used to effectively separate and identify different modified forms of *Sl*Gal83.

Next, the *in vivo* phosphorylation status of *Sl*Gal83 as expressed in tomato was analyzed. *Sl*Gal83-GFP was expressed in protoplasts, an extract made, the extract treated with λ phosphatase, and *Sl*Gal83-GFP analyzed using 1:200 gels/α-GFP western blot. In the presence of λ phosphatase *Sl*Gal83-GFP appeared as a single band (Figure 27A, lane 1). However, in the absence of λ phosphatase *Sl*Gal83-GFP appeared as at least four distinct protein bands, and by comparison to the λ phosphatase treatment this can be interpreted as one unphosphorylated form and three phosphorylated forms of *Sl*Gal83-GFP (Figure 27A, lane 2).

The contribution of Ser26 phosphorylation to the *Sl*Gal83 phosphorylated protein bands was analyzed by mutating *Sl*Gal83 Ser26 to the non-phosphorylatable Ala (*Sl*Gal83^{S26A}) and the phosphomimetic Asp (*Sl*Gal83^{S26D}). Expression of the GFP fusions of both of these proteins in tomato protoplasts appeared to reduce the number of *Sl*Gal83-GFP phosphorylated forms; *Sl*Gal83^{S26A} only had one phosphoprotein band (Figure 27, lane 3), while *Sl*Gal83^{S26D} showed a reduction of one phosphoprotein band (Figure 27, lane 5). The phosphoprotein bands for both *Sl*Gal83^{S26A} and *Sl*Gal83^{S26D} can be removed by λ phosphatase treatment (Figure 27A, lanes 4 and 6, respectively). This would suggest that Ser26 phosphorylation contributes to the *in vivo* phosphorylation status of *Sl*Gal83.

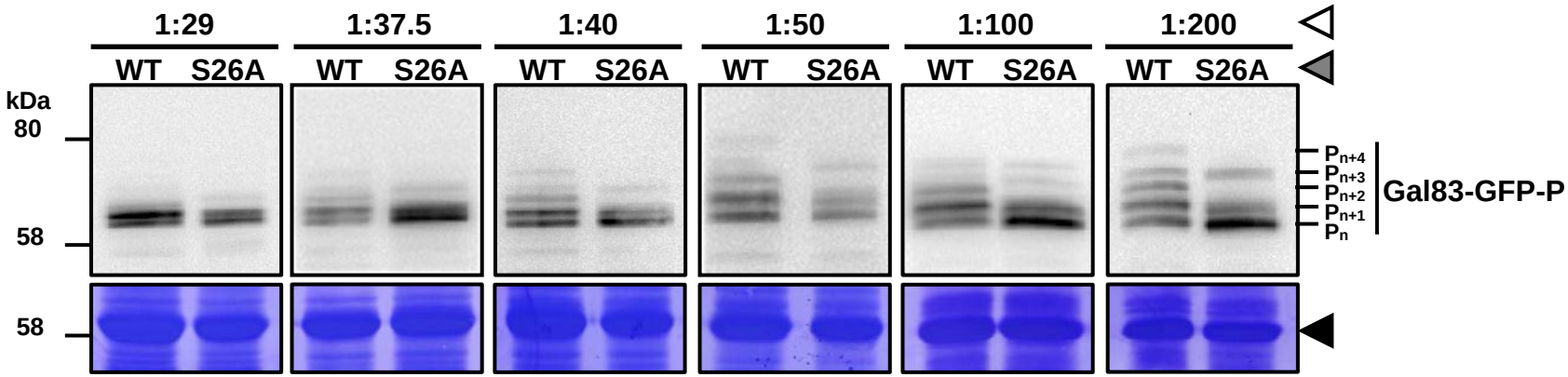

Figure 26. Separation of *Sl*Gal83-GFP phosphoproteins by SDS-PAGE with varying bis-acrylamide:acrylamide ratios. *Sl*Gal83-GFP was stably transformed into *A. thaliana*, protein extracts made from leaf tissue, and the extracts analyzed by SDS-PAGE. Open triangle, bis-acrylamide:acrylamide ratio; grey triangle, *Sl*Gal83-GFP protein; black triangle, RuBisCo

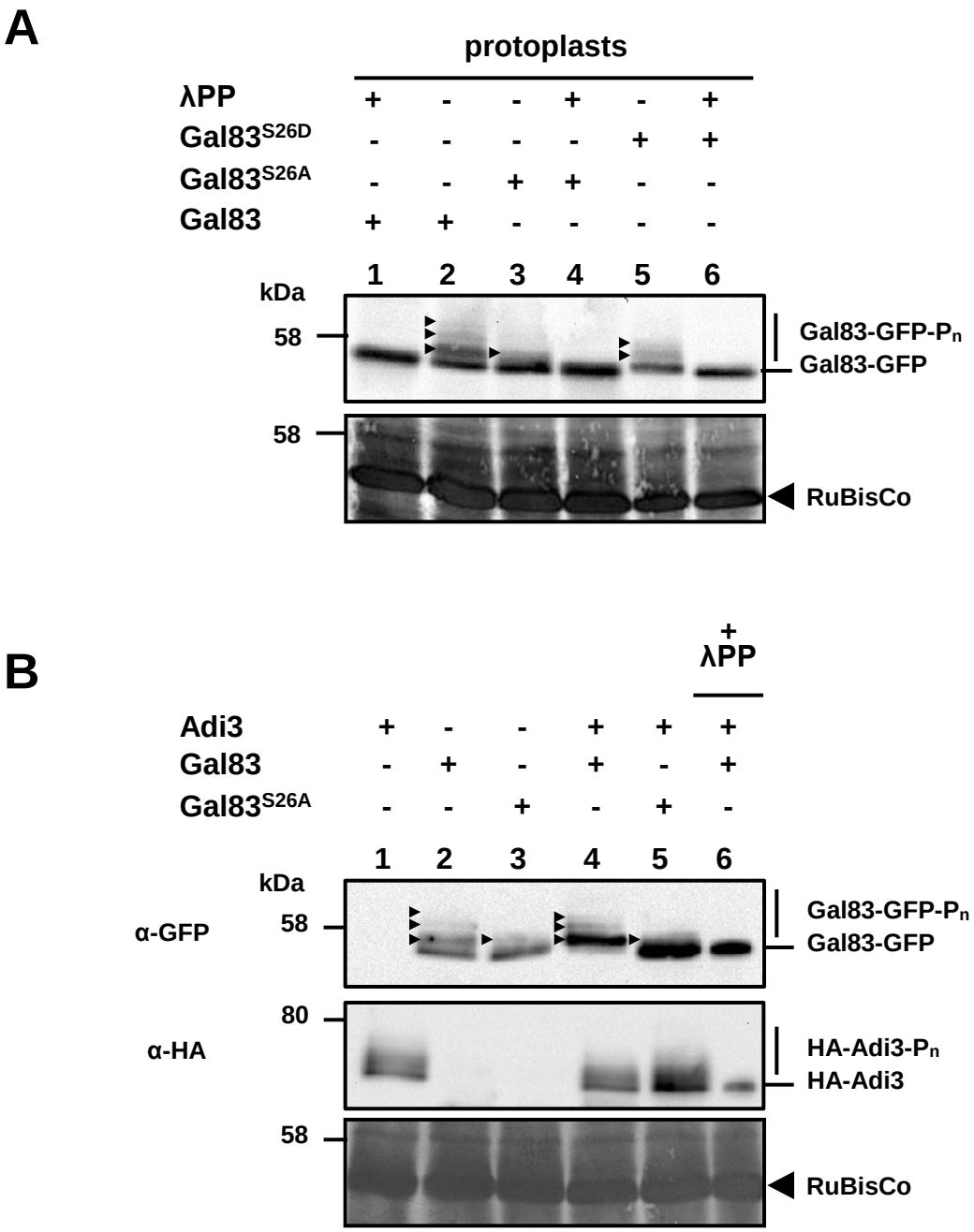

Figure 27. *In vivo* phosphorylation status of *Sl*Gal83. In both A and B, proteins were separated by SDS-PAGE using a 1:500 bis-acrylamide:acrylamide ratio followed by α-GFP or α-HA western blot. A, *Sl*Gal83 is phosphorylated in tomato protoplasts. Total protein extracts from *Sl*Gal83-GFP expressing protoplasts were treated with and without λ-phosphatase and analyzed by α-GFP western blot. Black arrow heads indicate different *Sl*Gal83-GFP phosphorylated forms. B, Adi3 phosphorylates *Sl*Gal83 *in vivo*. Protoplasts expressing the indicated combinations of HA-Adi3 and *Sl*Gal83-GFP were analyzed by α-GFP for analysis of the phosphorylation status of *Sl*Gal83-GFP, and α-HA western blot.

4.6 Adi3 phosphorylates *Sl*Gal83 *in vivo*

We looked for evidence that *Sl*Gal83 Ser26 is phosphorylated *in vivo* by Adi3 using a coexpression approach. *Sl*Gal83-GFP, *Sl*Gal83^{S26A}-GFP, and HA-Adi3 were coexpressed in tomato protoplasts and the banding pattern of phosphorylated *Sl*Gal83-GFP analyzed by 1:200 gels/*α*-GFP western blot. In the absence of HA-Adi3, *Sl*Gal83-GFP and *Sl*Gal83-GFP^{S26A} appeared as was seen in Figure 27A (Figure 27B, lane 2 and 3). However, in the presence of HA-Adi3, wild-type *Sl*Gal83-GFP protein appeared to shift upward (Figure 27, lane 4). Treatment of this sample with λ phosphatase reduced *Sl*Gal83-GFP to a single non-phosphorylated protein band (Figure 27B, lane 6, compare to lane 4). In the presence of HA-Adi3, the *Sl*Gal83-GFP^{S26A} protein appeared similar to that without HA-Adi3 (Figure 27B, lane 5). Taken together, these data would suggest *Sl*Ga83 is phosphorylated by Adi3 *in vivo*. Additionally, it was seen that HA-Adi3 exists as several phosphoprotein bands that can be reduced to a single band with λ phosphatase treatment (Figure 27B, middle panel).

4.7 Functional analysis of *Sl*Gal83 Ser26 phosphorylation

In order to begin to analyze possible roles for Adi3 phosphorylation of *Sl*Gal83 we first utilized the *sip1Δsip2Δgal83Δ* yeast complementation assay. The ability of the *Sl*Gal83^{S26A}-GFP and *Sl*Gal83^{S26D}-GFP proteins to complement the *sip1Δsip2Δgal83Δ* cells was tested and the results indicate these proteins complement to an extent similar to that of wild-type *Sl*Gal83-GFP (Figure 22A). This suggests Adi3 phosphorylation of *Sl*Gal83 may not affect the function, at least in a heterologous system, of controlling growth on alternate carbon sources.

Given the role of Adi3 in suppression of cell death (Devarenne et al., 2006, Ek-Ramos et al., 2010) and that Adi3 can phosphorylate *Sl*Gal83, the ability of *Sl*Gal83 and its Ser26 phosphorylation mutants to suppress cell death was analyzed in tomato cells. It is known that high levels of NaCl are capable of inducing cell death in plants (Affenzeller et al., 2009, Chen et al., 2009, Jiang et al., 2008, Katsuhara & Kawasaki, 1996, Lin et al., 2006, Tuteja, 2007, Wang et al., 2010) and a functional Snf1 complex has been shown to be required for yeast cell survival in the presence of high NaCl (Hong & Carlson, 2007). We expressed *Sl*Gal83-GFP, *Sl*Gal83^{S26A}-GFP, *Sl*Gal83^{S26D}-GFP, and GFP-Adi3 in tomato protoplasts, treated them with 200 mM NaCl, and measured cell viability over a 5.5 hr time course. Both Adi3 and *Sl*Gal83 were capable of CDS activity and provided increased cell viability in response to NaCl compared to the vector transformed sample (Figure 28A). The *Sl*Gal83 Ser26 phosphorylation mutants did not confer increased or decreased cell viability over wild-type *Sl*Gal83 (Figure 28D). These results indicated that *Sl*Gal83 does have a role in cell death suppression, but phosphorylation of Ser26 may not play a role in controlling *Sl*Gal83 CDS activity.

Next, the affect of *Sl*Gal83 phosphorylation on *Sl*SnRK1 complex kinase activity was tested. In order to carry out these assays, an *in vitro* active SnRK complex must be assembled. Thus, the *Sl*SnRK complex members studied here were analyzed for the formation of an active complex by testing kinase activity against the AMPK/SnRK1 SAMS peptide substrate (HMRSAMSGLHLVKRR; phosphorylation site bold and underlined) (Halford et al., 2003). We also cloned the tomato cDNA for Snf4, which encodes the γ-subunit of the *Sl*SnRK complex (Bradford et al., 2003) for inclusion in the

Figure 28. Functional analysis of *Sl*Gal83 Ser26 phosphorylation mutants. A, *Sl*Gal83 confers cell viability in the presence of high NaCl. Tomato protoplasts expressing GFP-Adi3 or the indicated *Sl*Gal83-GFP constructs for 18 hrs were treated with 200 mM NaCl and cell viability determined by Evans blue staining over a 5.5 hr time course. Values are averages of three independent experiments. Error bars are standard error. Data analysis was carried out using Duncan's multiple-range test. Samples with the same letter above the bars are not significantly different ($p < 0.05$). Protein expression detected by α-GFP western blot is shown on the right. B, *Sl*SnRK1 substrate phosphorylation with *Sl*Gal83^{S26D} mutant and Adi3. Kinase-active and inactive MBP-SnRK1 proteins were tested for phosphorylation of the SAMS peptide in combination with GST-*Sl*Snf4, MBP-*Sl*Gal83, and MBP-Adi3 using γ-[^{32}P]ATP in *in vitro* kinase assays. Values are shown as pmole of phosphate incorporated/mg of SnRK1 protein/min and are averages of three independent experiments. Error bars are standard error. One and two asterisks indicate significant increase or decrease, respectively, in SAMS phosphorylation as compared to phosphorylation by SnRK1^{T175D} alone (Student's t test, $p < 0.01$). SDS-PAGE gel shows proteins put into the assay. C, Expression of the data in (B) as a percentage of the GST sample, column 13. All other information as in (B). D, SAMS phosphorylation by protoplast extracts expressing *Sl*Gal83. The indicated *Sl*Gal83-GFP proteins were expressed in protoplasts for 16 hrs, an extract made, and tested for phosphorylation of SAMS as in (B). Values are averages of three independent experiments and error bars are standard error. One asterisk indicates significant decrease in SAMS phosphorylation as compared to the *Sl*Gal83 sample (Student's t test, $p < 0.01$).

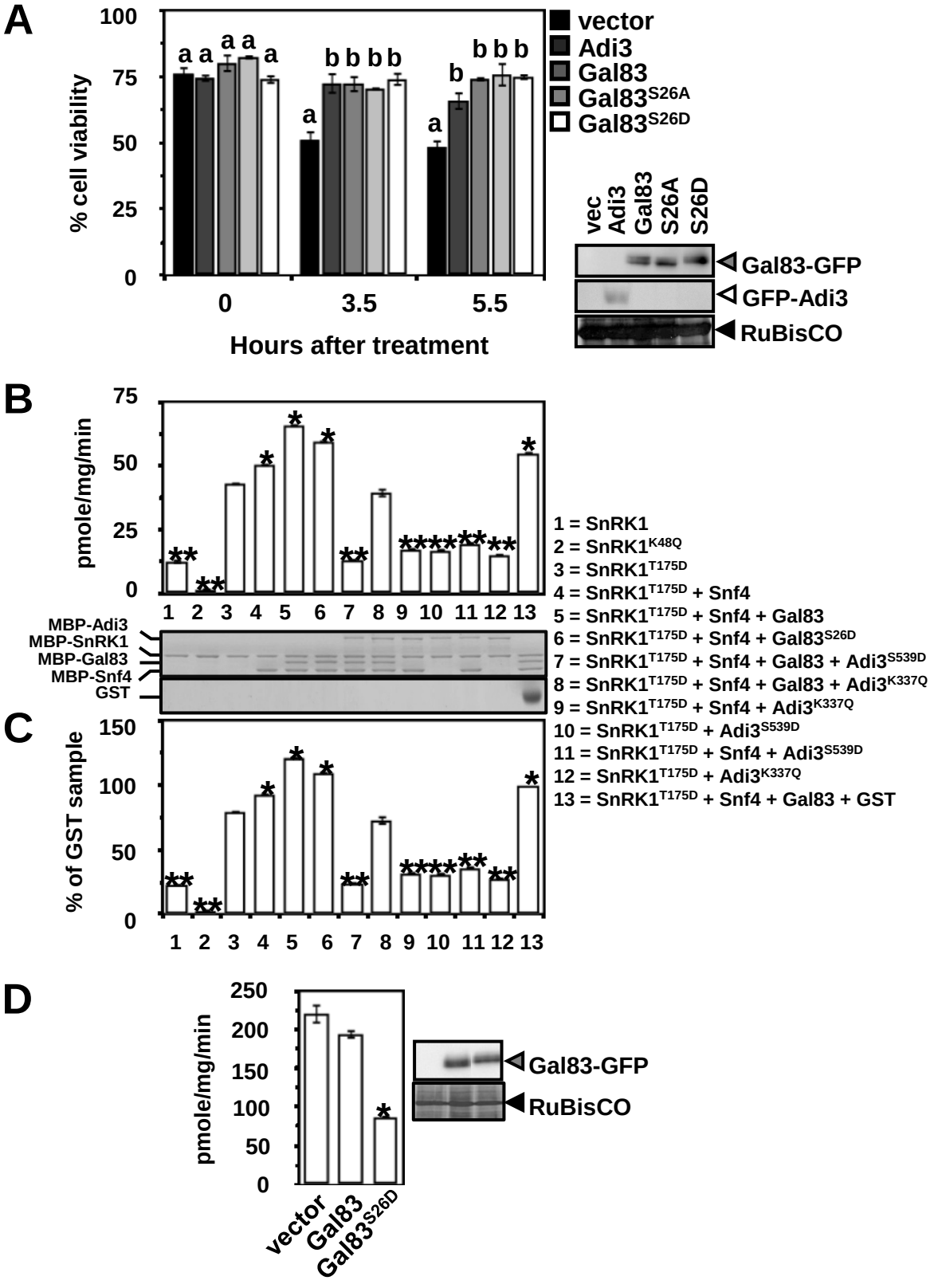
A
100
75
50
25
0
% cell viability
a a a a a
a b b b b
a b b b b
vector
Adi3
Gal83
Gal83S26A
Gal83S26D
0
3.5
5.5
Hours after treatment
vec
Adi3
Gal83
S26A
S26D
Gal83-GFP
GFP-Adi3
RuBisCO
B
75
50
25
0
pmole/mg/min
1 2 3 4 5 6 7 8 9 10 11 12 13
MBP-Adi3
MBP-SnRK1
MBP-Gal83
MBP-Snf4
GST
1 = SnRK1
2 = SnRK1K48Q
3 = SnRK1T175D
4 = SnRK1T175D + Snf4
5 = SnRK1T175D + Snf4 + Gal83
6 = SnRK1T175D + Snf4 + Gal83S26D
7 = SnRK1T175D + Snf4 + Gal83 + Adi3S539D
8 = SnRK1T175D + Snf4 + Gal83 + Adi3K337Q
9 = SnRK1T175D + Snf4 + Adi3K337Q
10 = SnRK1T175D + Adi3S539D
11 = SnRK1T175D + Snf4 + Adi3S539D
12 = SnRK1T175D + Adi3K337Q
13 = SnRK1T175D + Snf4 + Gal83 + GST
C
150
100
50
0
% of GST sample
1 2 3 4 5 6 7 8 9 10 11 12 13
D
250
200
150
100
50
0
pmole/mg/min
vector
Gal83
Gal83S26D
Gal83-GFP
RuBisCO

kinase assays. The α-subunit *Sl*SnRK1 by itself showed limited SAMS phosphorylation (Figure 28B, column 1). The phosphomimetic mutation of *Sl*SnRK1 Thr175 (*Sl*SnRK1^{T175D}), which corresponds to the identified phosphorylation activation site in AMPK (Thr172) and spinach and *A. thaliana* SnRK1 (Thr175; Hawley et al., 1996, Sugden et al., 1999; Figure 16), conferred an increase in SAMS phosphorylation (Figure 28B, column 3). Addition of *Sl*Snf4 marginally, but significantly increased *Sl*SnRK1^{T175D} SAMS phosphorylation (Figure 28B, column 4). Inclusion of all complex subunits (*Sl*SnRK1, *Sl*Snf4, *Sl*Gal83) imparted a greater increase in *Sl*SnRK1^{T175D} SAMS phosphorylation (Figure 28B, column 5). These assays show that the *Sl*SnRK1 subunits comprise a functional complex. To the best of our knowledge, this is the first report of reconstituting an active plant SnRK complex *in vitro*.

The contribution of *Sl*Gal83 Ser26 phosphorylation towards *Sl*SnRK1 kinase activity on the SAMS peptide was analyzed by including the *Sl*Gal83^{S26D} protein in the complex or adding Adi3 to the complex. The results show that *Sl*Gal83^{S26D} conferred a slight yet statistically significant decrease in *Sl*SnRK1 SAMS phosphorylation (Figure 28B, column 6), while the addition of Adi3^{S539D} to the assay drastically lowered the phosphorylation of SAMS to a level close to that of *Sl*SnRK1 alone (Figure 28B, column 7). This drop in SAMS phosphorylation appears to partially depend on Adi3 kinase activity as inclusion of the kinase-inactive Adi3^{K337Q} restored activity of the complex similar to *Sl*SnRK1^{T175D} alone, but not to the level of the full complex (Figure 28B, column 8). This would suggest that even though Adi3 does not phosphorylate

*Sl*SnRK1 (Figure 20A, lane 14), it may inhibit SnRK kinase activity through their interaction. This appears to be the case since kinase-active Adi3^{S539D} or kinase-inactive Adi3^{K337Q} reduced SAMS phosphorylation by *Sl*SnRK1^{T175D} and *Sl*SnRK1^{T175D} + Snf4 close to the level of *Sl*SnRK1 alone (Figure 28B, columns 9, 10, 11, 12). In order to analyze if the drop in complex kinase activity in the presence of Adi3 is due to an additional protein in the assay, the analysis was repeated with the addition of GST protein. This assay had strong kinase activity, but not to the level of the full complex (Figure 28B, column 13). This would suggest that some loss of kinase activity in the presence of Adi3 could be due to the addition of an additional protein. To take this into account, the values in Figure 28 were normalized to that of the assay in the presence of GST; i.e. the GST sample was set as 100% and the other samples were expressed as a percentage of this value. Figure 28C shows that when expressed in this manner, the trends do not change.

We extended the SnRK1 SAMS phosphorylation assays to an *in vivo* approach by expressing *Sl*Gal83-GFP or *Sl*Gal83^{S26D}-GFP in tomato protoplasts, making extracts of these cells, and using the extract to phosphorylate the SAMS peptide. We found that the extract from *Sl*Gal83^{S26D}-GFP expressing cells had greatly reduced SAMS phosphorylation compared to expression of *Sl*Gal83-GFP (Figure 28D). This reduction in SAMS phosphorylation is much lower than what was seen for the *in vitro* assay (Figure 28B, C) suggesting that a more *in vivo* context is needed to better realize the effects of Ser26 phosphorylation. Taken together, these kinase assay data suggest that the Adi3 interaction with the *Sl*SnRK complex has the ability to inhibit the kinase

activity of the complex. This may be mediated through two mechanisms, phosphorylation of *Sl*Gal83 and interaction with *Sl*SnRK1.

4.8 Discussion

In the present chapter we present evidence for the interaction of Adi3 with the SnRK complex in tomato. Our finding that Adi3 can only phosphorylate the *Sl*Gal83 SnRK β-subunit out of the four β-subunits identified in tomato has far-reaching implications since Snf1/AMPK/SnRK1 β-subunits control cellular localization and substrate specificity of the complex (Mitchelhill et al., 1997, Vincent et al., 2001, Warden et al., 2001). Additionally, β-subunit phosphorylation has been associated with regulation of some of these β-subunit functions (Hedbacker et al., 2004, Mangat et al., 2010, Mitchelhill et al., 1997, Warden et al., 2001), and the SnRK1 complex appears to link signaling connected with metabolism and stresses (Halford & Hey, 2009). Given the role of Adi3 in cell death control our studies add additional evidence for the connection of SnRK1 with stress signaling. Alternatively, Adi3 may also be involved in the direct regulation of metabolism through its interactions with the *Sl*SnRK1 complex.

4.8a A role for Adi3 phosphorylation in regulating SnRK complex kinase activity?

We have shown that Adi3 phosphorylates *Sl*Gal83 at Ser26 (Figure 23) and explored the functional relevance of this phosphorylation event. While, several β-subunits have been shown to be phosphorylated in yeast and mammals (Hedbacker et al., 2004, Mangat et al., 2010, Warden et al., 2001), our studies appear to be the first report of phosphorylation for a plant β-subunit. An *in vitro* functional analysis showed that kinase-active Adi3 has drastic affects on the kinase activity of the SnRK1 complex. If

Adi3 phosphorylation of *Sl*Gal83 at Ser26 is controlling this large decrease in SnRK1 complex activity, the *Sl*Gal83^{S26D} protein should also confer a decrease in kinase activity. A large reduction in SAMS phosphorylation in the presence of *Sl*Gal83^{S26D} was seen *in vivo* (Figure 28D), but was much less drastic *in vitro* (Figure 28) suggesting there is an *in vivo* role for Ser26 phosphorylation in controlling SnRK1 kinase activity.

Interestingly, the restoration of SAMS phosphorylation when including kinase-inactive Adi3^{K337Q} would suggest that Adi3 kinase activity is at least partially required for this large inhibition of SnRK1 activity *in vitro* and may suggest additional Adi3 phosphorylation sites on *Sl*Gal83 for controlling activity. It is possible that Ser30 is one of these sites since we identified phosphorylation of this *Sl*Gal83 residue both *in vitro* and *in vivo* by MS analysis. However, the inability of Adi3 to phosphorylate this site *in vitro* raises doubt about the role of Ser30 phosphorylation. Additionally, the complete loss of Adi3 phosphorylation of the *Sl*Gal83^{S26A} protein suggests Ser26 is the only Adi3 phosphorylation site on Gal83. Thus, the requirement of Adi3 kinase activity in the suppression of SnRK1 substrate phosphorylation still remains to be fully resolved.

While many studies have shown that phosphorylation of α-subunits controls complex kinase activity in yeast, mammals, and plants (Hawley et al., 2005, Hey et al., 2007, Hong et al., 2003, Hurley et al., 2005, Nath et al., 2003, Shen & Hanley-Bowdoin, 2006, Shen et al., 2009, Sutherland et al., 2003, Woods et al., 2003, Woods et al., 2005), only one previous study has shown that phosphorylation of a β-subunit affects complex kinase activity. A phosphorylation mutant of the human AMPKβ1 β-subunit reduced AMPK complex kinase activity by 60% (Warden et al., 2001). Thus, control of complex

kinase activity by β-subunit phosphorylation may be more common than previously thought. This could be supported by determining if phosphorylation of the conserved Ser26 residue in the *A. thaliana* Gal83 homologue, AKINβ1, affects *At*SnRK1 complex kinase activity.

Our results also suggest that the interaction of Adi3 with *Sl*SnRK1 is capable of suppressing *Sl*SnRK1 kinase activity (Figure 28B). In the absence of *Sl*Gal83 the kinase-active or -inactive forms of Adi3 are capable of suppressing *Sl*SnRK1 kinase activity (Figure 28B). This apparently contradicts the finding that the kinase-inactive Adi3 can restore activity of the complex in the presence of *Sl*Gal83. However, these results may indicate that the Adi3/*Sl*Gal83 interaction affects the ability of Adi3 to fully interact with and inhibit *Sl*SnRK1. Eliminating *Sl*Gal83 from the assay would then allow for full interaction between Adi3 and *Sl*SnRK1 and stronger activity inhibition. The interaction of Adi3 with *Sl*SnRK1 may be inhibiting the ability of *Sl*SnRK1 to bind the SAMS substrate or even ATP.

These data also help to explain the detection of *Sl*SnRK1 as an Adi3 Y2H interactor even though Adi3 does not phosphorylate *Sl*SnRK1 as well as shed light on the biological significance for this interaction. Given the role of Adi3 in the host response to *Pst* and the function of SnRK1 in stress signaling, Adi3 may be directing reallocation of cellular energy reserves by modulating *Sl*SnRK1 kinase activity during the resistance response of tomato to *Pst*. Studies using *Nicotiana attenuata* show that photosynthate is reallocated to the roots in response to herbivore attack through the down-regulation of SnRK β-subunit expression (Schwachtje et al., 2006). Our results

indicate that *Sl*Gal83 phosphorylation at Ser26 functions as an inhibitor of *Sl*SnRK kinase activity. Down regulation of this β-subunit may thus play a role in facilitating the activation of *Sl*SnRK1 and the metabolic modifications required to respond to pathogens. Phosphorylation of *Sl*GAL83 by *Sl*Adi3 offers an additional layer of control over *Sl*SnRK activity, a specificity required given the involvement of this complex in regulating metabolic responses to several environmental stresses (Cho et al., 2012, Hey et al., 2007, Hong & Carlson, 2007).

4.8b Multiple roles for β-subunit phosphorylation.

Snf1/AMPK/SnRK1 β-subunits appear to be phosphorylated on several amino acids and our studies also support phosphorylation at several residues on *Sl*Gal83. Expression of *Sl*Gal83-GFP in plant cells showed the existence of multiple phosphorylated protein bands based on our λ phosphatase treatments, one of which contains Ser26 phosphorylation (Figure 27A and B). One of these phosphorylated bands may also contain Ser30 phosphorylation. This and the identity of any additional *Sl*Gal83 phosphorylation sites remain to be determined. Multiple phosphorylation sites have been found for other β-subunits. Mass spectral analysis of human AMPKβ1 isolated from COS cells identified phosphorylation at Ser24/25, Ser108, and Ser182, but the responsible kinase has not been identified (Mitchelhill et al., 1997). Phosphorylation of AMPKβ1 Ser24/25 and Ser182, but not Ser108, appears to prevent nuclear localization (Warden et al., 2001). *Sc*Gal83 is phosphorylated by both the α-subunit Snf1 and casein kinase 2 (CK2), and while the exact sites of phosphorylation have not been identified they are predicted to be Ser64 or Ser65 for Snf1 and Ser87, *Thr*90 or Ser93 for CK2

(Mangat et al., 2010). The role for Snf1/CK2 phosphorylation of *Sc*Gal83 is not clear since deletion of the region containing both the Snf1 and CK2 phosphorylation sites did not affect glucose-regulated Snf1 function (Mangat et al., 2010). The situation for *Sc*Sip1 is similar. Protein kinase A (PKA) has been shown to be required for retaining *Sc*Sip1 cytoplasmic localization under high glucose conditions (Hedbacker et al., 2004). However, mutation of 4 potential PKA phosphorylation sites did not affect *Sc*Sip1 cellular localization (Hedbacker et al., 2004).

Taken together it appears that the role of Snf1/AMPK/SnRK1 β-subunit phosphorylation is not fully understood and will be an important area of research for the future. From our studies the full role of *Sl*Gal83 Ser26 phosphorylation by Adi3 is not clear. It appears to have only a minor role in controlling *Sl*SnRK1 complex kinase activity. So, additional functions attributable to this phosphorylation event will be important to identify in the future. Given the role of β-subunits in controlling Snf1/AMPK/SnRK1 complex localization and phosphorylation playing a role in this function, it will be important to examine the contribution of phosphorylation by Adi3 in controlling *Sl*Gal83 cellular localization. Consequently, the full extent of the *Sl*Gal83 Ser26 phosphorylation event by Adi3 remains to be determined.

4.8c Is there a link between cell death control and metabolism?

An important aspect of PCD is the reallocation of cellular resources such as proteins and sugars. This is particularly true of the cell death that occurs during leaf senescence (Doorn & EJ, 2004; Guiboileau et al., 2010). In fact, the reuse of cellular materials was suggested as early as 1891 from the examination of cell death associated

with xylem development (Lange, 1891). Thus, it may not be surprising that a gene controlling PCD would also be able to regulate how cells utilize and/or mobilize energy sources. This appears to be the case for mammalian PKB. While it is well known that PKB suppresses cell death by phosphorylating and inactivating proapoptotic proteins or activating antiapoptotic proteins (Carnero, 2010, Luo et al., 2003), PKB also functions in the regulation of metabolism through the control of glycolytic enzymes and glucose uptake (Carnero, 2010, Plas & Thompson, 2002). Such a connection between a specific plant gene controlling cell death and metabolism has been indirect at best. Our previous studies have shown that there are many striking activity and cellular localization similarities between Adi3 and PKB (Devarenne et al., 2006; Ek-Ramos et al., 2010).

The studies presented here showing Adi3 inhibition of *Sl*SnRK1 complex kinase activity adds one additional similarity between Adi3 and PKB since PKB is known to modulate AMPK activity. While PKB and AMPK do not directly interact with each other, there is substantial crosstalk between the pathways. For example, activation of PKB has been shown to down regulate AMPK activity and thus a decrease in AMP/ATP cellular ratios (Hahn-Windgassen et al., 2005, Kovacic et al., 2003). Conversely, activation of AMPK has been shown to inactivate PKB-regulated glycolysis (Grabacka & Reiss, 2008). Combining our current and previous Adi3 studies raises the possibility that Adi3 functions similarly to PKB in cell death and metabolism control. Further studies on the role of Adi3 association with the *Sl*SnRK1 complex, especially phosphorylation of Gal83, will be required to fully understand if there is a connection between Adi3-mediated cell death control and *Sl*SnRK1 metabolism control.

CHAPTER V

EFFECT OF GAL83 PHOSPHORYLATION ON CELLULAR LOCALIZATION

5.1 Rationale

In the previous chapter the interaction of Adi3 with the *Sl*SnRK complex was characterized. From these studies, it was established that the β-subunit *Sl*Gal83 was phosphorylated at multiple sites, one of which is Ser26 (Figure 24). It was then determined that this phosphorylation event decreases the kinase activity of the catalytic subunit *Sl*SnRK1. However, the kinase inhibition observed when the phosphomimic *Sl*Gal83^{S26D} is used *in vitro* is mild when compared to the inhibition observed when this mutant is overexpressed *in vivo.*

The difference in kinase activity is most likely explained by the additional roles *Sl*GAL83 plays in regulating the complex activity that cannot be recreated in an *in vitro* system. For instance, homologue β-subunits have been shown to regulate the intracellular localization of the SnRK complex and regulate its ability to interact with substrates. Similarly, β-subunits function as scaffolding units that facilitate the assembly of the complex bringing α- and γ-subunits together in response to the metabolic and developmental needs of the cell (Hardie, 2007).

These different regulatory mechanisms depend on β-subunit post-translational modifications such as phosphorylation and myristoylation (Mitchelhill et al., 1997, Pierre et al., 2007). In this chapter, I further explore the phosphorylation of *Sl*Gal83 in addition to its myristoylation in its effect on cellular localization.

5.2 Finding additional *Sl*Gal83 phosphorylation sites

Yeast and mammalian β-subunits are known to be phosphorylated at multiple sites (Mangat et al., 2010, Mitchelhill et al., 1997, Warden et al., 2001). Some of these residues are directly phosphorylated by the α-catalytic subunits with which the β-subunits form a complex, and are often called auto-phosphorylation residues despite the lack of β-subunit kinase activity *per se* (Mitchelhill et al., 1997).

The phosphorylation of *Sl*Gal83 and the related β-subunits *Sl*Sip1, *Tau*1, and *Tau*2 (Figure 18) by the catalytic subunit *Sl*SnRK1 was estimated in *in vitro* phosphorylation assays using recombinant *Sl*SnRK1 kinase inactive (K48Q) and constitutively active (T175D) mutants (Figure 29). *Sl*SnRK1 was found to be weakly phosphorylated by *Sl*Gal83 (Figure 29 A, B). *Sl*SnRK1 strongly phosphorylated *Sl*Sip1 and *Tau*2 with an approximate 6- and 3-fold increase in phosphorylation signal over *Sl*Gal83 respectively (Figure 29 compare lanes 1, 2 and 4). On the other hand, *Tau*1 and *Sl*Gal83 exhibit similar levels of phosphorylation (Figure 29 lanes 1 and 3).

Despite the weak phosphorylation of *Sl*Gal83, a phosphorylation screen using several Ser to Ala *Sl*Gal83 mutants was carried out in order to identify potential *Sl*SnRK1 phosphorylation sites on *Sl*Gal83. The screen revealed that a mutation removing Ser45 (S45A) drastically reduced the phosphorylation by *Sl*SnRK1. In addition to S45A, the double mutant S262A/S264R was found to significantly reduce phosphorylation (Figure 29 lanes 1 and 3).

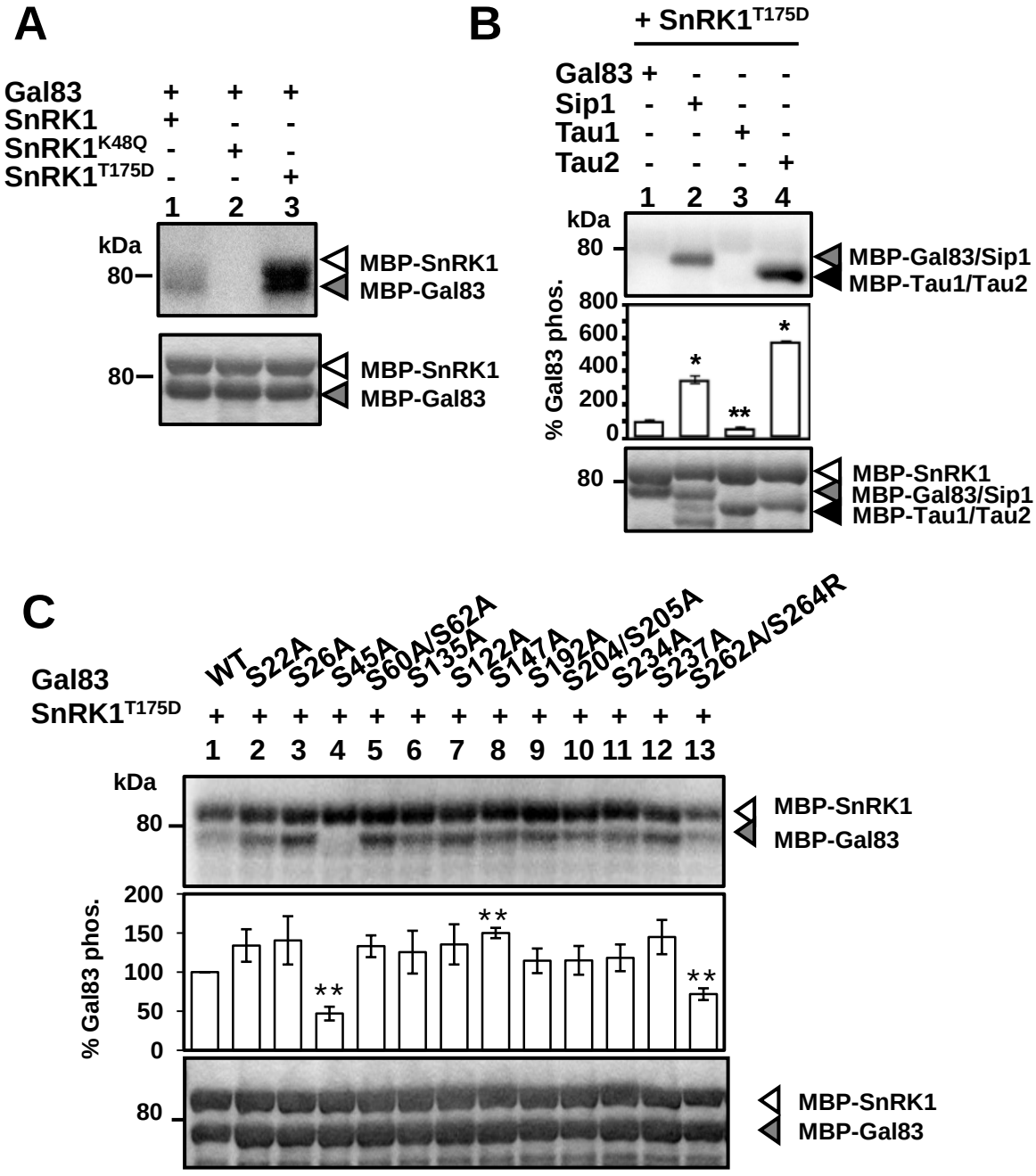

Figure 29. *Sl*SnRK1 phosphorylation of *Sl*Gal83. In A, B, and C the indicated proteins were incubated in an *in vitro* kinase assay with γ-[^{32}P]ATP, separated by SDS-PAGE and visualized by phosphorimager. Top panels, phosphorimage; bottom panels, Coomassie stained gel. A, The *Sl*SnRK1 α catalytic subunit can phosphorylate *Sl*Gal83. B, SnRK1strongly phosphorylates Sip1 and Tau2 β-subunits. Kinase-active MBP-SnRK1^{T175D} was tested for phosphorylation of MBP-*Sl*Gal83, MBP-*Sl*Sip1 MBP-Tau1, and MBP-Tau2 as in (B). C. Kinase-active MBP-*Sl*SnRK1^{T175D} was used to phosphorylate the indicated MBP-*Sl*Gal83 Ser to Ala mutants. Values are averages of three independent experiments. Error bars are standard error. One and two asterisks indicate significant increase or decrease, respectively, in β-subunit phosphorylation as compared to *Sl*Gal83 phosphorylation (Student's t test, * $p < 0.01$, ** $p < 0.05$).

SnRK complexes share a conserved phosphorylation motif, and the specific residues surrounding the Ser or Thr target residue for plant SnRK phosphorylation have been characterized (Figure 30A; Huang & Huber, 2001, Sugden et al., 1999). Using this motif, potential *Sl*SnRK1 phosphorylation residues on the β-subunits used in Figure 29 were identified. First, Ser45 in *Sl*Gal83 is absent in all of the other subunits Figure 30C). Whereas, the residues around Ser45 match the phosphorylation motif for SnRK with the exception of a polar amino acid at position -6, which in the motif appears at position -5 (Figure 30C lane 11). All β-subunits have between two and three Ser and Thr residues that align with Ser264 and Ser262 on *Sl*Gal83 (Figure 30B). However, each subunit has specific polymorphic sites within this motif that could help explain the differences observed in SnRK phosphorylation efficiency. For instance, both *Sl*Sip1 and Tau2 which are strongly phosphorylated by *Sl*SnRK1 have a match for the phosphorylation motif around Ser257 for *Sl*Sip1 and Ser244 for Tau2 (Figure 30B, alignment 5 and 7). This motif cannot explain, however, the low auto-phosphorylation of Tau1, which also has a Ser (S241) that perfectly fits the motif (Figure 30B, alignment 10). Instead, the phosphorylation differences could potentially be explained by the presence of a bulky Gln at position +2 on Tau1 instead of a Pro present in both Tau2 and *Sl*Sip1 (Figure 30B, marked in alignments 5, 7, 10). Taken together, these results suggest that the β-subunits studied are differentially phosphorylated by *Sl*SnRK. Additionally; the loss of SnRK phosphorylation observed using *Sl*Gal83^{S45A}, as well as the amino acid sequence analysis surrounding this residue, suggests that Ser45 is a unique target for *Sl*SnRK1 autophosphorylation absent in other tomato β-subunits.

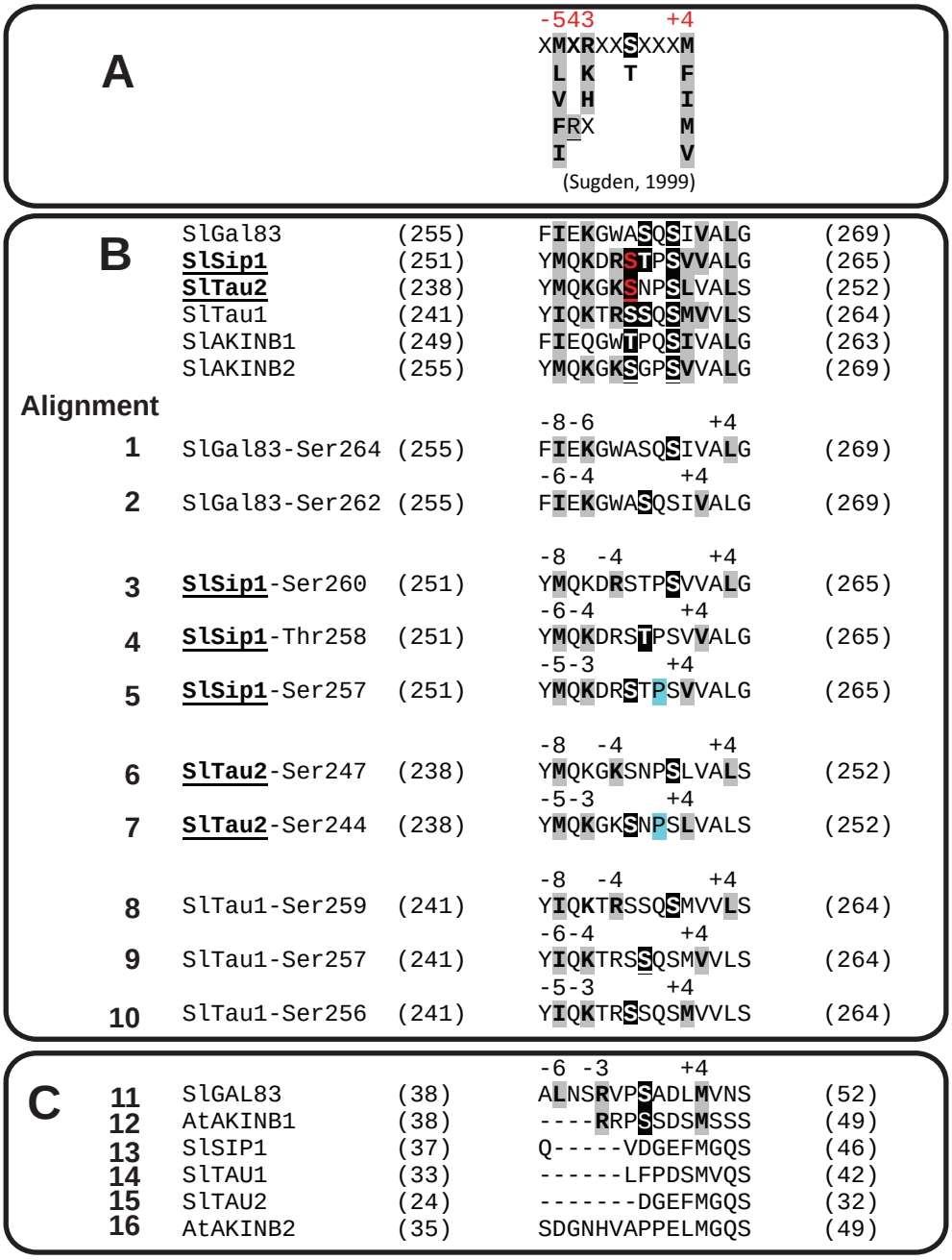

Figure 30. β-subunit *Sl*SnRK1 phosphorylation motif. Tomato and *A. thaliana* β-subunits were aligned using the BioEdit Sequence Alignment Editor (Hall, 1999) and SnRK phosphorylation motifs were identified. A, plant SnRK phosphorylation motif described by Sugden, 1999 and Huang, 1991. B, detailed analysis of the potential phosphorylation residues and motifs for each tomato β-subunit.C, motif surrounding Ser45 in *Sl*Gal83. Residues highlighted in grey correspond to conserved residues in motif sequence, highlighted in black are the Ser or Thr residues target of SnRK phosphorylation, and numbers in parenthesis show the amino acid location within each sequence. Highlighted in blue are Pro present in Tau2 and *Sl*Sip1, absent in Tau1 and *Sl*Gal83. Underlined are the β-subunits that are strongly phosphorylated by *Sl*SnRK1.

5.3 *Sl*Gal83 promoter isolation

In order to test the localization of *Sl*Gal83and phosphorylation mutants, we sought to isolate the native promoter that drives the expression of *Sl*Gal83 in tomatoes. Using BLAST searches against the genomic databases in the Solanacea Genomic Network (SGN) website (http://solgenomics.net/tools/blast/index.pl), the genomic region containing *Sl*Gal83 (U5356587) was mapped to chromosome 12 (Figure 31A). The vicinity upstream of the initiation site was analyzed and the stop codon of the closest upstream gene (U535657) was found to be 932 bp upstream of *Sl*Gal83 initiation site. Therefore, an 821bp fragment within this region excluding the 3'UTR of neighboring U535657 was amplified and subcloned into the plasmid pTEX driving the expression of *Sl*Gal83-GFP (*SlGal83pro*: Gal83-GFP; Figure 31).The original expression construct generated contained an ATG initiation immediately before the restriction site and the native initiation site for *Sl*Gal83. Thus, the translated protein has an additional three amino acids (+MGS) at its N-terminus (Figure 31A).

The expression of the construct *SlGal83pro*:Gal83-GFP (+MGS) was compared to the overexpression under the control of the 35S cauliflower mosaic virus CaMV promoter (*35SPro)* by transforming tomato protoplasts isolated from leaves and conducting α-GFP western blotting on total cell lysates 16 hours post-transformation. The level of *Sl*Gal83-GFP expressed under the native promoter (+MGS) was 20-fold lower than the *35SPro*-controlled expression as quantified by the intensity of the α-GFP immunoreactive bands (Figure 31B compare lanes 1 and 2).

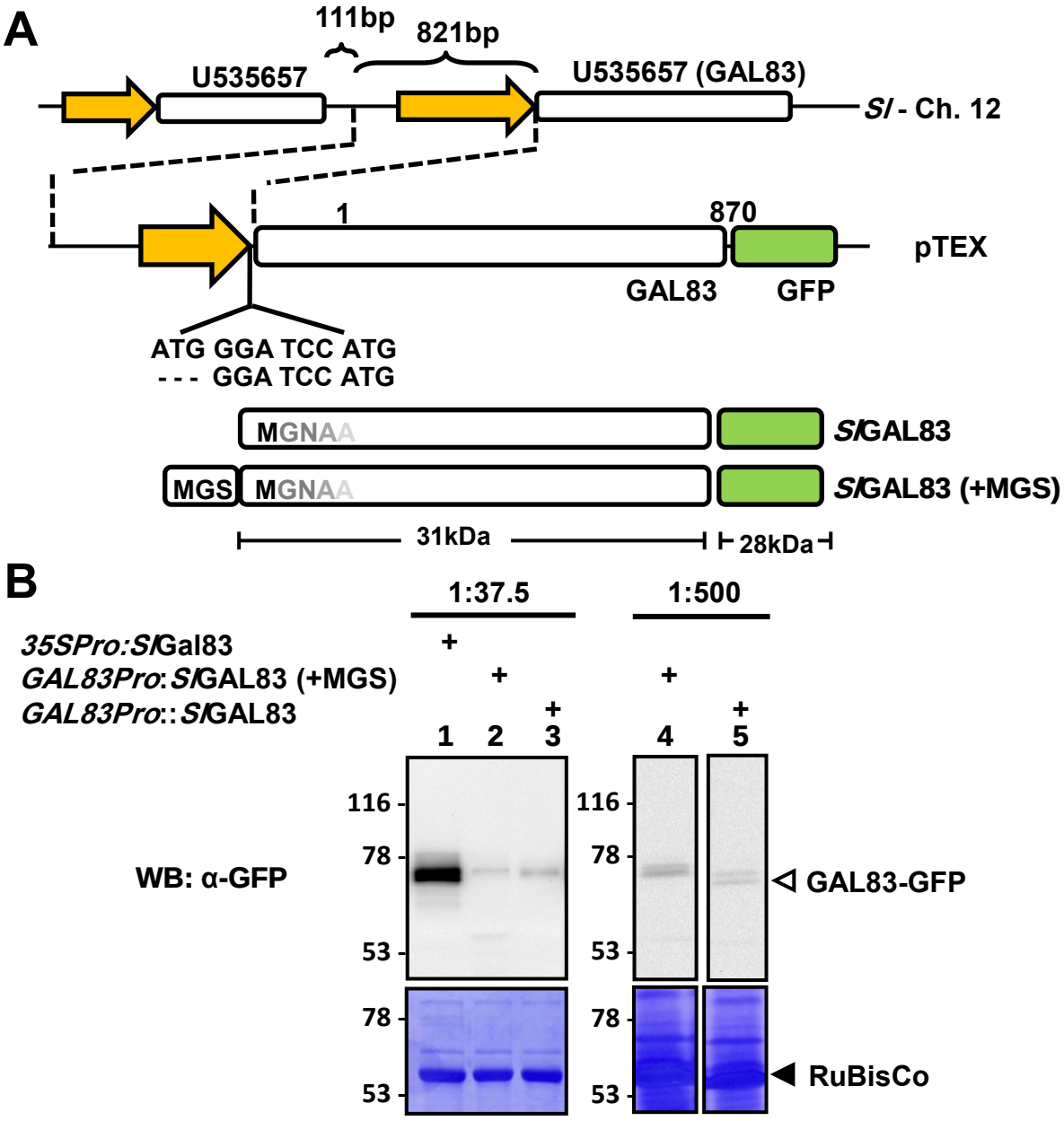

Figure 31. *Sl*GAL83 promoter isolation and expression profile. A, Schematic representation of the isolation of promoter region for *Sl*GAL83. The location of the *Sl*GAL83 gene was located in chromosome 12 using BLAST searches against the tomato whole-genome sequence database available at the Solanacea Genomic Network (SGN). An 821bp region flanked upstream by (U535657) and downstream by *Sl*GAL83 was isolated from tomato leaf genomic DNA and sub-cloned replacing upstream of *Sl*GAL83-GFP in the vector pTEX. Two constructs were generated: one carrying only the native initiation site (ATG) and one with an additional ATG prior to the restriction site (*Sl*GAL83+MGS). B. *Left*, The expression of the promoter constructs generated is compared to the over-expression of *Sl*Gal83-GFP under the control of the 35S cauliflower mosaic virus (CaMV) promoter. *Right*, detailed banding pattern of the promoter constructs generated in A. In both A and B proteins were transiently expressed in tomato protoplasts for 18 hours, extracts made in SDS-Sample buffer and proteins resolved by SDS PAGE (*Left:* 12% 1:37.5 Bis-:Acrylamide, *Right:* 10% % 1:500 Bis-:Acrylamide), and western blotting was performed using α-GFP 1:1000.

Evidence suggests plant β-subunits undergo N-terminal myristoylation. For instance, they have a typical N-terminal myristoylation motif: M-G-X(except EDFKRVWY)-X-X-[STACFGRV]-X (except DE), where Gly at position 2 is the residue to which myristate is attached, and X can be any amino acid, except where indicated (Boisson et al., 2003, Kakita et al., 2007; Figure 32A). On the other hand, both *A. thaliana* β-subunits are known to be myristoylated *in vitro* by N-myristoyltransferase (Pierre et al., 2007). Thus, it is possible that *Sl*Gal83 is myristoylated *in vivo,* and the addition of +MGS to the N-terminus disrupts the appropriate posttranslational processing or localization of the protein. To overcome this possible limitation, a construct lacking the additional initiation site was produced and its expression compared to that under the control of the *35Spro*. Both native promoter constructs, with or without the additional MGS residues, expressed similar protein levels (Figure 31B lanes 2 and 3). However, closer inspection of the expression of the promoter constructs under low Bis:Acrylamide ratio SDS-PAGE revealed a slight retardation in the migration of *Sl*Gal83-GFP when expressed under its native promoter and the residues MGS are present at the N-terminus (Figure 31B lanes 4 and 5).

5.4 Myristoylation affects *Sl*Gal83 phosphorylation

The small gel mobility retardation observed when the N-terminal region of *Sl*Gal83 is modified (Figure 31) is reminiscent of the protein mobility changes caused by protein phosphorylation (Figure 28). With this in mind, we asked whether complete removal of the myristoylation site would affect the phosphorylation state of *Sl*Gal83. A Gly to Ala myristoylation mutant (G2A) was expressed and its banding pattern

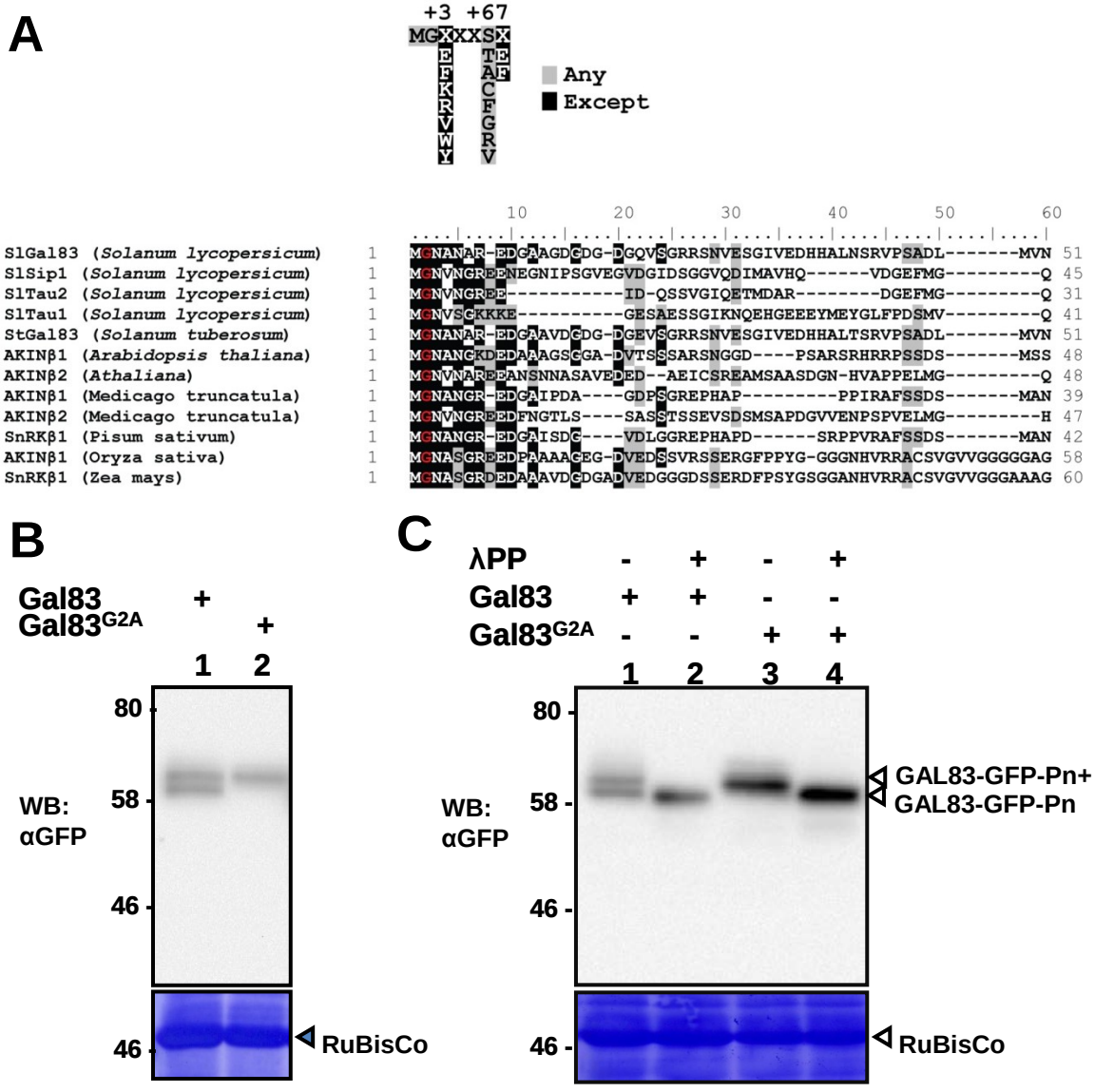

Figure 32. *Sl*Gal83 myristoylation knockout has increased phosphorylation *in vivo*. A, Plant β-subunits have an N-terminal myristoylation motif. Amino acid sequences were aligned using ClustalX and the N-terminus compared to the myristoylation motif. *Top:* residues highlighted in gray are required for myristoylation. X represents any amino acid except those highlighted in black. *Bottom:* Residues highlighted in black are identical, grey are similar, and Gly in red font is myristoylation site that matches the motif sequence. B, Substituting *Sl*Gal83 Gly-2 to Ala (*Sl*Gal83^{G2A}) decreases Gal83 electrophoretic mobility on an SDS PAGE. C, Gal83^{G2A} electrophoretic mobility is due to increased phosphorylation. Protoplast extracts expressing Gal83 and Gal83^{G2A} were treated with or without λ-phosphatase (λPP). In both B and C proteins were transiently expressed in tomato protoplasts for 18 hours after which total protein extracts were made. Proteins were resolved by SDS PAGE (10% 1:200 Bis-:Acrylamide), and western blotting was performed using α-GFP 1:1000.

compared to *Sl*Gal83 using α-GFP western blotting analysis. Expression of *Sl*Gal83^{G2A} – GFP displayed decreased electrophoretic mobility (Figure 32, B).

The differences in *Sl*Gal83 electrophoretic mobility have been shown to correspond to different phosphorylated forms (see Figure 24, Chapter IV). Thus, protoplast extracts expressing either *Sl*Gal83 or *Sl*Gal83^{G2A} were treated with λ phosphatase. Samples were resolved in 1:500 gels and analyzed with α-GFP western blotting. Untreated *Sl*Gal83 displays at least two defined phosphorylated forms as it has been seen before (Figure 32B lane 1, see Figure 27, Chapter IV), whereas *Sl*Gal83^{G2A} lacks the lower, faster-migrating band present in *Sl*Gal83 (Figure 32B lane 2). Phosphatase treated samples on the other hand, were found to migrate as a single, faster migrating band (Figure 32C lanes 2 and 4). These results indicate that the difference in electrophoretic mobility observed between Gal83 and Gal83^{G2A} is a consequence of an increase in phosphorylation in the myristoylation mutant.

5.5 Phosphorylation and myristoylation control *Sl*Gal83 localization

After the successful isolation of the *Sl*Gal83 promoter and the unexpected correlation between N-terminal myristoylation and phosphorylation, we sought to determine the effect of these post-translational modifications in the intracellular localization of *Sl*Gal83. Fluorescence microscopy and cellular fractionation were used to estimate the localization of *Sl*Gal83 using tomato protoplasts transformed with *Sl*Gal83-GFP and *Sl*Gal83 phosphorylation and myristoylation mutants transcribed under the control of the *35SPro* and *Gal83Pro*. Proteins were expressed for 16 hours and a cells visualized by fluorescence microscopy. The specific location of the nucleus was

determined by treating protoplasts with the DNA stain HOECHST 33342 (Arndt-Jovin and Jovin, 1977) and chlorophyll auto-fluorescence was used to estimate the location of the chloroplasts.

The expression of *Sl*Gal83 under *Gal83Pro* was low as predicted by low protein levels observed in western blotting analysis (Figure 31B), and no fluorescence signal was detected when cells were observed under the microscope (data not shown). On the other hand, *SlGal83* expressed under the *35SPro* was readily visible after 16 hours post-transfection (Figure 33A). Given the similar banding pattern observed between *Sl*Gal83-GFP expressed under *SlGal83Pro* and *35SPro*, *35SPro* was used for all subsequent fractionation and microscopy experiments.

*Sl*Gal83 displays different types of localization: cytosol, nucleus, around the chloroplasts, or forming discrete foci surrounding the chloroplast (Figure 33A top panels and B, Figure 34). These different localizations vary according to each individual cell analyzed and, while some cells can present all types of localization to some degree, cells appear to have one particular type or combination of intracellular localizations. The *Sl*Gal83 phosphorylation knockout mutant S26A for instance causes an increase in the localization around the chloroplast and a higher proportion of cells containing foci around the chloroplast. This localization is accompanied by a concomitant reduction in the *Sl*Gal83-GFP signal in the nucleus (Figure 33, Figure 35). Conversely, the phosphomimetic mutation S26D favors cytosolic and nuclear localization while the presence of cells with foci-localized *Sl*Gal83 is reduced (Figure 33). Similar localization patterns were observed when the SnRK1 phosphorylation target Ser45 was mutated to

Figure 33. Localization of *Sl*Gal83, Ser26 phosphorylation, and myristoylation mutants. A, Tomato protoplasts were transformed with pTEX plasmids containing the corresponding proteins with a C-terminal GFP tag under the expression of the 35S cauliflower mosaic virus (CaMV) promoter. Pictures were taken 18 hours after expression. Cells were treated with HOECHST 33342 (5 μg/ml) for 30 minutes to stain nuclei and visualized by fluorescence microscopy. Merge; *left*: chloroplast auto-fluorescence and GFP, *right*: chloroplasts autofluorescence, GFP, and nuclei. The white arrowhead points at the location of the nucleus. B, *Sl*Gal83 localizes to discrete foci, *left*, fluorescence, *right*: cartoon representation, red: chloroplasts, dotted circle: nucleus, green dots: foci-localized *Sl*Gal83.

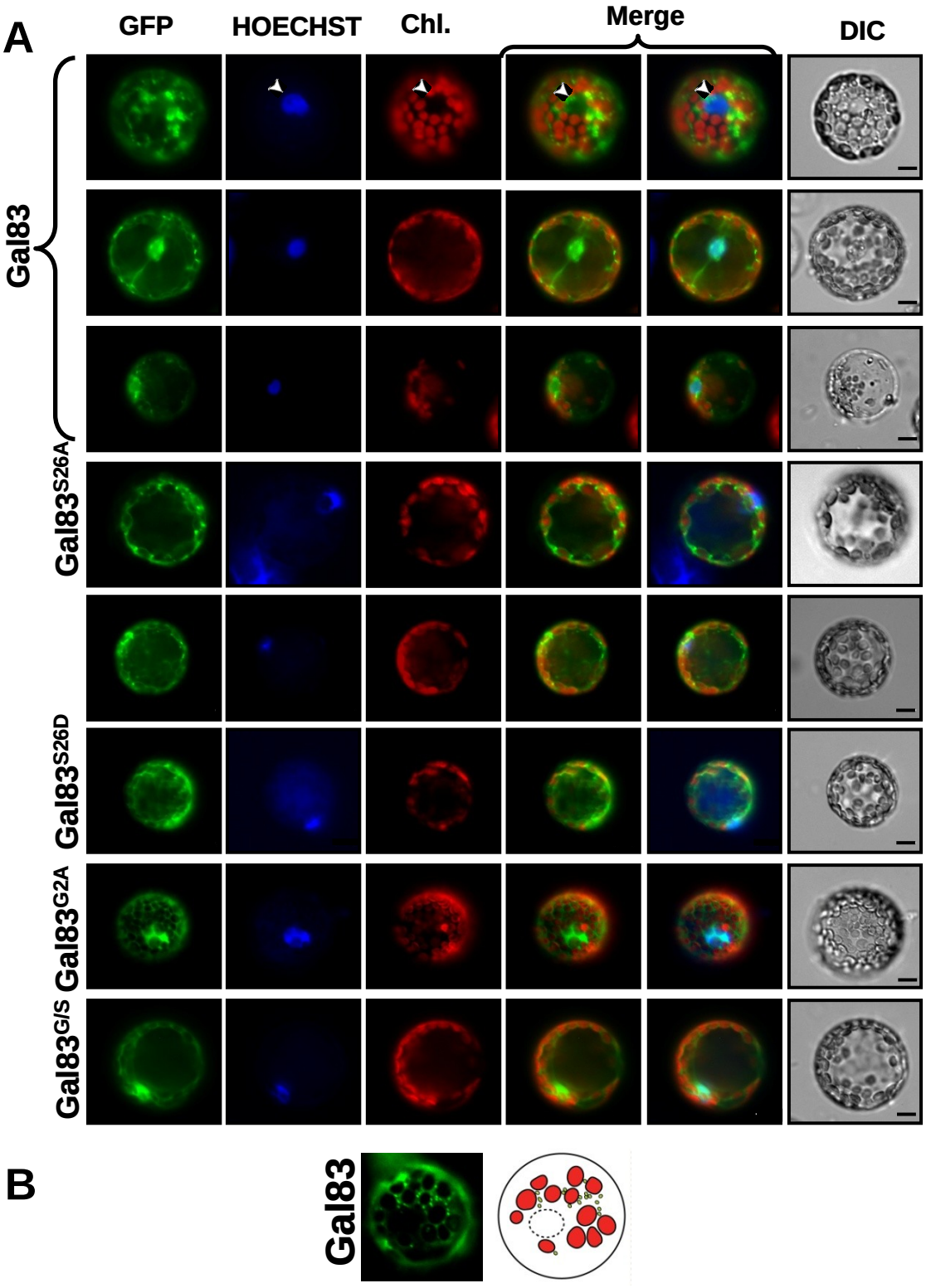
A
GFP
HOECHST
Chl.
Merge
DIC
Gal83
Gal83S26A
Gal83S26D
Gal83G2A
Gal83G/S
B
Gal83

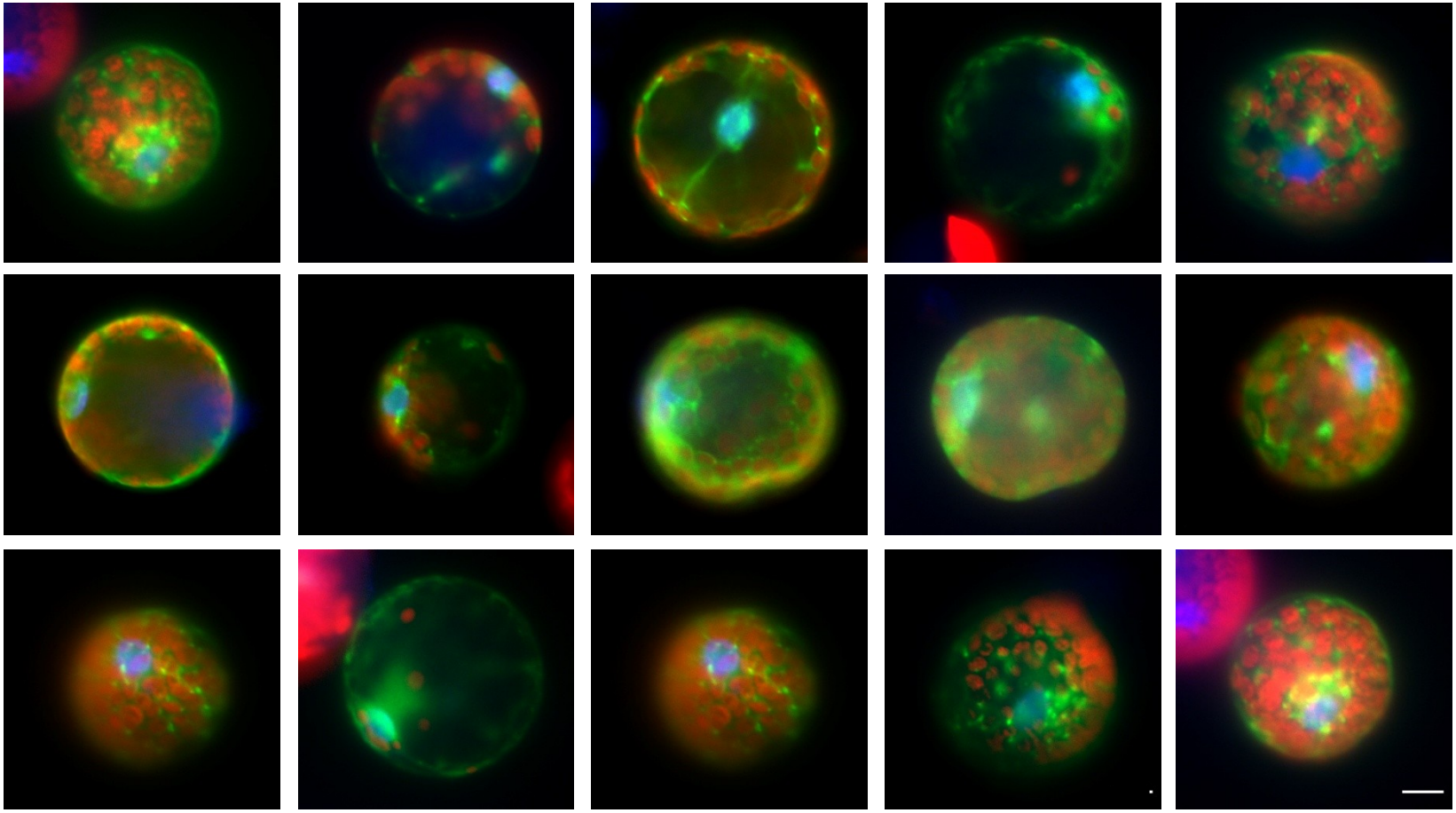

Figure 34. Localization of *Sl*Gal83. Protoplasts expressing C-terminal GFP-tagged *Sl*Gal83 under the expression of the 35S cauliflower mosaic virus (CaMV) promoter. Nuclei were stained using HOECHST 33342 (5 µg/ml) for 30 minutes. All images are a merged overlay of : chloroplast auto-fluorescence (red), GFP (green), and nuclei (blue).

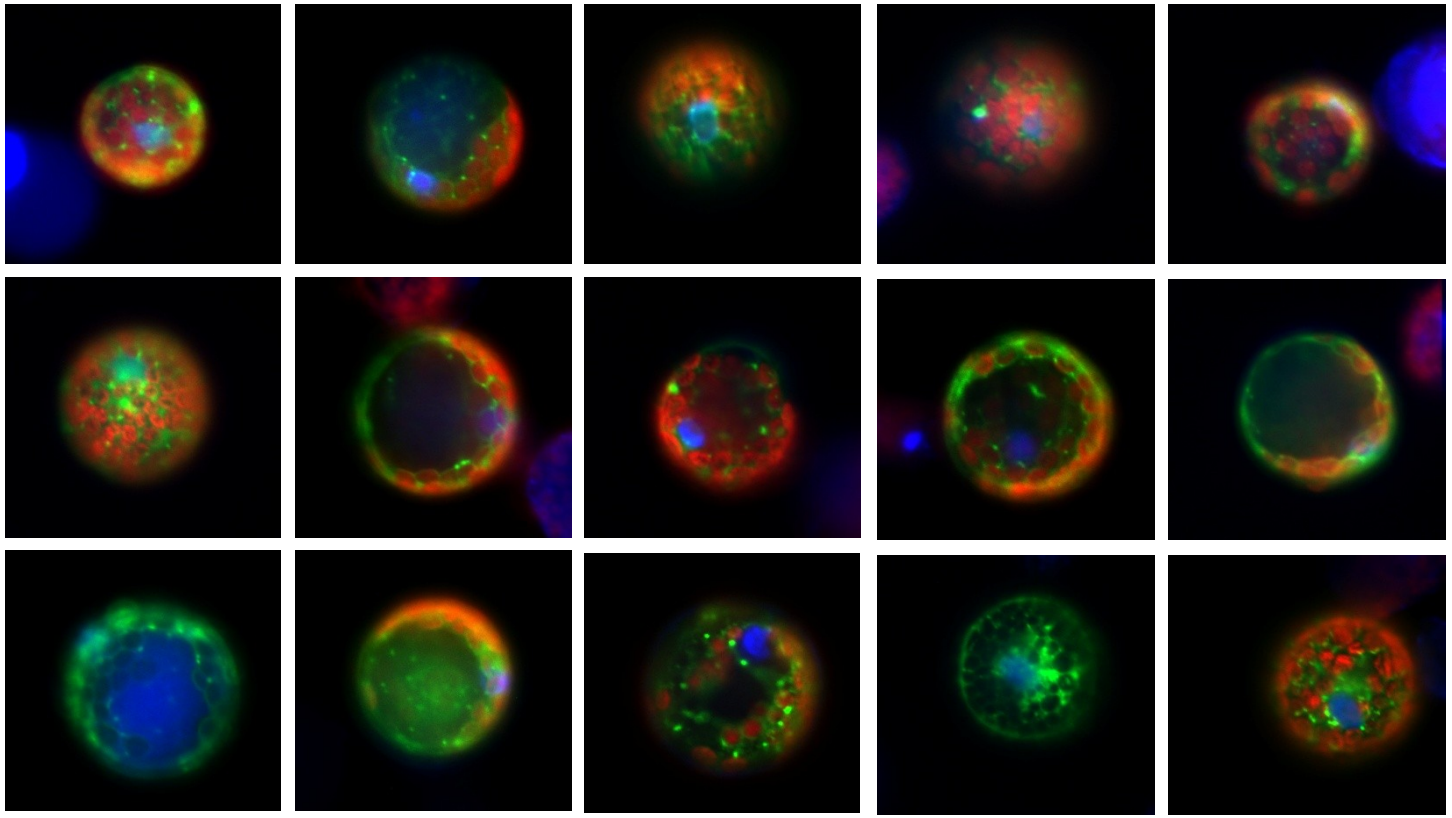

Figure 35. Localization of *Sl*Gal83^{S26A}. Protoplasts expressing C-terminal GFP-tagged *Sl*Gal83 under the expression of the 35S cauliflower mosaic virus (CaMV) promoter. Nuclei were stained using HOECHST 33342 (5 µg/ml) for 30 minutes. All images are a merged overlay of : chloroplast auto-fluorescence (red), GFP (green), and nuclei (blue).

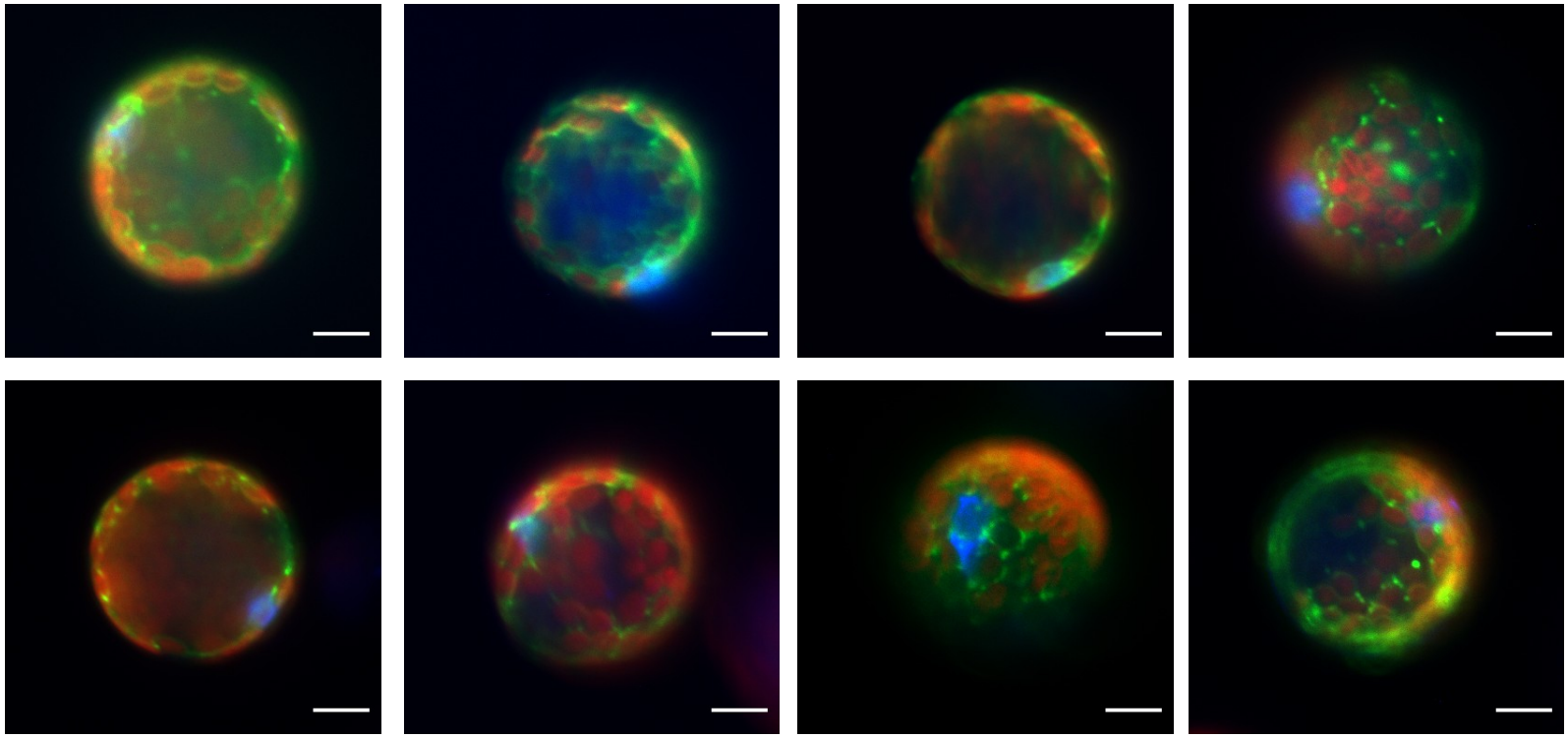

Figure 36. Localization of *Sl*Gal83^{S45A}. Protoplasts expressing C-terminal GFP-tagged *Sl*Gal83 under the expression of the 35S cauliflower mosaic virus (CaMV) promoter. Nuclei were stained using HOECHST 33342 (5 µg/ml) for 30 minutes. All images are a merged overlay of: chloroplast auto-fluorescence (red), GFP (green), and nuclei (blue).

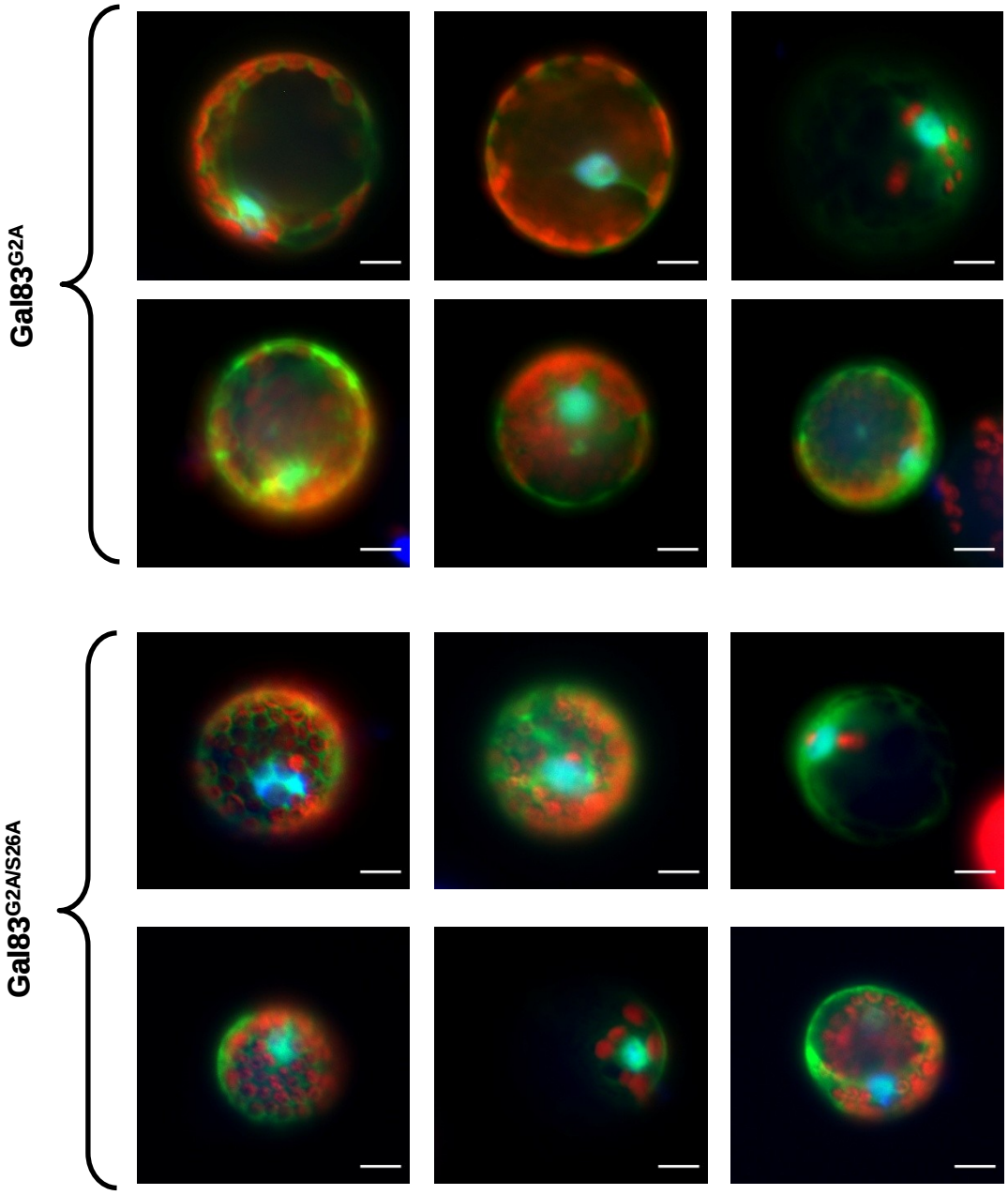

Figure 37. Localization of *Sl*Gal83^{G2A} and *Sl*Gal83$^{G2A/S26A}$. Protoplasts expressing C-terminal GFP-tagged *Sl*Gal83 under the expression of the 35S cauliflower mosaic virus (CaMV) promoter. Nuclei were stained using HOECHST 33342 (5 µg/ml) for 30 minutes. All images are a merged overlay of : chloroplast auto-fluorescence (red), GFP (green), and nuclei (blue).

Ala (Figure 33, Figure 36). The removal of the myristoylation signal which causes an increase in *Sl*Gal83 phosphorylation causes *Sl*Gal83 to adopt a diffuse cytosolic and nuclear localization (Figure 33, Figure 37). Similarly, the double phosphorylation /myristoylation mutant *Sl*Gal83$^{G2A/S26A}$ exhibits localization similar to *Sl*Gal83^{G2A}, indicating myristoylation is required for the foci and membrane localization of *Sl*Gal83^{S26A} or *Sl*Gal83^{S45A} phosphorylation deficient mutants (Figure 33, Figure 37).

To further explore the localization of *Sl*Gal83 fractionation experiments were conducted on transformed protoplasts 18 hours after transformation. First, nuclear (N) fractionations were obtained by gently lysing the cells in the presence of low detergent concentration (0.2% Triton-X100). After nuclei isolation, the remaining lysates were fractionated into total (T), soluble protein (S), and insoluble fractions (I) using ultracentrifugation as previously described (Ek-Ramos et al., 2010). Equivalent protein amounts of each fraction were resolved in SDS-PAGE, following α-GFP or α-Histone3 western blotting analysis to track *Sl*Gal83-GFP and nuclear enrichment, respectively. The nuclear enrichment of *Sl*Gal83 was calculated as follows: the ratio of band intensity in T and N was estimated for α-GFP (*Sl*Gal83) and α-H3 (Histone). The ratio obtained for αGFP was normalized by dividing by the T/N αH3 ratio (nuclear enrichment for each sample) and values for the mutations tested were normalized as a percentage of nuclear *Sl*Gal83 wild type. The amount of nuclear *Sl*Gal83 was found to decrease when Adi3 phosphorylation site (Ser26) was mutated (47% of *Sl*Gal83, Figure 38), while a slight increase in nuclear localization with the phosphomimetic mutant S26D was observed (120% of *Sl*Gal83, Figure 38A). The protein found in the insoluble fraction was low and

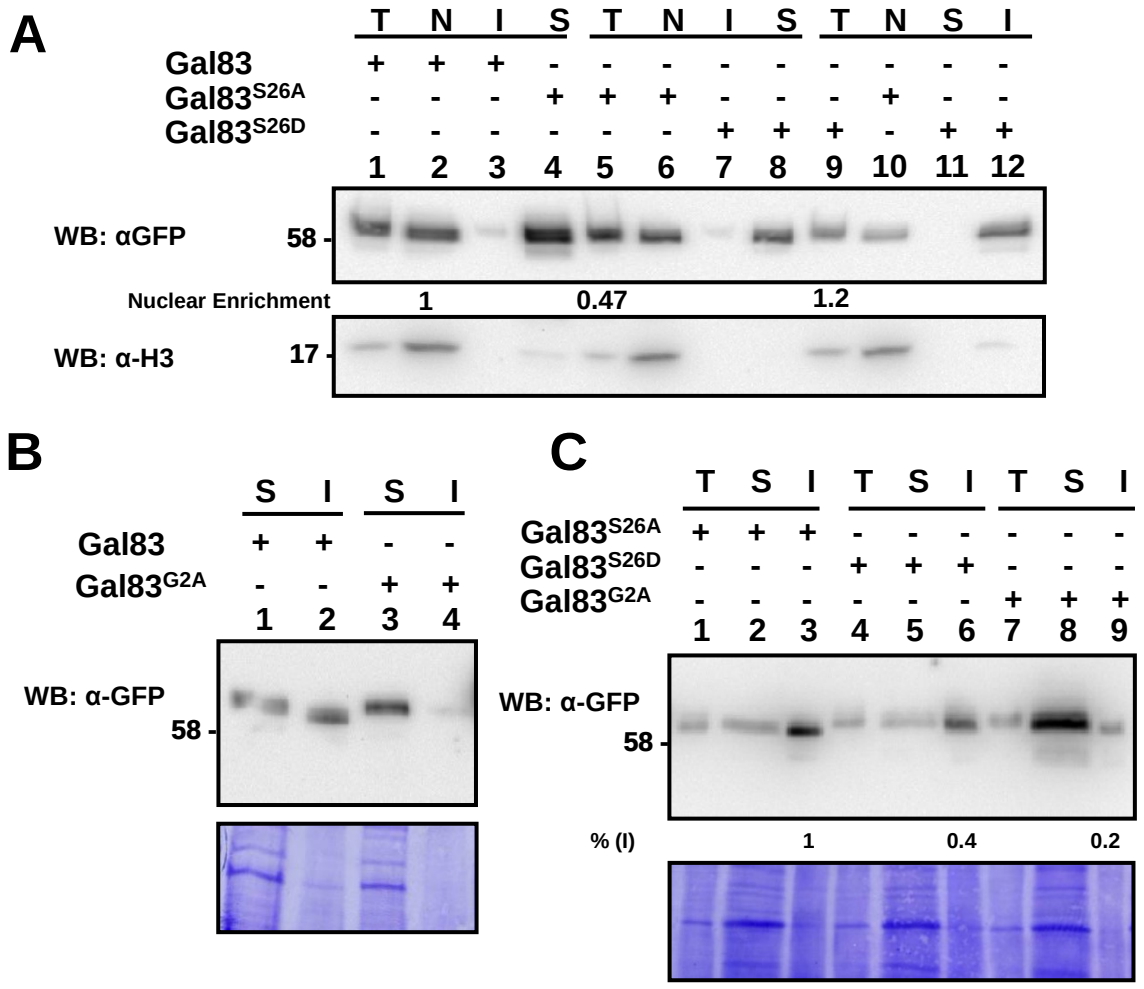

Figure 38. Myristoylation and phosphorylation affect *Sl*Gal83 cellular partitioning. A, Nuclear fractionation using low detergent concentration. B - C, Soluble and insoluble fractionation in the absence of detergent. Proteins were expressed for 18 hours in tomato protoplasts and nuclear or membrane fractionation was conducted, equivalent protein amounts were resolved in 10% SDS-PAGE and analyzed by western blotting with α-GFP and α-Histone 3 antibodies. Band intensity in T and N was estimated for α-GFP (*Sl*Gal83) and α-H3 (Histone) and the ratio obtained for αGFP was normalized by dividing by the T/N αH3 ratio (nuclear enrichment).All values were then made a percentage of *Sl*Gal83 nuclear fraction. Values are an average of two independent fractionation experiments. % (I) was calculated as the intensity of I divided by T and normalized to the value obtained for Gal83$^{S26A.}$Fractions: Total (T), Nuclei (N), Soluble (S), Insoluble (I).

could not be compared among mutants likely caused by the presence of detergent used during the lysis process. Therefore, a fractionation of total soluble and insoluble protein in the absence of detergent was conducted. The myristoylation mutant *Sl*Gal83^{G2A} was found enriched in the soluble fraction (Figure 38B lanes 3 and 4 and C, lanes 7-9). Similarly, the phosphorylation knockout *Sl*Gal83^{S26A} appears enriched in the insoluble fraction when compared to the phosphomimetic mutant *Sl*Gal83^{S26D} (Figure 38C, lanes 3 and 6). Detailed analysis of *Sl*Gal83 banding pattern under low Bis:acrylamide SDS-PAGE revealed that highly phosphorylated protein (slow mobility) is found mainly in the soluble fraction (Figure 38B lanes 1 and 3), while protein with lower phosphorylation (higher mobility) remains membrane-bound in insoluble fractions (Figure 38A lanes 1 and 3). Taken together, localization data suggest phosphorylation and myristoylation control the localization of *Sl*Gal83in which myristoylation is required for membrane association, while phosphorylation of Ser26 favors a cytosolic and nuclear localization.

5.6 Discussion

The control over the activity of the SnRK complex relies on several post-translational regulatory mechanisms. The myristoylation and phosphorylation of β-subunits have been widely characterized in yeast and mammals and is known to play a role in the regulation of SnRK complex activity and localization (Mitchelhill et al., 1997, Oakhill et al., 2010, Warden et al., 2001).

5.6a Differential phosphorylation of β-subunits

Our results show that the tomato β-subunits *Sl*Gal83, *Sl*Sip1, Tau1, and Tau2 are differentially phosphorylated by the α-catalytic subunit of the SnRK complex *Sl*SnRK1. To our knowledge, no other report of differential auto-phosphorylation of the β-subunits by *Sl*SnRK1 is available. Out of the four tomato β-subunits, *Sl*SnRK1 was found to strongly phosphorylate only *Sl*Sip1 and Tau2. The implications of these differences in phosphorylation are puzzling and could potentially reflect two different scenarios.

First, the *Sl*SnRK1α-subunit could have preferential binding affinity for and, thus phosphorylate the β-subunits *Sl*Sip1 and Tau2, while *Sl*Gal83 and Tau1are the target for a different catalytic subunit. Until recently, *Sl*SnRK1 was the only α-subunit characterized in tomato, but the availability of a genomic sequence (The tomato genome consortium, 2012) has allowed for the identification of *Sl*SnRK2 (SGN-U566966), an additional α-catalytic subunit that shares 67% identity with *Sl*SnRK1. The differences in phosphorylation observed could thus be an outcome of the α-subunit used in this study.

Second, several lines of evidence suggest that different combinations of plant α- and β-subunits can bind and form complexes *in vitro* and *in vivo* (Bouly et al., 1999; Ferrando et al., 2001; Kleinow et al., 2000). All of the tomato β-subunits studied contain a conserved kinase interacting domain and are likely to interact with both tomato *Sl*SnRKs. If their interaction with the kinase subunit is similar, β-subunit phosphorylation differences could be explained directly at the phosphorylation motif rather than the formation of different complexes with α-subunits. This scenario was studied by identifying and analyzing the potential phosphorylation residues present on

the β-subunits. Despite the low *Sl*Gal83 phosphorylation, the residues Ser45, Ser262, and Ser264 were identified as potential targets for *Sl*SnRK1 phosphorylation (Figure 29). These residues likely represent *in vivo Sl*SnRK phosphorylation targets because they match to different degrees the plant SnRK phosphorylation motif and are conserved among β-subunits in tomato as well as other orthologus plant β-Subunits (Figure 30). Furthermore, the likelihood of these residues being real phosphorylation sites, even when they deviate from a perfect SnRK phosphorylation motif, is supported by the observation that SnRKs can phosphorylate residues that are not a perfect match to the established consensus sequence (Tsai & Gazzarrini, 2012).

The detailed analysis of the motifs revealed that the reduced phosphorylation observed on *Sl*Gal83 and Tau1 could be explained by a Gln to Pro substitution present in the immediate vicinity of the phosphorylation site. Gln are bulky amino acids and Pro can cause kinks in protein structure. Further characterization of the phosphorylation site in the tomato β-subunits as well as their ability to interact and be phosphorylation the α-subunit SnRK2 will be required to understand the differential phosphorylation of the β-subunits and the two scenarios here proposed.

5.6b Multisite SlGal83 phosphorylation, which phosphorylation comes first?

Interestingly, out of the *Sl*Gal83 residues tested for *Sl*SnRK1 phosphorylation, only the removal of Ser45 completely blocks the phosphorylation by *Sl*SnRK1. Meanwhile, mutations affecting Ser262 and Ser264 significantly reduced phosphorylation but did not completely eliminate it. These observations suggest that phosphorylation of Ser45, a residue not present in other β-subunits, is required for the

phosphorylation of additional residues. We previously characterized (CHAPTER IV) the phosphorylation of Ser26 by the tomato PCD suppressor Adi3. When expressed *in vivo*, mutations affecting Ser26 cause a decrease in overall *Sl*Gal83 phosphorylation which is seen as an enrichment of lower-migrating less-phosphorylated bands (Figure 39). Like Ser45 phosphorylation, Ser26 phosphorylation seems to be required for the phosphorylation of additional unknown sites *in vivo*. However, unlike Ser26, *Sl*Gal83^{S45A} expression does not cause a substantial reduction in phosphorylation *in vivo* (Figure 26, Figure 27, Figure 39). This could indicate that Ser26 has a stronger disruptive effect over the hyper-phosphorylation of *Sl*Gal83 than Ser45 does. On the other hand, Ser26 phosphorylation could be a constitutive phosphorylation event, while *Sl*SnRK phosphorylation of *Sl*Gal83 could be induced by a, yet to be characterized, stimulus.

Proteins that are phosphorylated at multiple sites act as translators that convert kinases signals into sensitive switch-like responses (Kim & Ferrell, 2007, Koivomagi et al., 2011, Nash et al., 2001, Thomson & Gunawardena, 2009). Recently, the study of the hierarchical multisite phosphorylation of the yeast cell cycle regulator Sic1 demonstrated that phosphorylation of its N-terminal priming sites facilitates the phosphorylation of additional sites by enhancing its interaction with upstream kinases (Koivomagi et al., 2011). For a protein that is phosphorylated at multiple sites, *Sl*Gal83 could follow a similar regulatory mechanism, in which SnRK and Adi3 act as activating kinases that prime that phosphorylation of additional sites. Since β-subunits have no kinase activity, these priming phosphorylation events must facilitate the phosphorylation

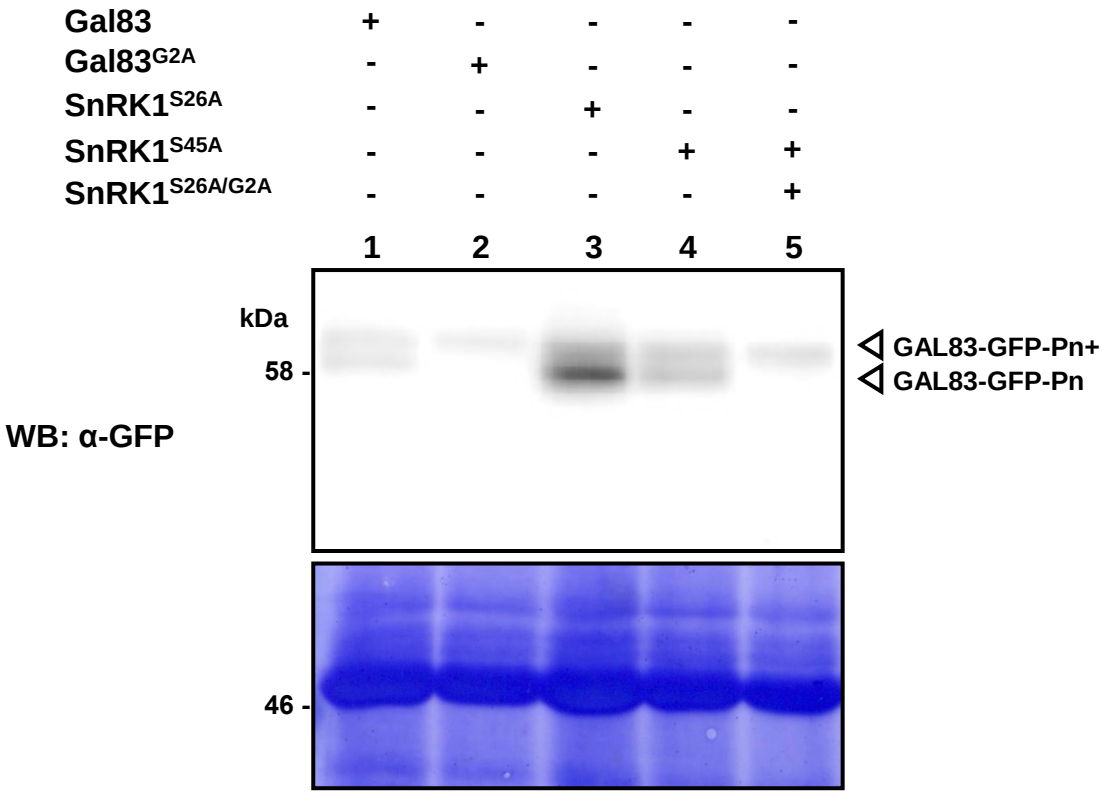

Figure 39. Electrophoretic mobility of *Sl*Gal83 Ser26 and Ser45 phosphorylation knockouts. Indicated proteins were transiently expressed in tomato protoplasts for 18 hours and cells collected and lysed in SDS sample buffer. Total proteins were resolved by SDS PAGE and analyzed by western with α-GFP 1:1000

of additional residues by enhancing the interaction with the upstream kinases or cause conformational changes that facilitate the access to suboptimal phosphorylation sites.

5.6c SlGal83 myristoylation and phosphorylation; myristoyl switch?

Myristoylation is a widespread β-subunit co-translational modification that is required for the proper localization and activation state of the SnRK complex (Iseli et al., 2008, Mitchelhill et al., 1997, Oakhill et al., 2010, Pierre et al., 2007, Steinberg & Kemp, 2009). The N-terminal attachment of myristate is commonly used as mechanism to attach proteins to membranes (Steinberg & Kemp, 2009). The removal of the mammalian AMPKβ myristoylation site, causes a mobilization between a cytosolic particulate localization to a diffuse cytosolic one (Mitchelhill et al., 1997, Oakhill et al., 2010). Similarly, the plant AKINβ2 myristoylation mutant is detached from membranes and found primarily in a diffuse cytosolic distribution (Pierre et al., 2007). Our results indicate that *Sl*Gal83 can adopt different localizations and be partitioned in nuclear, cytosolic, or in discrete foci around the nucleus and chloroplasts. This localization is dramatically affected by the removal of a myristoylation site (G2A) which causes the disappearance of foci-localized *Sl*Gal83 and favors a diffuse nucleo-cytosolic distribution. This indicates that *Sl*Gal83, like other β-subunits, relies on myristoylation to regulate localization.

Interestingly, the removal of *Sl*Gal83 myristoylation causes an increase in protein phosphorylation in which the lower, less phosphorylated, *Sl*Gal83 bands are completely absent. This observation suggests that different *Sl*Gal83 phosphorylation states localize differently. For instance, low phosphorylated *Sl*Gal83 which can be generated with the

removal of Ser26 or Ser45, promotes membrane association and potentially the formation of the observed foci. This association is dependent on myristoylation as removal of Ser26 loses its membrane binding affinity when the myristoylation mutation is introduced. These observations could explaining why, at a given time, *Sl*Gal83 can be found in different localizations, since different phosphorylation forms are always found when *Sl*Gal83 is expressed. This doesn't appear to be an artifact of protein overexpression, however, since *Gal83Pro* expressed protein has a similar phosphorylation pattern.

It has been proposed that β-subunits, like other myristoylated proteins, use a myristoyl switch regulatory mechanism to alter cellular localization in response to stimuli (McLaughlin & Aderem, 1995, Resh, 2006. Working with mammalian AMPKβ, Oakhill (2010) and Steinberg (2009) suggest that β-subunits are subject to an AMP-dependant myristoyl-switch, that sequesters the protein's N-terminus into a membrane, where it is incapable of inhibiting the catalytic activity of the complex (Oakhill et al., 2010). Our data supports a traditional electrostatic-myristoyl switch in which the phosphorylation of the N-terminus causes the dissociation of SlGal83 from membranes, due to the electrostatic clashes of the negatively charged phosphates with the membrane phospholipids. However, additional studies on the impact of these phosphorylation events on the interaction of SlGal83 with SnRK should be conducted to elucidate this regulatory model.

A detailed study of *Sl*Gal83 phosphorylation sites *in vivo* and their effect on the binding of the myristoylated protein to membranes and the SnRK complex should

provide information on the significance of these post-translational modifications in regulating protein localization and their interaction with *Sl*SnRK1, Adi3, or additional upstream kinases. In conclusion, the β-subunits are differentially phosphorylated by the α-subunit *Sl*SnRK1. *Sl*Gal83 phosphorylation by *Sl*SnRK1 appears to be part of a group of post-translational modifications, that along with Adi3 phosphorylation at Ser26 and N-terminal myristoylation, regulate the intracellular localization of this β-subunit.

CHAPTER VI

CONCLUSIONS AND FUTURE DIRECTIONS

6.1 Chapter III conclusions and future directions

6.1a A new set of tools for the study of plant ubiquitination

In Chapter III, the interaction of Adi3 with the RING-finger E3 ubiquitin ligase AdBiL was characterized. An *in vitro* ubiquitination system was standardized and optimized with the use of the *A.thaliana* and tomato E2 enzymes and the *A. thaliana* E1 enzyme *AtUBA1.* The successful activation and transfer of Ub using plant, but not commercially available mammalian E2 enzymes, highlights one of the limitations faced when studying plant ubiquitination *in vitro*. The addition of these ubiquitination enzymes to the plant biochemistry toolbox has allowed for the characterization of, not only the ubiquitination of AdBiL and Adi3 described in this chapter, but the study of other plant specific ubiquitination processes. For instance, the use of highly purified *AtUBA1* and *AtUBC8* derived from the *in vitro* studies in this chapter, allowed me to collaborate with the lab of Ping He in our department to characterize the ubiquitination of the PAMP receptor FLS2 (Lu et al., 2011). These tools have so far been shared with several other laboratories and should facilitate ubiquitination research in plant science.

In addition to the development of ubiquitination enzymes, an Adi3 specific antibody was generated. This antibody was found to efficiently recognize Adi3 when used in western blotting experiments with recombinant proteins. Unfortunately, the

antibody titer was low and endogenous Adi3 protein present in plant extracts was not detected. Thus, it was not useful for studying ubiquitination *in vivo.*

6.1b What does Adi3 ubiquitination mean in vivo?

The *in vitro* evidence presented in this chapter for the ubiquitination of both AdBiL and Adi3 is a first step in the characterization of the interaction between these two proteins. Additional evidence for the ubiquitination and its outcome should be addressed *in vivo.* The involvement of the 26S proteasome in the degradation of Adi3 indicates that Adi3 ubiquitination indeed takes place *in vivo,* but the involvement of AdBiL in this process is not known. Additional short term studies should address: the interaction of AdBiL and Adi3 *in planta*, the ubiquitination of Adi3 *in vivo*, and the role that AdBiL might play in such ubiquitination.

First, the interaction of both proteins can be studied *in vivo* by co-immunoprecipitation experiments or bi-molecular fluorescence complementation experiments (BiFC; Kerppola, 2008). This, because the *in vitro* and yeast two hybrid interactions do not guarantee these two proteins interact constitutively *in planta*. Preliminary data show that C-terminally GFP tagged AdBiL can be overexpressed in plant protoplasts (not shown). The co-expression with Adi3 could provide information on Adi3 protein stability and localization in the presence of AdBiL which are two of the potential Adi3 ubiquitination outcomes studied in this chapter.

Second, the ubiquitination of Adi3 has to be demonstrated *in vivo*. Identifying ubiquitinated proteins *in vivo* is challenging due to the low ubiquitination levels detected, the presence of de-ubiquitinating enzymes, and the involvement of the 26S

proteasome in removing certain types of poly-ubiquitinated proteins (Peng, 2003, Wilkinson, 2000). In order to overcome these complications, enrichment of ubiquitinated proteins can be accomplished by coexpressing Adi3 with epitope-tagged ubiquitin, followed by affinity purification of total ubiquitinated proteins and western blotting detection of Adi3. The selective immunoprecipitation of ubiquitinated Adi3 could facilitate the analysis of the type of ubiquitination (mono or poly) that is occurring on Adi3, another important element in determining the fate of ubiquitinated Adi3.

Finally, the role of AdBiL in Adi3 ubiquitination can be tested once an efficient mechanism to detect Adi3 ubiquitination *in vivo* has been standardized. AdBiL can be selectively removed and the impact on Adi3 ubiquitination tested. This can be accomplished either by outcompeting functional AdBiL by overexpressing inactive forms of AdBiL that are incapable of interacting with E2 ligases, or by directly knocking down expression levels through viral induced gene silencing.

6.1c Is Adi3 a target for plant metacaspases?

Adi3 was found to be rapidly degraded when incubated in the presence of plant extracts. In addition to proteasomal-mediated degradation, the formation of cleavage products indicates Adi3 is targeted by proteases. When compared in size, the degradation products suggest Adi3 is cleaved close to its N-terminus. The identification of the proteases involved in this cleavage could draw an interesting connection between regulation of Adi3 levels and programmed cell death. The characterization of the plant cysteine-proteases known as metacaspases and their role in cell death is, unlike metazoan caspases, still at its infancy. But several caspase-specific inhibitors can be

used to inhibit PCD induction in plants and could potentially be used to study the metacaspase cleavage of Adi3 (del Pozo & Lam, 1998, Solomon et al., 1999).

6.2 Chapter IV conclusions and future directions

In chapter IV I characterize the interaction of Adi3 with the SnRK complex which is a conserved eukaryotic master regulator of energy homeostasis (Halford et al., 2000, Polge & Thomas, 2007) . Studying this interaction, I found that Adi3 is capable of interacting with three subunits of the complex, the α-catalytic *Sl*SnRK1 and the β regulatory subunits *Sl*Gal83 and *Sl*Sip1. A detailed inspection of these interactions revealed that Adi3 phosphorylates only *Sl*Gal83. This phosphorylation event was pursued given the importance of this subunit and its posttranslational phosphorylation in regulating the complexes activation state, localization, and interaction with substrates. With this phosphorylation, a great opportunity was found to link cell death regulation by Adi3 with energy homeostasis with SnRK activity regulation; a connection that has long been drawn in mammalian PCD processes such as senescence and apoptosis (Steinberg & Kemp, 2009).

6.2a In vivo phosphorylation; technological limitations

A considerable portion of this chapter is focused on the detailed characterization of this phosphorylation event, and describing Ser26 as the phosphorylation site *in vitro* and *in vivo*. The *in vitro* identification of this site as the phosphorylation target of Adi3 was relatively easy. Translating this knowledge *in vivo*, however, proved a challenging feat because of the low expression levels of Gal83 and the difficulties obtaining enough protein from plant or protoplast tissue.

One of the challenging aspects of studying protein phosphorylation *in vivo* is demonstrating that both kinase and substrates interact *in vivo,* while directly linking this interaction with phosphorylation. All of the evidence collected in this chapter provided circumstantial *in vivo* evidence for the phosphorylation of *Sl*Gal83 by Adi3, but not a direct linkage of both phenomena *in vivo*. Our lab has experimented with an approach successfully used in yeast, in which a modified protein kinase can use bulky ATP analogues to study substrate phosphorylation *in vivo* (Dittrich & Devarenne, 2012). Unfortunately, despite working well *in vitro,* attempts to apply this technology to Adi3 *in vivo* have proven unsuccessful. While a new approach is developed to address these limitations, additional evidence could be collected to further demonstrate the connection between *Sl*Gal83 phosphorylation at Ser26 by Adi3. For instance, silencing or outcompeting endogenous Adi3 with kinase inactive Adi3^{K337Q} can be done in tomato leaves or protoplasts, and the phosphorylation state of *Sl*Gal83 estimated by mass spectrometry of gel shift assays as done in Figure 27.

6.2b Adi3, an inhibitor of SnRK kinase activity?

One of the most important findings in this study is the negative regulation Adi3 exerts on SnRK activity. Adi3 was found to inhibit SnRK activity by directly interacting with *Sl*SnRK1 or, indirectly, by phosphorylating *Sl*Gal83 at Ser26. The phosphorylation of Ser26 was found to decrease the kinase activity *in vivo* and *in vitro*. However, we have not investigated the effect overexpression of Adi3 might have on the activity of the SnRK complex *in vivo.* Adi3 overexpression could potentially reduce the activity of the complex, but as has been observed in mammals with PKB, the inhibitory activity over

AMPK requires signaling cues such as the kinase activation by insulin signaling (Beauloye et al., 2001, Kovacic et al., 2003).

So far, a few metabolites have been identified convincingly as negative regulators of plant SnRK activity (Halford & Hey, 2009). A few examples are the accumulation of trehalose-6-phosphate (Ananieva et al., 2008, Paul et al., 2010, Schluepmann et al., 2011, Zhang et al., 2009) and potentially glucose-6-phosphate (Toroser et al., 2000) .The effect on *Sl*Gal83 and Adi3 phosphorylation under these, as well as yet to be identified SnRK complex inhibitory conditions, should be studied to elucidate the signaling mechanisms that trigger SnRK inhibition by Adi3. In addition to Adi3 activating and SnRK inhibition stimuli, the expression profiles of *Sl*Gal83, especially during pathogenesis, should be taken into consideration since Adi3 could act as a conditional inhibitor of SnRK activity, inhibiting only when *Sl*Gal83 expression is induced.

6.2c SlGal83 in carbon reallocation

Recently, *Nicotiana attenuata* expression of Gal83 was found to be down-regulated during herbivore attack causing a reallocation of photosynthates to the root (Schwachtje et al., 2006). Conversely, antisense repression of potato StGal83 has been shown to interfere with the appropriate development of roots and tubers (Lovas et al., 2003) while SnRK activity appears to favor the allocation of carbon to the root (Halford & Hey, 2009). In this case, these conflicting results indicate *Sl*Gal83 can either function in reallocating carbon to the roots or inhibiting it. Further studies on the posttranslational modifications accompanying the transcription changes should help elucidate these

contrasting observations and the potential role of SlGal83 post-translational modifications, since these studies solely rely on expression data.

6.2d Towards a model for SlGal83 regulation in PCD

Very little information is available on the regulatory roles of β-subunits on the activity of plant SnRK complexes. This study provides important evidence linking β-subunit phosphorylation with negative complex activity regulation. Evidence indicates *Sl*Gal83 orthologues can act as negative regulators of SnRK activity in PCD regulation. For instance, the expression of the β-subunits in *A. thaliana* is strongly induced during senescence (Polge et al., 2008). Interestingly, SnRK appears to negatively regulate this type of PCD as observed with the overexpression of the active α-catalytic subunit (AKIN10, AKIN11) which delays the appearance of senescence markers (Cho et al., 2012) and represses the expression of the senescence associated genes 1 and 5 (Baena-Gonzalez et al., 2007). Our data supports a model in which both the overexpression of *Sl*Gal83 and its phosphorylation by Adi3 are required to inactivate SnRK in order to suppress its negative regulation over senescence.

In terms of pathogen-mediated PCD and HR, it will be fundamental to estimate if the activity of the SnRK complex is altered in plants exposed to susceptible or resistant interactions with *Pst.* Likewise, the phosphorylation state of *Sl*Gal83 during these cell death processes should provide information on the role of Adi3 in mediating pathogen-triggered or plant-controlled (HR) cell death.

6.3 Chapter V conclusions and future directions

6.3a Characterization of SlGal83 additional phosphorylation sites

In Chapter V, I attempted to characterize additional phosphorylation sites on SlGal83 and the overall impact of protein phosphorylation in cellular localization. In order to find phosphorylation sites we took advantage of the knowledge that β-subunits are phosphorylated within the SnRK complex by the α-catalytic subunit. Since a collection of *Sl*Gal83 Ser to Ala mutants had been developed for Chapter IV, the approach used these mutants to test for loss of *Sl*SnRK1 phosphorylation. Despite being a weak phosphorylation event, we identified Ser45 as a residue that is required for SnRK phosphorylation and the region around Ser262 and Ser264 as an additional potential phosphorylation target. I speculated that Ser262 and Ser264 phosphorylations are primed by the upstream phosphorylation on Ser45 resembling a hierarchical phosphorylation cascade observed in other multi-site phosphorylated proteins (Koivomagi et al., 2011). It has been described that priming phosphorylations enhance docking interactions with the kinase, facilitating the phosphorylation of sub-optimal sites. This hypothesis could be tested by evaluating the binding between a Ser45 phosphomimic *Sl*Gal83^{S45D} and *Sl*SnRK1. Similar to the description of Ser26 as an Adi3 phosphorylation site, the *in vivo* validation of Ser45 as a phosphorylation target of SlSnRK1 will have to be investigated using mass spectrometry of *Sl*Gal83 expressed *in planta*.

6.3b Myristoylation, phosphorylation, and localization; a model for SlGal83 regulation

In an attempt to estimate the localization of *Sl*Gal83-GFP, I isolated the *Sl*Gal83 promoter region to express fluorescently tagged protein at endogenous levels. This was

done with the goal to prevent spurious localization artifacts caused by the use of overexpression promoters. Unfortunately, the expression levels observed were low and no fluorescence was detectable. Luckily, the isolation of the promoter and the detailed analysis of its protein expression in SDS-PAGE and western blotting analysis lead me to two important observations. First, the banding pattern associated to *SlGal83Pro* and the *35Pro* is very similar, indicating that the SlGal83 phosphorylation bands observed when the protein is overexpressed are not likely an overexpression artifact. Second, mutations affecting the N-terminus of the protein, and an *Sl*Gal83 myristoylation signal, have an effect on the banding pattern of the protein and its phosphorylation state.

In this chapter, one of the most important findings was the connection established between phosphorylation and myristoylation. I found that removing the myristoylation causes an increase in *Sl*Gal83 phosphorylation. It is not known whether this observation is conserved in other β-subunits as most studies of their post-translational modifications aim to understand the effect of myristoylation in the activity or localization of the complex as a whole (Lin et al., 2003, Mitchelhill et al., 1997, Oakhill et al., 2010).

Unsurprisingly, the removal of *Sl*Gal83 myristoylation affects membrane binding and favors a diffuse nucleo-cytosolic localization; an observation that has been reported for many β-subunits (Mitchelhill et al., 1997, Oakhill et al., 2010, Pierre et al., 2007, Warden et al., 2001). Unlike most of these studies, however, this chapter provided evidence for a link between phosphorylation and cell localization in a myristoylation-dependent manner. In our model, *Sl*Gal83 is subject to a myristoyl-electrostatic switch

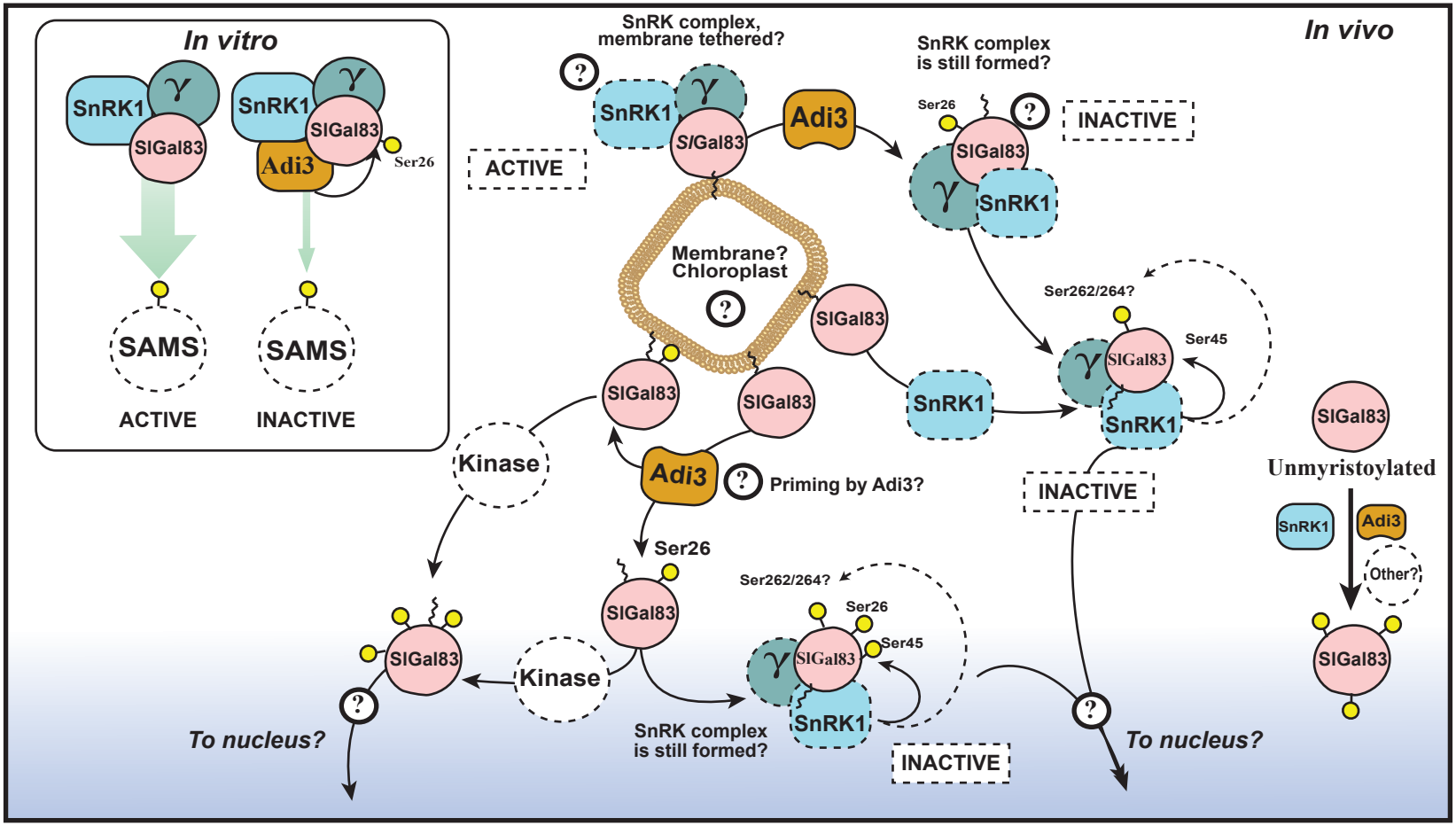

Figure 40. Building a model for *Sl*Gal83 phosphorylation. In this study I characterized the myristoylation and phosphorylation of *Sl*Gal83. The phosphorylation of *Sl*Gal83 Ser26 by Adi3 acts as an inhibitor of SnRK activity and appears to trigger additional phosphorylation events that release membrane localized *Sl*Gal83. Also, the catalytic subunit of the complex (*Sl*SnRK1) was found to phosphorylate *Sl*Gal83 in vitro at Ser45. Finally, myristoyaltion was found to be required for the proper localization and phosphorylation state of *Sl*Gal83. My results raise multiple questions that are summarized in this figure. The timing of these postranslational modification, their impact on the subcellular localization of the complex, and their effect on the activity of the SnRK should be addressed to begin to understand the role of these events in the light of PCD regulation.

which causes myristoylated *Sl*Gal83 to dissociate from membranes (Figure 40). However, many questions remain unanswered and further studying will be required in order to validate this model.

First, where in the cell is Adi3 phosphorylating *Sl*Gal83? Furthermore, which membrane is *Sl*Gal83 attached to? Myristoylation is traditionally linked to plasma membrane targeting, however, our localization studies indicate *Sl*Gal83 localizes to discrete foci and what appears to be the chloroplast membrane (Figure 33). Further membrane and organelle fractionation experiments should be conducted, preferentially using stable transformed transgenic plants in order to avoid the variability in expression and localization observed in protoplasts systems. Several lines of two *A. thaliana* plants expressing *Sl*Gal83 and *Sl*Gal83^{S26A} were generated for studies in Chapter IV and could be used to obtain preliminary information on the exact identity of *Sl*Gal83 cellular localization.

Second, it appears as if the phosphorylation of additional sites other than Ser26 on SlGal83 takes place, not at the membrane, but in the soluble cytosolic distribution, because *Sl*Gal83^{S26D} and *Sl*Gal83^{G2A}, which are preferentially found in the cytosol, are highly phosphorylated when analyzed in western blotting analyses (Figure 40). Adi3 could phosphorylate Ser26 causing the dissociation of SlGal83 from membranes and its phosphorylation by a set of cytosolic or nuclear kinases (Figure 40).

Third, Gal83^{S26D} inhibits SnRK kinase activity, however, the mechanism of such inhibition is not known. A model has been proposed for mammalian AMPKβ, in which the myristoyl group binds a hydrophobic pocket within the catalytic subunit causing its

inhibition. With our data, this model would imply that Adi3 causes the dissociation of *Sl*Gal83 from the membrane and the membrane-free myristoyl group binds *Sl*SnRK causing its inhibition. This model would help explain the differences in *Sl*SnRK1 kinase activity inhibition observed when *Sl*Gal83^{S26D} was used *in vivo* and *in vitro* SAMS phosphorylation assays (Figure 28, Chapter IV), since the recombinant *Sl*Gal83 used in these experiments is not myristoylated. If this model is correct, no reduction in *Sl*SnRK activity should be observed when *Sl*Gal83^{G2A} is overexpressed since the myristoyl exerts the inhibitory effect. Also, Ser26 phosphorylation should cause an increase in *Sl*Gal83 association to *Sl*SnRK *in vivo*.

6.4 Final conclusions

In this study I have provided additional evidence in support of the functional homology between the tomato cell death regulator Adi3 and the mammalian AGC kinase PKB. I show that like PKB, Adi3 is ubiquitinated, potentially processed by proteases, and an inhibitor of SnRK activity. The mechanisms and outcomes of the post-translational modifications involving Adi3 and its interactors, AdBiL and the SnRK complex, are far from being fully understood. However, I believe these studies pave the road for a better understanding of Adi3 function, not only in PCD regulation, but in different signaling pathways that integrate the different decisions that plants have to make when encountering a pathogen. Future studies should frame the significance of the current findings under a framework that fully elucidates their involvement, if any, in PCD and pathogen interactions.

REFERENCES

Abramovitch RB, Kim YJ, Chen S, Dickman MB, and Martin GB. (2003) Pseudomonas type III effector AvrPtoB induces plant disease susceptibility by inhibition of host programmed cell death, *EMBO J* **22**: 60-69.

Abramovitch RB, and Martin GB. (2004) Strategies used by bacterial pathogens to suppress plant defenses, *Curr Opin Plant Biol* **7**: 356-364.

Abramovitch RB, and Martin GB. (2005) Avrptob: A bacterial type III effector that both elicits and suppresses programmed cell death associated with plant immunity, *FEMS Microbiol Lett* **245**: 1-8.

Affenzeller MJ, Darehshouri A, Andosch A, Lütz C, and Lütz-Meindl U. (2009) Salt stress-induced cell death in the unicellular green alga *Micrasterias denticulata*, *J Exp Bot* **60**: 939-954.

Ahn J-Y, Liu X, Liu Z, Pereira L, Cheng D, Peng J, Wade PA, Hamburger AW, and Ye K. (2006) Nuclear Akt associates with Pkc-phosphorylated Ebp1, preventing DNA fragmentation by inhibition of caspase-activated dnase, *EMBO J* **25**: 2083-2095.

Ananieva EA, Gillaspy GE, Ely A, Burnette RN, and Erickson FL. (2008) Interaction of the WD40 domain of a myoinositol polyphosphate 5-phosphatase with SnRK1 links inositol, sugar, and stress signaling, *Plant Phys* **148**: 1868-1882.

Anthony RG, Henriques R, Helfer A, Meszaros T, Rios G, Testerink C, Munnik T, Deak M, Koncz C, and Bogre L. (2004) A protein kinase target of a PDK1 signalling pathway is involved in root hair growth in arabidopsis, *EMBO J* **23**: 572-581.

Asai T, Tena G, Plotnikova J, Willmann MR, Chiu W-L, Gomez-Gomez L, Boller T, Ausubel FM, and Sheen J. (2002) MAP kinase signalling cascade in Arabidopsis innate immunity, *Nature* **415**: 977-983.

Ashrafi K, Lin SS, Manchester JK, and Gordon JI. (2000) Sip2p and its partner Snf1p kinase affect aging in *S. cerevisiae*, *Genes Dev* **14**: 1872-1885.

Bachmair A, Novatchkova M, Potuschak T, and Eisenhaber F. (2001) Ubiquitylation in plants: A post-genomic look at a post-translational modification, *Trends Plant Sci* **6**: 463-470.

Baena-Gonzalez E, Rolland F, Thevelein JM, and Sheen J. (2007) A central integrator of transcription networks in plant stress and energy signalling, *Nature* **448**: 938-942.

Barberon M, Zelazny E, Robert S, Conéjéro G, Curie C, Friml J, and Vert G. (2011) Monoubiquitin-dependent endocytosis of the iron-regulated transporter 1 (Irt1) transporter controls iron uptake in plants, *PNAS* **108**: 450–458.

Beauloye C, Marsin A-S, Bertrand L, Krause U, Hardie DG, Vanoverschelde J-L, and Hue L. (2001) Insulin antagonizes AMP-activated protein kinase activation by ischemia or anoxia in rat hearts, without affecting total adenine nucleotides, *FEBS L* **505**: 348-352.

Bent AF, and Mackey D. (2007) Elicitors, effectors, and R genes: The new paradigm and a lifetime supply of questions, *Annu Rev Phytopathol* **45**: 399-436.

Beutler BA. (2009) TLRs and innate immunity, *Blood* **113**: 1399-1407.

Biondi RM. (2004) Phosphoinositide-dependent protein kinase 1, a sensor of protein conformation, *Trends Biochem Sci* **29**: 136-142.

Block A, and Alfano JR. (2011) Plant targets for *Pseudomonas syringae* type III effectors: Virulence targets or guarded decoys?, *Curr Opin in Microbiol* **14**: 39-46.

Bogdanove AJ, and Martin GB. (2000) Avrpto-dependent Pto-interacting proteins and AvrPto-interacting proteins in tomato, *PNAS* **97**: 8836-8840.

Bögre L, Ökrész L, Henriques R, and Anthony RG. (2003) Growth signalling pathways in Arabidopsis and the AGC protein kinases, *Trend Plant Scie* **8**: 424-431.

Boisson B, Giglione C, and Meinnel T. (2003) Unexpected protein families including cell defense components feature in the n-myristoylome of a higher eukaryote, *J Biol Chem* **278**: 43418-43429.

Borden KLB. (2000) Ring domains: Master builders of molecular scaffolds?, *J Mol Biol* **295**: 1103-1112.

Bradford KJ, Downie AB, Gee OH, Alvarado V, Yang H, and Dahal P. (2003) Abscisic acid and gibberellin differentially regulate expression of genes of the Snf1-related kinase complex in tomato seeds, *Plant Physiol* **132**: 1560-1576.

Brunet A, Bonni A, Zigmond MJ, Lin MZ, Juo P, Hu LS, Anderson MJ, Arden KC, Blenis J, and Greenberg ME. (1999) Akt promotes cell survival by phosphorylating and inhibiting a forkhead transcription factor, *Cell* **96**: 857-868.

Busch H, and Goldknopf IL. (1981) Ubiquitin — protein conjugates, *Molecular and Cellular Biochemistry* **40**: 173-187.

Callis J, Carpenter T, Sun CW, and Vierstra RD. (1995) Structure and evolution of genes encoding polyubiquitin and ubiquitin-like proteins in *Arabidopsis thaliana* ecotype columbia, *Genetics* **139**: 921-939.

Cao J, F J, and Sodmergen CK. (2003) Time-course of programmed cell death during leaf senescence in eucommia ulmoides, *J Plant Res* **162**: 7.

Carlson M, Osmond BC, and Botstein D. (1981) Mutants of yeast defective in sucrose utilization, *Genetics* **98**: 25-40.

Carlson M, Osmond BC, Neigeborn L, and Botstein D. (1984) A supressor of Snf1 mutation causes constitutive high-level invertase synthesis in yeast, *Genetics* **107**: 19-32.

Carnero A. (2010) The Pkb/Akt pathway in cancer, *Curr Pharm Des* **16**: 34-44.

Celenza J, and Carlson M. (1986) A yeast gene that is essential for release from glucose repression encodes a protein kinase, *Science* **233**: 1175-1180.

Chang JH, Rathjen JP, Bernal AJ, Staskawicz BJ, and Michelmore RW. (2000) AvrPto enhances growth and necrosis caused by *Pseudomonas syringae* pv. Tomato in tomato lines lacking either pto or prf, *MPMI* **13**: 568-571.

Chang JH, Urbach JM, Law TF, Arnold LW, Hu A, Gombar S, Grant SR, Ausubel FM, and Dangl JL. (2005) A high-throughput, near-saturating screen for type III effector genes from pseudomonas syringae, *PNAS***102**: 2549-2554.

Chau V, Tobias J, Bachmair A, Marriott D, Ecker D, Gonda D, and Varshavsky A. (1989) A multiubiquitin chain is confined to specific lysine in a targeted short-lived protein, *Science* **243**: 1576-1583.

Chen X, Wang Y, Li J, Jiang A, and Zhang W (2009) Mitochondrial proteome during salt stress-induced programmed cell death in rice, *Plant Phys Biochem* **47:**407-415.

Cheng W, Munkvold Kathy R, Gao H, Mathieu J, Schwizer S, Wang S, Yan Y-b, Wang J, Martin Gregory B, and Chai J. (2011) Structural analysis of

Pseudomonas syringae AvrPtoB bound to host BAK1 reveals two similar kinase-interacting domains in a type III effector, *Cell Host Microbe* **10**: 616-626.

Chinchilla D, Zipfel C, Robatzek S, Kemmerling B, Nurnberger T, Jones JDG, Felix G, and Boller T. (2007) A flagellin-induced complex of the receptor FLS2 and BAK1 initiates plant defence, *Nature* **448**: 497-500.

Chisholm ST, Coaker G, Day B, and Staskawicz BJ. (2006) Host-microbe interactions: Shaping the evolution of the plant immune response, *Cell* **124**: 803-814.

Cho Y-H, Hong J-W, Kim E-C, and Yoo S-D. (2012) Regulatory functions of snrk1 in stress-responsive gene expression and in plant growth and development, *Plant Phys* **158**: 1955-1964.

Coll NS, Vercammen D, Smidler A, Clover C, van Breusegem F, and Dangl JL. (2010) Arabidopsis type I metacaspases control cell death, *Science* **330**: 1393-1397.

Coll NS, Epple P, and Dangl JL. (2011) Programmed cell death in the plant immune system, *Cell Death Differ* **18**: 1247-1256.

Collier SM, and Moffett P. (2009) NB-LRRs work a bait and switch on pathogens, *Trend Plant Sci* **14**: 521-529.

Collmer A, Schneider DJ, and Lindeberg M. (2009) Lifestyles of the effector rich: Genome-enabled characterization of bacterial plant pathogens, *Plant Physiol* **150**: 1623-1630.

Dale S, Arró M, Becerra B, Morrice NG, Boronat A, Hardie DG, and Ferrer A. (1995) Bacterial expression of the catalytic domain of 3–hydroxy-3–methylglutaryl-CoA reductase (isoform HMGR1) from *Arabidopsis thaliana*, and its inactivation by phosphorylation at Ser577 by *Brassica oleracea* 3-hydroxy-3-methylglutaryl-CoA reductase kinase, *Eur J Biochem* **233**: 506-513.

Dale S, Wilson WA, Edelman AM, and Hardie DG. (1995) Similar substrate recognition motifs for mammalian AMP-activated protein kinase, higher plant HMG-CoA reductase kinase-A, yeast Snf1, and mammalian calmodulin-dependent protein kinase I, *FEBS Lett* **361**: 191-195.

Dangl JL, and Jones JDG. (2001) Plant pathogens and integrated defence responses to infection, *Nature* **411**: 826-833.

Dangl JL, and McDowell JM. (2006) Two modes of pathogen recognition by plants, *PNAS* **103**: 8575-8576.

Datta SR, Dudek H, Tao X, Masters S, Fu H, Gotoh Y, and Greenberg ME. (1997) Akt phosphorylation of BAD couples survival signals to the cell-intrinsic death machinery, *Cell* **91**: 231-241.

de Vries JS, Andriotis VME, Wu A-J, and Rathjen JP. (2006) Tomato Pto encodes a functional N-myristoylation motif that is required for signal transduction in *Nicotiana benthamiana*, *Plant J* **45**: 31-45.

Deak M, Casamayor A, Currie RA, Peter Downes C, and Alessi DR. (1999) Characterisation of a plant 3-phosphoinositide-dependent protein kinase-1 homologue which contains a pleckstrin homology domain, *FEBS Letters* **451**: 220-226.

Debener T, Lehnackers H, Arnold M, and Dangl JL. (1991) Identification and molecular mapping of a single *Arabidopsis thaliana* locus determining resistance to a phytopathogenic *Pseudomonas syringae* isolate, *Plant J* **1**: 289-302.

del Pozo O, and Lam E. (1998) Caspases and programmed cell death in the hypersensitive response of plants to pathogens, *Curr Biol* **8**: 1129-1132.

Delaney TP. (1997) Genetic dissection of acquired resistance to disease, *Plant Phys* **113**: 5-12.

Delatte TL, Sedijani P, Kondou Y, Matsui M, de Jong GJ, Somsen GW, Wiese-Klinkenberg A, Primavesi LF, Paul MJ, and Schluepmann H. (2011) Growth arrest by trehalose-6-phosphate: An astonishing case of primary metabolite control over growth by way of the snrk1 signaling pathway, *Plant Phys* **157**: 160-174.

Demmel L, Beck M, Klose C, Schlaitz A-L, Gloor Y, Hsu PP, Havlis J, Shevchenko A, Krause E, Kalaidzidis Y, and Walch-Solimena C. (2008) Nucleocytoplasmic shuttling of the golgi phosphatidylinositol 4-kinase PIK1 is regulated by 14-3-3 proteins and coordinates golgi function with cell growth, *Mol Biol Cell* **19**: 1046-1061.

Deshaies RJ. (1999) Scf and Cullin/RING H2-based ubiquitin ligases, *Annual Review of Cell and Developmental Biology* **15**: 435-467.

Deslandes L. (2003) Physical interaction between Rss1-R, a protein conferring resistance to bacterial wilt, and Popp2, a type III effector targeted to the plant nucleus, *Proc Natl Acad Sci USA* **100**: 8024-8029.

Devarenne TP, Ekengren SK, Pedley KF, and Martin GB. (2006) Adi3 is a Pdk1-interacting agc kinase that negatively regulates plant cell death, *EMBO J* **25**: 255-265.

Devarenne TP. (2011) The plant cell death suppressor Adi3 interacts with the autophagic protein Atg8h, *Biochemical and Biophysical Research Communications* **412**: 699-703.

DeYoung BJ, and Innes RW. (2006) Plant NBS-LRR proteins in pathogen sensing and host defense, *Nat Immunol* **7**: 1243-1249.

Dijkers PF, Medema† RH, Lammers J-WJ, Koenderman* L, and Coffer PJ. (2000) Expression of the pro-apoptotic Bcl-2 family member bim is regulated by the forkhead transcription factor fkhr-l1, *Curr Biol* **10**: 1201-1204.

Dikic I, and Robertson M. (2012) Ubiquitin ligases and beyond, *BMC Biology* **10**: 22.

Dittrich ACN, and Devarenne TP. (2012) An ATP analog-sensitive version of the tomato cell death suppressor protein kinase Adi3 for use in substrate identification, *Biochimica et Biophysica Acta (BBA) - Proteins & Proteomics* **1824**: 269-273.

Dodds PN. (2006) Direct protein interaction underlies gene-for-gene specificity and coevolution of the flax resistance genes and flax rust avirulence genes, *Proc Natl Acad Sci USA* **103**: 8888-8893.

Doorn Wv, and EJ W. (2004) Senescence and programmed cell death: Substance or semantics, *J Exp Bot* **55**: 2147.

Downes BP, Stupar RM, Gingerich DJ, and Vierstra RD. (2003) The HECT ubiquitin-protein ligase (upl) family in arabidopsis: Upl3 has a specific role in trichome development, *Plant J* **35**: 729-742.

Du X, Miao M, Ma X, Liu Y, Kuhl JC, Martin GB, and Xiao F. (2012) Plant programmed cell death caused by an autoactive form of Prf is suppressed by co-expression of the Prf LRR domain, *Mol Plant* **5:** 1058-1067.

Durek P, Schmidt R, Heazlewood JL, Jones A, MacLean D, Nagel A, Kersten B, and Schulze WX. (2010) Phosphat: The arabidopsis thaliana phosphorylation site database. An update, *Nucleic Acids Research* **38**: 828-834.

Dyck JRB, Gao G, Widmer J, Stapleton D, Fernandez CS, Kemp BE, and Witters LA. (1996) Regulation of the 5AMP-activated protein kinase activity by the noncatalytic β and γ subunits, *J Biol Chem* **271**: 17798-17803.

Ek-Ramos MJ, Avila J, Cheng C, Martin GB, and Devarenne TP. (2010) The T-loop extension of the tomato protein kinase AvrPto-dependent Pto-interacting protein 3 (Adi3) directs nuclear localization for suppression of plant cell death, *J Biol Chem* **285**: 17584-17594.

Ellis HM, and Horvitz HR. (1986) Genetic control of programmed cell death in the nematode *C. elegans*, *Cell* **44**: 817-829.

Elmore S. (2007) Apoptosis: A review of programmed cell death, *Toxicologic Pathology* **35**: 495-516.

Erbs G, Silipo A, Aslam S, Castro CD, and Liparoti V. (2008) Peptidoglycan and muropeptides from pathogens agrobacterium and Xanthomonas elicit plant innate immunity: Structure and activity, *Chem Biol* **15**: 438.

Eulgem T, Rushton PJ, Robatzek S, and Somssich IE. (2000) The WRKY superfamily of plant transcription factors, *Trends Plant Sci* **5**: 199-206.

Felix G, and Boller T. (2003) Molecular sensing of bacteria in plants. The highly conserved RNA-binding motif Rnp-1 of bacterial cold shock proteins is recognized as an elicitor signal in tobacco, *J Biol Chem* **278**: 6201-6208.

Feng Z, Hu W, de Stanchina E, Teresky AK, Jin S, Lowe S, and Levine AJ. (2007) The regulation of AMPK β1, Tsc2, and PTEN expression by p53: Stress, cell and tissue specificity, and the role of these gene products in modulating the igf-1-akt-mtor pathways, *Cancer Research* **67**: 3043-3053.

Freemont PS. (1993) The RING finger, *Annals of the New York Academy of Sciences* **684**: 174-192.

Fritz-Laylin LK, Krishnamurthy N, Tor M, Sjolander KV, and Jones JD. (2005) Phylogenomic analysis of the receptor-like proteins of rice and arabidopsis, *Plant Physiol* **138**: 611-623.

Fukuda H. (2000) Programmed cell death of tracheary elements as a paradigm in plants, *Plant Mol Biol* **44**: 245-253.

Ghillebert R, Swinnen E, Wen J, Vandesteene L, Ramon M, Norga K, Rolland F, and Winderickx J. (2011) The AMPK/Snf1/SnRK1 fuel gauge and energy regulator: Structure, function and regulation, *FEBS Journal* **278**: 3978-3990.

Gimenez-Ibanez S, Hann DR, Ntoukakis V, Petutschnig E, Lipka V, and Rathjen JP. (2009) AvrPtoB targets the lysm receptor kinase CERK1 to promote bacterial virulence on plants, *Curr Biol : CB* **19**: 423-429.

Gissot L, Polge C, Bouly J-P, Lemaitre T, Kreis M, and Thomas M. (2004) AKINβ3, a plant specific snrk1 protein, is lacking domains present in yeast and mammals non-catalytic β-subunits, *Plant Mol Biol* **56**: 747-759.

Gissot L, Polge C, Jossier M, Girin T, Bouly J-P, Kreis M, and Thomas M. (2006) AKINβγ contributes to snrk1 heterotrimeric complexes and interacts with two proteins implicated in plant pathogen resistance through its kis/gbd sequence, *Plant Physiol* **142**: 931-944.

Glickman MH, and Ciechanover A. (2002) The ubiquitin-proteasome proteolytic pathway: Destruction for the sake of construction, *Physiol Rev* **82**: 373-428.

Glücksmann A. (1951) Cell deaths in normal vertebrate ontogeny, *Biological Reviews* **26**: 59-86.

Gohre V, and Robatzek S. (2008) Breaking the barriers: Microbial effector molecules subvert plant immunity, In *Annu Rev Phytopathol*, pp 189-215, Annual Reviews, Palo Alto.

Gomez-Gomez L, and Boller T. (2000) Fls2: An LRR receptor-like kinase involved in the perception of the bacterial elicitor flagellin in arabidopsis, *Mol Cell* **5**: 1003-1011.

Gonzalez-Lamothe R. (2006) The u-box protein Cmpg1 is required for efficient activation of defense mechanisms triggered by multiple resistance genes in tobacco and tomato, *Plant Cell* **18**: 1067-1083.

Grabacka M, and Reiss K. (2008) Anticancer properties of PParalpha; effects on cellular metabolism and inflammation, *PPAR Research* **2008**.

Grant SR, Fisher EJ, Chang JH, Mole BM, and Dangl JL. (2006) Subterfuge and manipulation: Type III effector proteins of phytopathogenic bacteria, *Annu Rev Microbiol* **60**: 425-449.

Greenberg JT, and Yao N. (2004) The role and regulation of programmed cell death in plant–pathogen interactions, *Cell Microbiol* **6**: 201-211.

Groover A, DeWitt N, Heidel A, and Jones A. (1997) Programmed cell death of plant tracheary elements differentiating in vitro, *Protoplasma* **196**: 197-211.

Gu YQ. (1998) Molecular mechanisms involved in bacterial speck disease resistance of tomato, *Philos Trans R Soc London* **353**: 1455-1461.

Guiboileau A, Sormani R, Meyer C, and Masclaux-Daubresse C. (2010) Senescence and death of plant organs: Nutrient recycling and developmental regulation, *Comptes rendus biologies* **333**: 382-391.

Hahn-Windgassen A, Nogueira V, Chen C-C, Skeen JE, Sonenberg N, and Hay N. (2005) Akt activates the mammalian target of rapamycin by regulating cellular atp level and ampk activity, *J Biol Chem* **280**: 32081-32089.

Häkli M, Lorick KL, Weissman AM, Jänne OA, and Palvimo JJ. (2004) Transcriptional coregulator snurf (rnf4) possesses ubiquitin e3 ligase activity, *FEBS Letters* **560**: 56-62.

Halford NG, Boulyz JP, and Thomas M. (2000) Snf1-related protein kinases (SnRKs) -- regulators at the heart of the control of carbon metabolism and partitioning, *Adv Bot Res* **32**:405-434.

Halford NG, Hey S, Jhurreea D, Laurie S, McKibbin RS, Paul M, and Zhang Y. (2003) Metabolic signalling and carbon partitioning: Role of Snf1-related (SnRK1) protein kinase, *J Exp Bot* **54**: 467-475.

Halford NG, and Hey SJ. (2009) Snf1-related protein kinases (SnRKs) act within an intricate network that links metabolic and stress signalling in plants, *Biochem J* **419**: 247-259.

Hall T. (1999) Bioedit: A user-friendly biological sequence alignment editor and analysis program for windows 95/98/nt, *Nucleic Acids Symp* **41**: 95-98.

Hamilton KS, Ellison MJ, Barber KR, Williams RS, Huzil JT, McKenna S, Ptak C, Glover M, and Shaw GS. (2001) Structure of a conjugating enzyme-ubiquitin thiolester intermediate reveals a novel role for the ubiquitin tail, *Structure* **9**: 897-904.

Hammond-Kosack KE, and Jones JDG. (1997) Plant disease resistance genes, *Annual Review of Plant Phys and Plant Mol Biol* **48**: 575-607.

Hao L, Wang H, Sunter G, and Bisaro DM. (2003) Geminivirus al2 and l2 proteins interact with and inactivate snf1 kinase, *Plant Cell* **15**: 1034-1048.

Hara-Nishimura I, and Hatsugai N. (2011) The role of vacuole in plant cell death, *Cell Death Differ* **18**: 1298-1304.

Hardie DG, Carling D, and Carlson M. (1998) The AMP-activated/SNF1 protein kinase subfamily: Metabolic sensors of the eukaryotic cell?, *Annu Rev Biochem* **67**: 821-855.

Hardie DG. (2007) AMP-activated/SNF1 protein kinases: Conserved guardians of cellular energy, *Nat Rev Mol Cell Biol* **8**: 774-785.

Harthill JE, Meek SEM, Morrice N, Peggie MW, Borch J, Wong BHC, and MacKintosh C. (2006) Phosphorylation and 14-3-3 binding of Arabidopsis trehalose-phosphate synthase 5 in response to 2-deoxyglucose, *Plant J* **47**: 211-223.

Hatfield PM, Gosink MM, Carpenter TB, and Vierstra RD. (1997) The ubiquitin-activating enzyme (E1) gene family in *Arabidopsis thaliana*, *Plant J* **11**: 213-226.

Hawley SA, Davison M, Woods A, Davies SP, Beri RK, Carling D, and Hardie DG. (1996) Characterization of the AMP-activated protein kinase kinase from rat liver and identification of Threonine 172 as the major site at which it phosphorylates amp-activated protein kinase, *J Biol Chem* **271**: 27879-27887.

Hawley SA, Pan DA, Mustard KJ, Ross L, Bain J, Edelman AM, Frenguelli BG, and Hardie DG. (2005) Calmodulin-dependent protein kinase kinase-beta is an alternative upstream kinase for amp-activated protein kinase, *Cell Metab* **2**: 9-19.

Hayashi F. (2001) The innate immune response to bacterial flagellin is mediated by toll-like receptor 5, *Nature* **410**: 1099-1103.

Heazlewood JL, Durek P, Hummel J, Selbig J, Weckwerth W, Walther D, and Schulze WX. (2008) Phosphat: A database of phosphorylation sites in arabidopsis thaliana and a plant-specific phosphorylation site predictor, *Nucleic Acids Res* **36**: D1015-D1021.

Hedbacker K, Hong S-P, and Carlson M. (2004) Pak1 protein kinase regulates activation and nuclear localization of snf1-gal83 protein kinase, *Mol Cell Biol* **24**: 8255-8263.

Hedbacker K, Townley R, and Carlson M. (2004) Cyclic amp-dependent protein kinase regulates the subcellular localization of snf1-sip1 protein kinase, *Mol Cell Biol* **24**: 1836-1843.

Hedbacker K, and Carlson M. (2006) Regulation of the nucleocytoplasmic distribution of snf1-gal83 protein kinase, *Eukaryot Cell* **5**: 1950-1956.

Hershko A, and Ciechanover A. (1998) The ubiquitin system, *Annu Rev Biochem* **67**: 425-479.

Hey S, Mayerhofer H, Halford NG, and Dickinson JR. (2007) DNA sequences from arabidopsis, which encode protein kinases and function as upstream regulators of snf1 in yeast, *J Biol Chem* **282**: 10472-10479.

Hirt H, Garcia AV, and Oelmüller R. (2011) AGC kinases in plant development and defense, *Plant Signal Behav* **6**: 1030-1033.

Hong S-P, Leiper FC, Woods A, Carling D, and Carlson M. (2003) Activation of yeast SNF1 and mammalian AMP-activated protein kinase by upstream kinases, *PNAS* **100**: 8839-8843.

Hong S-P, and Carlson M. (2007) Regulation of SNF1 protein kinase in response to environmental stress, *J Biol Chem* **282**: 16838-16845.

Horman S, Vertommen D, Heath R, Neumann D, Mouton V, Woods A, Schlattner U, Wallimann T, Carling D, Hue L, and Rider MH. (2006) Insulin antagonizes ischemia-induced thr172 phosphorylation of amp-activated protein kinase α-subunits in heart via hierarchical phosphorylation of ser485/491, *J Biol Chem* **281**: 5335-5340.

Huang J-Z, and Huber SC. (2001) Phosphorylation of synthetic peptides by a cdpk and plant SNF1-related protein kinase. Influence of proline and basic amino acid residues at selected positions, *Plant Cell Physiol* **42**: 1079-1087.

Huibregtse JM, Scheffner M, Beaudenon S, and Howley PM. (1995) A family of proteins structurally and functionally related to the E6-AP ubiquitin-protein ligase, *PNAS* **92**: 2563-2567.

Hurley RL, Anderson KA, Franzone JM, Kemp BE, Means AR, and Witters LA. (2005) The Ca^{2+}/calmoldulin-dependent protein kinase kinases are amp-activated protein kinase kinases, *J Biol Chem* **280**: 29060-29066.

Iseli TJ, Oakhill JS, Bailey MF, Wee S, Walter M, van Denderen BJ, Castelli LA, Katsis F, Witters LA, Stapleton D, Macaulay SL, Michell BJ, and Kemp BE. (2008) AMP-activated protein kinase subunit interactions: B1:Γ1 association requires β1 Thr-263 and Tyr-267, *J Biol Chem* **283**: 4799-4807.

Janjusevic R, Abramovitch RB, Martin GB, and Stebbins CE. (2006) A bacterial inhibitor of host programmed cell death defenses is an E3 ubiquitin ligase, *Science* **311**: 222-226.

Jeworutzki E, Roelfsema MRG, Anschütz U, Krol E, Elzenga JTM, Felix G, Boller T, Hedrich R, and Becker D. (2010) Early signaling through the *Arabidopsis* pattern recognition receptors Fls2 and Efr involves Ca^{2+}-associated opening of plasma membrane anion channels, *Plant J* **62**: 367-378.

Jia Y, Loh YT, Zhou J, and Martin GB. (1997) Alleles of Pto and Fen occur in bacterial speck-susceptible and fenthion-insensitive tomato cultivars and encode active protein kinases, *Plant Cell* **9**: 61-73.

Jia Y, McAdams SA, Bryan GT, Hershey HP, and Valent B. (2000) Direct interaction of resistance gene and avirulence gene products confers rice blast resistance, *EMBO J* **19**: 4004-4014.

Jiang AL, Cheng Y, Li J, and Zhang W. (2008) A Zinc-dependent nuclear endonuclease is responsible for DNA laddering during salt-induced programmed cell death in root tip cells of rice, *J Plant Phys* **165**: 1134-1141.

Jiang R, and Carlson M. (1997) The Snf1 protein kinase and its activating subunit, Snf4, interact with distinct domains of the Sip1/Sip2/Gal83 component in the kinase complex, *Mol Cell Biol* **17**: 2099-2106.

Jones J. (1991) Bacterial speck, In *Compendium of tomato diseases* (Jones, J., Jones, J. P., Stall, R. E., and Zitter, T. A., Eds.), pp 26-27, APS Press, St, Paul, MN.

Jones JD, and Dangl JL. (2006) The plant immune system, *Nature* **444**: 323-329.

Jung J-Y, Kim Y-W, Kwak JM, Hwang J-U, Young J, Schroeder JI, Hwang I, and Lee Y. (2002) Phosphatidylinositol 3- and 4-phosphate are required for normal stomatal movements, *Plant Cell***14**: 2399-2412.

Kakita M, Murase K, Iwano M, Matsumoto T, Watanabe M, Shiba H, Isogai A, and Takayama S. (2007) Two distinct forms of M-locus protein kinase localize to the plasma membrane and interact directly with S-locus receptor kinase to transduce self-incompatibility signaling in brassica rapa, *Plant Cell***19**: 3961-3973.

Katsuhara M, and Kawasaki T. (1996) Salt stress induced nuclear and DNA degradation in meristematic cells of barley roots, *Plant Cell Physiol* **37**: 169-173.

Kerppola TK. (2008) Bimolecular fluorescence complementation: Visualization of molecular interactions in living cells, In *Methods Cell Biol* (Kevin, F. S., Ed.), pp 431-470, Academic Press.

Khosravi-Far R, White E, Zakeri Z, and Lockshin RA. (2007) Cell death: History and future programmed cell death in cancer progression and therapy, pp 1-11, Springer Netherlands.

Kim SY, and Ferrell JE. (2007) Substrate competition as a source of ultrasensitivity in the inactivation of wee1, *Cell* **128**: 1133-1145.

Koivomagi M, Valk E, Venta R, Iofik A, Lepiku M, Balog ERM, Rubin SM, Morgan DO, and Loog M. (2011) Cascades of multisite phosphorylation control Sic1 destruction at the onset of S phase, *Nature* **480**: 128-131.

Kovacic S, Soltys C-LM, Barr AJ, Shiojima I, Walsh K, and Dyck JRB. (2003) Akt activity negatively regulates phosphorylation of amp-activated protein kinase in the heart, *J Biol Chem* **278**: 39422-39427.

Kraft E. (2005) Genome analysis and functional characterization of the E2 and RING-type E3 ligase ubiquitination enzymes of Arabidopsis, *Plant Physiol* **139**: 1597-1611.

Kuchin S, Vyas VK, and Carlson M. (2002) Snf1 protein kinase and the repressors nrg1 and nrg2 regulate flo11, haploid invasive growth, and diploid pseudohyphal differentiation, *Mol Cell Biol* **22**: 3994-4000.

Kuo A, Cappelluti S, Cervantes-Cervantes M, Rodriguez M, and Bush DS. (1996) Okadaic acid, a protein phosphatase inhibitor, blocks calcium changes, gene expression, and cell death induced by gibberellin in wheat aleurone cells, *Plant Cell* **8**: 259-269.

Lam E. (2004) Controlled cell death, plant survival and development, *Nat Rev Mol Cell Biol* **5**: 305-315.

Lange T. (1891) Beiträge zur kenntniss der entwicklung der gefässe und tracheiden., *Flora* **74**: 391-434.

Larkin MA, Blackshields G, Brown NP, Chenna R, McGettigan PA, McWilliam H, Valentin F, Wallace IM, Wilm A, Lopez R, Thompson JD, Gibson TJ, and Higgins DG. (2007) Clustal w and clustal x version 2.0, *Bioinformatics* **23**: 2947-2948.

Lee DH, and Goldberg AL. (1996) Selective inhibitors of the proteasome-dependent and vacuolar pathways of protein degradation in saccharomyces cerevisiae, *J Biol Chem* **271**: 27280-27284.

Lee SB, Xuan Nguyen TL, Choi JW, Lee K-H, Cho S-W, Liu Z, Ye K, Bae SS, and Ahn J-Y. (2008) Nuclear Akt interacts with B23/NPM and protects it from proteolytic cleavage, enhancing cell survival, *PNAS* **105**: 16584-16589.

Lettre G, and Hengartner MO. (2006) Developmental apoptosis in *C. elegans*: A complex cednario, *Nat Rev Mol Cell Biol* **7**: 97-108.

Li W, Ahn I-P, Ning Y, Park C-H, Zeng L, Whitehill JGA, Lu H, Zhao Q, Ding B, Xie Q, Zhou J-M, Dai L, and Wang G-L. (2012) The U-box/arm E3 ligase PUB13 regulates cell death, defense, and flowering time in arabidopsis, *Plant Phys* **159**: 239-250.

Li X-F, Li Y-J, An Y-H, Xiong L-J, Shao X-H, Wang Y, and Sun Y. (2009) AKINβ1 is involved in the regulation of nitrogen metabolism and sugar signaling in Arabidopsis, *J Integr Plant Biol***51**: 513-520.

Lim MTS, and Kunkel BN. (2004) The *Pseudomonas syringae* type III effector AvrRpt2 promotes virulence independently of RIN4, a predicted virulence target in arabidopsis thaliana, *Plant J* **40**: 790-798.

Lim P, HR W, and HG N. (2003) Molecular genetics of leaf senescence in arabidopsis, *Trends Plant Sci* **8**: 272.

Lim PO, Kim HJ, and Gil Nam H. (2007) Leaf senescence, *Annu Rev Plant Biol* **58**: 115-136.

Lin J, Wang Y, and Wang G. (2006) Salt stress-induced programmed cell death in tobacco protoplasts is mediated by reactive oxygen species and mitochondrial permeability transition pore status, *J Plant Phys* **163**: 731-739.

Lin N-C, and Martin GB. (2007) Pto- and Prf-mediated recognition of AvrPto and AvrPtoB restricts the ability of diverse pseudomonas syringae pathovars to infect tomato, *MPMI***20**: 806-815.

Lin S-S, Martin R, Mongrand S, Vandenabeele S, Chen K-C, Jang I-C, and Chua N-H. (2008) RING1 E3 ligase localizes to plasma membrane lipid rafts to trigger FB1-induced programmed cell death in arabidopsis, *Plant J* **56**: 550-561.

Lin SS, Manchester JK, and Gordon JI. (2003) Sip2, an N-myristoylated β subunit of Snf1 kinase, regulates aging in saccharomyces cerevisiae by affecting cellular histone kinase activity, recombination at rdna loci, and silencing, *J Biol Chem* **278**: 13390-13397.

Lochman J, and V M. (2006) Ergosterol treatment leads to the expression of a specific set of defence-related genes in tobacco, *Plant Mol Biol* **62**: 43.

Lockshin RA. (1969) Programmed cell death. Activation of lysis by a mechanism involving the synthesis of protein, *J Insect Physiol* **15**: 1505-1516.

Lorenz DR, Cantor CR, and Collins JJ. (2009) A network biology approach to aging in yeast, *PNAS* **106**: 1145-1150.

Lovas Á, Bimbó A, Szabó L, and Bánfalvi Z. (2003) Antisense repression of StubGal83 affects root and tuber development in potato, *Plant J* **33**: 139-147.

Lu D, Wu S, Gao X, Zhang Y, Shan L, and He P. (2010) A receptor-like cytoplasmic kinase, BIK1, associates with a flagellin receptor complex to initiate plant innate immunity, *PNAS* **107**: 496-501.

Lu D, Lin W, Gao X, Wu S, Cheng C, Avila J, Heese A, Devarenne TP, He P, and Shan L. (2011) Direct ubiquitination of pattern recognition receptor FLS2 attenuates plant innate immunity, *Science* **332**: 1439-1442.

Lumbreras V, Alba MM, Kleinow T, Koncz C, and Pages M. (2001) Domain fusion between Snf1-related kinase subunits during plant evolution *EMBO reports* **2**: 55-60.

Luo HR, Hattori H, Hossain MA, Hester L, Huang Y, Lee-Kwon W, Donowitz M, Nagata E, and Snyder SH. (2003) Akt as a mediator of cell death, *PNAS* **100**: 11712-11717.

Luo Z, Zang M, and Guo W. (2010) AMPK as a metabolic tumor suppressor: Control of metabolism and cell growth, *Future Oncology* **6**: 457-470.

Mackey D, Holt IB, Wiig A, and Dangl JL. (2002) RIN4 interacts with *Pseudomonas syringae* type III effector molecules and is required for Rpm1-mediated resistance in Arabidopsis, *Cell* **108**: 743-754.

Mangat S, Chandrashekarappa D, McCartney RR, Elbing K, and Schmidt MC. (2010) Differential roles of the glycogen-binding domains of β subunits in regulation of the Snf1 kinase complex, *Eukaryoc Cell* **9**: 173-183.

Manning G, Whyte DB, Martinez R, Hunter T, and Sudarsanam S. (2002) The protein kinase complement of the human genome, *Science* **298**: 1912-1934.

Masuyama N, Oishi K, Mori Y, Ueno T, Takahama Y, and Gotoh Y. (2001) Akt inhibits the orphan nuclear receptor Nur77 and T-cell apoptosis, *J Biol Chem* **276**: 32799-32805.

McLaughlin S, and Aderem A. (1995) The myristoyl-electrostatic switch: A modulator of reversible protein-membrane interactions, *TIBS* **20**: 272-276.

Medina EA, Afsari RR, Ravid T, Castillo SS, Erickson KL, and Goldkorn T. (2005) Tumor necrosis factor-α decreases Akt protein levels in 3t3-l1 adipocytes via the caspase-dependent ubiquitination of Akt, *Endocrinology* **146**: 2726-2735.

Melotto M, Underwood W, Koczan J, Nomura K, and He S. (2006) The innate immune function of plant stomata against bacterial invasion, *Cell* **126**: 969-980.

Mishina TE, and Zeier J. (2007) Pathogen-associated molecular pattern recognition rather than development of tissue necrosis contributes to bacterial induction of systemic acquired resistance in arabidopsis, *Plant J* **50**: 500-513.

Mitchelhill KI, Michell BJ, House CM, Stapleton D, Dyck J, Gamble J, Ullrich C, Witters LA, and Kemp BE. (1997) Posttranslational modifications of the 5′-AMP-activated protein kinase β1 subunit, *J Biol Chem* **272**: 24475-24479.

Mucyn TS. (2006) The tomato NBARC-LRR protein Prf interacts with Pto kinase in vivo to regulate specific plant immunity, *Plant Cell* **18**: 2792-2806.

Munnik T, and Testerink C. (2009) Plant phospholipid signaling: "in a nutshell", *J Lipid Res* **50**: S260-S265.

Mur LA, Kenton P, Lloyd AJ, Ougham H, and Prats E. (2008) The hypersensitive response; the centenary is upon us but how much do we know?, *J Exp Bot* **59**: 501-520.

Nash P, Tang X, Orlicky S, Chen Q, Gertler FB, Mendenhall MD, Sicheri F, Pawson T, and Tyers M. (2001) Multisite phosphorylation of a Cdk inhibitor sets a threshold for the onset of DNA replication, *Nature* **414**: 514-521.

Nath N, McCartney RR, and Schmidt MC. (2003) Yeast Pak1 kinase associates with and activates Snf1, *Mol Cell Biol* **23**: 3909-3917.

Navarro L, Zipfel C, Rowland O, Keller I, Robatzek S, Boller T, and Jones JD. (2004) The transcriptional innate immune response to flg22. Interplay and overlap with avr gene-dependent defense responses and bacterial pathogenesis, *Plant Physiol* **135**: 1113-1128.

Nomura K, DebRoy S, Lee YH, Pumplin N, Jones J, and He SY. (2006) A bacterial virulence protein suppresses host innate immunity to cause plant disease, *Science* **313**: 220-223.

Nomura K, Mecey C, Lee Y-N, Imboden LA, Chang JH, and He SY. (2011) Effector-triggered immunity blocks pathogen degradation of an immunity-associated vesicle traffic regulator in *Arabidopsis*, *PNAS* **108**: 10774-10779.

Nürnberger T, Brunner F, Kemmerling B, and Piater L. (2004) Innate immunity in plants and animals: Striking similarities and obvious differences, *Immunological Reviews* **198**: 249-266.

Oakhill JS, Chen ZP, Scott JW, Steel R, Castelli LA, Linga N, Macaulay SL, and Kemp BE. (2010) B-subunit myristoylation is the gatekeeper for initiating

metabolic stress sensing by amp-activated protein kinase (AMPK), *PNAS***107**: 19237-19241.

Oh C-S, and Martin GB. (2011) Effector-triggered immunity mediated by the pto kinase, *Trend Plant Scie* **16**: 132-140.

Oldroyd GED, and Staskawicz BJ. (1998) Genetically engineered broad-spectrum disease resistance in tomato, *PNAS* **95**: 10300-10305.

Osterlund MT, Hardtke CS, Wei N, and Deng XW. (2000) Targeted destabilization of Hy5 during light-regulated development of Arabidopsis, *Nature* **405**: 462-466.

Page RDM. (1996) Tree view: An application to display phylogenetic trees on personal computers, *Computer applications in the biosciences : CABIOS* **12**: 357-358.

Paul MJ, Jhurreea D, Zhang Y, Primavesi LF, Delatte T, Schluepmann H, and Wingler A. (2010) Up-regulation of biosynthetic processes associated with growth by trehalose 6-phosphate, *Plant Signal Behav* **5**: 386-392.

Pearce LR, Komander D, and Alessi DR. (2010) The nuts and bolts of AGC protein kinases, *Nat Rev Mol Cell Biol* **11**: 9-22.

Pedley KF, and Martin GB. (2003) Molecular basis of pto-mediated resistance to bacterial speck disease, *Annu Rev Phytopathol* **41**: 215-243.

Peng J. (2003) A proteomics approach to understanding protein ubiquitination, *Nature Biotech* **21**: 921-926.

Pennell RI, and Lamb C. (1997) Programmed cell death in plants, *Plant Cell***9**: 1157-1168.

Pickart CM. (2001a) Ubiquitin enters the new millennium, *Molecular Cell* **8**: 499-504.

Pickart CM. (2001b) Mechanisms underlying ubiquitination, *Annu Rev Biochem* **70**: 503-533.

Pierre M, Traverso JA, Bertrand B, Domenichini S, Bouchez D, Giglione C, and Meinnel T. (2007) N-myristoylation regulates the SnRK1 pathway in Arabidopsis, *The Plant Cell* **19**: 2804-2821.

Plas D, and Thompson C. (2002) Cell metabolism in the regulation of programmed cell death, *Trends Endocrinol Metab* **13**: 75-78.

Polge C, and Thomas M. (2007) Snf1/AMPK/SnRK1 kinases, global regulators at the heart of energy control?, *Trend Plant Scie* **12**: 20-28.

Polge C, Jossier M, Crozet P, Gissot L, and Thomas M. (2008) Beta-subunits of the SnRK1 complexes share a common ancestral function together with expression and function specificities; physical interaction with nitrate reductase specifically occurs via AKINβ1-subunit, *Plant Physiol* **148**: 1570-1582.

Ptiblado R, and Kerr E. (1980) Resistance to bacterial speck (Pseudomonas tomato) in tomato, *Acta Horticulturae* **100**: 379-382.

Reiland S, Messerli G, Baerenfaller K, Gerrits B, Endler A, Grossmann J, Gruissem W, and Baginsky S. (2009) Large-scale arabidopsis phosphoproteome profiling reveals novel chloroplast kinase substrates and phosphorylation networks, *Plant Physiol* **150**: 889-903.

Resh MD. (2006) Trafficking and signaling by fatty-acylated and prenylated proteins, *Nat Chem Biol* **2**: 584-590.

Rokudai S, Fujita N, Hashimoto Y, and Tsuruo T. (2000) Cleavage and inactivation of antiapoptotic Akt/PKB by caspases during apoptosis, *J Cell Physiol* **182**: 290-296.

Ronald PC, and Beutler B. (2010) Plant and animal sensors of conserved microbial signatures, *Science* **330**: 1061-1064.

Rosebrock TR. (2007) A bacterial E3 ubiquitin ligase targets a host protein kinase to disrupt plant immunity, *Nature* **448**: 370-374.

Sanabria N, Goring D, Nürnberger T, and Dubery I. (2008) Self/nonself perception and recognition mechanisms in plants: A comparison of self-incompatibility and innate immunity, *New Phytologist* **178**: 503-514.

Saunders JW. (1966) Death in embryonic systems, *Science* **154**: 604-612.

Sauvonnet N, Lambermont I, Bruggen Pvd, and Cornelis GR. (2002) YopH prevents monocyte chemoattractant protein 1 expression in macrophages and t-cell proliferation through inactivation of the phosphatidylinositoi 3-kinase pathway, *Mol Microbiol* **45**: 805-815.

Schluepmann H, Berke L, and Sanchez-Perez GF. (2011) Metabolism control over growth: A case for trehalose-6-phosphate in plants, *J Exp Bot*.

Schmidt MC, and McCartney RR. (2000) β-subunits of Snf1 kinase are required for kinase function and substrate definition, *EMBO J* **19**: 4936-4943.

Schuhegger R, A I, S G, G B, and C K. (2006) Induction of systemic resistance in tomato by N-acyl-l-homoserine lactone-producing rhizosphere bacteria, *Plant Cell Environ* **29**: 909.

Schwachtje J, Minchin PEH, Jahnke S, van Dongen JT, Schittko U, and Baldwin IT. (2006) Snf1-related kinases allow plants to tolerate herbivory by allocating carbon to roots, *PNAS* **103**: 12935-12940.

Scott JW, Ross FA, Liu JKD, and Hardie DG. (2007) Regulation of amp-activated protein kinase by a pseudosubstrate sequence on the γ subunit, *EMBO J* **26**: 806-815.

Segonzac C, and Zipfel C. (2011) Activation of plant pattern-recognition receptors by bacteria, *Curr Opin in Microbiol* **14**: 54-61.

Sessa G, D'Ascenzo M, and Martin GB. (2000) The major site of the Pti1 kinase phosphorylated by the pto kinase is located in the activation domain and is required for Pto–Pti1 physical interaction, *Eur J Biochem* **267**: 171-178.

Shen W, and Hanley-Bowdoin L. (2006) Geminivirus infection up-regulates the expression of two arabidopsis protein kinases related to yeast Snf1- and mammalian AMPK-activating kinases, *Plant Phys* **142**: 1642-1655.

Shen W, Reyes MI, and Hanley-Bowdoin L. (2009) Arabidopsis protein kinases GRIK1 and GRIK2 specifically activate SnRK1 by phosphorylating its activation loop, *Plant Phys* **150**: 996-1005.

Shimmen T, and Yokota E. (2004) Cytoplasmic streaming in plants, *Curr Opin Cell Biol* **16**: 68-72.

Shiu SH, and Bleecker AB. (2003) Expansion of the receptor-like kinase/pelle gene family and receptor-like proteins in arabidopsis, *Plant Physiol* **132**: 530-543.

Silipo A, L S, D G, G E, and TT J. (2008) The acylation and phosphorylation pattern of lipid a from *Xanthomonas campestris* strongly influence its ability to trigger the innate immune response in arabidopsis, *Chem Bio Chem* **9**: 896.

Simeonova E, S S, M C, and A M. (2000) Aspects of programmed cell death during leaf senescence of mono- and dicotyledonous plants, *Protoplasma* **214**: 93.

Smalle J, and Vierstra RD. (2004) The ubiquitin 26S proteasome proteolytic pathway, *Annu Rev Plant Biol* **55**: 555-590.

Solomon M, Belenghi B, Delledonne M, Menachem E, and Levine A. (1999) The involvement of cysteine proteases and protease inhibitor genes in the regulation of programmed cell death in plants, *Plant Cell***11**: 431-443.

Stakman EC. (1915) Relation between puccinia graminis and plants highly resistant to its attack, *J Agric Res* **4**: 193-200.

Stapleton D, Mitchelhill KI, Gao G, Widmer J, Michell BJ, Teh T, House CM, Fernandez CS, Cox T, Witters LA, and Kemp BE. (1996) Mammalian AMP-activated protein kinase subfamily, *J Biol Chem* **271**: 611-614.

Steinberg GR, and Kemp BE. (2009) AMPK in health and disease, *Physiol Rev* **89**: 1025-1078.

Stone SL. (2005) Functional analysis of the RING-type ubiquitin ligase family of Arabidopsis, *Plant Physiol* **137**: 13-30.

Stulemeijer IJE, and Joosten MHAJ. (2008) Post-translational modification of host proteins in pathogen-triggered defence signalling in plants, *Molecular Plant Pathology* **9**: 545-560.

Sugden C, Crawford RM, Halford NG, and Hardie DG. (1999) Regulation of spinach snf1-related (SnRK1) kinases by protein kinases and phosphatases is associated with phosphorylation of the T loop and is regulated by 5′-AMP, *Plant J* **19**: 433-439.

Sugden C, Donaghy PG, Halford NG, and Hardie DG. (1999) Two Snf1-related protein kinases from spinach leaf phosphorylate and inactivate 3-hydroxy-3-methylglutaryl-coenzyme a reductase, nitrate reductase, and sucrose phosphate synthase in vitro, *Plant Physiol* **120**: 257-274.

Sutherland CM, Hawley SA, McCartney RR, Leech A, Stark MJR, Schmidt MC, and Hardie DG. (2003) Elm1p is one of three upstream kinases for the *Saccharomyces cerevisiae* Snf1 complex, *Curr Biol* **13**: 1299-1305.

Takken FL, Albrecht M, and Tameling WI. (2006) Resistance proteins: Molecular switches of plant defence, *Curr Opin Plant Biol* **9**: 383-390.

Tan X. (2007) Mechanism of auxin perception by the Tir1 ubiquitin ligase, *Nature* **446**: 640-645.

Tang D, Kang R, Coyne CB, Zeh HJ, and Lotze MT. (2012) PAMPs and DAMPs: Signals that spur autophagy and immunity, *Immunological Reviews* **249**: 158-175.

Thelander M, Olsson T, and Ronne H. (2004) Snf1-related protein kinase 1 is needed for growth in a normal day-night light cycle, *EMBO J* **23**: 1900-1910.

Thomson M, and Gunawardena J. (2009) Unlimited multistability in multisite phosphorylation systems, *Nature* **460**: 274-277.

Toft C, and Andersson SGE. (2010) Evolutionary microbial genomics: Insights into bacterial host adaptation, *Nat Rev Genet* **11**: 465-475.

Toroser D, Plaut Z, and Huber SC. (2000) Regulation of a plant Snf1-related protein kinase by glucose-6-phosphate, *Plant Phys* **123**: 403-412.

Tsai AY-L, and Gazzarrini S. (2012) AKIN10 and FUSCA3 interact to control lateral organ development and phase transitions in arabidopsis, *Plant J* **69**: 809-821.

Tsiatsiani L, Van Breusegem F, Gallois P, Zavialov A, Lam E, and Bozhkov PV. (2011) Metacaspases, *Cell Death Differ* **18**: 1279-1288.

Tuteja N. (2007) Mechanisms of high salinity tolerance in plants, *Methods in enzymology* **428**: 419-438.

Van der Biezen EA, and Jones JD. (1998) Plant disease-resistance proteins and the gene-for-gene concept, *Trends Biochem Sci* **23**: 454-456.

Van der Hoorn RA, De Wit PJ, and Joosten MH. (2002) Balancing selection favors guarding resistance proteins, *Trends Plant Sci* **7**: 67-71.

van der Hoorn RAL, and Kamoun S. (2008) From guard to decoy: A new model for perception of plant pathogen effectors, *Plant Cell***20**: 2009-2017.

van Ooijen G, van den Burg HA, Cornelissen BJC, and Takken FLW. (2007) Structure and function of resistance proteins in solanaceous plants, *Annu Rev Phytopathol* **45**: 43-72.

Vaux DL, and Korsmeyer SJ. (1999) Cell death in development, *Cell* **96**: 245-254.

Vierstra RD. (2009) The ubiquitin-26S proteasome system at the nexus of plant biology, *Nat Rev Mol Cell Biol* **10**: 385-397.

Vincent O, Townley R, Kuchin S, and Carlson M. (2001) Subcellular localization of the Snf1 kinase is regulated by specific β subunits and a novel glucose signaling mechanism, *Genes Dev* **15**: 1104-1114.

Vivanco I, and Sawyers CL. (2002) The phosphatidylinositol 3-kinase-akt pathway in human cancer, *Nat Rev Cancer* **2**: 489-501.

Wang DY-C, Kumar S, and Hedges SB. (1999) Divergence time estimates for the early history of animal phyla and the origin of plants, animals and fungi, *Proc R Soc Lond [Biol]* **266**: 163-171.

Wang H, Li J, Bostock RM, and Gilchrist DG. (1996) Apoptosis: A functional paradigm for programmed plant cell death induced by a host-selective phytotoxin and invoked during development, *Plant Cell***8**: 375-391.

Wang J, Li X, Liu Y, and Zhao X. (2010) Salt stress induces programmed cell death in thellungiella halophila suspension-cultured cells, *J Plant Physiol* **167**: 1145-1151.

Wang Z, Wilson WA, Fujino MA, and Roach PJ. (2001) Antagonistic controls of autophagy and glycogen accumulation by snf1p, the yeast homolog of amp-activated protein kinase, and the cyclin-dependent kinase pho85p, *Mol Cell Biol* **21**: 5742-5752.

Warden S, Richardson C, O'Donnell J, Satpleton D, Kemp BE, and Witters LA. (2001) Post-translational modifications of the β-1 subunit of amp-activated protein kinase affect enzyme activity and cellular localization, *Biochem J* **354**: 275-283.

Wiborg J, O'Shea C, and Skriver K. (2008) Biochemical function of typical and variant Arabidopsis thaliana U-box E3 ubiquitin-protein ligases, *Biochem J* **413**: 447-457.

Wilkinson KD. (2000) Ubiquitination and deubiquitination: Targeting of proteins for degradation by the proteasome, *Sem Cell Dev Biol* **11**: 141-148.

Woffenden BJ, Freeman TB, and Beers EP. (1998) Proteasome inhibitors prevent tracheary element differentiation in zinnia mesophyll cell cultures, *Plant Phys* **118**: 419-430.

Woods A, Johnstone SR, Dickerson K, Leiper FC, Fryer LG, Neumann D, Schlattner U, Wallimann T, Carlson M, and Carling D. (2003) Lkb1 is the upstream kinase in the amp-activated protein kinase cascade, *Curr Biol* **13**: 2004-2008.

Woods A, Dickerson K, Heath R, Hong SP, Momcilovic M, Johnstone SR, Carlson M, and Carling D. (2005) Ca^{2+}/calmodulin-dependent protein kinase kinase-beta acts upstream of amp-activated protein kinase in mammalian cells, *Cell Metab* **2**: 21-33.

Xiang T, Zong N, Zou Y, Wu Y, Zhang J, Xing W, Li Y, Tang X, Zhu L, Chai J, and Zhou J-M. (2008) *Pseudomonas syringae* effector avrpto blocks innate immunity by targeting receptor kinases, *Curr Biol* **18**: 74-80.

Xiao B, Heath R, Saiu P, Leiper FC, Leone P, Jing C, Walker PA, Haire L, Eccleston JF, Davis CT, Martin SR, Carling D, and Gamblin SJ. (2007) Structural basis for amp binding to mammalian amp-activated protein kinase, *Nature* **449**: 496-500.

Xing W, Y Z, Q L, J L, and X L. (2007) The structural basis for activation of plant immunity by bacterial effector protein AvrPto, *Nature* **449**: 243.

Yaeno T, and Iba K. (2008) Bah1/nla, a ring-type ubiquitin e3 ligase, regulates the accumulation of salicylic acid and immune responses to pseudomonas syringae dc3000, *Plant Phyisiol* **148**: 1032-1041.

Yang C-W, González-Lamothe R, Ewan RA, Rowland O, Yoshioka H, Shenton M, Ye H, O'Donnell E, Jones JDG, and Sadanandom A. (2006) The e3 ubiquitin ligase activity of arabidopsis plant u-box17 and its functional tobacco homolog acre276 are required for cell death and defense, *Plant Cell* **18**: 1084-1098.

Yang P, Fu H, Walker J, Papa CM, Smalle J, and Ju YM. (2004) Purification of the arabidopsis 26S proteasome: Biochemical and molecular analyses revealed the presence of multiple isoforms, *J Biol Chem* **279**: 6401-6413.

Yang W-L, Wang J, Chan C-H, Lee S-W, Campos AD, Lamothe B, Hur L, Grabiner BC, Lin X, Darnay BG, and Lin H-K. (2009) The E3 ligase Traf6 regulates Akt ubiquitination and activation, *Science* **325**: 1134-1138.

Zeng L, Velásquez AC, Munkvold KR, Zhang J, and Martin GB. (2012) A tomato Lysm receptor-like kinase promotes immunity and its kinase activity is inhibited by AvrPtoB, *Plant J* **69**: 92-103.

Zhang Y, Shewry PR, Jones H, Barcelo P, Lazzeri PA, and Halford NG. (2001) Expression of antisense snrk1 protein kinase sequence causes abnormal pollen development and male sterility in transgenic barley, *Plant J* **28**: 431-441.

Zhang Y, and McCormick S. (2009) AGCVIII kinases: At the crossroads of cellular signaling, *Trend Plant Scie* **14**: 689-695.

Zhang Y, Primavesi LF, Jhurreea D, Andralojc PJ, Mitchell RAC, Powers SJ, Schluepmann H, Delatte T, Wingler A, and Paul MJ. (2009) Inhibition of Snf1-related protein kinase1 activity and regulation of metabolic pathways by trehalose-6-phosphate, *Plant Phys* **149**: 1860-1871.

Zhou J, Loh Y-T, Bressan RA, and Martin GB. (1995) The tomato gene Pti1 encodes a serine/threonine kinase that is phosphorylated by Pto and is involved in the hypersensitive response, *Cell* **83**: 925-935.

Zipfel C, and Felix G. (2005) Plants and animals: A different taste for microbes?, *Curr Opin Plant Biol* **8**: 353-360.

Zipfel C, Kunze G, Chinchilla D, Caniard A, Jones JDG, Boller T, and Felix G. (2006) Perception of the bacterial pamp EF-TU by the receptor efr restricts Agrobacterium-mediated transformation, *Cell* **125**: 749-760.